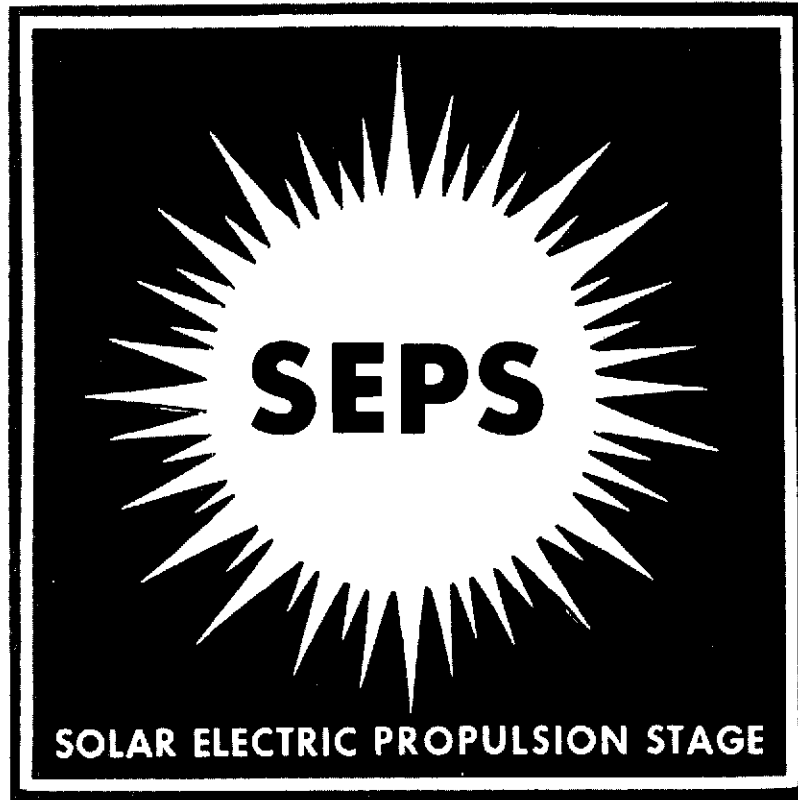


LMSC-D384250  
1 SEPTEMBER 1974

# SOLAR ARRAY TECHNOLOGY EVALUATION



N74-35199

(NASA-CR-120483) SOLAR ARRAY TECHNOLOGY  
EVALUATION PROGRAM FOR SEPS (SOLAR  
ELECTRICAL PROPULSION STAGE) Final  
Report (Lockheed Missiles and Space Co.)  
253 p HC \$15.75

Unclas  
51013

G3/28

CSCI 21C

SUBMITTED TO: GEORGE C. MARSHALL SPACE CENTER  
NATIONAL AERONAUTICS AND SPACE ADMINISTRATION



## FINAL REPORT

LOCKHEED MISSILES & SPACE COMPANY, INC.

A GROUP DIVISION OF LOCKHEED AIRCRAFT CORPORATION  
SPACE SYSTEMS DIVISION • SUNNYVALE, CALIFORNIA

**LMSC-D384250**

**1 September 1974**

**SOLAR ARRAY TECHNOLOGY EVALUATION  
PROGRAM FOR SEPS  
(SOLAR ELECTRICAL PROPULSION STAGE)**

**FINAL REPORT**

**NAS8-30315**

**Prepared for**

**National Aeronautics and Space Administration  
George C. Marshall Space Flight Center  
Huntsville, Alabama**

**by**

**Space Systems Division**

**LOCKHEED MISSILES & SPACE COMPANY**

Page intentionally left blank

## FOREWORD

This final report summarizes the effort and technical progress achieved in the technology evaluation and preliminary design for a 25 KW Solar Array System for SEPS. This document is required by Contract NAS8-30315 Exhibit A Statement of Work. It was prepared by the Space Systems Division of Lockheed Missiles and Space Company, Inc. for the National Aeronautics and Space Administration's Marshall Space Flight Center, Huntsville, Alabama. The contents are not necessarily endorsed by the Marshall Space Flight Center or the National Aeronautics and Space Administration.



Page intentionally left blank

# TABLE OF CONTENTS

	<u>Page</u>
Foreword	iii
Table of Contents	v
List of Figures	vii
List of Tables	ix
SECTION 1 INTRODUCTION AND SUMMARY	1-1
SECTION 2 TECHNICAL DISCUSSION	2-1
2.1 Program Objectives	2-1
2.2 Design Requirements	2-2
2.3 Mechanical Design	2-7
2.3.1 Design Baseline	2-7
2.3.2 Mechanical Design Studies	2-20
2.4 Electrical Design	2-47
2.4.1 Electrical Design	2-43
2.4.2 Electrical Design Studies Tradeoffs	2-63
2.5 Design Support Studies	2-89
2.5.1 Dynamics Analysis	2-89
2.5.2 Thermodynamics Analysis	2-100
2.5.3 Solar Cell Radiation Analysis	2-111
2.5.4 Structures Analysis	2-120
2.6 State Of The Art Assessment	2-127
2.6.1 Cell Cover	2-129
2.6.2 Solar Cells	2-137
2.6.3 Solar Cell Interconnect	2-140
2.6.4 Cell Joining Techniques	2-148
2.6.5 Solar Array Flexible Substrate	2-156
2.6.6 Modular Joints	2-169
2.6.7 Array Electrical Harness	2-175
2.6.8 Composite Material for Containment Box Structure	2-179
2.6.9 Extension and Retraction Mast	2-181
2.6.10 Extension Mast Motors	2-193
2.6.11 Lubricants	2-198
2.7 Component Design, Fabrication and Test	2-200
2.7.1 On Array Padding	2-200
2.7.2 Harness Joining Techniques	2-208
2.7.3 Thin Array Substrate Fabrication and Test	2-213
2.8 Root Section Model	2-117

TABLE OF CONTENTS CONT'D.

	<u>Page</u>
SECTION 3    SEPS Solar Array Technology Developmentwork Plan	3-1
SECTION 4    REFERENCES	4-1
APPENDIX A   HARNESS CALCULATIONS	A-1

## LIST OF FIGURES

<u>Figure</u>		<u>Page</u>
2-1	SEPS Solar Array Design Requirements	2-1
2-2	SEPS Solar Array Configuration	2-8
2-3	Array System Assembly Container Configuration	2-9
2-4	Array Extension Sequence	2-13
2-5	Panel Stowage Method Study Results	2-21
2-6	Substrate Tensioning Methods	2-24
2-7	On-Array Padding Concepts	2-29
2-8	Pad Concept Effects on Solar Array	2-31
2-9	On-Array Padding - FEP Teflon Over Cell Sheet	2-33
2-10	Criss-Cross Padding Concept	2-35
2-11	Ascent Preload Methods	2-37
2-12	Flat-Fold Preload Concepts	2-41
2-13	Substrate System Options	2-49
2-14	Integral Interconnects - Substrate Design	2-50
2-15	Chronology of Wraparound Cell Development	2-53
2-16	Required Efficiency of Covered Cell	2-56
2-17	FCC Harness Inboard End Termination	2-62
2-18	Intensity Vs. Sun Distance	2-64
2-19	Cell Temperature - Normal Incidence	2-66
2-20	$V_{oc}$ As a Function of Displacement, Intensity and Temperature	2-67
2-21	Panel Voltage Characteristics	2-69
2-21a	Shadowed Module I-V Characteristics	2-72
2-22	Electrical Module Selection	2-73
2-23	Array Panel Configuration	2-73
2-24	Harness Option - Backside Integral	2-76
2-25	Harness Option - Edge Mounted	2-77
2-26	Harness Option - Backside Transverse	2-78
2-27	Harness Option - Primary Substrate	2-80
2-28	Harness Option - Pantograph	2-81
2-29	Harness Option - Segmented Printed Circuit	2-82
2-30	Power Feeder Harness Concept Tradeoffs	2-84
2-30a	Array P / Po vs Distance From Sun	2-88
2-31	SEPS Solar Array Configuration	2-91
2-32	Array Finite Element Model	2-92
2-33	First Mode Frequency Variation	2-97
2-34	Array Blanket/Tension System Model	2-99
2-35	Tension for Minimum Mast EI	2-99
2-36	Tension for Minimum Mast EI, Dual Blanket Density	2-101
2-37	Extension Mast Stiffness Requirements	2-101
2-38	Substrate Copper Trace Pattern	2-103
2-39	Array Panel Detail	2-103

<u>Figure</u>		<u>Page</u>
2-40	Reflectivity and Transmissivity vs Solar Incidence Angle	2-106
2-41	Solar Cell and Substrate Base Temperature vs Sun Distance	2-108
2-42	Solar Cell Temperature Vs Heliocentric Distance and Array Tilt	2-109
2-43	Array Front-to-Back Temperature Difference	2-110
2-44	Transient Temperature Response of Mast Elements	2-112
2-45	SEPS Solar Array Degradation	2-118
2-46	Inboard Tension Distribution Model	2-121
2-47	Deflection of Edge Beam and First Hinge	2-121
2-48	On-Array Padding Test Specimens	2-201
2-49	Slip Resistance Test Fixture	2-204
2-50	Padding Slip Resistance Test Setup	2-205
2-51	Qualification Test Levels - Random Vibration	2-207
2-52	Padding Concept Slip Resistance	2-209
2-53	Summary of Slip Resistance Tests	2-210

## LIST OF TABLES

<u>TABLE</u>		<u>Page</u>
2-1	SEPS Solar Array Weight Summary	2-14
2-2	Extension Mast Design	2-18
2-3	Candidate Panel Materials	2-43
2-5	FCC Harness Design	2-86
2-6	SEPS Solar Array Performance	2-88
2-7	Dynaics Study Results	2-95
2-8	Solar Array Modes	2-96
2-9	Surface Radiation Properties Used in Therm Model of the SEPS Solar Array	2-104
2-10	SEPS Equivalent 1 MeV Electron Fluence	2-115
2-11	Partially Stored SEPS Equivalent 1 MeV Electron Fluence	2-117
2-12	Probability of Solar Flare Events	2-119
2-13	Criteria for State of the Art Assessment	2-128
2-14	Summary of Vibration Test	2-211
2-15	Thin Flexible Printed Circuit Substrate Tests	

## SECTION 1

### INTRODUCTION AND SUMMARY

This report presents a summary of the work performed under NASA-MSFC Contract NAS8-30315. The program objectives were to evaluate technology and to develop a preliminary design for a 25 KW Solar Array System for SEPS with a power to weight ratio of 65 watts/Kg. The Solar Array System is composed of two wings. Each wing consists of a solar array blanket, a blanket launch storage container, an extension/retraction mast assembly, a blanket tensioning system, an array electrical harness, and necessary brackets and attach points for supporting the solar array system for launch and in the operating position.

The technology evaluation was performed to assess the applicable solar array state-of-the-art, and to define supporting research necessary to achieve technology readiness for meeting the SEPS solar array design requirements. The major design requirements for the SEPS solar array are:

- o operation between 0.3 and 6.0 au
- o operation in free space and in the earth's radiation environments with specified allowable degradation
- o power availability of 25 KW BOL and 21 KW EOL after 5 years in free space at 1 au
- o full deployment, full retraction, to and from one intermediate deployment position
- o a weight limit of 385 Kg

The major program tasks are:

<u>Task No.</u>	<u>Task Title</u>
1.0	Preliminary Design
2.0	Assessment of State-of-the-Art
3.0	Test Component Design
4.0	Hardware Fabrication and Assembly
5.0	Design Verification Testing

1.0 Preliminary Design. The design requirements for the solar array system were used to define the trade-off and analysis activity during the program first half. The major design support analysis effort was in the areas of space radiation effects, deployed array dynamics, and thermodynamics evaluations. The space radiation study generated parametric data on the power degradation of candidate cell and cell cover designs when exposed to the free space radiation environment at 1 au. Degradation data for cell/cell cover combinations were also generated for a partially stowed flat-fold array to evaluate designs using partial array retraction to limit average array power loss due to proton flare events. It is apparent that this type of operation is required to limit total power degradation from 25 KW BOL to 21 KW EOL during 5 years in free space at 1 au.

The deployed array dynamics have been evaluated with a finite element computer model for out-of-array-plane and torsional modes. Extension mast and blanket tensioning system performance requirements have been defined and are within the state-of-the-art capabilities. Since the in-plane mode results are only approximate solutions with this model, a new in-plane motion model was developed and evaluated.

The thermodynamics studies that were performed characterized the baseline array blanket solar cell and substrate backside temperatures as a function of heliocentric distance under normal illumination. Cell temperature as a function of heliocentric distance and array tilting angle, and extension mast transient heating under non-nominal sun exposure at 0.3 au have also been evaluated.

Solar array mechanical and structural design studies in the areas of flat-fold vs roll-up, array blanket guide-wire and tensioning system concepts, containment box cover mechanism for release and re-application of stored blanket compression pre-load, and on-array padding concepts have been completed. Electrical design studies were performed for module size, series/parallel arrangement, array harness design concept comparisons, and array harness sizing.

2.0 Assessment of State-of-the-Art. The elements of the SEPS solar array have been reviewed from the standpoints of past development and specific application



to the SEPS solar array. Much of the technology required has been classified as Category I - Sufficient. These items fall mostly in the areas defined by either;

- a) Successfully used for similar missions, or
- b) Not in use but substantiated by test and analysis, or
- c) Substantiation achievable within span and scope of this technology program.

Sample Category I elements are: fused silica coverglasses, lubricants, extension mast drive motors, thin substrate fabrication, thin substrate electrical and mechanical performance, and module hinge strength.

The technology for several array elements is classed as Category II - Insufficient, But Development Progress Will Achieve Required Readiness. These items are mostly in areas defined by: Insufficiency due to lack of analytical or test data and not due to known functional or physical limitation. Sample Category II elements are: Intermediate Efficiency (11.4%) 8 mil Solar Cell, Solar cell/thin substrate/module hinge performance after exposure to SEPS UV/space radiation/temperature/and thermal cycling environments, and Array Electrical Module NDT Inspection-Acceptance Techniques for fabrication.

A few items were classed Category III - Insufficient but an alternate is feasible and Category IV - Insufficient and no alternates or potential devices defined. These items were all additional design candidates where Category I or II designs and developments were available for the SEPS solar array design.

3.0 Test Component Design. Several on-array padding concepts were generated and screening test modules designed using 12 mil thick 2 x 4 cm fused silica cover glasses as cell simulators with each padding concept. A tool for holding the padding concepts in a four layer configuration was designed to test interlayer slip resistance force as a function of compression load, and to be used in vibration table testing of selected designs. Thin solar array substrate lamination designs using different laminating "adhesives" with a basic 0.5 mil Kapton film were completed for 1) a laminated circuit test pattern (dielectric strength, peel strength, shrinkage, and

tensile strength, 2) for a 10 cell substrate for testing joining of solar cells to the thin substrate designs, and 3) for UV exposure testing of the substrates.

Aluminum flat cable conductor (FCC) harness joints to copper array panel interconnects were designed for testing a variety of solder, braze and welding techniques for strength and for humidity exposure resistance.

The array root section functional model (full scale width and 3 m (10 ft) tall) design specification was completed. The solar cell and cover specifications for the  $0.757 \text{ m}^2$  ( $8.18 \text{ ft}^2$ ) model electrical modules (two incorporated in the model and one separately delivered  $2.5 \text{ ft}^2$  module) and the model extension mast design specification were completed and issued to vendors with RFQ's. Vendors were selected and orders placed. Glass cell mass simulators were ordered for the remainder of the model array blanket. A vendor for the aluminum FCC selected for the design was found and an order placed.

4.0 Hardware Fabrication and Assembly. Nine on-array padding screening test items composed of 4 layers of cell simulators in a 4 x 5 cell configuration were fabricated. A test tool for slip resistance force and vibration testing of the on-array padding concepts was built. Samples of aluminum FCC were fabricated using an etched printed circuit technique along with samples copper pads in the array substrate. These were used to make sample joints between the Al FCC and the copper pads using five candidate joining techniques. Three thin substrate candidate material systems were used to fabricate laminated circuit test patterns and 10-cell substrate test modules.

Centralab, the selected model solar cell vendor has completed the fabrication of all but 432 of each 2800 each 2 x 4 cm, wraparound contact, 200 micron (8 mil) cells. The 150 micron (6 mil) fused silica cell cover vendor, Heliotek completed 1059 covers before equipment problems forced cancellation of the remainder of the order. OCLI is fabricating the remaining covers required. Astro Research Corp., Santa Barbara built and delivered a 3.7 m (12 ft) long, 25.4 cm (10 in) diameter continuous

coilable longeron Astromast for the root section model. The model fabrication has been delayed due to delays in deliveries of solar cells and cell covers. Fabrication will be completed in October 1974.

5.0 Design Verification Tests. Slip force resistance tests were performed on nine on-array padding concepts by varying the compression load on 4 layers of test substrates and pulling on the clamped edge of one of the two inner layers until relative motion or slip was observed. Illumination tests in a thermal vacuum chamber were performed on a solar cell test module covered with an embossed FEP Teflon sheet, an on-array padding concept. An uncovered module was tested at the same time to determine the effect on transmission and "greenhouse" heating of the Teflon sheet. The test was repeated with two 1.25 cm diameter holes over the 2 x 4 cm solar cells to reduce the cell heating effects. The padding concepts were also vibration tested.

Three thin flexible printed circuit substrate designs concepts were subjected to dielectric strength, high temperature exposure, temperature/humidity, and peel tests. Several concepts for joining aluminum FCC conductors to the copper circuitry in the printed circuit were evaluated for ease of fabrication and pull strength. UV irradiation (3210 E.S.H at 5 suns) and humidity exposure tests were performed on several array blanket components. The test results supported the preliminary design selections in the areas of substrate, harness, panel hinge and harness/panel joining techniques.

### CONCLUSIONS

1. The flat fold array concept is recommended by LMSC for the SEPS solar array design.
2. The design and weight evaluations completed in this study indicate that the required power to weight ratio for the array can be obtained by the recommended technology advances with minimum risk.
3. The beginning of life, 1 au array performance meets the design requirements. New technology effort is required primarily in the testing of materials and

designs that seem viable for application to the array design but are lacking in testing to the SEPS mission environments.

4. The development of minimum cost materials, fabrication processes, and testing techniques are desired technology advancements. Definition of the ground test techniques for the assembled solar array that provide a true test of the assembly, without perturbing the results, is an important requirement.

## SECTION 2 TECHNICAL DISCUSSION

### 2.1 PROGRAM OBJECTIVES

The objectives of the Solar Array Technology Evaluation Program for SEPS are to:

1. Plan and conduct an assessment of the solar array state-of-art in order to define necessary research and technology advancements that may be required in the next 30 to 36 months to support the SEPS solar array development.
2. Develop a 25 KW SEPS solar array preliminary design capable of performing the SEPS mission between 0.3 and 6 au and limited in weight to 385 Kg.
3. Design, fabricate and test those array component designs that require testing to adequately assess and verify the validity of the solar array design concept that is developed.
4. Define the most cost effective approach to demonstrate technology readiness through the fabrication and test of components, subassemblies, assemblies and a full scale solar array wing.

## 2.2 DESIGN REQUIREMENTS

A summary of the design requirements is shown in Figure 2-1.

### ELECTRICAL DESIGN REQUIREMENTS

The most distinctive and demanding requirements are those requiring:

- o operation between 0.3 and 6.0 au
- o operation in free space and in the earth's radiation environments with specified allowable degradation
- o power availability of 25 KW BOL and 21 KW EOL after 5 years in free space at 1 au
- o a weight limit of 385 Kg
- o minimum array cost

#### 0.3 to 6.0 au

The major parameters associated with the stated solar intensity range are varying spectral distribution and intensity as they relate to the temperature and electrical output of the arrays, and the UV or degrading constituents of the varying spectrum as it relates to the thermal optical material stability of the proposed array.

The 25 KW power output requirement is specified at 1 au at BOL. It is necessary to incorporate versatility into the module design so that series-parallel combinations can be readily changed for a planetary mission and acceptable array voltages will be produced which are compatible with the vehicle EPS voltage levels.

Previous studies indicate promise for array systems which operate at pre-selected off angles from the solar vector for increased intensity (solar flyby) phases. This approach for the Solar Probe and Mercury Orbiter missions has more merit than using high percent area grid coverage cells because of reduced power at sun distances (above 0.65 au) where the array will be normal to the sun.

Parameter	Requirements	Parameter	Requirements
Electrical Power, B.O.L	25 KW, in free space at 1 au.	Deployment/Retraction	Full deployment, full retraction to and from intermediate positions of deployment
Point of Power Measurement	Input to power regulation, conditioning and control circuits	No. of Intermediate Positions	One per mission, weights based on 30% deployed intermediate position
Operating Environment	Free space between 0.3 and 6 au	Range of Intermediate Positions	Design to allow range of 25% to 75% deployed intermediate positions
Operating Lifetime	Not less than 5 years	Deployed Array Dynamics Characteristics	Natural system vibration frequency greater than 0.04 Hz; in plane, normal to plane and torsional
Electrical Power, E.O.L.	21 KW, in free space at 1 au.	Array Voltage	In range of 200 vdc to 400 vdc over particular SEPS mission
Power Degradation Limits	Degrade from B.O.L. 25 KW to 21 KW from all effects after 5 years at 1 au, free space	Electrical and Dynamic Characteristics	Compatible with the SEPS defined in Attachment 1 to RFP
Radiation Degradation Limits	Not more than 25% for a total equivalent 1 Mev electron fluence of $10^{15}$ electrons/square cm	Docking Loads	+0.5g with blanket retracted
Weight, including deployment mechanisms and all mounting bracketry	385 Kg	Launch Environments	Withstand launch on Titan III/Centaur, Shuttle/Tug or Shuttle/Centaur
Stowage volume	0.456m (18 in) x 0.456m (18 in) x 3.56m (140 in)	Reentry Loads	Table 2-1, Rockwell International Report SD2-SA-0177-2-2

Figure 2-1 SEPS Solar Array Design Requirements

### Radiation Environment

The SEPS array may be used in a large number of trajectories ascending to geosynchronous orbit and in performing missions in the 0.3 to 6 au range. Design requirements have been set to assure that the array degradation is acceptable over this range of applications. These requirements state that the design power should not degrade more than 25 percent for a specified fluence of  $10^{15}$  E/cm<sup>2</sup>, 1 MeV equivalent electron fluence regardless of source and type radiation. The cost of the candidate designs required to provide this limitation in power degradation will be considered in the study to provide a minimum cost design.

A companion requirement limits the amount of power degradation from 25 KW BOL to 21 KW EOL as a result of all power degrading effects after 5 years at 1 au in free space. These degrading effects, in addition to the space radiation input to the solar cells, include the effects of UV and space radiation on thermal-optical properties of materials and coatings that result in higher array temperatures and decreased power.

## MECHANICAL DESIGN REQUIREMENTS

### Volume and Launch Constraints

The stowage volume length in Table 2-1 was increased to 4.06m (160 in.) during the study to use the Shuttle as the baseline launch system. Any new technology required for a design to fit a volume limited by a Centaur shroud (array module length 3.56m) was to be defined for development. The stowed array module must survive the launch and ascent environments of the Titan III/Centaur, Shuttle/Tug or Shuttle/Centaur.

### Deployment and Retraction Requirements

Once in orbit, the solar array is required to deploy and retract fully or partially along the spacecraft Y-axis. The array's position along the spacecraft longitudinal axis must be such that it does not interfere with the engine plume, payload protuberances and payload view angles. Full array deployment will provide sufficient electrical power to satisfy the 5 year mission requirements while full retraction is necessary to accommodate Space Shuttle return to earth for refurbishment. During the refurbishment activities the fully-retracted array must be capable of withstanding impact loads up to 0.5 g's and the re-entry/landing loads without cell damage.



Since high radiation environments will be experienced, partial extension and retraction is required during the mission and must be adjustable from 25% to 75% deployed area. To assure a minimum weight approach this adjustment should be made prior to launch. In the fully and partially deployed positions, the combined solar array strip tension and structural stiffness must be sufficient to exhibit natural frequency characteristics equal to or greater than 0.04 Hz to be compatible with the SEPS stabilization and control system.

#### Orbital Replacement

The design shall provide for solar array wing replacement in orbit.

#### Space Environment

During the 5 year space mission, the solar array structural components and mechanisms must be capable of surviving the applied loads from the sun tracking system, thermal environments from 0.3 au to 6 au and radiation environments from operating in space and in the Van Allen belts.

#### Cost

The cost of the mechanical system designs to achieve the required system power/weight factors will be considered with the cost of the associated array blanket designs to provide the minimum system cost.

### EMI AND MAGNETIC CONTROL REQUIREMENTS

#### Grounding

All electrical circuits installed on the solar cell array shall be completely isolated from structure ground. Electrical grounding of these circuits shall be made at a single point within the power control and conditioning subsystem. Electrical bonding of the array structure shall be accomplished in such a manner so as to create a unipotential RF ground plane.

Leakage

Surfaces between adjacent electrical terminals on the solar panel shall be sufficiently long and of a material which will minimize electrode to electrode breakdown such that a voltage of 500 vdc will not cause a current flow of more than 1 microampere under all storage, checkout, and operating modes specified herein.

Magnetic Fields

Solar cell circuits as well as power harnesses, panel arrangement, and other wiring shall incorporate current counter-flow considerations in their arrangement such that induced magnetic fields are minimized and do not exceed the allowed magnetic field limits. These are: the magnetic field at six (6) meters from the rotation axis of the solar cell panel shall be no greater than 0.05 nT due to residual magnetism when the array is stored and 0.5 nT during operation at maximum power in earth orbit.

## 2.3 MECHANICAL DESIGN

### 2.3.1 Design Baseline

The SEPS baseline solar array is shown in Figure 2-2. The major components are the extendible/retractable 105 ft mast, a solar cell blanket 30.99 m (1220 inches by 3.99 m (157 inches), a preloadable cover, an ascent support container and a tension/guide system.

The mast is a continuous longeron Astromast similar to the "Moon beam" designed and fabricated by Astro Research, Santa Barbara, California. It can be extended to or retracted from its full length of 32.01 m (105 ft) or any intermediate point. The mast canister is 39.62 cm (15.6 inches) in diameter, 120.7 cm (47.5 inches) long and weighs 19.09 Kg (42 lbs). The mast is required to provide a preload force to the container levers less than 533N (120 lbs) for a distance less than 38.1 cm (15 inches) at the beginning and end of its travel. In the fully extended length it is required to support a 93.3 N (21 lb) tip load offset 15.24 cm (6 inches) from a flat side of the triangular cross section. It extends and retracts the foldable blanket with solar cells (section 2.4.1) which is separated into 41 panels with additional leaders at the blanket ends. The outboard leader is necessary to eliminate cell shadowing at soltices for the geosynchronous mission and provide an attachment interface. The panels are attached through a piano hinge formed out of 3 mil fiberglass which is laminated into the substrate. An 0.081 cm (0.032 inch) graphite/epoxy hinge pin is used to integrate the hinge halves. The fiberglass is also bonded into the substrate along the panel sides to form a tear resistant edge and provide a base for harness attachment. The blanket is mechanically attached to the cover allowing easy separation for maintenance. Between panel 28 and 29, a dual fiberglass hinge is bonded into a graphite/epoxy tension distribution bar, as shown in Figure 2-3, which is fastened to the intermediate tension mechanism cable. The dual hinge allows movement of the mid-tension point with negligible impact on assembly techniques. The blanket inboard leader is silicone rubber bonded into a graphite/epoxy bar which distributes the fully extended tension forces from the tension mechanism into the first solar array panel.

The cover and container components, shown in Figure 2-3, work as a team during ascent to provide support for the folded blanket. The cover is a honeycomb assembly

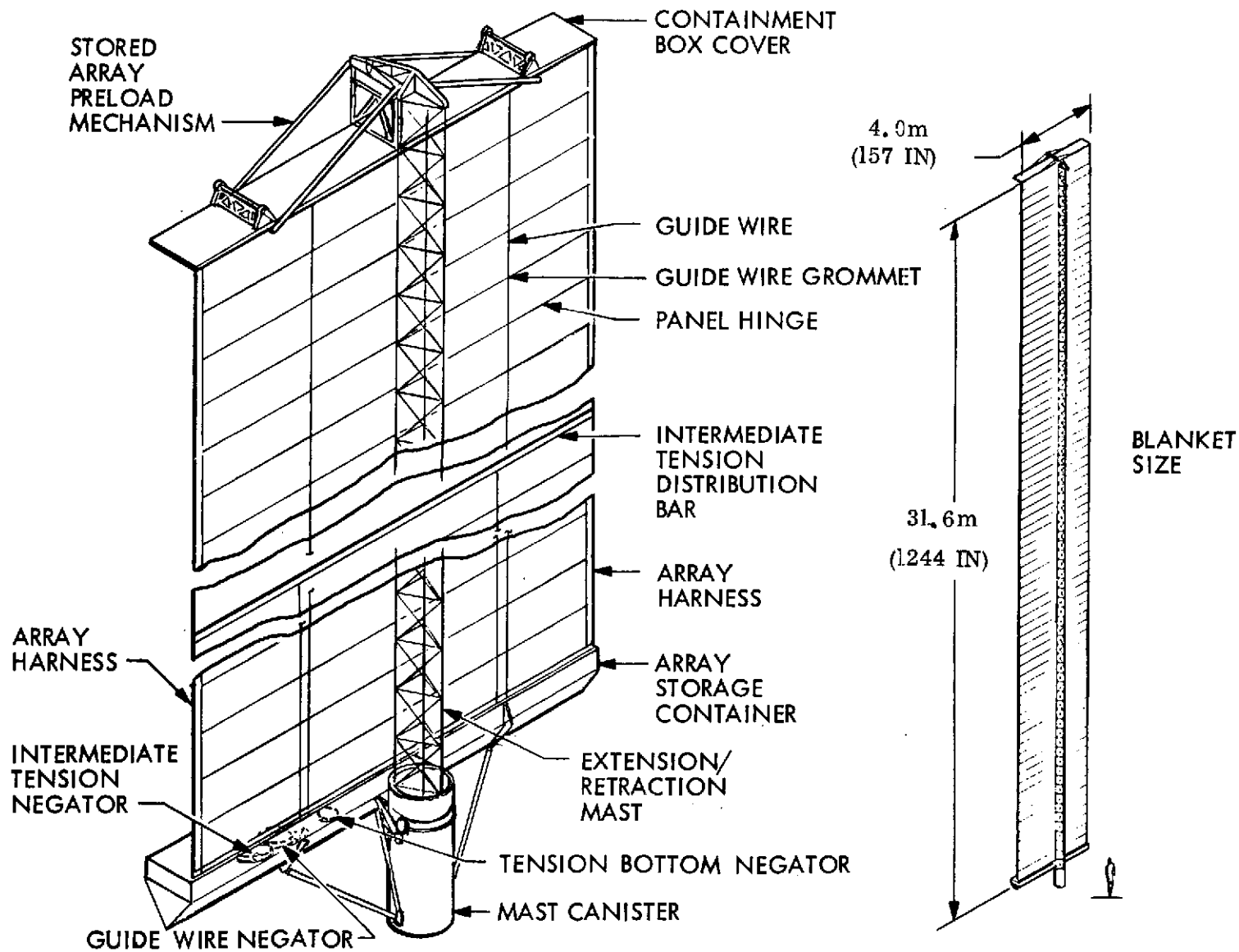


Figure 2-2 SEPS Baseline Configuration

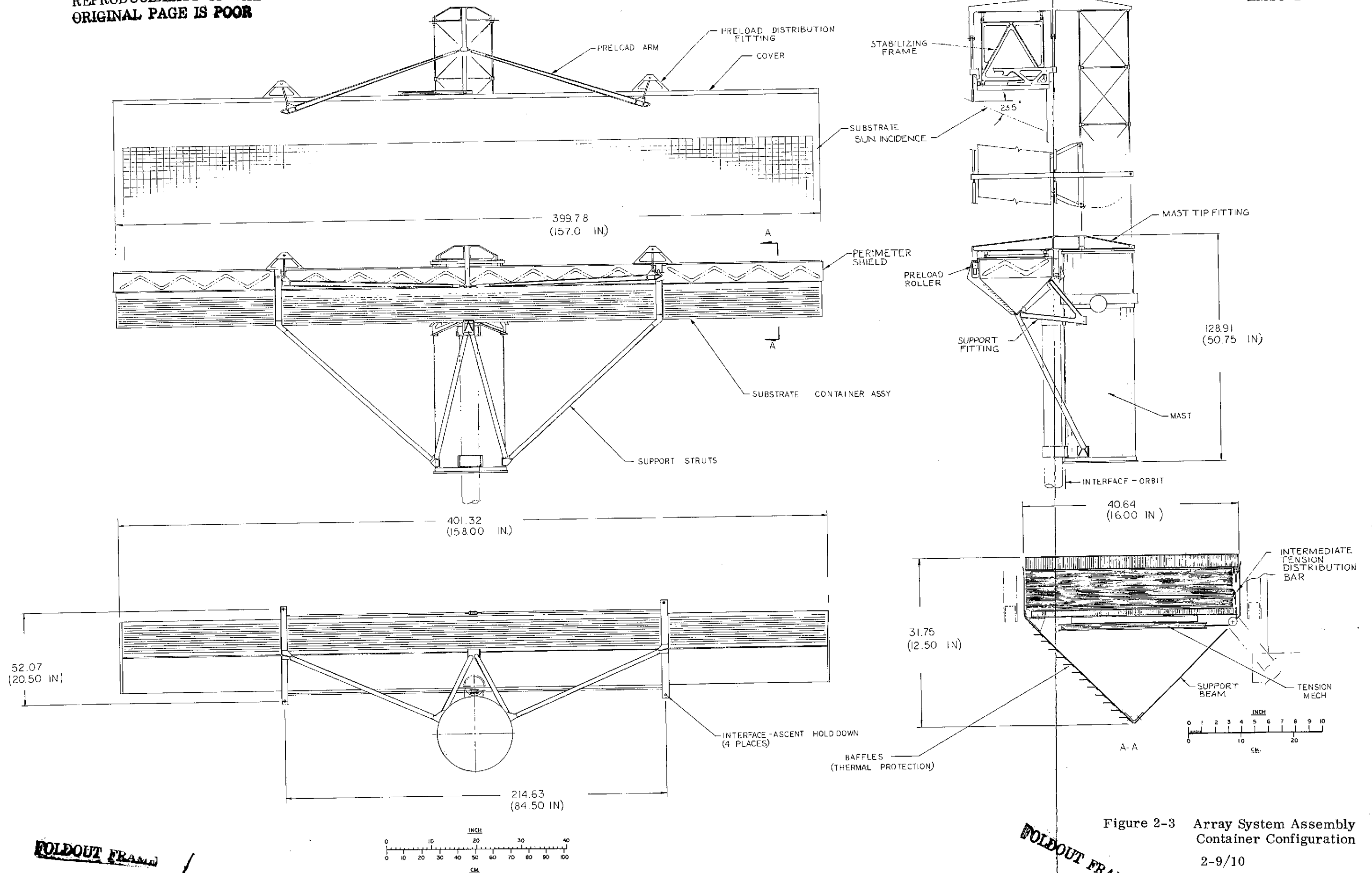


Figure 2-3 Array System Assembly  
Container Configuration  
2-9/10

FOLDED FRAME

with graphite skins and perforated aluminum core. It is contoured to maintain the compression variable on the folded blanket to within 10%. A polyurethane foam is bonded to the cover inner surface to compensate for minor surface depressions in the honeycomb. Two fittings are mounted to the top surface to distribute the preload forces from the four lever links into the cover. The levers are fabricated from graphite/epoxy tubes and aluminum end fittings. The levers are attached to the mast tip fitting through pivot points. A rectangular frame is attached to the cover and mast tip fitting to laterally stabilize the cover during extension and retraction. The frame lies flat against the array container cover when the array is stored. The initial 15 inches of mast extension unlocks the cover, unloads the stored array, and causes the frame to align itself with the mast. The end of the frame next to the cover has two rollers that are guided in slots parallel to the cover. The last 15 inches of mast retraction causes the bottom of the frame to be deflected by two cams installed on the cover. The frame then returns to its stored position. The container is the major support component for the folded substrate, mast, and tension mechanism and the interface structure to the spacecraft. The container shape shown in Figure 2-3 is triangular. A semi-circular shape is a more efficient torsion section but the triangular shape is more cost effective with a weight penalty of only 0.5 Kg (1.1 lbs). Four fittings are used to provide load paths for the preload and module/spacecraft interface. These fittings are located one-fourth the length of the container from each end. Rollers within the fitting at each lever preload point are used to minimize friction during preloading. A honeycomb panel with graphite skins and aluminum core along with two thin 0.051 cm (0.020 inch) skins form the main beam for module torsional and bending stiffness. The ends are closed to satisfy the structural needs. Thin skins, 0.051 cm (0.020 inch) thick, form a perimeter shield and surround the folded blanket on four sides to provide radiation and damage protection. The mast is supported for the ascent period by the container with two fittings and 4 tubular struts.

The tension and guide wire systems are similar in that they are negator powered. The mechanisms differ only in the travel and force required. There are 3 pairs of mechanisms, 2 guide, 2 intermediate tension and 2 full tension. Each one is powered by two negators. In addition a friction override can be provided in each mechanism to assure deployment will occur if a reel seizure should occur. The basic reel size is determined by the length of tension cable travel, negator length and tension required. The mechanisms

are mounted inside the triangular support beam of the container on the bottom of the honeycomb panel. The cable passes through the beam skin to a pulley which routes it to either the lower tension bar, intermediate tension bar, or to the cover depending on its function. The guide cable is routed through Delrin tabs attached to the panel hinge pins at each hinge line.

The array extension sequence is shown in Figure 2-4. It is initially released from the spacecraft and deployed to its extension position. From this position, extension is initiated by a signal to the mast. The blanket preload is released as the mast begins to extend. The guide wires and the blanket are pulled from the container as extension continues until the intermediate tensioning point is reached when the upper segment of panels are tensioned to 8.9N (2 lbs). Extension can be stopped at this point or continued until the blanket is fully extended when an additional 75.6N (17 lbs) will be applied to assure an overall 0.04 Hz minimum frequency. The retraction cycle is merely the extension in reverse, after which, the array will again be preloaded and prepared for Shuttle contact, stowage and return to earth for refurbishment.

The preliminary design weight summary in Table 2-1 reflects a conservative cell thickness and interconnect selection of 8 mil cell and 1 oz copper over 20% of substrate area. This is combined with the incorporation of lightweight materials and processes in structural design elements. The design meets the 385 Kg total weight requirement with low technology advancement risk which is possible because of the inherent low weight characteristics of the flatfold stowage system.

The selection of the continuous coilable longeron Astromast was based on a minimum weight design and on the fabrication experience that Astro Research Corp. has with this design. A major advantage of the continuous longeron design is also the minimization of the dead band around zero deflection as compared to an articulated lattice design. A major disadvantage is that the temperature limits on the mast element, 200°F, requires that non-nominal exposure of the mast element to the sun at near sun positions be of limited time, on the order of one minute or less. Development of a passive thermal control coating with good adhesion would extend this period but development of a high temperature resin system would provide more margin for non-nominal operation. The extension mast design is summarized in Table 2-2.

2-13

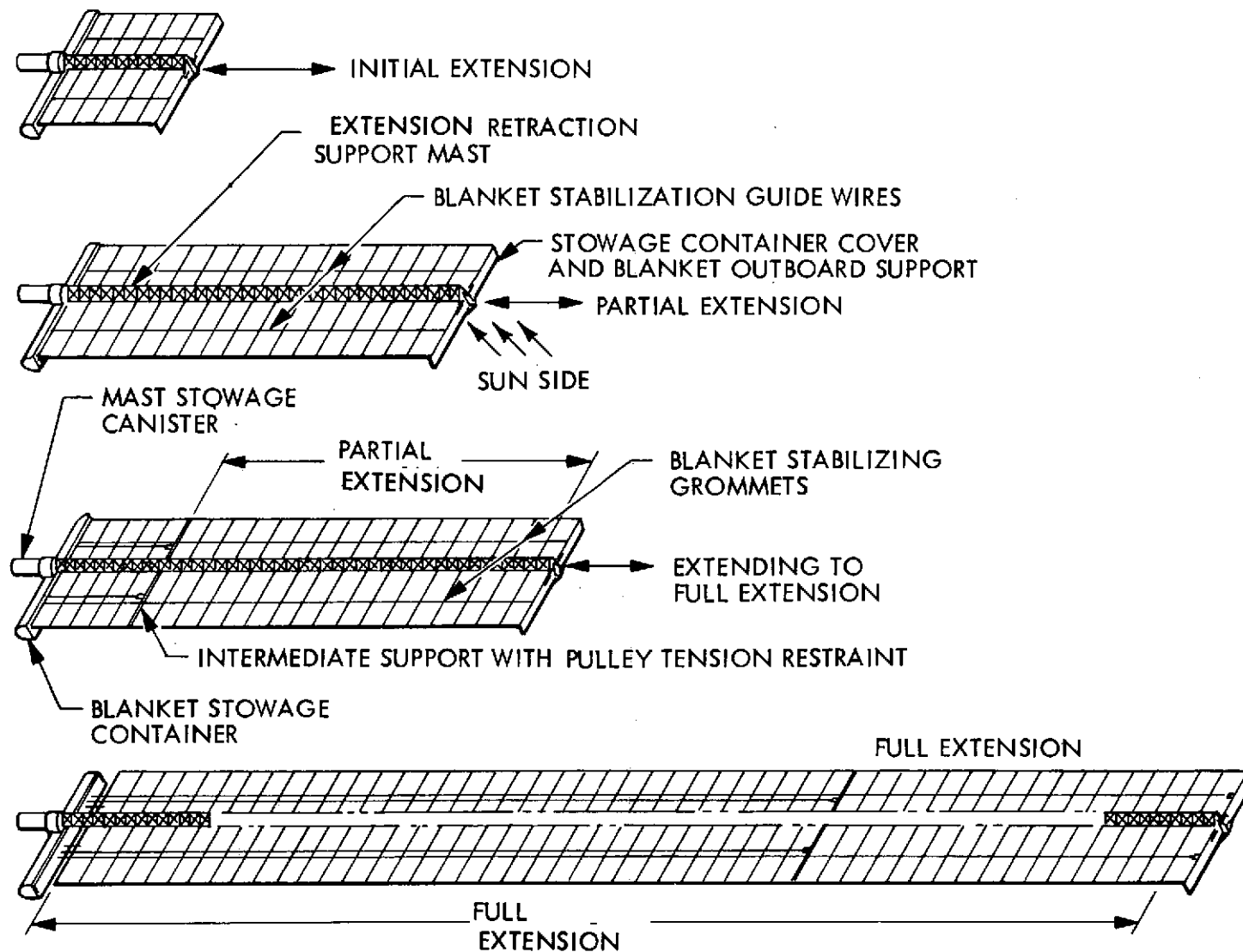


Figure 2-4 Array Extension Sequence

LMSC-D384250



Table 2-1 SEPS Solar Array Weight Summary

ITEM NO.	COMPONENT TREE	ESTIMATED WT (KG)	CONT. FACTOR	WEIGHT WITH CONTINGENCY FACTOR (KG)	NO. PER MODULE	WEIGHT/MODULE (KG)
	Required Module Weight				1	192.50
	Design Weight	181.96			1	192.49
1.0	Mast	32.04	.05	33.64	1	33.64
1.1	Cannister	16.31				
1.2	Mast Element	15.73				
2.0	Guide Wire Mechanism	1.412	.10	1.55	2	3.10
2.1	Wire (31.6 M) (2)	.34				
2.2	Negator (2)	.23				
2.3	Wire Reel (1)	.26				
2.4	Negator Hub (1)	.15				
2.5	Negator Reel (2)	.10				
2.6	Shaft (3)	.04				
2.7	Frame (1)	.28				
2.8	Panel/Wire Retainer (82)	.002				
3.0	Intermediate Tension Mechanism	1.29	.10	1.42	2	2.84
3.1	Wire (21.7M)	.29				
3.2	Negator (2)	.22				
3.3	Wire Reel (1)	.21				
3.4	Negator Hub (1)	.15				
3.5	Negator Reel (2)	.10				
3.6	Shaft (3)	.04				
3.7	Frame (1)	.28				
4.0	Full Tension Mechanism	.87	.10	0.96	2	1.92
4.1	Wire (1 M)	.01				
4.2	Negator (2)	.26				
4.3	Wire Reel (1)	.06				
4.4	Negator Hub (1)	.18				
4.5	Negator Reel (2)	.14				
4.6	Shaft (3)	.04				
4.7	Frame (1)	.18				

EXTENSION/RETRACTION ASSEMBLY

Table 2-1 CONT'd

ITEM NO.	COMPONENT TREE		ESTIMATED WT (KG)	CONT. FACTOR	WEIGHT WITH CONTINGENCY FACTOR (KG)	NO. PER MODULE	WEIGHT/MODULE (KG)
5.0	STORAGE ASSEMBLY	Tension Transfer	.08*	.0	.08	1	.08
5.1		Pulleys (6)					
5.2		Brackets (2)					
5.3		Pins (2)					
6.0		Mast Tip Fitting	.69	.0	.69	1	.69
6.1		Support (1)	.60*				
6.2		Brace (2)	.09*				
7.0		Cover Assembly	10.40	.10	11.44	1	11.44
7.1		Honeycomb Panel (1)	6.87				
7.1.1		Skin (2)	2.96				
7.1.2		Core (1)	2.60				
7.1.3		Edging	.61				
7.1.4		Inserts	.70				
7.2		Preload Distribution Fitting (2)	1.18				
7.3		Load Transfer Links (4)	.24				
7.4		Preload Level Arm (4)	1.12				
7.4.1		Tube (1)	.10				
7.4.2		Fittings (2)	.18				
7.5		Pivot Pins (4)	.04				
7.6		Control Frame	.95				
7.6.1		Frame (1)	.39				
7.6.2		Guide Rail (2)	.34				
7.6.3		Attach Fitting (2)	.06				
7.6.4		Roller (2)	.04				
7.6.5		Pivot Pins (4)	.04				
7.6.6		Cams (2)	.04				
7.6.7		Spring (2)	.04				
7.7	EXTENSION/RETRACTION ASSEMBLY	Pad (2)	.35				
7.8		Adhesive	.72				
7.8.1		Honeycomb	.48				
7.8.2		Pad	.24				

Table 2-1 CONT'd

ITEM NO.	COMPONENT TREE	ESTIMATED WT (KG)	CONT. FACTOR	WEIGHT WITH CONTINGENCY FACTOR (KG)	NO. PER MODULE	WEIGHT/MODULE (KG)
8.0	Container					
8.1	Honeycomb Panel (1)	4.20	.10	4.62	1	4.62
8.2	Skin (2)	2.67				
8.3	Core (1)	.80				
8.4	Edging	.28				
	Inserts	.45				
9.0	Triangular Beam	8.35	.10	9.19	1	9.19
9.1	Skin (2)	2.43				
9.2	Bulkhead (2)	.15				
9.3	Longeron (3)	3.50				
9.4	Support Fitting (4)	.38				
9.4.1	Fitting (4)	.27				
9.4.2	Roller (4)	.05				
9.4.3	Pin (4)	.06				
9.5	Baffles (12)	.05				
9.6	Perimeter Shield (1)	.77				
9.7	Pad (1)	.35				
9.8	Adhesive	.72				
9.8.1	Honeycomb	.48				
9.8.2	Pad	.24				
10.0	Support Struts	1.55	.0	1.55	1	1.55
10.1	Long (2)	.82*				
10.2	Medium (2)	.59*				
10.3	Short (2)	.14*				

STORAGE ASSEMBLY

Table 2-1 CONT'd

ITEM NO.	COMPONENT TREE	ESTIMATED WT (KG)	CONT. FACTOR	WEIGHT WITH CONTINGENCY FACTOR (KG)	NO. PER MODULE	WEIGHT/MODULE (KG)
11.0	BLANKET ASSEMBLY	Solar Cell Blanket	111.014	.05	116.56	116.56
11.1		Upper Leader	.14			
11.2		Upper Attach Bar	.16			
11.3		Full Tension Dist. Bar	.88			
11.4		Intermediate Tension Dist. Bar	.03			
11.5		Lower Leader	.17			
11.6		Panel (41)	109.634			
11.6.1		Substrate W/Pad	.467			
11.6.2		Solar Cells (3060)	1.171*			
11.6.3		Cover Adhesive (3060)	.130*			
11.6.4		Coverslide (3060)	.845			
11.6.5		Hinge (2)	.058			
11.6.6		Hinge Pin (1)	.003			
		Total	2.674			
12.0		Interconnect Harness	5.59	.05	5.87	1
		FCC Power	5.22			
		FCC (Instrumentation)	.25			
		Receptacles (4)	.12			
13.0		Misc Nuts & Bolts	.90	.10	0.99	1
						0.99

\* Actual Weights of Fabricated Hardware

TABLE 2-2  
EXTENSION MAST DESIGN

MAST ELEMENT DATA

Mast Diameter: 37.1 cm (14.6 in.) (nominal)

Mast Weight: 15.6 Kg (34.3 lb) (for 105-ft extended length plus 4 ft remaining in canister)

Longerons:

Cross section - 0.50 x 0.50 cm (0.197 x 0.197 in.) (square)

Material - S-glass/epoxy resin composite using 20-end glass roving/  
epoxy resin conforming to WS 1028 B

Battens:

Cross section - 0.50 x 0.37 cm (0.197 x 0.145 in.) (rectangular)

Material - S-glass/epoxy resin composite using 20-end glass  
roving/epoxy resin conforming to WS 1028 B

Diagonals: 3/64 in. diameter, 3 x 7 strand, stainless-steel cable

Bay Length: 20.4 cm (8.03 in.)

Mechanical Properties:

Bending stiffness - 66.1 KN-m<sup>2</sup> (23.1 x 10<sup>6</sup> lb-in.<sup>2</sup>) (mast element)

Ultimate bending strength - 3.58 m-Kg(3100 in.-lb)(for two longerons equally loaded)

Shearing stiffness - 102.2 KN (23,000 lb)

Shearing strength - 182 N (41 lb)

Torsional stiffness - 1.75 KN-m<sup>2</sup> (0.612 x 10<sup>6</sup> lb-in.<sup>2</sup>)

Torsional strength - 2.99 m-Kg (259 in.-lb)

Table 2-2 (cont'd)

Canister Data

Canister Height: 1.2 m (47.5 in.)

Canister Diameter: 0.40 m (15.6 in.) (nominal and excluding motors)

Canister Weight: 19.1 Kg (42.0 lb)

Extension Motors: Two Model T2950 dc torque motors manufactured by Inland Motors, Division of Kollmorgen Corporation

Dimensions - 9.5 cm o.d. x 3.4 cm wide (3.73 in. o.d. x 1.34 in. wide)

Stall torque - 0.166 m-Kg (1.2 ft-lb)

Power at stall - 79 W

Torque sensitivity - 0.064 m-Kg/A (0.46 ft-lb/A)

Dc resistance - 11.6 ohm

Operating temperature - 105°C max., TBD min.

Canister Materials: Principally aluminum (2024-T4 and 6061-T6)

Dissimilar materials to touch one another -

- a) Stainless-steel Kaydon bearings, 15 in. (nominal) o.d. mounted in 2024-T4 aluminum deployment nut. Thrust load per bearing is one-half maximum tension or compression in mast. Radial load is minimal.
- b) Delrin pinion gears which drive 2024-T4 aluminum ring gear on deployment nut. Tooth pressure is 19 lb at stall torque, 5.25 lb at 120-lb mast force.
- c) Steel bearings in aluminum mast-base turntable. Thrust load is no greater than 5 lb; minimal radial load.

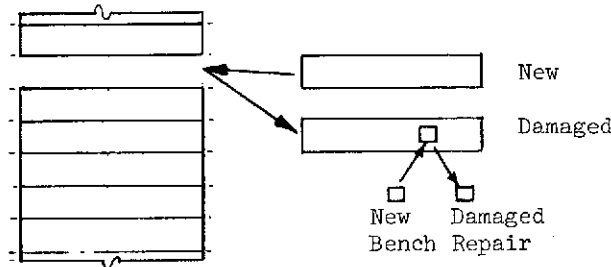
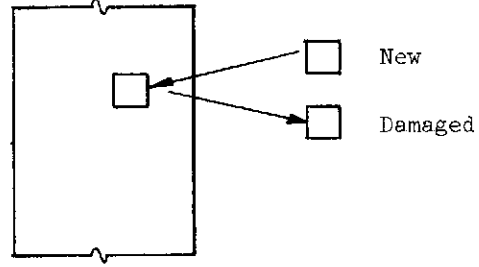
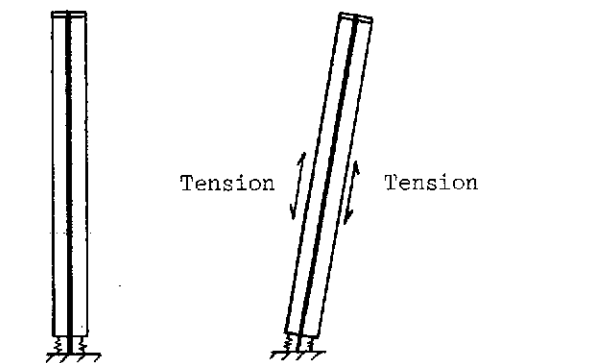
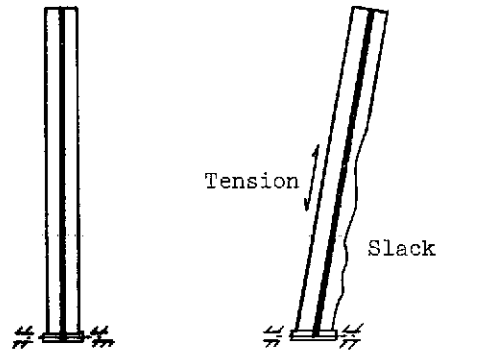
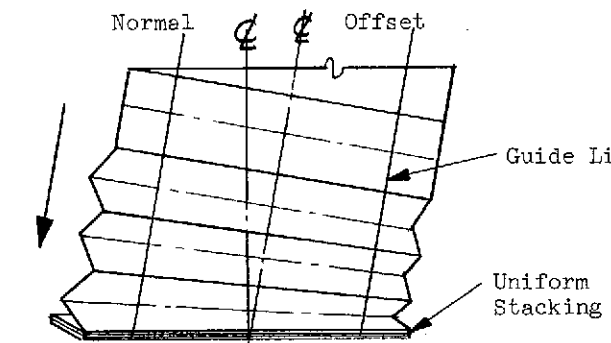
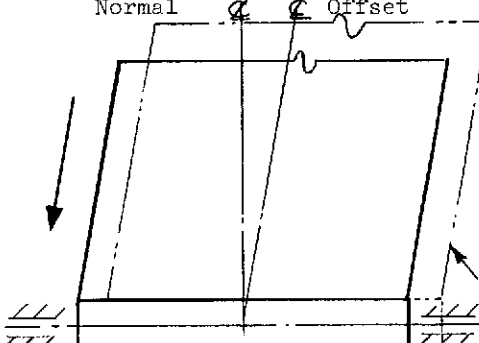
Lubrication System: A good possibility for all bearing surfaces is Ball Brothers' "Vac Kote". Note that aluminum boom rollers rotate on aluminum pivots and bear on deployment nut. These interfaces can be permanently lubricated with Vac Kote or equivalent (e.g., Micro Seal).

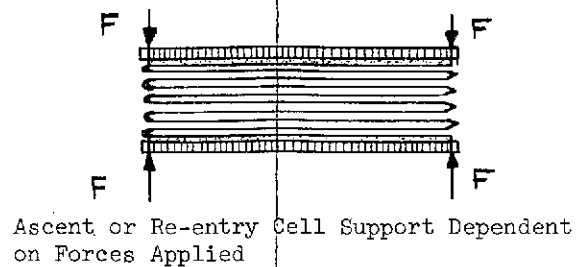
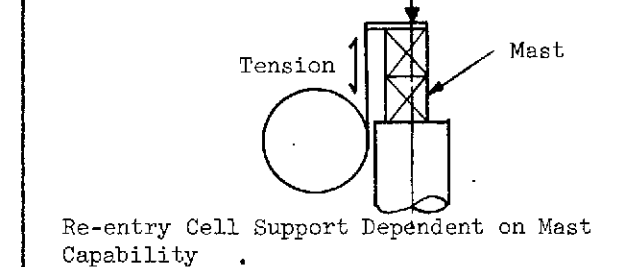
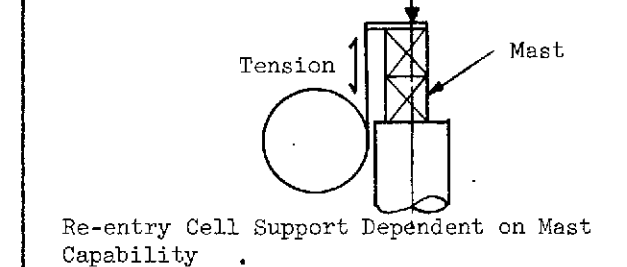
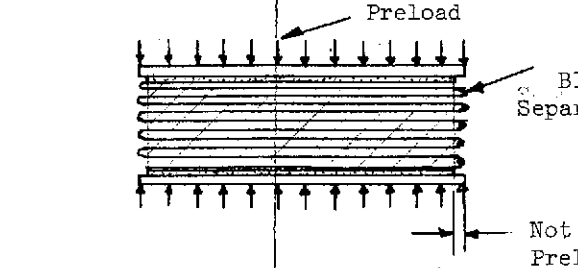
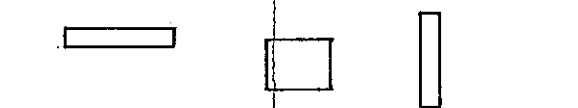


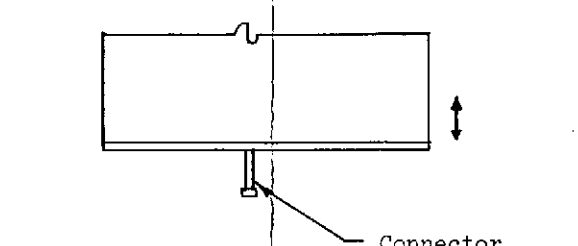
## 2.3.2 Mechanical Design Studies

### 2.3.2.1 Selection of Panel Stowage Method

Selection of the single mast per wing design was based on studies accomplished by LMSC during the Large Space Station Solar Array (LSSSA) Program and the Rockwell International (RI) SEPS Solar Array conceptual design study. The LSSSA studies showed that a central mast on each wing was preferred on the basis of minimum weight and simplicity since only a single mechanism for extension/retraction was required and no connecting or phasing components between masts are necessary. The studies also showed that the flatfold method of packaging the solar cells was preferable from the standpoint of:

- o Modularity. As shown in Figure 2-5, the flatfold packaging method for the blanket provides 40 easily separated hinge joints, thus simplifying and reducing the costs of manufacturing, ground testing and refurbishment of damaged modules.
- o Alignment. The flatfold method has demonstrated satisfactory deployment and retraction with in-plane misalignments up to  $10^0$  (20 ft. tip displacement with 115 ft. mast) which is a definite consideration with arrays in the 100 foot long class. This characteristic of the flatfold allows small perturbations, such as attitude control operation, to occur during the retraction cycle without impairing the panel stowage. It also allows less stringent fabrication tolerances in mast tip to stowage container and the panel assemblies which make up the solar cell blanket. In addition, the method of tensioning provides a mechanism which eliminates cross wrinkling of the blanket with lateral in-plane deflections of the mast tip.
- o Preload. The preload necessary to prevent cell damage to the cells during ascent is adjustable after complete stowage at any time up to launch thus allowing for low pressure ground storage and final adjustment without deployment. The same or lesser preload can be applied to the cells for reentry/landing without compromising the mast capabilities. The preload is uniform throughout the folded panels and not limited by the cell bending properties.

BASELINE		ALTERNATE		
MODULARITY	 <p>Hinge Separation</p>	 <p>Cut and Replace</p>		
ALIGNMENT	 <p>Tension</p>	 <p>Tension</p>		
	 <p>Normal</p> <p>Offset</p> <p>Guide Line</p> <p>Uniform Stacking</p>	 <p>Normal</p> <p>Offset</p> <p>Runoff Due to Misalignment</p>		

BASELINE		ALTERNATE	
PRELOAD	 <p>Ascent or Re-entry Cell Support Dependent on Forces Applied</p>	 <p>Re-entry Cell Support Dependent on Mast Capability</p>	 <p>Re-entry Cell Support Dependent on Mast Capability</p>
	 <p>Preload</p> <p>Blanket Separation Joint</p> <p>Not Preloaded</p>		
STOWED VOLUME	 <p>Dimension Limited by Electrical Module size and Shape</p>	 <p>Minimum Diameter Dependent on Cell Bending Properties</p>	 <p>Minimum Diameter Dependent on Cell Bending Properties</p>
	 <p>Connector</p>		

FOLDOUT FRAME

Figure 2-5 Panel Stowage Method Study Results

FOLDOUT FRAME

2



The hinge joints are external to the folded and preloaded cell area thus assuring that no high load concentration points exist to cause cell breakage during the ascent phases.

- o Stowed Volume. The shape of the stowed volume is reasonably flexible and can be varied within the electrical module restraints to accommodate the spacecraft configuration design. In addition, the flatfold is not restricted to ascent structural support at its ends or require use of two blankets with a middle support.
- o Power Transfer. No power transfer device is required, other than the interconnect harness itself, to carry power to the tracking power transfer unit.

#### 2.3.2.2 Tensioning Methods

Four major tensioning arrangements investigated for the SEPS flatfold array are shown in Figure 2-6. Each system combines a means for guiding the panels during the extension/retraction cycles with minimum tension capability of 8.9 N (2 lbs.) at an intermediate deployment point and 75.6 N (17 lbs) at the fully extended position.

Arrangement No. 1 includes two guide lines shown which are attached to the cover and pass through small plastic grommets at each strip panel hinge-line. On the bottom of the storage container honeycomb panel in two positions are five pulleys, three of which are attached to the panel and two to the blanket leaders of high stiffness material such as graphite or beryllium to distribute the tension loads. The line is passed through these pulleys to the tension mechanisms in such a manner that when the blanket is partially extended the leader pulls a traveling pulley up, thus tensioning the array blanket to twice the guide line tension. Further extension maintains tension on the outer section and no tension on the extending section.

This continues until the blanket is fully extended at which time the final pulley is pulled up by the bottom leader tensioning this section to twice the guideline tension. The two tension mechanisms are powered by negator springs which operate through a mechanical disadvantage to the guide line reel. The guide line reels, negator take up drum, negator torque and length (Space Station 36.5 ft for an 84 ft length of array) are proportional to accommodate the ultimate strip tension and length.

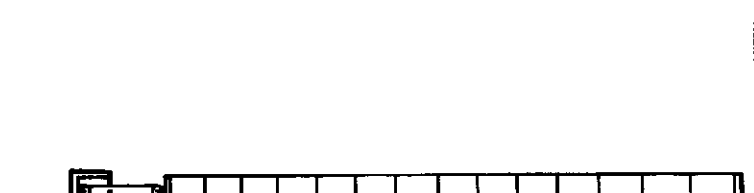
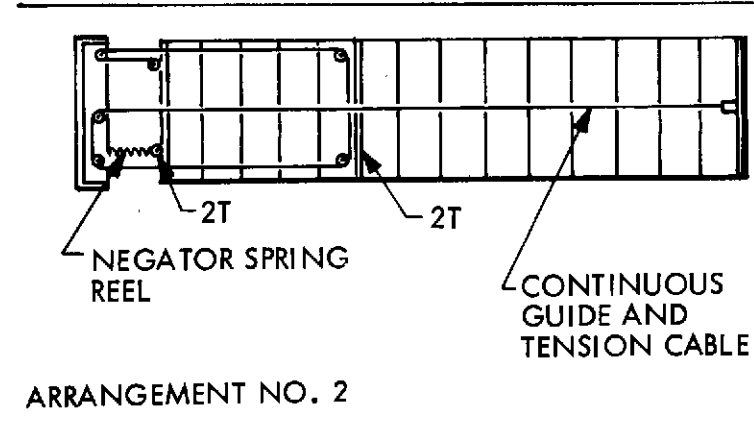
 <p>NEGATOR SPRING REELS — 2 PLACES</p> <p>CONTINUOUS GUIDE AND TENSION CABLE</p> <p>ARRANGEMENT NO. 1</p>	MAST TIP LOAD (LBS)	MAJOR PARTS COUNT	ESTIMATED WEIGHT $\Delta$ FROM 1 (LBS)	COMMENTS
	85	14	0	<ul style="list-style-type: none"> <li>• PULLEY FRICTION VARIABLES COULD CAUSE UP TO 1% TENSION UNBALANCE</li> <li>• NEGATOR TOLERANCE COULD CAUSE TENSION UNBALANCE UP TO 10%</li> <li>• SINGLE FAILURE COULD CAUSE LOSS OF 1/2 GUIDE WIRE, MID-TENSION AND FULL TENSION</li> <li>• ON ARRAY, PULLEYS COMPLICATE STOWAGE</li> </ul>
 <p>NEGATOR SPRING REEL</p> <p>2T</p> <p>2T</p> <p>CONTINUOUS GUIDE AND TENSION CABLE</p> <p>ARRANGEMENT NO. 2</p>	85	9	-4	<ul style="list-style-type: none"> <li>• PULLEY FRICTION VARIABLE COULD CAUSE UP TO 1% TENSION UNBALANCE</li> <li>• SINGLE GUIDE WIRE DOES NOT PROVIDE TORSIONAL STABILITY</li> <li>• SINGLE FAILURE WOULD RESULT IN LOSS OF COMPLETE GUIDE AND TENSION SYSTEM</li> <li>• ON ARRAY, PULLEYS COMPLICATE STOWAGE</li> </ul>

Figure 2-6 Substrate Tensioning Methods

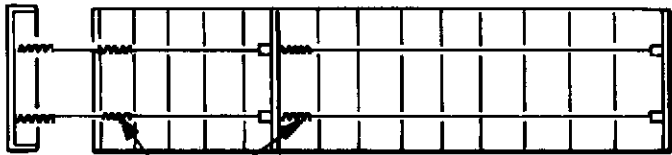
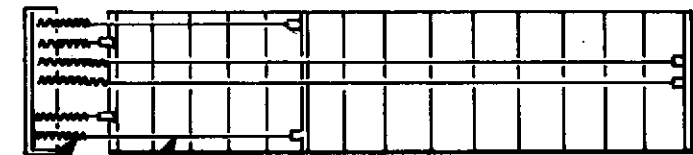
 <p>NEGATOR SPRING REEL</p> <p>ARRANGEMENT NO. 3</p>	MAST TIP LOAD (LBS)	MAJOR PARTS COUNT	ESTIMATED WEIGHT $\Delta$ FROM 1 (LBS)	COMMENTS
	21	12	-13	<ul style="list-style-type: none"> <li>• DIFFICULT TO BALANCE NEGATORS TO PROVIDE PROPER SUBSTRATE TENSIONS</li> <li>• DIFFICULT TO STOW NEGATORS ON THE ARRAY</li> <li>• NEGATOR TOLERANCES COULD CAUSE TENSION UNBALANCE UP TO 20%</li> <li>• SINGLE FAILURE WOULD RESULT IN LOSS OF 1/2 GUIDE, MID OR FULL TENSION SYSTEM</li> </ul>
<p>SELECTED ARRANGEMENT</p>  <p>BASE MOUNTED NEGATOR SPRING REEL</p> <p>ARRANGEMENT NO. 4</p>	21	12	-12	<ul style="list-style-type: none"> <li>• NEGATOR TOLERANCES COULD CAUSE TENSION UNBALANCE UP TO 20%</li> <li>• SINGLE FAILURE WOULD RESULT IN LOSS OF 1/2 GUIDE, MID OR FULL TENSION SYSTEM</li> </ul>

Figure 2-6 Substrate Tensioning Methods (Cont'd)

This system results in a 378 N (85lb) tip load on the mast requiring an EI of nearly twice that for arrangements 3 and 4. The on-array pulleys must be extremely compact with a minimum diameter using journal bearings to accommodate the minimum profile stowage system. The bearing friction of the on array pulleys could result in a mid-point tension variation up to 1% (0.2 lbs) with a journal bearing using solid film as the lubricant. Pulley and wire guidance is necessary to assure orderly retraction and will complicate the stowage in the container.

The force tolerance between negators could be up to 10% resulting in up to 20% tension variable between the two tension cables. This variable can be reduced to 10% with special springs and handling at a higher component cost.

A failure in one of the two tensioning mechanisms could result in loss of 1/2 guide, intermediate deployment and full tension phases. A friction override in the negator mechanism to eliminate a single point failure would increase the mast tip load by a factor of 5 times the override force and affect each tension phase with an off balance.

Arrangement No. 2 accomplishes the guide and both tensioning functions with 1 cable and negator motor. The single cable is attached to the cover and routed through grommets on the panels to the container where it passes over two pulleys then to the midpoint tension bar. Two low profile pulleys are integrated into the graphite composite bar where they transfer the cable back to the container. After passing over a single container pulley the cable is routed to the inboard tension pulleys and finally to the negator spring motor. This system would require up to 87 m (285ft) of cable routed to a single tension mechanism which would require up to a 0.8 m (32 inch) diameter reel to satisfy a direct drive with a standard maximum length spring. The reel diameter is larger than space is available, therefore, gearing must be used.

The mast tip load is 378 N (85 lbs) requiring the larger mast size and weight, but the system weight is estimated at 4 lbs less than Arrangement No. 1. The same panel tension unbalance as Arrangement No. 1 is experienced in the pulley system, but since only one tension mechanism is used there is no unbalance due to spring tolerances. A failure in the tensioning system could result in loss of tension throughout the array for all tension phases. A friction override on the tension reel would increase the mast tip load by a factor of 5 times the override force but it would be balanced.

One other shortcoming of this system is the single guide wire. During the extension phase from stowed position to partial deployment point tension and back to stowed during retraction, the panels will have no torsional stability other than their own inherent stiffness. This condition could lead to abnormal panel movement during extension and improper placement in the container during retraction.

Arrangement No. 3 requires a mast tip load capability of only 93 N (21 lbs) and is 5.9 Kg (13 lbs) lighter than No. 1 (3 lbs mechanism and 10 lbs in mast). It has dual guide, intermediate tension and full tension cables. Individual negators tension each cable to the appropriate level. The negator tension mechanisms located on the intermediate and full tension distribution bars must be extremely compact. Careful attention must be given to opposing force alignments between substrate and tensioning elements to minimize panel distortions during both stowage and tensioning phases. Unless the substrate tension, guide cable and mid tension forces are aligned, torques will result on the tension bar forcing it to rotate. This in turn will result in a bar of larger cross section to maintain its bending properties when rotated into a stable position. Higher weights and stowage difficulties will be experienced. Also it will be difficult to provide the proper balance between guide wire and mid tension forces and between mid tension and full tension forces.

The same 20% unbalance due to spring tolerance will be experienced as in Arrangement No. 1. A single failure in the system would result in loss of 1/2 guide, mid, or full tension of the panels. A reel friction override would result in an unbalance of the mid tension if the failure was in the guide or mid tension mechanism and in the full half if the failure was in the mid or full tension mechanisms.

Arrangement No. 4 is the selected system and is described in Section 2.3.1. It requires only a 93 N (21 lb) mast tip load capability and is 5.5 Kg (12 lbs) lighter than No. 1. It has a potential 20% unbalance due to negator tolerances and the same failure condition as No. 3. This arrangement was selected because of its low mast tip load, weight savings, failure level, and its ease of stowage.

### 2.3.2.3 On Array Padding

The ascent and re-entry phases of the SEPS mission require a form of cell protection from the environments. This has generally been accomplished with some type of separate padding system which is withdrawn or rolled up independent from the array blanket. The demands for a simple, lightweight, retractable solar array which could meet the SEPS requirements laid the groundwork for a flatfold on-array padding study. The range went from no padding, with the exception on the storage container cover and base, to padding throughout the array blanket. They were required to conservatively withstand the preloads necessary to survive the accelerations of the Titan (8 g's) along the worst case axis which is parallel to the folded panels. In addition to extension/retraction, and vibration, the padding materials are required to meet the long term orbit environments.

Several concepts were developed and separated into three categories: 1) no padding, 2) over cells and 3) between cells as shown in Figure 2-7. The no padding concept depends on cushioning on the ascent support cover and base to minimize the effects of shock loading, provide a high slip resistant surface, and to distribute the preload variables caused by local discontinuities in the storage box honeycomb structures. The ascent interpanel shear forces on the stowed panels are carried by friction between substrate-to-substrate, cell-to-cell or cell to cover/base padding surfaces. This means, particularly on the outermost panels, that these shear forces are transmitted through the cell-to-interconnect weld joints, but the joint capability is approximately 34 times the maximum expected Titan produced shear loads, and in addition, is helped by the slip resistance between the cell back and substrate.

Titan longitudinal load factor = 8 g's

Substrate weight <  $1.23 \text{ kg/m}^2$  ( $0.25 \text{ lbs/ft}^2$ )

Layers of substrate cells = no. of panels x 2 = 82

Load at pad-cell interface/area =  $0.25 \text{ lbs/ft}^2 \times 8 \text{ g's} \times \frac{82}{2} = 3942 \text{ N/m}^2$  ( $82 \text{ lbs/ft}^2$ )

Cell interconnect shear strength =  $106 \frac{\text{cells}}{\text{ft}^2} \times 8 \frac{\text{joints}}{\text{cell}} \times 4.1 \frac{\text{lbs}}{\text{joint}} = 167,000 \text{ N/m}^2$  ( $3477 \text{ lbs/ft}^2$ )

The over cell concepts were aimed at providing a padding surface between stowed cell-to-cell surfaces with minimum cell degradation. Three approaches were taken, a button

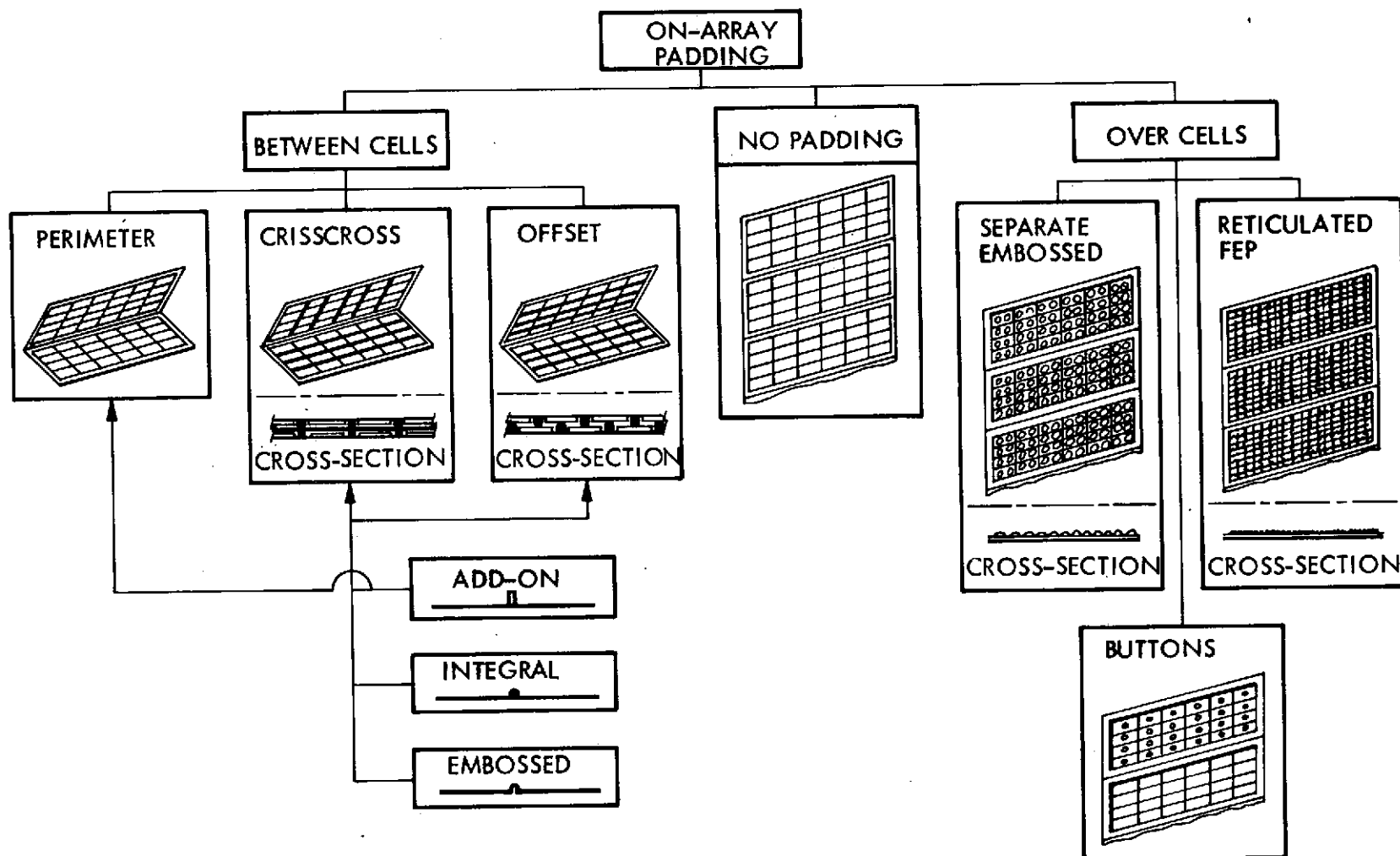


Figure 2-7 On-Array Padding Concepts

bonded to the cell coverslide surface and a pad of either separate embossed or reticulated FEP attached to the substrate and not the cell. The buttons would be located on every other panel.

The material selected for the button concept was Sylgard 182 which was cast into a sheet 0.020 in. thick with a layer of 2 mils thick FEP on the outer surface. The FEP layer would assure that no adhesion occurs in solar array storage which could damage the cells during the initial phases of extension and would serve as a separating agent which would produce a transparent pad. The button was then bonded to the cell coverslide with the same Sylgard 182 adhesive. The button was configured as a disc 0.250 in. in diameter by 0.020 in. thick and as an annulus 0.380 in. O.D., 0.25 in. I.D., by 0.020 in. thick. The annulus would provide a more stable base for preload transfer through the stowed cells but also may produce undesirable moments in the cells. Electrical performance tests were run to determine the reduction in characteristics. These tests indicated a power reduction of 0.142% for the disc and 0.65% for the annulus. Referring to Figure 2-8 this results in an increase in mast lengths of 0.15 ft and 0.67 ft and in cell number of 178 and 815, and in weight of 0.37 lbs and 1.69 lbs respectively.

An opaque button was run to determine a worst case effect and resulted in a 4.2% power reduction with 5018 additional cells and 16.8 lbs plus higher mast weight. The separate embossed FEP shown in Figure 2-9 along with a control specimen. It would be attached only at the hinge lines on every other panel. Two 0.5 inch diameter holes were cut into the 2 mil FEP above each cell to lower the cell performance degradation. The holes decreased the degradation from 16% to 10%. This in turn decreased the additional mast length from 17 ft to 10 ft, additional cells required from 20,070 to 12,418, and weight from 64.5 lbs plus mast to 38 lbs, plus mast. Due to its plastic memory the raised embossments in the FEP cover will completely disappear at the materials recovery temperature of 135-177°C (275-350°F). The FEP must also remain quite loose to prevent thermal distortion of the panel.

The reticulated FEP is not available in industry and therefore no further evaluation was conducted. With this concept it would be difficult to prevent cell edges and corners from being caught by the fibers of the reticulated FEP during solar array extension and, therefore, a potential damage mode would be present.



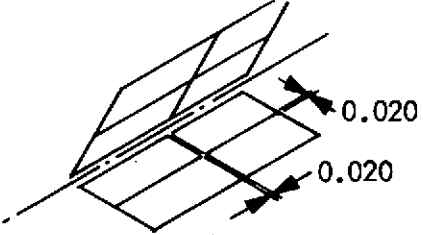
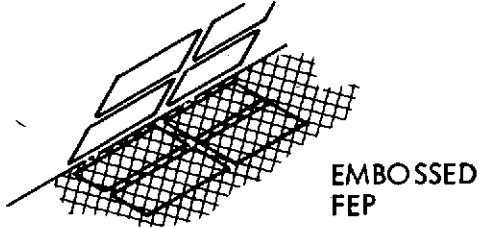
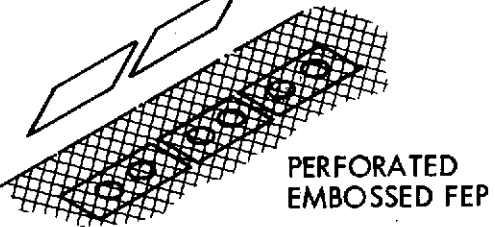
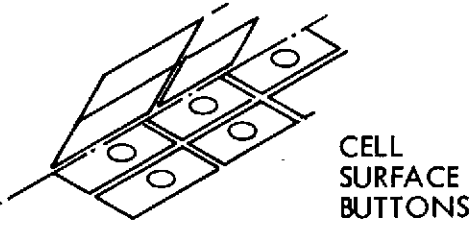
PAD TYPE		$\Delta L$ (FT)	$\Delta NO.$ CELL	$\Delta W$ (LB)	SLIP RESISTANT COEFFICIENT	SURVIV- ABILITY	PRODUC- IBILITY
NO PAD		0	0	0	0.518	TBD	TBD
		17	20070	64.5 +MAST $\Delta$	—	—	—
		10.2	12418	38 $\Delta$	—	—	—
		4.2	5018	16.8 + MAST $\Delta$	0.660	TBD	TBD
OVER CELLS		0.15	178	0.37			
		0.67	815	1.69			

Figure 2-8 Pad Concept Effects on Solar Array

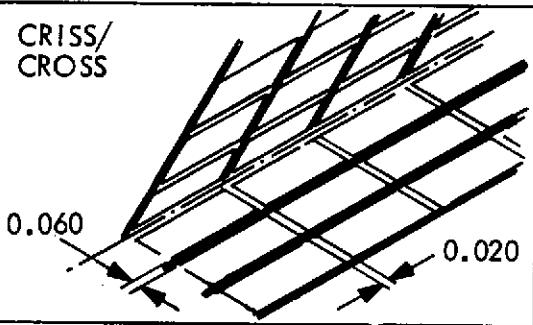
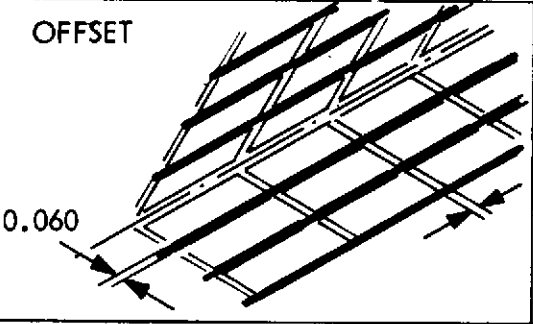
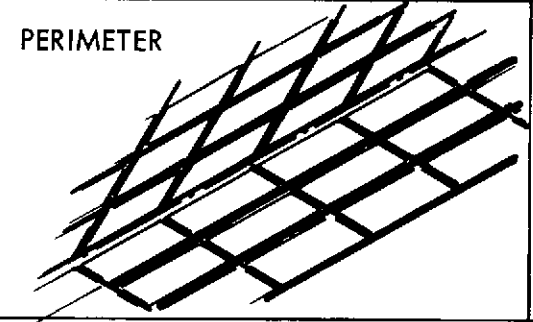
PAD TYPE		$\Delta L$ (FT)	$\Delta NO.$ CELL	$\Delta W$ (LB)	SLIP RESISTANT COEFFICIENT	SURVIVABILITY	PRODUCIBILITY
BETWEEN CELLS	CRISS/CROSS 	5.4	0	RTV 10.5+ MAST $\Delta$ TFE 17.3+ MAST $\Delta$	0.904	TBD	TBD
	OFFSET 	6.9	0	RTV 10.9 + MAST $\Delta$	0.538	TBD	TBD
	PERIMETER 	8.0	0	RTV 16.44 + MAST $\Delta$	0.474	TBD	TBD

Figure 2-8 Pad Concept Effects on Solar Array (Cont'd)

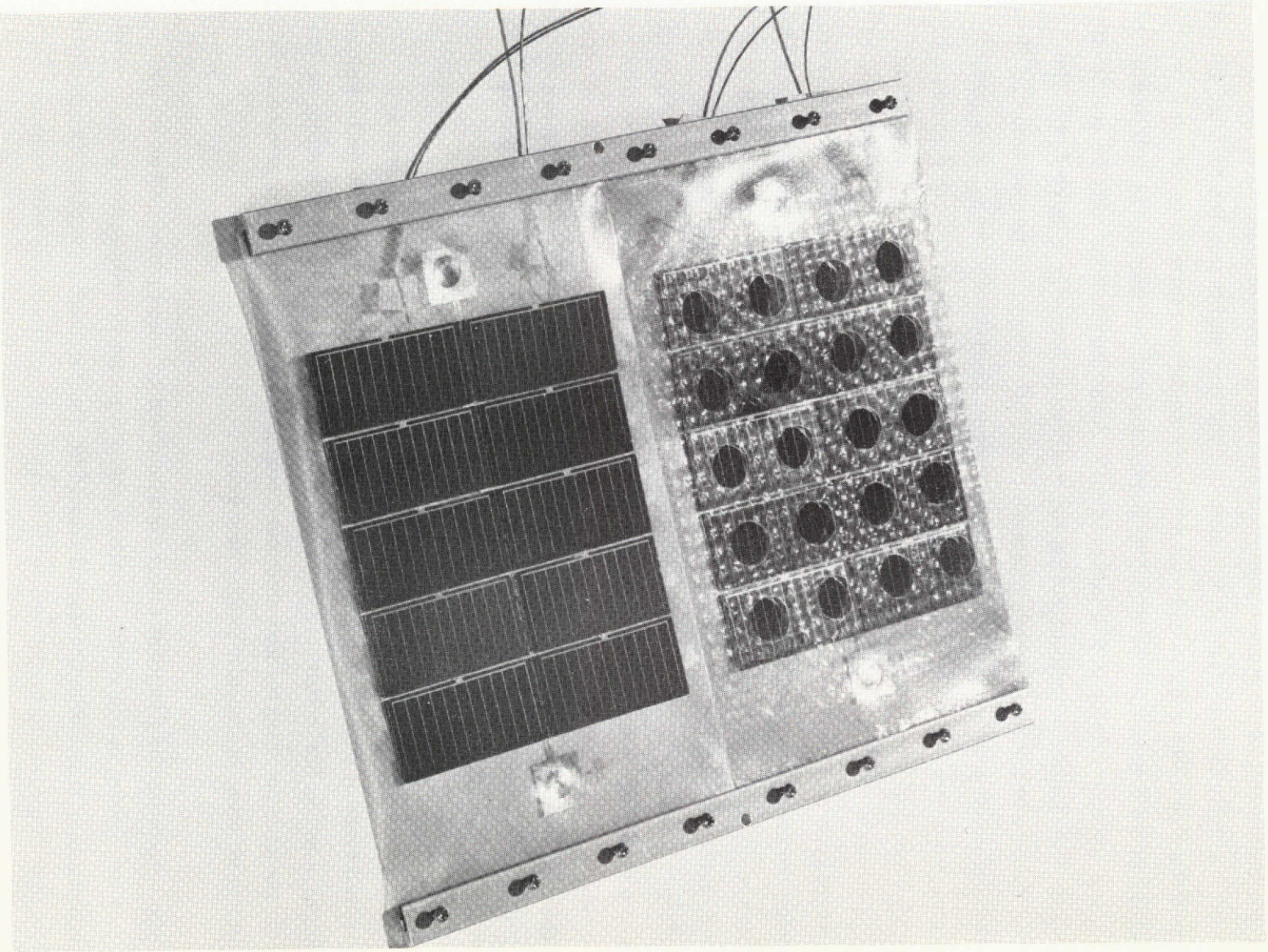


Figure 2-9 On-Array Padding-FEP Teflon Over Cell Sheet



The between-the-cell concepts are aimed at providing a way of separating the cells which are normally face-to-face in the stowed condition and taking the preload through the pads rather than the cells. The concepts are separated into three classes: perimeter, criss cross, and offset. The perimeter pad surrounds the cell and is 0.02 to 0.03 inches wide by 0.032 inches high. These dimensions may be varied in width up to 0.06 inches without affecting the evaluation levels in Figure 2-8. The height is limited to the point where shadowing will affect the cell performance. This becomes a tradeoff between cell packing factor (cell area/total array area), pad height and pad width. The pad design specified above allows up to  $\pm 41$  degrees from the normal sun incidence angle before some cell shading is caused by the padding. If the cell positions are biased to one side this angle is increased to  $+55^{\circ}$ . The use of transparent type materials such as the Sylgard would minimize the power losses from shadowing during large off angle operating modes. The use of this material may also minimize or even eliminate the need for removing the flash which was difficult with the crude methods applied in fabricating the test specimens. The material used for the test specimen padding was RTV-41 Silicone. The RTV-41 which is initially white, is a space qualified material but does not meet the SRI outgassing requirements. Another candidate material, which is very similar in properties, is GE 566 which does meet the requirements, is red in color and is also more expensive. As shown in Figure 2-8, this type of padding increases the mast length 2.44 m (8 ft) and the weight 7.45 Kg (16.4 lbs) compared to a no padding array.

A modified perimeter using crosses at the cell corners is also a candidate and was tested since it could reduce padding weight by 60%. Only the add-on technique is applicable to the perimeter padding concept since cross overs on the same section of substrate with the integral and embossed techniques would result in severe wrinkling and panel distortion in the fabricating process.

The criss-cross padding concept alternates between adjacent panel halves so that when they are folded in the stowed position the pad patterns cross each other providing cell separation. The padding material should be rigid enough to support the preload not allowing compression to the cell level and yet compress a sufficient amount to produce depressions in the mating pad surfaces. The depressions will develop a slip resistance higher than the friction coefficients of the mating materials.

The padding ribs are oriented parallel to the length of the array on the panel half nearest the storage container to increase the panel stiffness and, therefore, aid position control during the retraction process as shown in Figure 2-10.

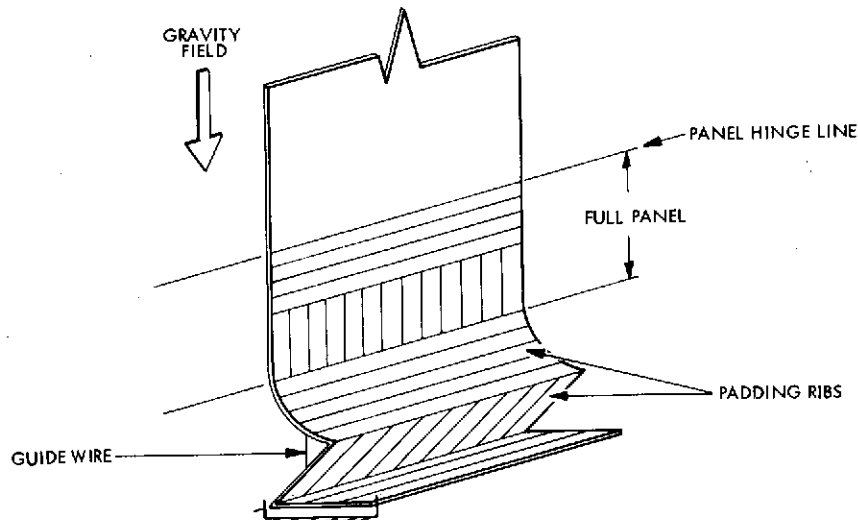
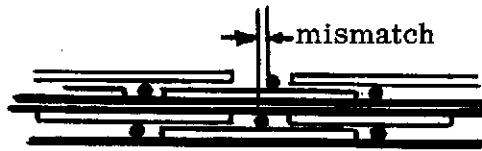


Figure 2-10 Criss Cross Padding Concept

Sections of TFE 0.032 in. x 0.032 in. were satisfactorily integrated between 0.015 in. sheets of Kapton/FEP for the test specimens.

Candidates which have coefficients of expansion very close to Kapton and even Kapton itself were considered for pad filler material in order to minimize thermal distortion of the panels but it would not allow sufficient local depressions because of its relatively high modulus. All three techniques, add-on, integral, and embossed, can be used for this concept. Rows of Silicone with an 0.032 inch cross section were bonded to the Kapton substrate by locally abrading and priming the Kapton surface, then molding and bonding in one operation. Problems were encountered in limiting the flash but good bonds were achievable. The system penalties are 1.64 m (5.4 ft) additional mast

length and 7.86 Kg (17.3 lbs) plus mast weight which is less than the RTV perimeter pad since a denser cell packing factor can be used and cross padding on each panel is not required. By using the silicon pad material rather than the TFE Teflon, the pad weight could be reduced by 40 percent. The offset pad is an exception to the between-cell concept because it uses the cell to transmit the compressive preloads. The panels which are face-to-face have parallel rows of pads. The pads on one panel mate with the cells on the adjacent panel. The padding material should be of a low durometer to distribute the load over as much cell area as possible and provide a mismatch capability for the total padding stack when the panels are in the stowed position.



All three techniques can be applied with this concept. The one fabricated for the test specimen used a low durometer silicon applied as on the criss-cross specimen. The system penalties associated with this concept are 2.10 m (6.9 ft) additional mast length and 4.95 Kg (10.9 lbs) plus mast weight delta.

Slip resistance testing (Section 2.7) showed that the criss-cross padding concept would require the least preload and structure weight to launch the array container in any orientation. It was therefore selected for the preliminary design. The RTV-41 is the selected material although further testing of this material and other candidates to the SEPS environments is required. The no-pad concept also remains a candidate for further evaluation.

#### 2.3.2.4 Preload Methods

The ascent phase of any space vehicle requiring solar cells for mission power subjects the cells to a severe acceleration, vibration and acoustic environments. Figure 2-11 shows types of preload methods which can be used to support the solar cells during ascent and their associated advantages and disadvantages. Small solar arrays (250 ft<sup>2</sup> or less) have generally used rigid substrate panels in the form of honeycomb.

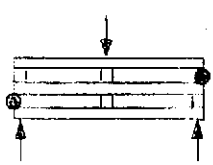
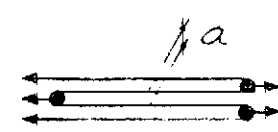
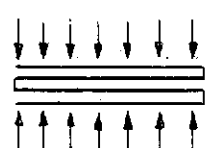
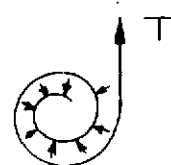
RIGID SUBSTRATE	BENDING	ADVANTAGES		DISADVANTAGES	
			<ul style="list-style-type: none"> <li>o Small shear load in cells induced by panel bending but none directly induced by preload.</li> <li>o No padding other than local spacers for separation</li> </ul>		<ul style="list-style-type: none"> <li>o Difficult to re-establish preload once extended.</li> </ul>
FLEXIBLE SUBSTRATE	TENSION		<ul style="list-style-type: none"> <li>o No loads directly induced in cells by preload.</li> </ul>		<ul style="list-style-type: none"> <li>o Large volume to provide sufficient clearance "a" to allow for dynamic deflection if no pad is used or extremely high tensions in substrate.</li> <li>o Difficult to initially apply and then re-establish preload once extended.</li> </ul>
	COMPRESSION		<ul style="list-style-type: none"> <li>o Preload can be re-established to original levels.</li> <li>o Uniform throughout stowed panels.</li> <li>o Can be stored un-preloaded.</li> <li>o Preload can be adjusted without extension prior to flight.</li> </ul>		<ul style="list-style-type: none"> <li>o Shear loads in cells.</li> <li>o Requires linkages to re-establish preload.</li> </ul>
			<ul style="list-style-type: none"> <li>o Low level preload can be easily re-established after extension.</li> </ul>		<ul style="list-style-type: none"> <li>o Preload varies throughout roll depth from low outside to high inside.</li> <li>o Preload limited by mast capabilities when retracted.</li> <li>o Shear loads in cells.</li> <li>o Must be stored preloaded.</li> <li>o Preload cannot be adjusted without extension.</li> </ul>

Figure 2-11 Ascent Preload Methods

The solar cells are bonded to the rigid substrate with adhesives. The folded panels are then preloaded to hold them in place during ascent while the cells are supported by the rigidity of the panels. Small shear loads due to panel bending when preloaded are induced through the adhesive to the cell. Spacers are placed between panels to prevent contact during ascent and to transfer preload from one panel to another. The extension mechanism on these arrays are generally not designed for retraction, but with certain modifications this can be accomplished and preloading would be accomplished by an independent system.

Flexible substrate arrays require external support for the cells during ascent. Two methods are shown in Figure 2-11, one employing tension and the other compression to support the cells. The tension scheme distributes tensile forces along the edge of each panel which does not induce loads directly into the cells. Sufficiently large space and tension must be designed into the arrangement to prevent panel contact during the expected vibration environment. Padding could be added with a slight compressive preload to prevent lateral motion, but the complexity of tensioning 100 layers initially, then re-establishing it after retraction, and then adding compression to minimize the volume is not warranted since pure compression would simplify the solution.

Compression is used in both flatfold and rollup solar array concepts to support the cells. In the flatfold system compression is applied uniformly to the folded solar panels by the honeycomb cover and base plate. The preload magnitude is determined by the mass of the panels, the interpanel slip resistance, the acceleration loads and acceleration direction. The SEPS array is

- (G) Titan Launch Acceleration - 8 g's
- (Wp) Panel Weight -  $0.982 \text{ Kg/m}^2$  ( $0.2 \text{ lbs/ft}^2$ )
- ( $\mu_{\text{sr}}$ ) Slip Resistance - 0.5
- (n) Panel Layers - 82

The preload (P) necessary to provide sufficient friction at the base and cover to support the solar panels is

$$P = \frac{GW_p n}{2 \mu_{\text{sr}}} = \frac{8 \times 0.2 \text{ lbs/ft}^2 \times 82}{2 \times 0.5} = 6307 \text{ N/m}^2 \text{ (131 lbs/ft}^2\text{)}$$



Applying factor of safety of 2,  $P = 12615 \text{ N/m}^2$  ( $1.82 \text{ lbs/in}^2$ )

For the storage container cover to produce this preload level, the preload mechanism must be capable of producing  $1.82 \text{ lbs/in}^2 \times 157 \text{ in} \times 15 \text{ in} = 19.07 \text{ KN}$  (4290 lb) between the honeycomb cover and base. Component test results on padding specimens indicate slip resistance values from 0.55 to 0.90 for preload levels from  $0.5 \text{ lbs/in}^2$  to  $4 \text{ lbs/in}^2$  are achieved on each specimen (see Section 2.7 for test description). A slip resistance value of 0.9 would reduce the preload value from 19.07 KN (4290 lbs) to 10.6 KN (2383 lbs). Lateral launch accelerations will act on the mass of the solar array to decrease preload on either the cover or the base. A small increase in preload will provide the required margin.

Additional levers and linkages which add to the weight are required on the cover to establish the preloads. On the other hand this preload can be re-established at the ascent levels after retraction allowing safe re-entry to earth for refurbishment. The preload can be adjusted from zero during the storage stage, which would prevent long term set in the padding, to full preload prior to flight. This can be accomplished without extension of the array.

The rollup is also preloaded by compression but it is accomplished by tensioning the substrate during retraction. The tension can be artificially induced on the ground to adjust the preload to levels sufficient for ascent survival but below the cell bending limits. A low level preload can be easily re-established during retraction but is limited by the mast properties. The preload varies from a low value on the outer layers to a higher value on the inner layers depending on substrate tension and number of layers. This variable is necessary since only one surface is stationary and available for shear support to prevent slippage of the stowed array during ascent. As in the flat-fold, the shear loads are carried through the cell-substrate. The preloads are always applied to the stowed substrate during all storage periods. The levels can be minimized during storage and increased prior to flight by extending the array and inducing the preload artificially during retraction.

The preload concepts were divided into two categories associated with how the storage container cover is oriented during extension. The first category, as shown in Figure 2-12, maintains the cover parallel to its original stowed position during extension and retraction while category two rotates at  $90^{\circ}$  at the beginning of extension and at the end of retraction. The concepts in each category shown in Figure 2-12 were evaluated on the basis of the several factors shown in the figure.

Concept 1A was selected for the following reasons.

- 1) The design requires no rotational change in lid attitude to align and lock to the container.
- 2) It provides a simple linkage arrangement with a low moving parts count which allows easy and adequate adjustment provisions.
- 3) It provides built-in locking alignment features in that the latches open wide enough to clear any obstructions.
- 4) The latch closing action wants to push the lid into exact closure alignment before locking.
- 5) Moment arm ratio varies to provide a progressively greater moment arm mechanical advantage as the latch closes. This provides a great final force that increases along a hyperbolic function curve thus reducing the area under the curve (work of closure) to a tailored minimum, while still providing the final compressive force.
- 6) Since the only energy source available comes from the astro-mast retraction motion, this means that the mast force and travel distance tapped to effect closure will be at a minimum.
- 7) Although it does not optimize fold control prior to final preload as does concept 2B, it provides a reasonable compromise.

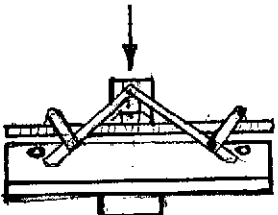
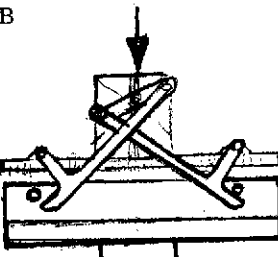
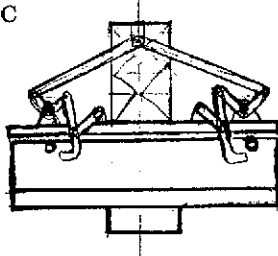
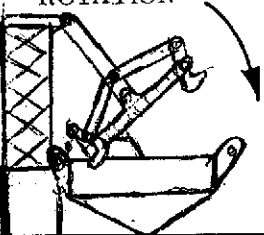
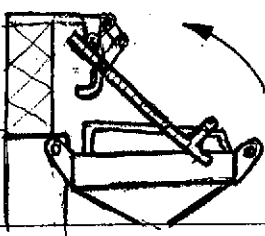
CATE- GORY	CONCEPT (SCHEMATIC REPRESENTATION)	PRELOAD APPLICATION	MAST $\Delta L$ (IN.)	STABILITY	LOCKING ACTION	FOLD CONTROL	LOCKING ENERGY	LID CLOSURE ALIGNMENT
1	A SELECTED 	.75 IN POSSIBLE COMPRESSION DISTANCE TO ACHIEVE 4200 LBS HOLD DOWN FORCE	33	REQUIRES HINGE FROM TIP FITTING TO COVER. DEPENDS ON LINKAGE AND JOINT STIFFNESS	MAX ADJUSTABILITY WITH LOCKING MOMENT INCREASING TO MAX AT FINAL LOCK	LEADER STIFFENER REQUIRED TO PROPERLY POSITION PANELS PRIOR TO PRELOAD	19 IN. OF ASTROMAST TRAVEL WITH 50 LBS OF MOVING FORCE	VERY GOOD DUE TO POSITIVE LID RESTRAINTS AND LARGE LOCKING HOOK ENGAGEMENT TRAVEL
	B 		40		LINKAGE SEQUENC- ING OF LOCKING ACTION IS NOT SIMULTANEOUS BUT INCREASES TO MAX AT FINAL LOCK		25 IN. OF ASTROMAST TRAVEL WITH 63 LBS OF MOVING FORCE	GOOD LID RESTRAINT BUT LOCKING ENGAGEMENT TRAVEL IS LESS
	C 		30		PROVIDES MORE ADJUSTABILITY THAN NECESSARY		15 IN. OF ASTROMAST TRAVEL WITH 50 LBS OF MOVING FORCE	VERY GOOD DUE TO LID RESTRAINT AND EXCELLENT LATCH HOOK TRAVEL FLEXIBILITY
2	A CLOCKWISE ROTATION 	.75 IN COMPRESS- ION DISTANCE NOT POSSIBLE WITH THIS ARRANGEMENT WITHOUT INVOLVED 4 BAR LINKAGE FORCE MULTIPLI- CATION TO REDUCE ASTROMAST FORCE	10	REQUIRES SPRING AND STOP TO MAIN- TAIN ROTATIONAL POSITION BUT OTHERWISE STABLE	MARGINAL MECHANI- CAL ADVANTAGE AND ADJUSTMENT WITH MINIMUM FOLDED BLANKET COM- PRESSIVE DISTANCE	PANELS AUTOMATI- CALLY FOLDED TO PROPER PRELOAD POSITION	LOCKING REQUIRES TOO MUCH ASTRO- MAST FORCE UNLESS LONG TRAVEL LINKAGES ARE ADAPTED	GOOD BUT REQUIRES GUIDANCE FOR IN- BOARD LATCH INITIAL ROTATION ENGAGE- MENT
	B COUNTERCLOCK- WISE ROTATION 	.75 IN POSSIBLE COMPRESSION DISTANCE TO OBTAIN 4200 LBS HOLD DOWN FORCE IF FINAL MOMENT ARM = .22 & ASSUME ASTROMAST FORCE IS LIMITED TO 50Lbs	18		OUTBOARD LATCH MOMENT ADEQUATE. INBOARD LATCHING THROUGH OVER- CENTER 4 BAR LOCKING WHICH MUST BE TAILORED FOR ADEQUACY	COVER SLIDES OVER CELLS UNLESS TOP PANEL IS STIFFENED AND GUIDED TO PROPER PRELOAD POSITION	18 IN OF ASTROMAST TRAVEL FOR OUT BOARD LATCH TRAVEL ASTROMAST CLOSURE FORCE REQUIRED MAY BE AS HIGH AS 135 LBS BECAUSE OF MOMENT ARM LIMITATIONS	GOOD BUT REQUIRES GUIDE RAILS FOR OUTBOARD LATCH INITIAL ENGAGEMENT

Figure 2-12 Flat-Fold Preload Concepts

FOLDOUT FRAME

FOLDOUT FRAME

## 2.3.2.5 Honeycomb Panel Materials Evaluation

The choice of materials composing the panel was predicated on those materials meeting the following requirements:

- o high temperature stability
- o high stiffness (EI)
- o low weight
- o producibility with fabrication equipment
- o ease of manufacture
- o cost

Table 2-3 lists the candidate panel (skins and core) materials.

TABLE 2-3  
CANDIDATE PANEL MATERIALS

<u>SKINS:</u>	<u>CORE:</u>
1. PRD-49	1. Aluminum
2. Steel	2. Glass
3. S-Glass	3. Graphite - Polyimide
4. Graphite - Epoxy	
5. Graphite - Polyimide	
6. Aluminum	

The skin candidates were traded-off using maximum stiffness and minimum weight as the guideline. Assuming a constant area moment of inertia for each candidate, maximizing stiffness reduced to maximizing the tensile modulus of elasticity. The candidates are ranked below according to their tensile modulus.

<u>CANDIDATE</u>	<u>TENSILE MODULUS</u>
1. Graphite	$36 \times 10^6$ psi
2. Steel	$29 \times 10^6$ psi
3. Aluminum	$10 \times 10^6$ psi
4. PRD-49	$4 \times 10^6$ psi
5. S-Glass	$5 \times 10^6$ psi

According to weight

	<u>CANDIDATE</u>	<u>DENSITY</u>
1.	PRD-49	1.45 g/cm <sup>3</sup>
2.	Graphite	1.95 g/cm <sup>3</sup>
3.	S-Glass	2.49 g/cm <sup>3</sup>
4.	010 Aluminum	2.72 g/cm <sup>3</sup>
5.	Steel	7.75 g/cm <sup>3</sup>

It can be clearly seen that the graphite skin has the highest strength to weight performance of the candidate systems. In the honeycomb system, the core serves three distinct functions: 1) It lowers the weight of the system, at the same time increasing the area moment of inertia and retaining the structural stability of the system; and 2) transfers the loads to the skins. Of the three candidate materials, aluminum is selected as it has the most manufacturing and flight usage experience and is available in a wide selection of core heights, cell diameters, alloys, wall thickness and density. A honeycomb panel is a closed system. To insure that pressure differentials do not exist when the system is in a space environment, the cell walls are perforated.

For applications requiring operation at temperatures in the 300 to 500<sup>o</sup>F range, structural adhesives can be classified\* according to strength as follows.

- 1) polyimides
- 2) polybenzimidazoles (PBI)
- 3) epoxy-phenolic
- 4) epoxy

Both the polyimide and the PBI adhesives were not considered for the panel skin to core adhesive because

- 1) both require extended (high temperature and pressure) cure cycles
- 2) due to the nature of the reaction, there is little reproducibility

\* in the absence of air

The epoxy-phenolics, as a family, are well suited for applications involving very short (1 minute) exposures up to 1000°F and long term exposures at 500°F in the absence of air.

The candidate adhesives chosen were:

Aerobond 430  
 Bloomingdale HT 432  
 Bloomingdale HT 424

By weight - these adhesives rank:

HT 432                      -0.08 lb/ft<sup>2</sup>  
 Aerobond 430              -0.12 lb/ft<sup>2</sup>  
 HT 424                      -0.135 lb/ft<sup>2</sup>

The following information is reported in vendor data:

	HT-424 0.135 psf	HT-432 0.07 psf	Aerobond 430 0.12 psf
Tensile Shear, psi at 75 ± 5°F	3550	3125	3150
Tensile Shear, psi at 300 ± 5°F	2760	2325	2530
Tensile Shear, psi 500 ± 5°F	2000	1700	2100
Tensile Shear, psi at 300 ± 5°F, 192 hours	2890	2390	2570
Tensile Shear, psi at 500 ± 5°F, 192 hours	--	--	770

The skin to core adhesive selection is Bloomingdale HT 424 because:

- 1) It is a stronger adhesive than the other candidates.
- 2) It is qualified as Type III\* adhesive for bonding honeycomb panels
- 3) It has extensive history of use in space applications

\*MMM-A-132, Federal Specification, Adhesives, Heat Resistant, Airframe Structural, Metal to Metal.

Table 2-4 compares two 1/2 inch thick panels that were tested for an array program at LMSC. As shown, the composite panel design has the highest stiffness to weight ratio.

TABLE 2-4  
SUMMARY OF PANEL DESIGN TEST RESULTS

<u>Candidate Skins</u>	<u>Adhesive Properties</u>		<u>Bending Stiffness</u> <u><math>\times 10^{-5}</math> lb-in<sup>2</sup></u>	<u>Weight</u> <u>(lb-ft<sup>2</sup>)</u>
	<u>Climbing Drum</u> <u>Peel</u> (lb-in/3 in-width)	<u>Flatwise</u> <u>Tensile</u> (psi)		
Composite (12 mil)	18.6	934.74	1.04	0.63
Al (10 mil)	11.4	763.33	0.26	0.61

## 2.4 ELECTRICAL DESIGN

This section of the study final report describes the portions of the SEPS solar array system which are categorized as being directly associated with the conversion of solar energy to electrical power, the collection of current at the cells, and conveyance inboard from the array to appropriate interface connectors. This section includes the analysis to support design selection of the solar cells, the cell covers, the cell interconnect, the method of assembly of the cell covers to the cells and the cells to the interconnect, the selection of the correct complement of cells in parallel and series, the integration of cell assemblies with the array modules and panels, and the design selection of the configuration, routing and termination of the array power feeder harnesses.

### 2.4.1 Electrical Design

The components and elements of the array electrical system are described in the following sections and are listed below starting in sequence progressing with the cell cover through the cell stack to the substrate.

Component	PRELIMINARY DESIGN	
	Description	Thickness
Cell Cover	Fused Silica	150 micron (6 mil)
Cover Adhesive	DC93-500	50 micron max
Solar Cell	2 x 4 cm W.A. Solderless 2 ohm-cm, hybrid	200 micron (8 mil)
(Parallel Gap Welding)	Assembly Method	
Interconnect	Printed Etched OFHC Copper	25 micron (1 mil max)
Substrate	Integral Interconnect Kapton/high temp. polyester adhesive	50 micron (2 mil)
Harness	FCC Aluminum Conductor	Conductor thickness 75 micron (3 mil)



The preliminary design list is considered a low or no risk system with its elements well demonstrated. Though not as well demonstrated or documented there are certain other candidates that due to distinctive advantages are listed as alternates and their potential use should be reviewed periodically prior to production design selection.

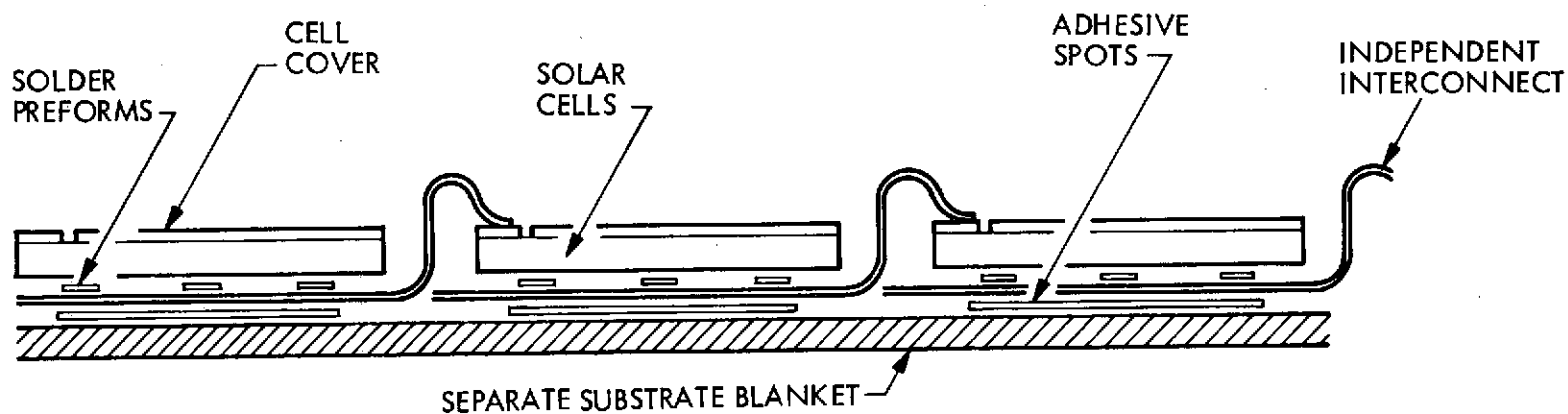
ALTERNATE		
Component	Description	Feature
Cell Cover	Ceria Glass	Lower cost, stronger
Solar Cell	Violet or Helios	Improved efficiency
Interconnect	Ag Plated Moly	Lower thermal coefficient (but higher weight and lower electrical conductivity)
Substrate	Kapton-Pyralux	Better control of shrinkage

A very recent cell cover system wherein 7070 Boro Silicate glass is electrostatically bonded to solar cells is being developed by Simulation Physics. If it becomes feasible in the future, it could also be considered as a cover alternate. Additional discussions of the selected and alternate components are incorporated in Section 2.6.

#### 2.4.1.1 Substrate - Interconnect System

The selection of the substrate system is largely dependant upon the interconnect system, whether it is an integral interconnect system or an independent interconnect system. Figure 2-13 illustrates the heaviest substrate, interconnect combination, wherein a conventional soldered cell is solder connected to an independent interconnect, then the cell submodule is glued to the array blanket or substrate. An intermediate design is also depicted in the same illustration wherein a solderless conventional top side N bus electrode cell would be parallel gap welded to interconnects that are laminated in between layers of the Kapton assembly. The baseline system is shown in Figure 2-14 where a wraparound electrode cell is used with the integral printed circuit interconnect. Some of the major advantages associated with the use of the integral interconnect are as follows:

- INDEPENDENT INTERCONNECT — CONVENTIONAL SOLDERED CELLS (HEAVIEST SYSTEM)



- INTEGRAL INTERCONNECT — CONVENTIONAL CELL OPTION

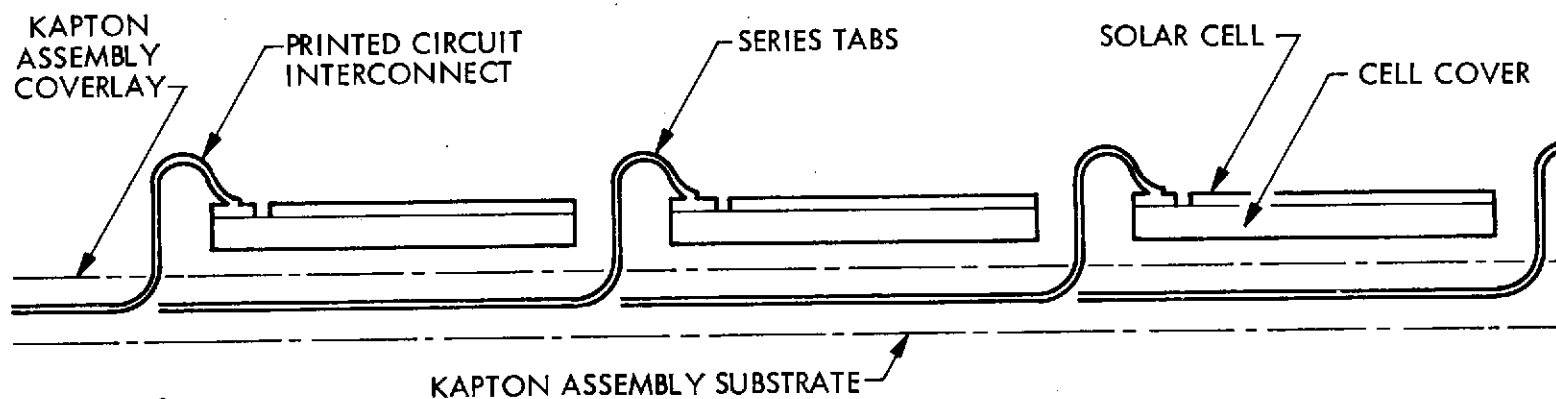


Figure 2-13 Substrate System Options

- GOOD JOINT ACCESS
- HIGHER PACKING FACTOR
- REDUCED ASSEMBLY STEPS AND COST
- ELIMINATES N-BUS GAP PROBLEM
- REDUCED WEIGHT

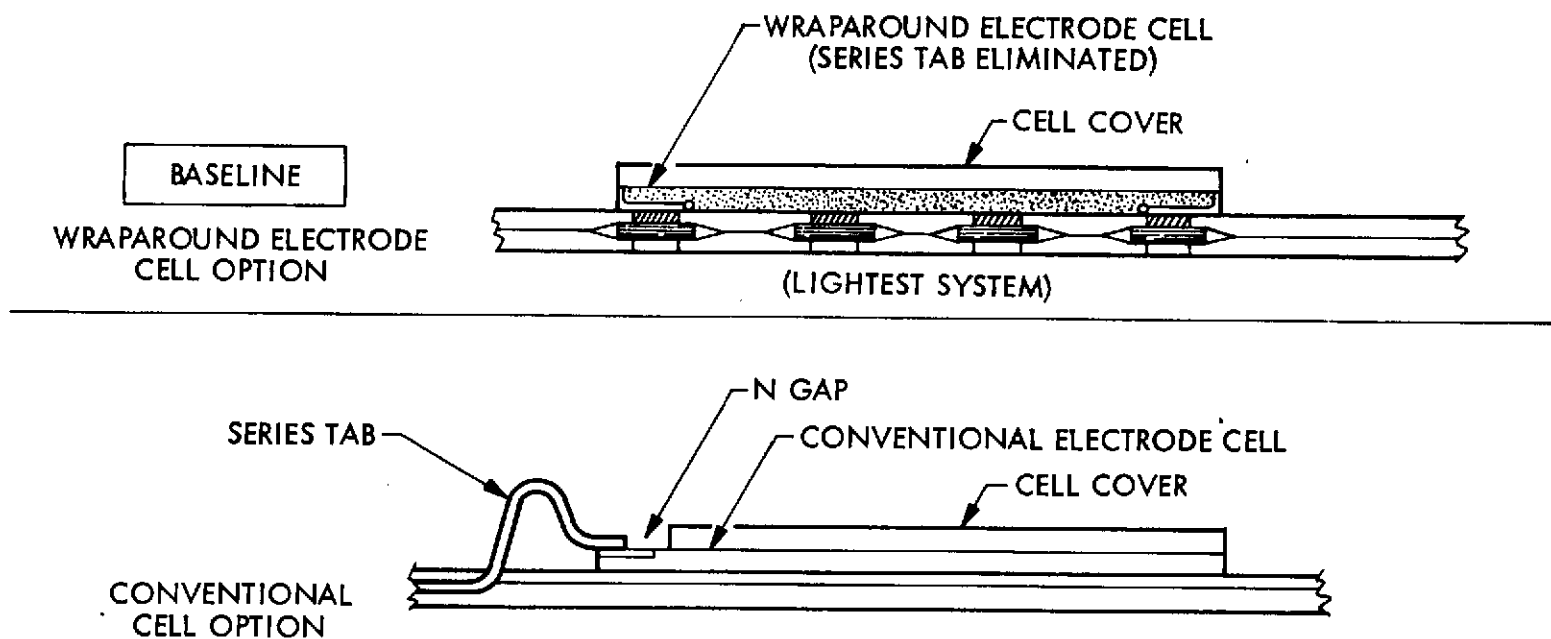


Figure 2-14 Integral Interconnects - Substrate Design

1. Weight and assembly functions are eliminated by not requiring adhesive to mount the interconnect and cells to the substrate.
2. The electrical joint (parallel gap weld) also performs the mechanical function of holding the cell to the array.
3. Thin foils of interconnect metal can be accommodated, protected, and held in exact registration through the entire assembly process.
4. A wide variety of interconnect stress relief-geometric patterns can be incorporated by precise step and repeat camera photographic processes to form the circuitry for entire modules or panels.

#### 2.4.1.2 Solar Cell

A wraparound electrode solar cell design has been selected because:

1. Its use eliminated the necessity of a discreetly formed, damage susceptible series tabs.
2. Greater active surface is available with relocation of the N bus to the rear surface of the cell resulting in higher cell power.
3. With both electrodes on one surface of the cell, cell assembly becomes a single side function wherein series contacts can be formed at the same time parallel contacts are made.
4. The N gap problem is eliminated by allowing the use of uniform covers over the entire cell surface.
5. A higher packing factor (more cells per unit area) can be achieved by reducing the additional series spacing formerly required for forming and routing the series tab.

6. Fully automated assembly becomes feasible. (This has been achieved in Europe by bonding tabs to the cells top side N contacts prior to final bonding so an automated "single surface" function can occur.)
7. Padding is minimized or eliminated because there are no series tabs protruding above the cover surface which can cause tab deformation or padding hang up.
8. All contacts (bonds) can be made in line along the backside centerline of the cell forming a pivot axis such that electrode flexure is minimized and increased load carrying capability occurs.

The Bell Telephone Laboratory solar cell patented by Chapin, Fuller and Pearson in 1954 depicted a rear surface contact (wraparound electrode) solar cell and all of the initial silicon solar cells were of this type. In 1965 the three cell vendors Texas Instruments, Centralab and Heliotek introduced commercial wraparound electrode cells as catalog items. These were received by the industry with mixed reaction because of the position that joint inspection was no longer possible after assembly. This was in the era when the cells were mounted to rigid substrate or honeycomb panels, but the argument was only half right because the parallel contacts or "P" contacts were always made on the cell under side and thus hidden after bonding to the rigid substrate. With the advent of lightweight, flexible, transparent substrates a strong interest was revived in wraparound electrode cells. Figure 2-15 summarizes the major milestones associated with development of the wraparound electrode cell. Its development has been accelerated in recent years and its use enhances long term temp cycle survivability by elimination of the series tab or the so called pretabbed cell. Exotic and complicated stress relieved series tabs have been proposed, most of which are susceptible to handling damage and interference in stowage or deployment with either a drum or flatpack array. The wraparound electrode cell is the recommended design for the SEPS application.

Preliminary evaluations of the array electrical performance, sizing and weights, including the extension mast and array container, indicated that the array weight density with on-array padding would have to be in the range of 0.78 to 0.88 Kg/m<sup>2</sup>

BOTH POSITIVE AND NEGATIVE ELECTRODES FORMED ON THE BACK OR INACTIVE SIDE OF THE CELL DURING FABRICATION

- MARCH 5, 1954 — ORIGINAL SOLAR CELL PATENT BY CHAPIN, FULLER, AND PEARSON OF BELL LABS WAS WRAPAROUND ELECTRODE REFERENCE DATED 2,780,765.
- COMMERCIAL W. A. CELLS — INTRODUCED BY CENTRALAB, HELIOTEK, AND T.I. IN 1965.
- 100 W.A. CELLS INCORPORATED IN A.F. PROTOTYPE ARRAY AND MET PREFLIGHT QUALIFICATION IN FLAT PACK STOWAGE 1970.
- FERRANTI BUILT 1,000 FOUR-MIL W.A. CELLS FOR R.A.E.
- 1,000 EACH, 2 x 2 FABRICATED BY CENTRALAB AND HELIOTEK FOR NASA LEWIS, REFERENCE NAS 3-15345.
- 1,000 EACH, 2 x 4 FABRICATED BY CELL VENDORS FOR SPACE STATION SOLAR ARRAY REFERENCE JSC/LMSC NAS 9-11039.
- 300 EACH, 2 x 4 END TAB W.A. CELLS FABRICATED BY CELL VENDORS FOR IMPROVED SUBSTRATE TEMPERATURE CYCLE TESTS, REFERENCE MSFC/LMSC NAS 8-28432.
- 1,200 EACH, 2 x 4 END TAB W.A. CELLS PROCURED FOR LMSC ID PROGRAMS.
- 120 EACH, HIGH EFFICIENCY WRAPAROUND CELLS BEING FABRICATED FOR ADDITIONAL TEMPERATURE CYCLE TEST MODULES.
- 2,800 EACH, 2 x 4 END TAB W.A. CELLS IN FABRICATION FOR SEPS (NAS 8-30315)

Figure 2-15 Chronology of Wraparound Cell Development

(0.16 to 0.18 lbs/ft<sup>2</sup>) to avoid high risk technology developments for extension mast and container materials and designs. The evaluation of the array harness weight resulted in a minimum weight harness plus array blanket when the harness power loss was 4.0 percent. The covered solar cell power requirement is based on the following assumed losses:

Assembly loss:	3 percent
Bussing loss:	3.7 percent
Diode loss:	0.5 percent

The required covered cell power at 50°C (122°F flexible array solar cell operating temperature at 1 au) is  $25 \text{ KW}/0.929 = 26,899 \text{ W}$ . A six mil fused silica cover is selected for the array design. A 2 ohm-cm base resistivity cell is also selected based on data reported in Reference 3 where the Pmp of 10 ohm-cm cells at higher illumination intensities ( $> 250 \text{ mW/cm}^2$ ) falls off with respect to Pmp of 2 ohm-cm cells. The higher initial specific power of the 2 ohm-cm cell also provides a lighter array design. The temperature of the SEPS array will be controlled going toward the sun by array tilting starting at 0.62 au with the illumination intensity limited to  $364 \text{ mW/cm}^2$ .

Based on 3060 cells on a panel (30" x 157"), there are 93.6 cells/ft<sup>2</sup>. The panel size is essentially a function of the storage container volume constraints. The use of a 0.050 in. cell spacing to allow for the selected on array padding concept (between cells) produces a lower than usual number of 2 x 4 cm cells per unit area.

The weight density of the array blanket is shown below in a concept for the SEPS array.

8 mil cell	0.0831 lbs/ft <sup>2</sup>	(0.429 gm/cell)
6 mil cover	0.0569	(0.276 gm/cover)
Cover adhesive	0.0092	(0.0446 gm/cover)
1 mil Kapton	0.0074	
1 mil FEP Teflon	0.0112	
1 mil copper	0.0116	(25% area)
<hr/>		
0.1794 lbs/ft <sup>2</sup>		$= 0.881 \text{ Kg/m}^2$

The copper interconnect material was a second choice to silver-plated molybdenum because it is approximately one-third as heavy. The 1 mil Kapton, 1 mil FEP Teflon is a lamination of two 0.5 mil Kapton/0.5 mil FEP Teflon sheets. This design is considerably lighter than a 1 mil Kapton/0.5 mil FEP Teflon film which had been used in previous LMSC designs. An array blanket weight was developed based on an eight mil cell with an uncovered efficiency of 11.2% (an improvement in conventional technology is required). The 8 mil thickness was a conservative selection based on having to raise the conventional efficiency of a 8 mil cell from 10.7 percent to 11.2 percent while avoiding the higher costs of 6 mil cells and of the new high efficiency technology. At the same time, the required weight of the other components in the array blanket, i.e., covers, interconnect and flexible substrate did not require large reductions over present technology. The resulting array blanket size and weight was compatible with the extension mast and container technology that satisfied the deployed array dynamics requirements and the total array weight of 385 Kg. To evaluate other candidate solar cell designs, the total weight of the blanket was held constant, the blanket weight density, excluding the solar cells, was held constant and the thickness of the solar cells was varied. The resulting solar cell efficiency required vs cell thickness is shown in Figure 2-16. The effect of increased cell efficiency on required array area is included in the curve.

The component evaluations performed under this study have led to the replacement of the 0.5 mil FEP Teflon laminating "adhesive" specific gravity of 2.15 with a 0.5 mil high temperature polyester adhesive (sp. gr. of 1.4). The resulting blanket design is:

8 mil cell	0.0831 lbs/ft <sup>2</sup>	(0.429 gm/cover)
6 mil cover	0.0569	(0.276 gm/cover)
Cover adhesive	0.0092	(0.0446 gm/cover)
1 mil Kapton	0.0074	
1 mil Adhesive	0.0073	
1 mil copper	0.0116	(25% area)

---


$$0.1755 \text{ lbs/ft}^2 = 0.862 \text{ Kg/m}^2$$



2-56

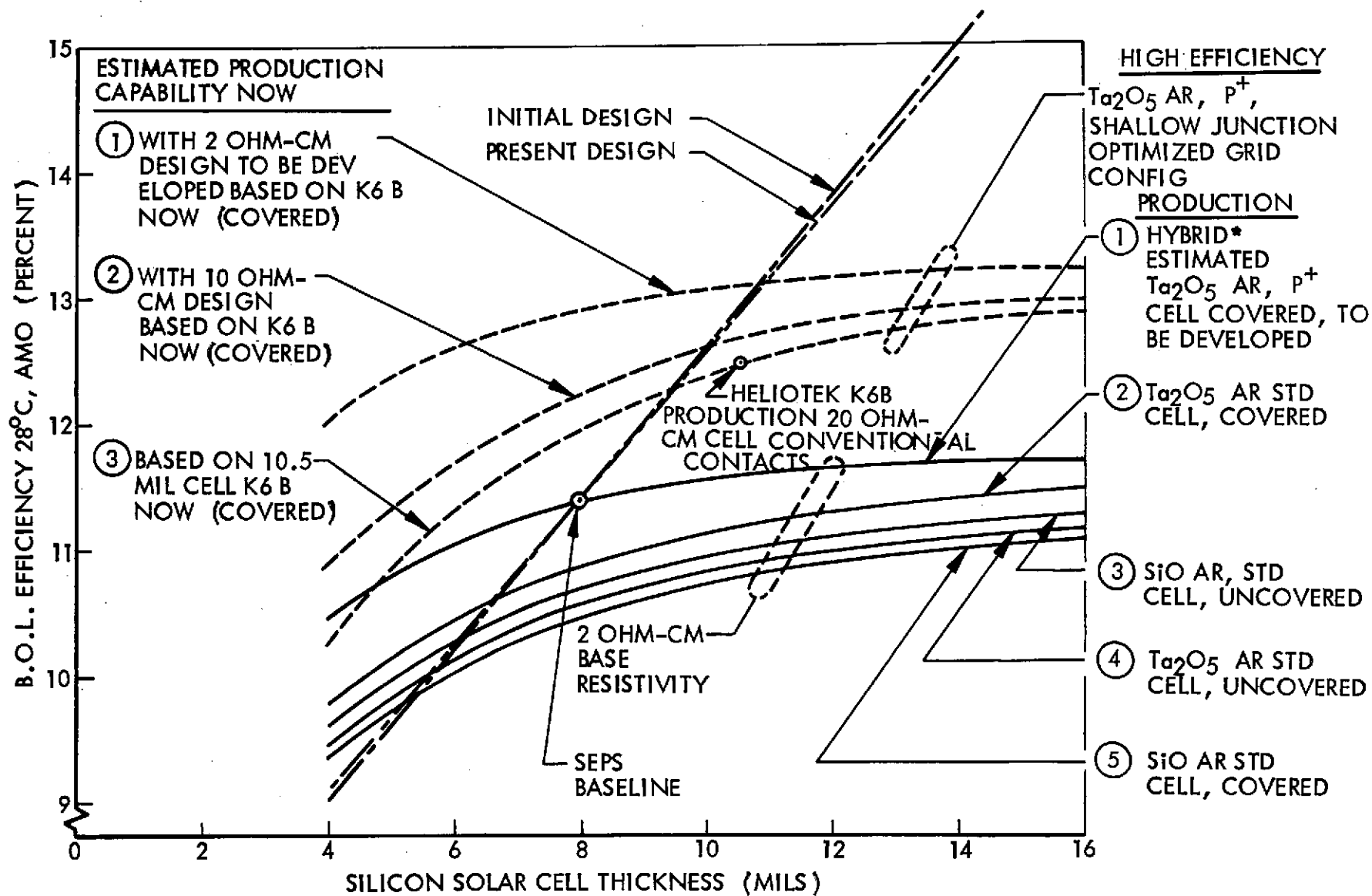


Figure 2-16 Required Efficiency of Covered Cell

LMSC-D384250

The resulting curve of required covered cell efficiency vs solar cell thickness for the final weight summary is also shown in Figure 2-16. No significant change is noted from the first curve. The SEPS baseline cell design is shown in the figure along with cell performance for various designs. The hybrid cell is selected as the most cost effective in the wraparound contact 2 x 4 cm design. A cell 6 mils thick or less is not desired from a breakage standpoint but can be a weight improvement in the future. The initial baseline SEPS solar cell was an SiO AR coated 11.2 percent average efficiency cell that provided 11.0% efficiency when covered. This design assumed an array harness loss of one percent. The design studies reveal that a 4.0 percent harness loss provides a minimum blanket plus harness weight. This results in an 11.4% covered 8 mil cell design requirement. Laboratory built cells of the baseline design have an average uncovered efficiency of 11.4 and provide 11.6% when covered.

The covered solar cell costs of cells meeting the required B. O. L. efficiencies are:

Covered Cell	Thickness	Req'd Covered Eff.	No. Req'd	R. O. M. Cost/SEPS
SEPS Baseline	8 mils	11.4%	250,920	\$3.849 M
K6B (Modified to 2 x 4 WA)	10.5 mils	12.9%	221,742	\$3.880 M to \$4.324
High Efficiency	12 mils	13.8%	207,281	\$3.627 M to \$4.020

The number of cells required is determined by:  $26,899 \text{ W of cell power} / (135.3 \text{ mW/cm}^2 \times 8.088 \text{ cm}^2/\text{cell} \times 11.4\% \text{ eff} \times 0.868 (50^\circ\text{C}) \text{ temp. factor}) = 248,410 \text{ cells.}$

The use of a  $P^+$  backside treatment on an 8 mil cell provides a dramatic improvement in cell performance. At 12 mils, the  $P^+$  treatment has a much smaller impact. The  $P^+$  treatment provides an 8 mil cell with conventional 12 mil cell performance and, equally significant, the radiation degradation of the  $P^+$  8 mil cell is very much like that of the conventional 12 mil cell according to Heliotek. The radiation degradation of high efficiency cells is showing a faster rate of power decay once degradation commences. This latter fact is not of great significance if only total energy (SEPS impulse) is important. This is not the case if end-of-life (E. O. L.) power is important as in stage power to synchronous equatorial satellites.

NASA/MSFC under NAS8-28432 is developing shallow junction cell technology for a 2 x 4 cm wraparound contact design. This activity plus that of other existing programs at the vendors will continue to improve the available high efficiency cell technology. This technology is considered a backup to the SEPS Solar Array. It is not recommended for primary SEPS technology development because of cost, radiation performance, and because it is not essential to meeting the SEPS Solar Array requirements.

The use of high efficiency cell technology to obtain maximum beginning of life (B. O. L.) specific power is recognized. While production of cells with average efficiencies of 14 percent or higher has not yet been demonstrated, significant specific power improvements have been demonstrated in the K6B cell design. LMSC's recommendation is to meet the SEPS solar array weight requirements with the minimum solar cell cost. A change in this guideline would result in a re-evaluation of the present solar cell selection.

#### 2.4.1.3 Cell Cover

Within the SEPS hardware time frame there will be a domestic source for cerium stabilized glass in that OCLI has added this option along with the other cover types Fused Silica and Microsheet. Fused Silica and Cerium Stabilized Glass both have a state of the art status Category I, reference Section 2.6. Ceria glass and 7070 borosilicate electrostatically bonded glass have lower cost in all thicknesses, and greater flexibility and bending strength in thinner configurations than fused silica. For testing purposes, in that fused silica is a more fragile system, there is impetus to use fused silica because if it survives ascent/reentry simulated loads in selected stowage configurations, the survivability of the glass options is insured. The 6 mil thickness of fused silica is selected since it is the lightest design that is presently available in production quantities. The radiation damage studies also show that this thickness, with an 8 mil cell, provides reduced power degradation compared to thinner covers. The cover has an AR coating on the surface facing the sun and blue filter is selected for the cover to protect the cover adhesive which would be exposed to high intensity solar UV. The filter cut-on wavelength is 0.400 microns. The cover adhesive is DC93-500. This material is a highly refined version of Sylgard 182 and has good transmission stability in the space environment.

#### 2.4.1.4 Interconnect

The selected interconnect material is copper. Copper, silver, aluminum, Kovar and molybdenum have been used in printed circuit substrates. Invar has also been investigated but its very low electrical conductivity is not advantageous. Of the metals requiring plating, molybdenum has the best electrical conductivity, is non-magnetic unlike Kovar, and has been successfully used in many flight applications in an independent (non-laminated) interconnect category. As a result, molybdenum is the current recommended interconnect material in the low thermal expansion category. Copper, silver and aluminum are in the higher thermal expansion category. The high cost and lower tensile strength of silver as compared to copper, and the developmental status of Al contacted cells where Al interconnects would be most compatible, favors the selection of copper based on weight if orbit thermal cycles are not extreme. There is sufficient versatility in the printed/laminated circuit technology that metal selection does not appreciably impact schedule.

Copper is selected for the SEPS design for the following reasons:

1. A low density interconnect material is mandatory to meet the SEPS weight requirements. One mil molybdenum with 0.5 mil Ag plating weighs 0.0213 lbs/ft<sup>2</sup> while 1 oz. copper weighs 0.0125 lbs/ft<sup>2</sup> (both 20% area).
2. It has established produceability advantages in printed circuit etching and is compatible with parallel gap welding application.

#### 2.4.1.5 Assembly Technique

The selected assembly technique for joining the solar cells and the copper interconnect is parallel gap electric resistance welding. The present array blanket design temperature upper limit is set at 150°C (302°F). At distances closer to the sun than 0.62 au this temperature can be exceeded. The above limit is not set by known materials limitation but combined high temperature and UV effects on materials are known to accelerate mechanical and optical property damage. At 0.3 au, the temperature limit establishes the maximum amount of array tilt required and this in turn affects the degree of sun shading of the array extension mast by the array blanket. The melting point of a typical solder, Sn 63, is 183°C (361°F) with an operating temperature limit set lower.

The advantages of welded arrays over soldered arrays are as follows:

#### Operational Reliability Advantages

- o Thermal Cycling Durability. Thermal cycling produces large stresses at the interconnect/cell interface due to the difference in thermal expansion coefficients. This condition can be minimized by keeping the amount of metal at the interface as small as possible. Welding offers a better potential than soldering for controlling the thickness of metal to achieve this result.

#### Array Assembly (Manufacturing) Advantages

- o Possible Lower Cost, High Reliability Interconnections. The welding process selected, parallel gap welding, is inherently more consistent and controllable for high volume production than present soldering. Fluxing and washing are eliminated. Electrical losses due to contact resistance are minimized.

Parallel gap electric resistance welding was selected since:

- 1) More development work has been performed by other investigators with this technique for solar array fabrication than with other techniques.
- 2) The required welding equipment is developed, available and compatible with requirements for production operations.
- 3) This joining technique is compatible with a) the selected cell contact metal and the copper interconnect and b) the joining operation from the back of the flexible circuit to the wraparound contact solar cells.

#### 2.4.1.6 Array Harness

The selected array harness is mounted on the back of solar array blanket at the two long edges. The harness uses flat cable conductor (FCC) and aluminum conductors 75 microns (3 mils) thick. The width of the conductors varies from 0.635 cm (0.25 in.) to 0.127 cm (0.050 in.) to provide a constant voltage drop to the base of the array for 41 electrical modules (100 volts nominal) one side of the array and for 41 electrical

modules (100 volts nominal) on the other side of the array. The FCC is 7.6 cm (3.0 in) wide and the number of conductors per cable varies from 7 to 20. The conductors are laminated between two sheets of 1 mil Kapton/1 mil high temperature polyester adhesive and the nominal spacing between conductors is 0.254 cm (0.10 in). Aluminum conductors are selected since they provide an approximate weight saving of 2.5 Kg (5.5 lbs) per array wing. The polyester adhesive is selected, as in the substrate, to provide a significant weight savings over FEP Teflon. It is 1 mil thick to assure that the spaces between the 3 mil thick conductors are completely filled during lamination. The conductor widths are tailored for each module distance from the array base since this is not difficult to fabricate when the conductor width is held constant.

The solar cells do not cover the panel edges immediately in front of the harness so that the temperature of the cells is not affected by the harness. Printed circuit copper pads at the ends of the electrical modules extend into this area and are exposed so that the FCC can be terminated on the panel. Alusol solder and 673 flux are used to join the aluminum conductors to the copper pads. The joint is encapsulated with an epoxy adhesive to prevent humidity damage prior to array operation. The minimum aluminum conductor width is limited to 0.127 cm (0.050 in) to facilitate fabricating the joints. The harness is attached to the array panels with adhesive on 1.77 cm (0.5 in) wide areas on either side of a hinge. The harness is wrapped with a 0.5 in wide adhesive tape at these locations to fix the location of the FCC bundle which has 9 cables at the inboard end. Lightweight plastic ties and thermal control aluminized film tapes provide additional support of the harness weight in 1 "g" and control of the position of cables with respect to each other. The mounting method allows some movement of the cables and prevents the harness from being loaded by the tension being placed in the array blanket. The fold to fold distance on the harness is slightly longer than that on the flat fold solar array. The edge of each solar panel is cut out in the fold area where the harness will project forward of the panel folds.

The termination of the FCC harness on the inboard end of the array is shown in Figure 2-17. Individual RWC copper wires are fused, balled, flattened and attached to the aluminum conductors near the RWC connector receptacles on the array storage container near the extension mast. The joining technique is the same as for the FCC to array panel joints and the joints are also encapsulated. The array harness sizing is described in Section 2.4.2

2-62

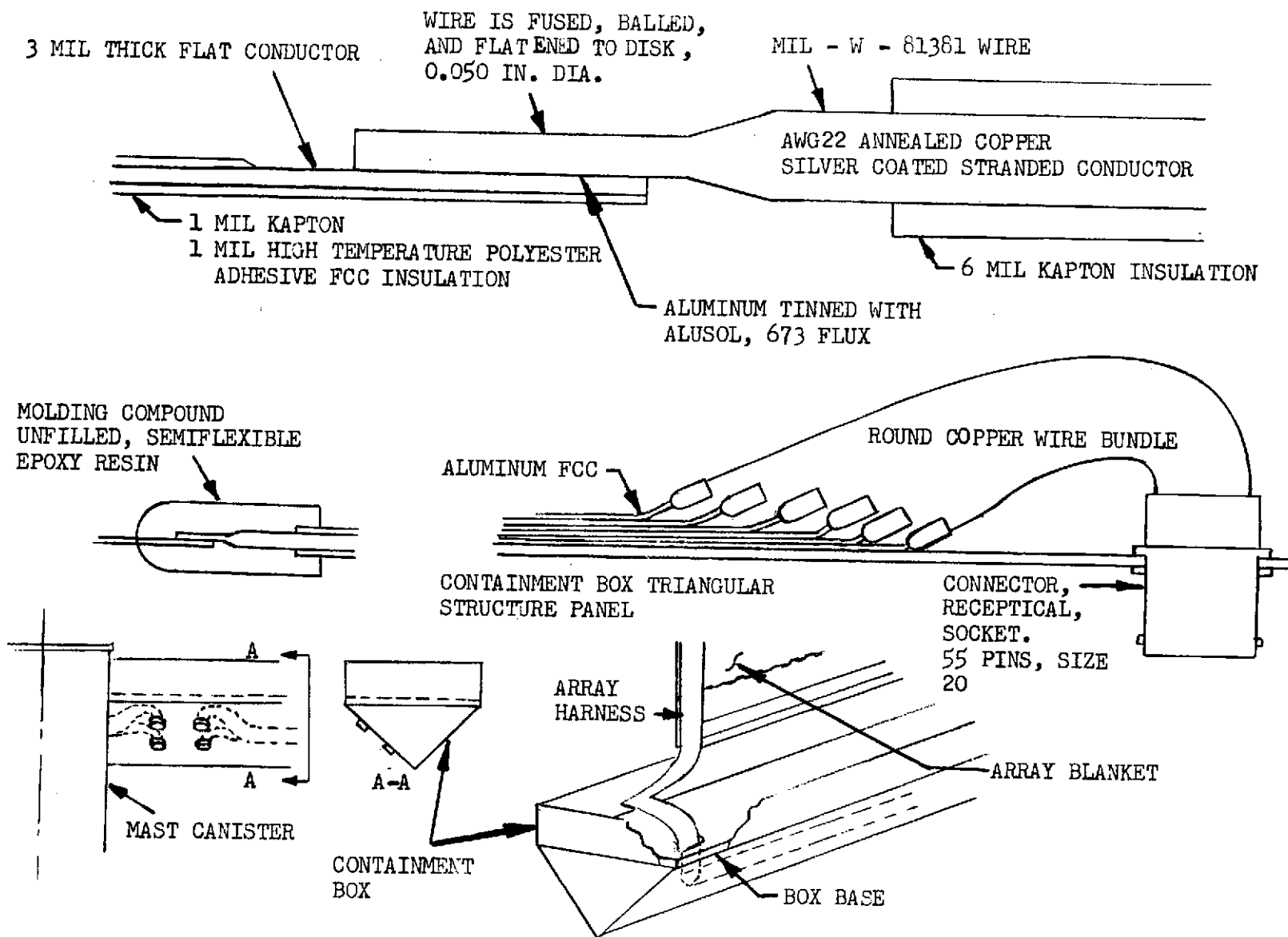


Figure 2-17 FCC Harness Inboard End Termination

LMSC-D384250

## 2.4.2 Electrical Design Studies and Tradeoffs

This section of the SEPS Solar Array Study final report discusses the important areas of system analysis, component design and selection that pertain to the electrical portions of the solar array. By nature of the fact that there are dominant weight restraints, the array is of a large size, and there are stowed volume space allocation limitations, only the lightweight flexible substrate type of solar array (as opposed to rigid substrate) was a candidate for consideration. This and the selection of flat fold stowage discussed in Section 2.3.2 directly impacted the Harness tradeoffs and selection.

### 2.4.2.1 Panel Electrical Configuration Analysis

The main parameters to be considered in the correct selection of the parallel and series string for the SEPS panels are: a) allowable periphery dimensions (space allocation), b) solar intensity, c) cell temperature and d) voltage range. The current Shuttle launch concept can accommodate an array width in the 160 in. category and the resultant array panel length, which is in the direction transverse to the deployment direction, could be in the space left after allocation for stowage box structure, edge spacing and a harness width allocation. The other allowable periphery dimension of the panel, panel width, was found to be about 0.76 m (2.5 ft.).

Shift in solar displacement from 1 au to 0.3 au, ingoing missions, and from 1 au to 6 au, outgoing missions, has the direct effect of changing illumination intensity which results in the secondary effect of changing the array temperature. Change in illumination intensity by itself changes the output current of the cells but has little effect on cell voltage. Change in cell temperature dramatically changes the Voc open circuit voltage and correspondingly the Vmp voltage at maximum power. In order to assess the number of cells which should be in series to obtain a module, or multiples thereof, that satisfy the unreg. source range of 200V to 400V, it is necessary to develop array temperature reference data. Figure 2-18 presents solar flux, in milliwatts per square centimeter as a log function, as it relates to distance from the sun--AU astronomical units, 1 au being the distance from the sun to the earth. This data is used to develop cell temperature and, knowing conversion efficiency, determining power output at different mission displacements.



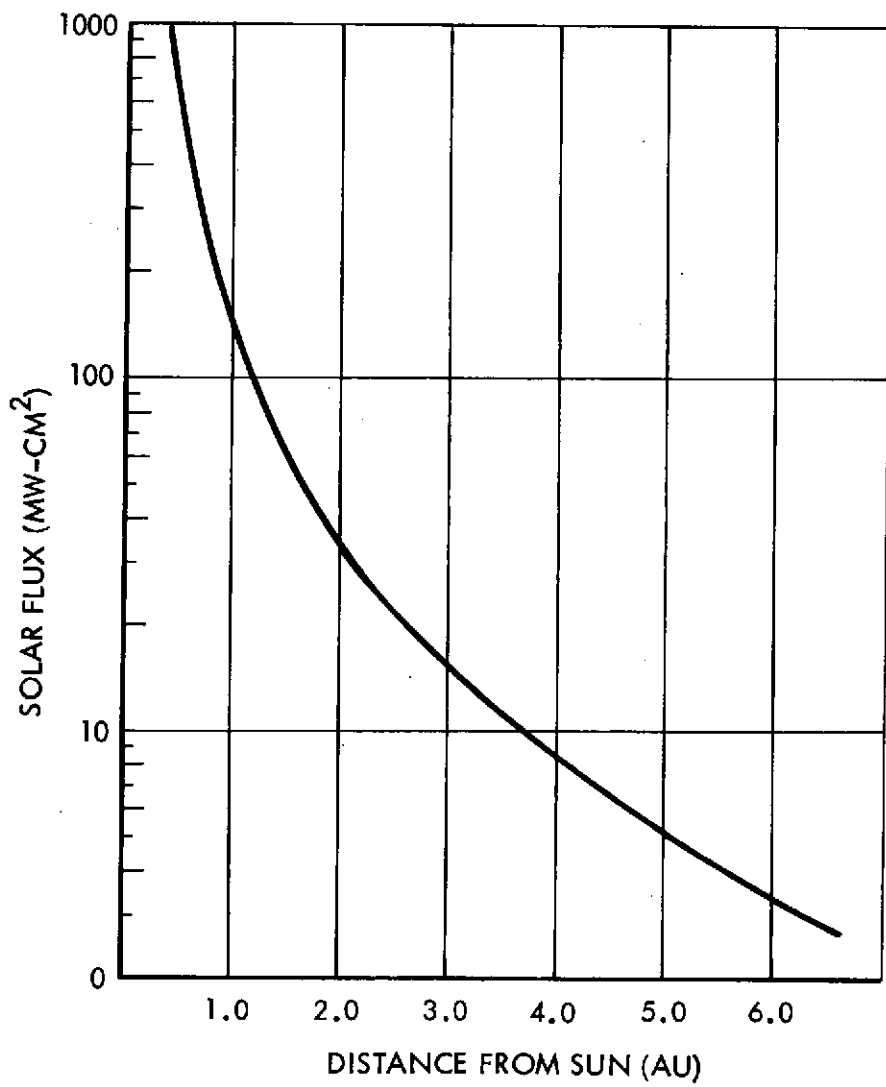


Figure 2-18 Intensity Vs Sun Distance

With solar intensity known and using the thermal optical properties of the cell covers and substrate materials, computer runs were made to project array temperature. From these runs the temperatures were determined to be  $159^{\circ}\text{C}$  at 0.6 au,  $50^{\circ}\text{C}$  at 1.0 au,  $-23^{\circ}\text{C}$  at 1.6 au and  $-145^{\circ}\text{C}$  at 6 au. This data is plotted in Figure 2-19 and is shown to correlate well with data from reference 1 for 0.72, 1.0, 1.52, 2.77 and 5.2 au corresponding to Venus, Earth, Mars, Asteroid Belts and Jupiter respectively. Also depicted on the figure are indications of temperature limiting by tilting the arrays away from normal incidence for the three following cases.

The next step in the analysis was to develop plots showing cell voltage as a function of temperature and intensity combined. Data exists in the literature which depicts cell performance at varying illumination intensities, but with temperature held constant--usually at  $28^{\circ}\text{C}$ . This is meaningful for showing general cell parameter changes but for exact simulation, temperatures must be incorporated that correspond to intensity at varying au.

Using as a baseline the 2 ohm-cm base resistivity, 200 micron (8 mil) N on P cell, data was plotted to depict cell open circuit voltage as a function of sun distance. This is shown in Figure 2-20 along with a curve depicting cell voltage at maximum power,  $V_{mp}$  at beginning of life, BOL. For this study EOL power level is down 16% from 25 KW to 21 KW from all degradation effects for five years at 1 au, free space. The degradation mechanism which will dominantly effect cell voltage shift-down is particulate radiation. The radiation causes a greater reduction in current than it does in voltage, however, this specific portion of the study addresses itself to sizing the series string therefore the voltage shift-down component of specified EOL limits was factored into Figure 2-20 to develop the dash line which is a representation of EOL voltage at max power. The shaded curve band then represents the range of maximum power voltages over the projected mission life from 0.3 au to 6.0 au.

It should be noted that in future contract phases when specific mission trajectory, ephemeris, life and launch dates are known, the trapped plus solar flare particulate radiation environments will be mapped and corresponding factors developed for cell/cover degradation, and that final cover thickness selections will be made accordingly, as will voltage shift-down analysis. It is further noted that the trend in the improved

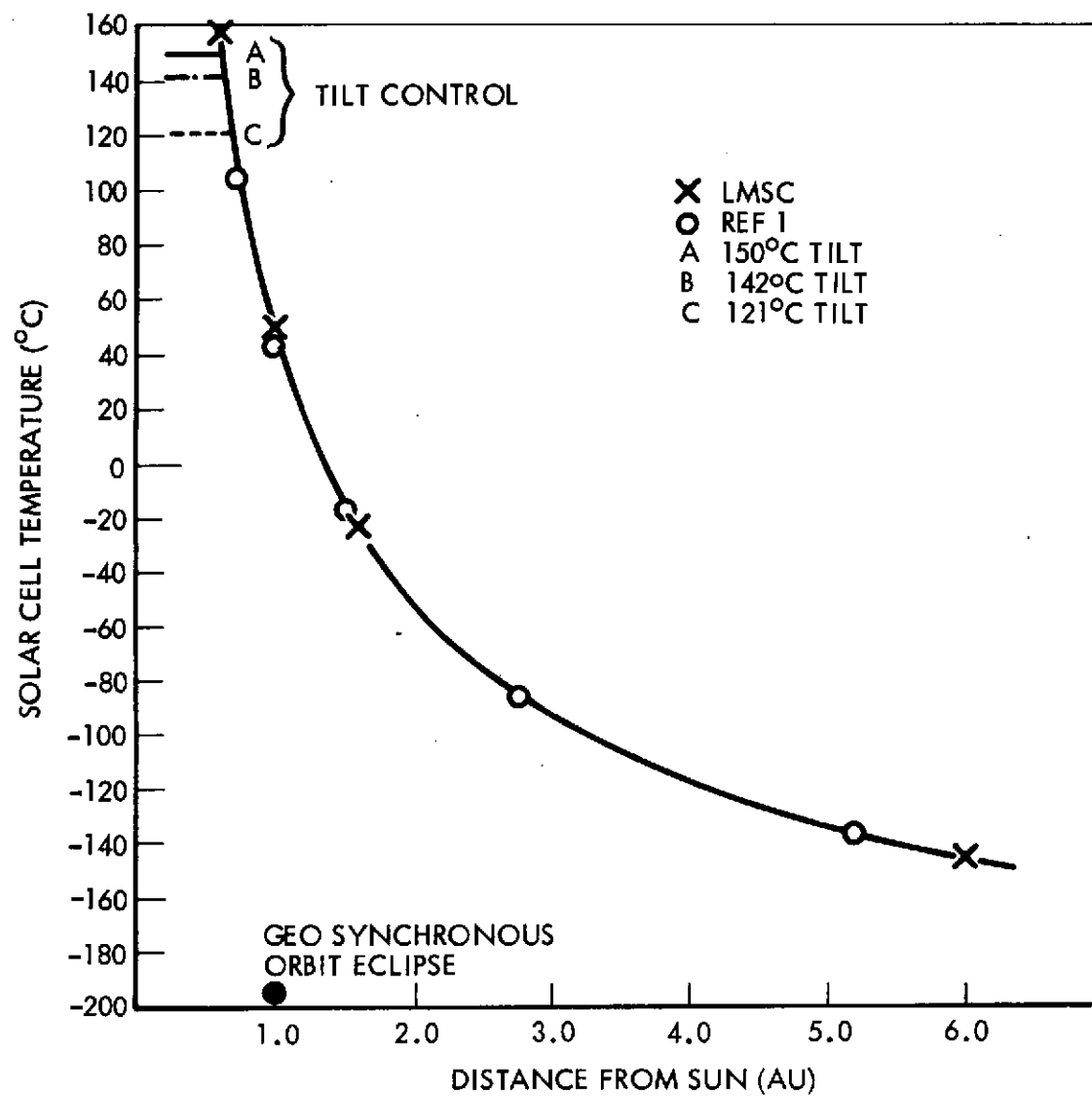


Figure 2-19 Cell Temperature - Normal Incidence

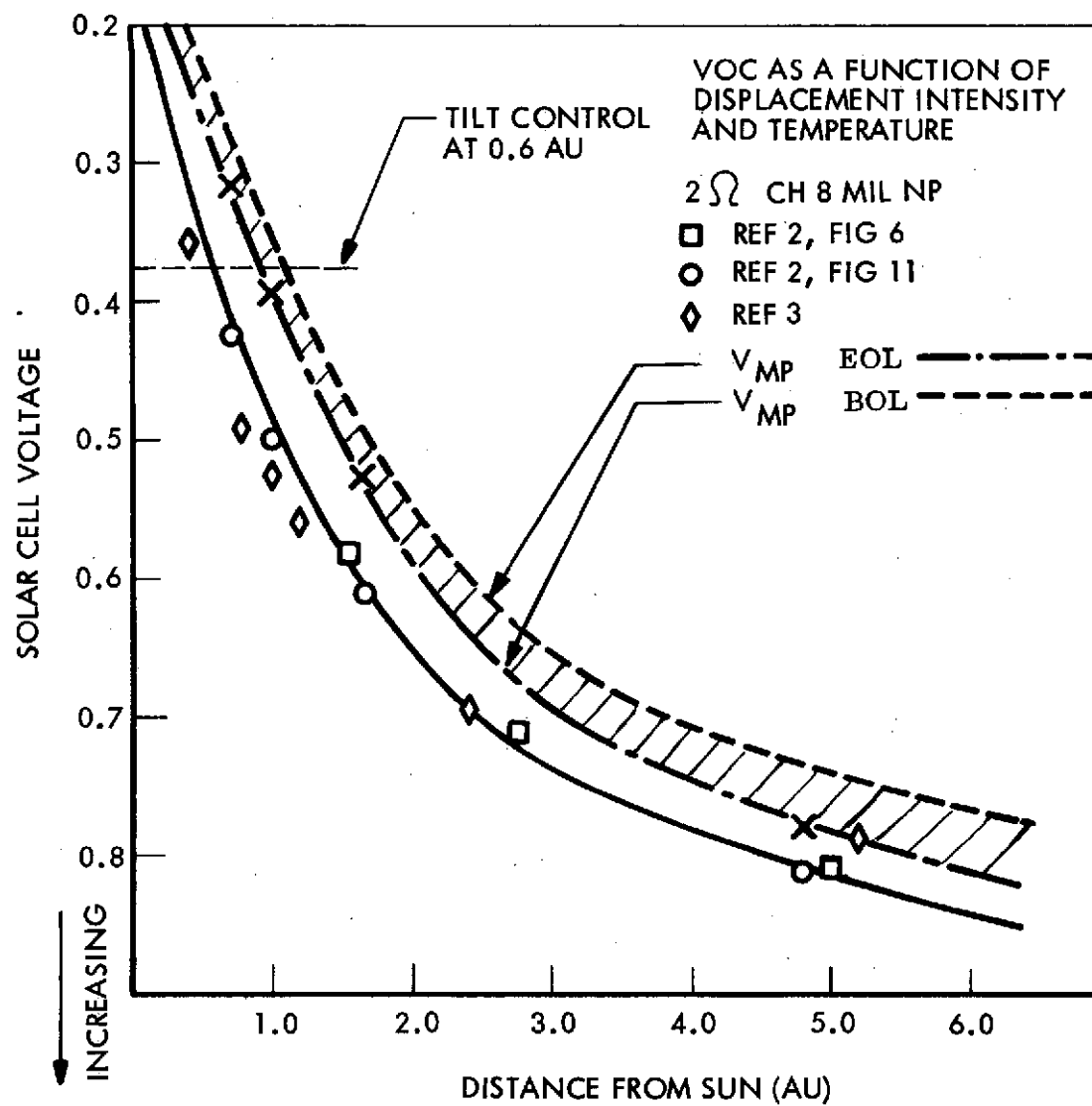


Figure 2- 20  $V_{oc}$  As a Function of Displacement, Intensity and Temperature

efficiency solar cells, both the Heliotek 1050 types and the Centralab Violets, is toward voltage enhancement partly due to back surface field effects. The selected SEPS cell design will require characterization of voltage and current at maximum power vs temperature, illumination, and electron and proton irradiation prior to fabrication of flight hardware.

2.4.2.1.1 Series String Selection . For inbound missions going from 1 to 0.3 au or for solar flyby missions where solar intensity initially increases, individual cell max power voltage could go through a BOL shift from 0.43 V at 1 au to Zero V at 0.3 au with no tilt control. However, with tilt control occurring at 0.64 au and limiting of array temperature to 121°C the voltage shift would be only 0.14 volts from 0.43 to 0.29 BOL. Assuming a mission situation where tilt control did not occur until 0.61 au, temperature went to 150°C, and that the full assumed radiation degradation shift back had set in, voltage shift would be 0.21 volts from 0.43 to 0.22 for a single cell. Looking at three different complements of 600 cells in series (cis), 640 cis and 680 cis, for the array module and 600, 640 and 680 for the panel, the following voltages would be achieved at the solar array panel level bus.

<u>Cells in Series (cis)</u>	B. O. L. Module Voltage Range for Ingoing Missions	
	<u>121°C Max</u>	<u>150°C + Degradation</u>
600 cis	174 - 258	132 - 258
640 cis	185 - 275	141 - 275
680 cis	197 - 292	150 - 292

With a 25% harness voltage drop at 0.3 au due to high temperature and current, a module series string of 306 cells (612/panel) and four modules (2 panels) switched in series in the stage will provide 200 volts at the vehicle bus.

For outbound missions going from the Earth at 1 au towards and past Jupiter to 6.0 au, the cell temperature is greatly reduced increasing cell voltage and requiring inflight series string switching to stay within the prescribed 200 to 400 volt range. Figure 2-21 illustrates panel voltage characteristics as a function of cells in series from 1 au to 6 au. It can be seen that the three cases, 600, 640 and 680 dependent upon when they

AS A FUNCTION OF CELLS IN SERIES FROM 1 AU TO 6 AU (OUTGOING MISSIONS)

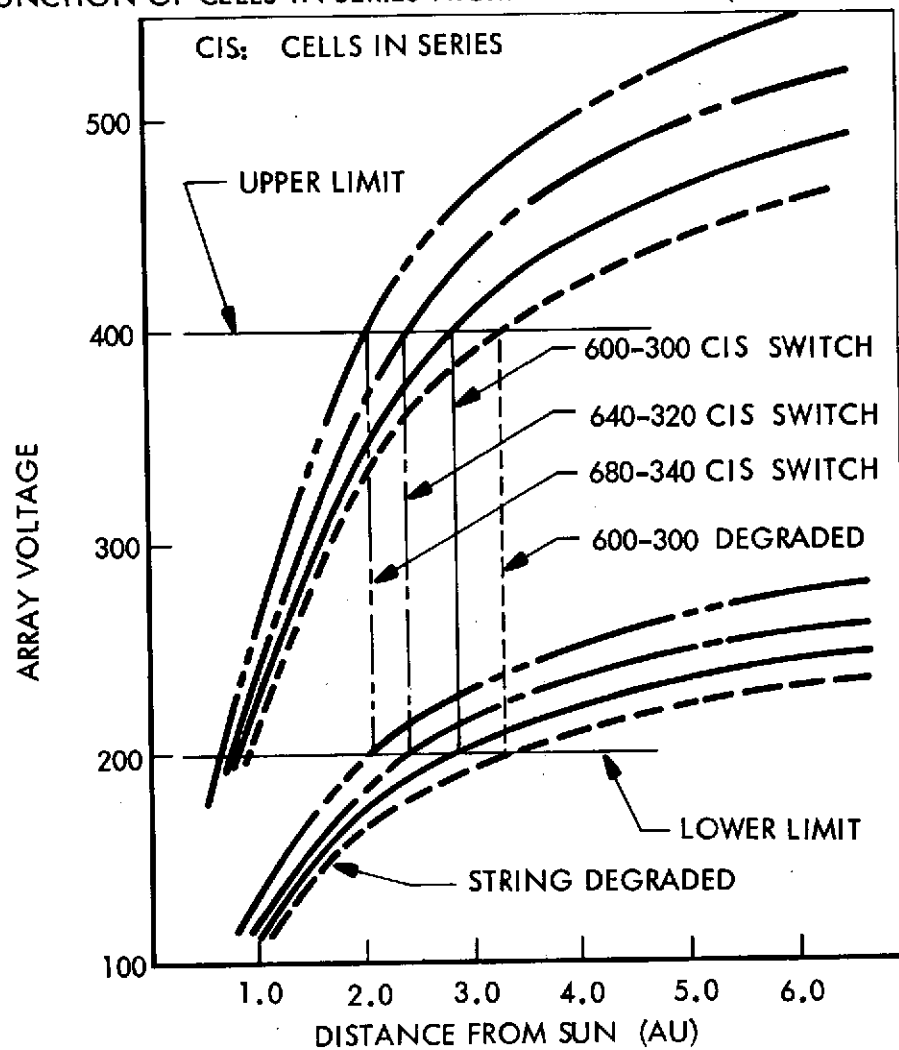


Figure 2-21 Panel Voltage Characteristics

are switched down to the module string level, would all stay within the prescribed voltage range between 1.0 and 6.0 au. The switching would occur between 2.08 au and 3.1 au dependent upon which series complement was selected.

Several factors favor the smaller series string range: 1) Voltage change is more gradual (flatter) with the 600-300 cis case, 2) Should some malfunction occur which precluded switch down from the panel to module (1/2 panel) string level, with the 600-300 case, voltage would go 15% above upper limit (undegraded) whereas with 680-340 it would go 37.5% above upper limit, 3) As alluded to previously, if higher efficiency-voltage enhanced cells are used for flight hardware, they can be accommodated with minimum impact as a direct substitution into the lower count series string.

2.4.2.1.2 Cell Paralleling Selection. The dominant factors associated with selection of cells in parallel are: 1) redundancy for reliability, 2) efficient use of allocated area (high packing factor), and 3) cell shadowing. The SEPS arrays will rotate, for sun orientation purposes, about the centerline of their longitudinal axis. This sweeps a cylinder approximately 14 feet in diameter and 105 feet long per wing. To avoid mechanical interference between the solar array and structure projecting from the vehicle, the structure would have to offset sufficiently to avoid mechanical interference with the array as it rotates  $360^{\circ}$ . With the weight constraints on SEPS, the potential shadow casting components such as antenna, boom, probes, etc., would probably be clustered close to the vehicle to minimize heavy stand-off and dog leg root structure. Should non-avoidable, consistently static shadowing occur it would most likely occur at the inboard end near the vehicle. Therefore, if such were the case, the innermost array panels could contain single series strings or by-pass diodes.

Developmental work is also being done on integral diode wraparound electrode solar cells. Multi string modules could be accommodated with least impact on harness design at the inboard location because this would result in the shortest runs for the required multi conductor FCC.

For the SEPS array the solderless cells that will be interconnected using non-soldered techniques can withstand very high transient and static localized temperature without sustaining damage as compared to the earlier soldered assembly cells.

The 5 solar-cells-in-parallel design was evaluated for hot spot conditions in free space at one au and  $50^{\circ}\text{C}$  cell temperature. A condition of stationary full shadowing was assumed on one cell and on two cells in the same parallel 5 cell submodule. The reverse current-voltage characteristic of the unshadowed cells was assumed to be the same as the "low leaker" (Type 8L Solar Cell, Figure 2-32, pg 2-30, "SAS z-local Vertical Study", Vol 1, Summary, TRW Systems, November 1971). The resulting operating points of the "100 volt" SEPS solar array module at beginning of life is shown in Figure 2-21. The power dissipated in each unshadowed solar cell is 1.77 watts with one cell shadowed and 3.64 watts with two cell shadowed. The predicted cell operating temperature based on these dissipation levels and Large Space Station Solar Array thermal studies is  $125^{\circ}\text{C}$  for one cell shadowed and  $180^{\circ}\text{C}$  for two cells shadowed in the same 5 cell parallel submodule.

**2.4.2.1.3 Cell Paralleling vs Array Width.** The array blanket width associated with the 160 in long storage volume is 3.99 m (157 in), and the selected module layout is depicted in Figure 2-22 with 5 cells in parallel and 306 in series. The circuit routing is serpentine to cancel any current induced torques plus adjacent panels can be mirror images to further enhance torque cancellation as shown in Figure 2-23. The module is basically a 100 volt unit at 1 au. Two modules can be interconnected in series to provide 200 volts.

A group of five cells in parallel by 17 in series forms the basic module segment (85 cells) of which there are 18 per module. There are then 9 module segment bays per module which results in the module being 45 cells by 34 cells. This corresponds, with dimensions of 1.591 in x .788 in. for the solar cell plus 0.050 in. spacing, to a module cell area width of 1.87 m (73.80 inches). Allowing 0.25 inches at the panel center line the panel cell area width becomes 3.76 m (147.85 inches). Subtracting this from the 3.99 m (157 inches) allocated,  $\frac{9.15}{2} = 4.58$  inches is available at each edge of the panel for the power feeder harness.

Another method of gaining the right fit if edge space is limited (which is primarily a function of cells in parallel) would be to slightly modify cell size, shaving cell length ( $< 1.591$ ) and adding to cell width ( $> .788$ ). The size/area correlations of the cells are as follows.



2-72

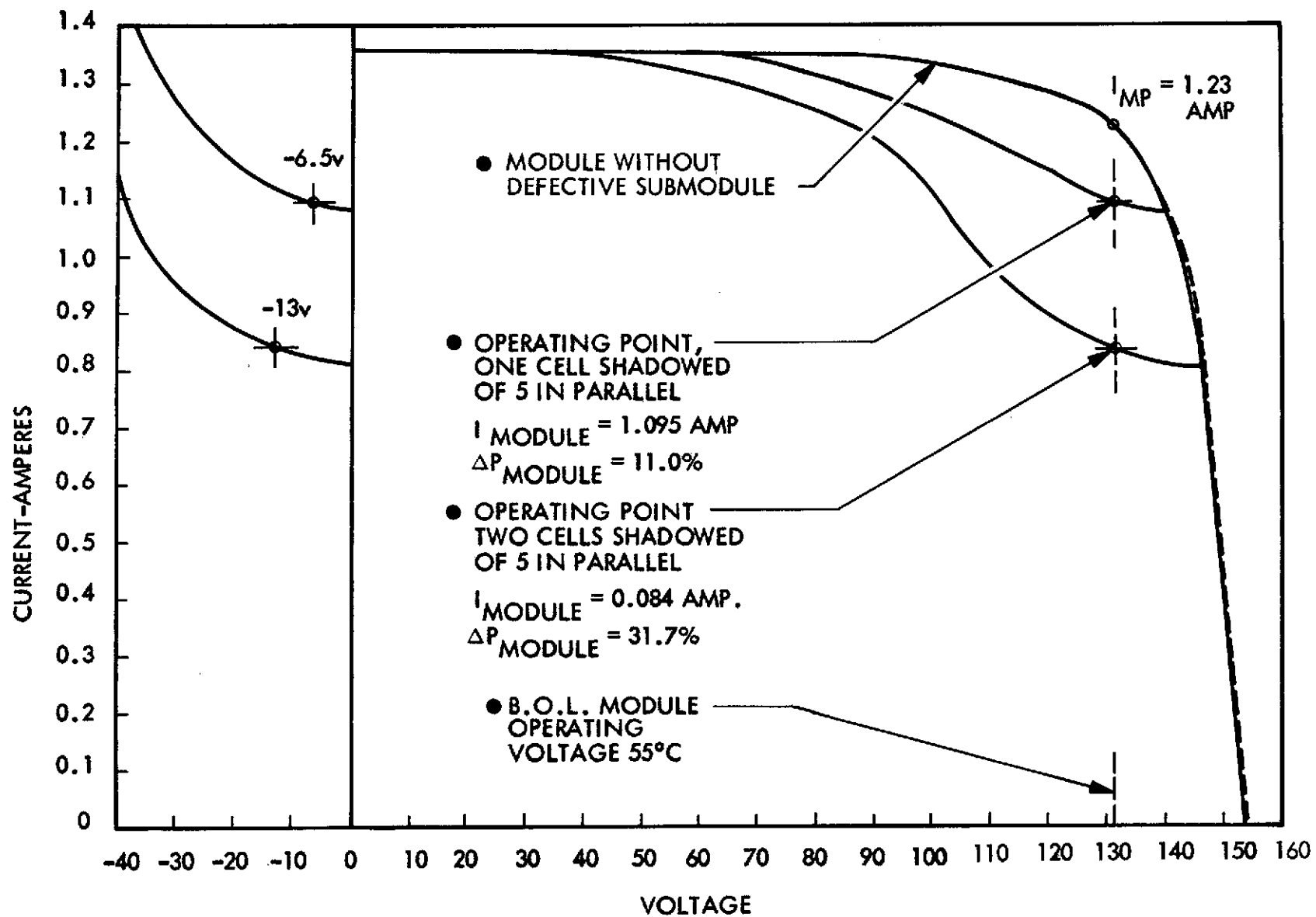


Figure 2-21a Shadowed Module I-V Characteristics

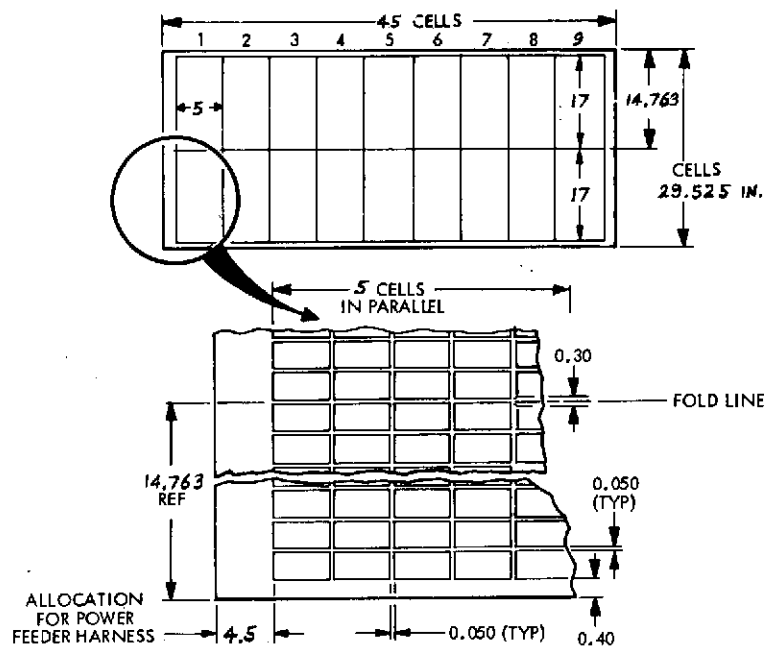
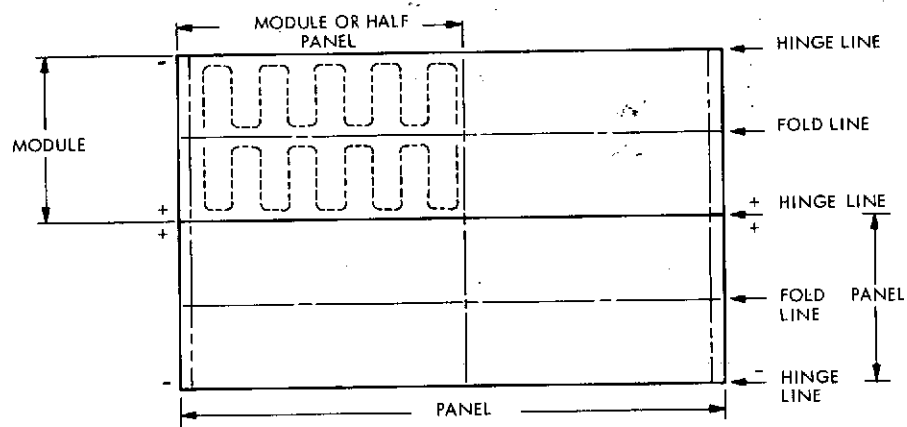


Figure 2-22 Electrical Module Selection

SOLAR ARRAY MODULE**5** CELLS IN PARALLEL BY **306** IN SERIES**1530** CELLS TOTALSOLAR ARRAY PANEL

2 EA MODULES

**3060** CELLS TOTAL

Figure 2-23 Array Panel Configuration

Reference		2 cm (.7874)	x	4 cm (1.5748)	Area 8 cm <sup>2</sup>
Baseline Cell		.788	x	1.591	8.09 cm <sup>2</sup>
(Delta)	+	.0006	x	+ .0162	
True 4 cm		.796	x	1.575	8.09 cm <sup>2</sup>
(Delta)	+	.0086	x	Net	
Under 4 cm		.799	x	1.568	8.09 cm <sup>2</sup>
(Delta)	+	.012	x	- .007	

Maintaining the same cell area as the baseline cell, if cell length is held to the net 4 cm dimension, 1.44 inches would be picked up to allocate for harness width, going under net dimension .007, 2.06 inches would be picked up. A variety of examples including current Air Force and communication satellite programs can be cited where in final design, cell size has been tuned to achieve the best packing factor for the specific application. The cell vendors can accommodate minor changes of this type where the cell quantity is of sufficient size to amortize tooling costs.

From a reliability standpoint multiple cells in parallel are recommended to effect redundant series paths. The greater the length of the series string the more impetus for redundant series paths via paralleling.

The baseline parallel selection for the narrow aspect solar array is 5 cells in parallel. This number provides a good fit with the number of cells-in-series desired and the containment box short dimension 0.46 m (18 in.).

The total voltage change of the solar cells, as seen at the stage, including the effect harness voltage drop at high temperature, (0.3 au), over the au range of 0.3 to 6 is 0.165 V to 0.75 V for the radiation degraded cell voltage. This represents a factor of 4.5 and necessitates changing the number of electrical modules in series by switching in the vehicle to provide the required configurations:

	<u>0.3 to 0.75 au</u>	<u>0.75 to 3.1 au</u>	<u>3.1 to 6.0 au</u>
No. of Electrical Modules (306 CIS) In Series	4	2	1
Stage Voltage	200 to 400	200 to 400	200 to 240

#### 2.4.2.2 Array Power Feeder Harness Analysis

The first task in arriving at the specific configuration of the Power Feeder Harness Analysis was to perform tradeoffs to assess the suitability of the various harness design options which are possible candidates for the SEPS array. There are six separate, distinctive harness design options that were considered. It is acknowledged that there are several adaptations and refinements of these options, but it is noted that the salient option characteristics are represented in the six designs depicted.

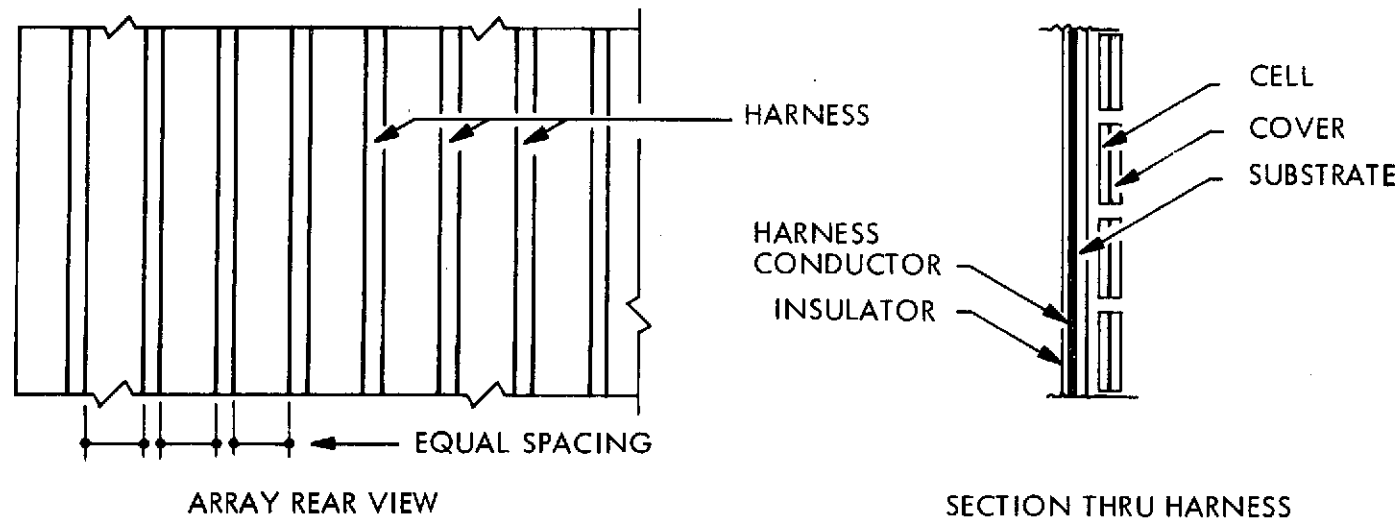
##### 2.4.2.2.1 Power Feeder Harness Options

1. Backside Integral
2. Edge Mounted
3. Backside Transverse
4. Primary Substrate
5. Pantograph
6. Segmented Printed Circuit

Backside Integral - This harness concept refers to the incorporation of FCC on the rear surface of the array substrate spaced at even intervals (Figure 2-24). The section shown would be the lightest version of the backside integral concept with a single sided insulator, the array substrate providing the insulation on the side adjacent to the bare conductor.

Edge Mounted - With this power feeder harness option the conductors are grouped into FCC layers at the edges of the array in flat fold (firehose fold) fashion similar to the array layers (Figure 2-25). This is the concept which was developed and used for the Space Station Solar Array (Ref. 4, Fig. 3.2-19, page 3.2-52). As shown in edge view the FCC harness has a large radius at the hinge and fold lines so the array can be properly tensioned without supplementary loading from the harness. The harness has a greater fold radius than the array proper so that it will lay flat and so that it is essentially untensioned when the array is fully deployed.

Backside Transverse - The backside transverse harness, similar to the End Mounted, is a layup of FCC (Figure 2-26). Its routing somewhat parallels the geometry of the



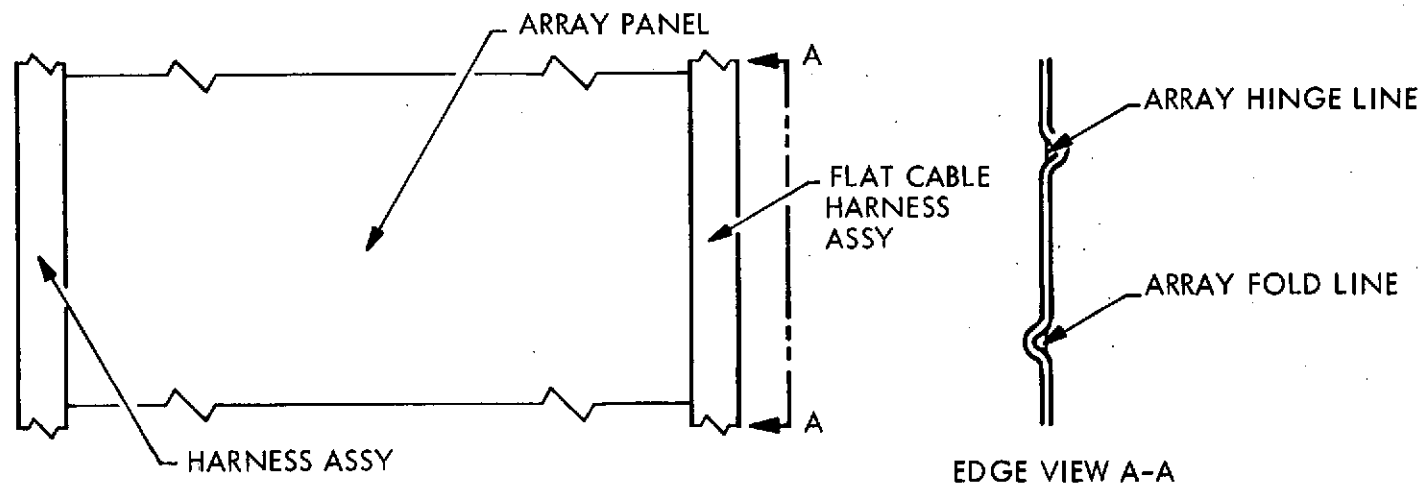
#### ADVANTAGES

1. MAY EFFECT WEIGHT SAVINGS BY USING ARRAY SUBSTRATE AS ONE LAYER OF INSULATOR

#### DISADVANTAGES

1. CREATES BACKSIDE THERMAL BARRIER CAUSING LOCALIZED INCREASE IN CELL TEMPERATURE
2. CREATES NON UNIFORM STACK CROSS SECTION COMPLICATING AND COMPROMISING STOWAGE PRESSURE DESIGN
3. CONTRIBUTES TO LAMINATED BEAM EFFECT CAUSING DIFFICULT FOLD LINE DESIGN
4. COMPLICATES MODULARITY – EASE OF PANEL REPLACEMENT AND REPAIR

Figure 2-24 Harness Option - Backside Integral



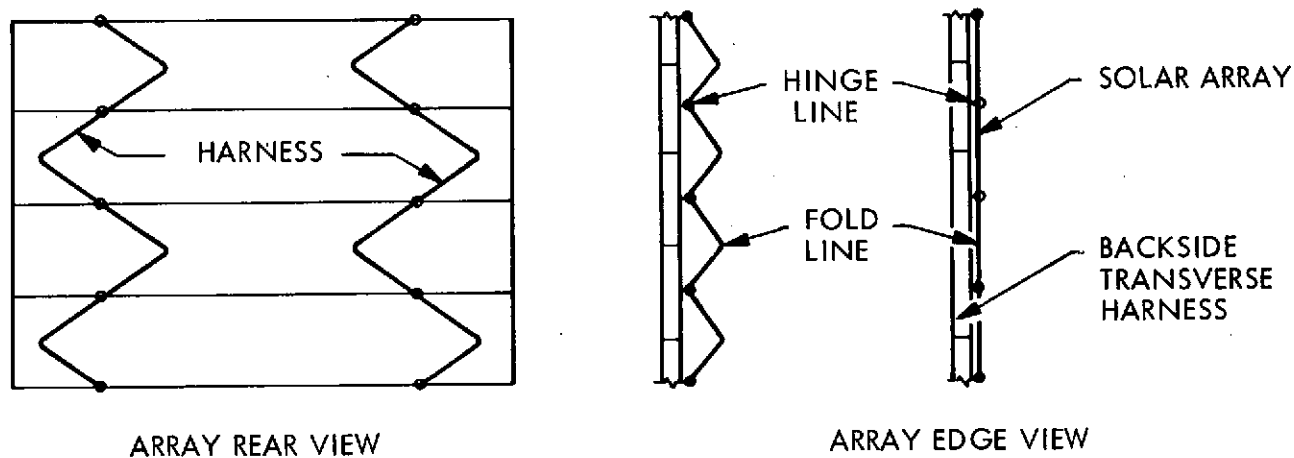
#### ADVANTAGES

1. COMPATIBLE WITH MODULARITY, PANEL REPLACEMENT AND REPAIR
2. SEPARATE FROM CELLS SO APPROPRIATE PRELOADING CAN BE INCORPORATED
3. DOES NOT CREATE BACK SIDE THERMAL BARRIER
4. DEMONSTRATED ON SPACE STATION SOLAR ARRAY TEST QUADRANT AND AF PROGRAM QUAL TEST ARRAY

#### DISADVANTAGES

1. REQUIRES ADDITIONAL ARRAY WIDTH OR ADDITIONAL ARRAY LENGTH IF ARRAY IS WIDTH LIMITED

Figure 2-25 Harness Option - Edge Mounted



#### ADVANTAGES

1. MINIMAL IMPACT ON ARRAY WIDTH
2. HARNESS SEEN "ON EDGE" THEREFORE LESS THERMAL IMPACT  
BACKSIDE INTEGRAL HARNESS
3. SEPARATE FROM CELLS SO APPROPRIATE PRELOADING CAN OCCUR

#### DISADVANTAGES

1. INCREASED LENGTH AND WEIGHT SO HARNESS DOESN'T GO OVER CENTER OR INTRODUCE ADDITIONAL LOADS
2. TERMINATION JUMPER DESIGN INVOLVES TWIST AS WELL AS SIMPLE BENDING MOTION

Figure 2-26 Harness Option - Backside Transverse

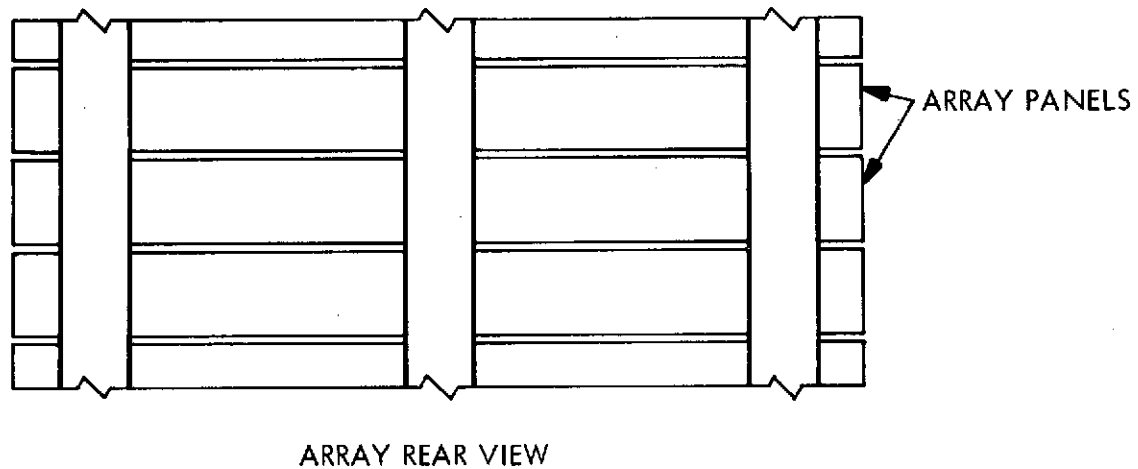
transverse folding beam used on the Skylab workshop solar array. The harness is attached to the array at the hinge lines, at which location the module power jumpers route from the cable to the module terminals.

Primary Substrate - With the Primary Substrate option the harness serves the electrical function of conducting power and the mechanical function of being the "attach-to" base for the panels, and the folds and hinges for the panels (Figure 2-27 ). The P. S. harness runs the entire length of the array with the harness acting as the major structural tension members. The panels are independently fabricated and assembled to the harnesses to make electrical and mechanical connections.

Pantograph - General Electric during the 110 watt per kilogram study developed an interesting "alternative blanket folding approach" for flat-fold arrays wherein the array panels are articulated with supplementary edge membrane pantographs or scissors elements such that the panels do not mate cell face to cell face in the stowed condition (Figure 2-28). Each panel rotates  $90^{\circ}$  as it is deployed and in the stack condition each cell face is against the padding on the backside of the next panel. The supplementary membranes added at the edge could be FCC for routing power inboard from the panels. The harness could comprise the forward or rear section of the scissors assembly as shown in the above illustration from Ref. 5.

Segmented Printed Circuit - The solar array harnessing concept, as its name denotes, is made using printed circuit techniques (Figure 2-29 ). It therefore is length limited due to restraints on photoresist, exposure, etch equipment to maximums of approximately 12' to 20'. If step and repeat procedures can be used without objectionable registration problems, longer lengths can be achieved. The best current example of a Segmented Printed Circuit solar array power harness is the one used for the Canadian Technology Satellite (Ref. 6). The SPC harnesses are attached to several solar panels, four in the case of the CTS application, and supplementary "bridge piece wiring" is used to electrically interconnect the panel sets to each other.





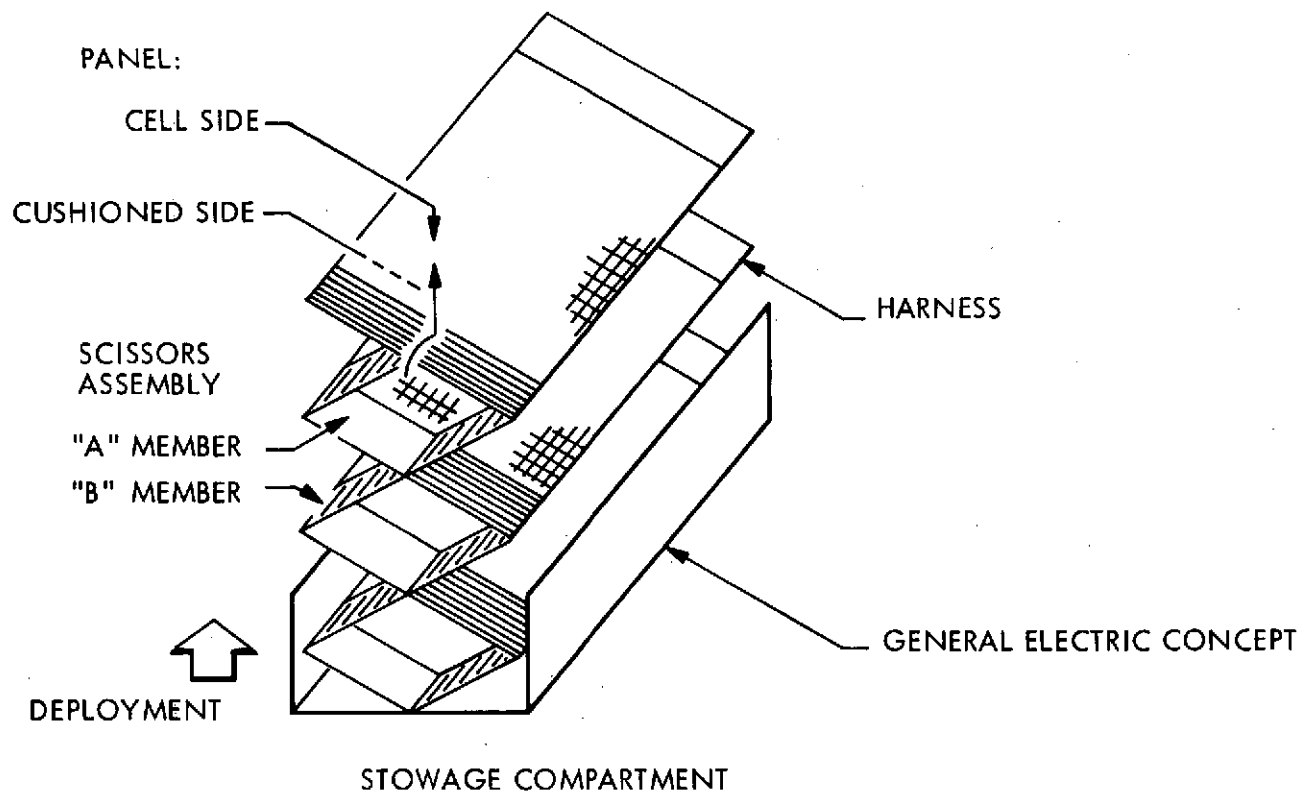
#### ADVANTAGES

1. SERVES DUAL FUNCTION

#### DISADVANTAGES

1. ADDITIONAL BACKSIDE THERMAL BARRIER
2. NON UNIFORM STACK CROSS SECTION
3. COMPLICATES MODULARITY
4. POOR PANEL PERIPHERY STABILITY
5. WEIGHT PENALTY

Figure 2-27 Harness Option - Primary Substrate



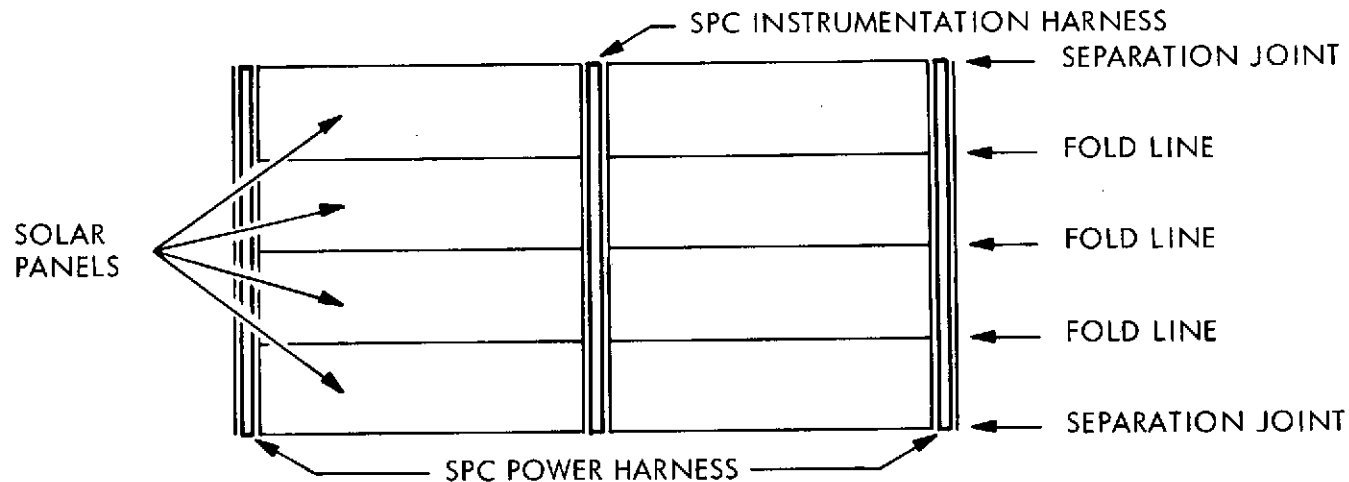
#### ADVANTAGES

1. NATURAL ELEMENT UTILIZATION IF PANTOGRAPH TYPE ARRAY IS USED

#### DISADVANTAGES

1. RESTRICTED TO USE WITH THE G.E. ARRAY CONCEPT
2. REQUIRES ADDITIONAL ARRAY WIDTH OR ADDITIONAL ARRAY LENGTH IF ARRAY IS WIDTH LIMITED

Figure 2-28 Harness Option - Pantograph



#### ADVANTAGES

1. CONDUCTOR RUNS CAN BE DESIGNED WITH DISCRETE JUMPER RUNS FOR TERMINATION TO PANEL BUSSES
2. PROVIDES A LEVEL OF MODULARITY
3. DOES NOT CREATE BACKSIDE THERMAL BARRIER

#### DISADVANTAGES

1. MANY IN SERIES CONNECTIONS IN EVERY POWER RUN
2. REQUIRES ADDITIONAL ARRAY WIDTH OR ADDITIONAL ARRAY LENGTH IF ARRAY IS WIDTH LIMITED
3. WOULD REQUIRE SACRIFICIAL TABS OR PADS AT EACH BRIDGE PIECE SO SUBSEQUENT JOINTS COULD BE MADE IN A NONSOLDERED SYSTEM
4. LEVEL OF MODULARITY REQUIRES DISRUPTION OF RUNS FOR MULTIPLE PANELS (8 ON CTS) TO ACCOMMODATE REPLACEMENT OF ONE PANEL

Figure 2-29 Harness Option - Segmented Printed Circuit

#### 2.4.2.2.2 Power Feeder Harness Concept Tradeoffs

The next step in the harness analysis after description of candidate concepts and their general advantages and disadvantages, was to evaluate them against six important evaluation criteria. Figure 2-30 summarizes the harness concepts ratings in consideration of the weighted criteria which are discussed below.

Weight/Size Impact - The major restraint of the SEPS application is keeping weight to a minimum, therefore this factor was given the highest point value out of 10, i.e., 2.2. Concepts that increase array temperature decrease cell output and thereby increase required array size to meet fixed power minimums. Therefore array backside membrane insulation sharing and harness placement behind the array reduce width, but not without a temperature penalty resulting in increased area and weight.

Compatibility with Modularity - The SEPS array is significantly larger than the FRUSA array, the CTS array and most flexible arrays which have progressed through design and testing phases with the exception of the Space Station Solar Array. By nature of its very size it must be modular in nature to be compatible with accessibility for fabrication and repair, spares, logistics and for low impact damage susceptibility. Column two of Figure 2-30 rates the harness concepts pertaining to their compatibility with achieving modularity in the array panel design. A backside integral harness concept, with multi conductors traversing the backside of the array, (even if they could be semi-permanently adhered with an acceptable adhesive) void the possibility of incorporating easily serviceable modular panels.

Maintainability - The maintainability assessment pertains to maintenance of the harness itself, i.e., how easy is the harness to a) get at in the first place, and b) to repair or replace should it sustain some fabrication or preflight damage. Maintainability is also important as a refurbishment factor if any inflight and or return by shuttle missions occur for sake of making modifications or repairs.

Interface Compatibility - This evaluation criteria pertains primarily to how well the selected harness design can be incorporated into an assembly with minimum impact on the mechanical design for launch survivability (padding and ascent preloading), and deployment and retraction.

WEIGHTING FACTOR*	2.2	1.5	1.7	2.0	1.5	1.1	CUM POINTS	RANK
EVALUATION CRITERIA CONCEPT	WEIGHT/SIZE IMPACT	COMPATIBILITY WITH MODULARITY	MAINTAINABILITY	INTERFACE COMPATIBILITY	MINIMAL THERMAL EFFECTS	PRIOR USE		
BACKSIDE INTEGRAL	Weight savings via possible insulation commonality, but some thermal/weight increase impact (2) 4.4	Dependent on level of mechanical and insulation sharing. May have to spare entire wing.	Poor access, tied to entire array (1) 1.7	Non uniform stack height, bad pre-loading (1) 2.0	Differential backside thermal barrier (1) 1.5	Flown on FRUSCA (3) 3.3	12.9	6
EDGE MOUNTED	Additional mandatory width (1) 2.2	Only remove power terminals to remove module (3) 4.5	Single function, easy access (3) 5.1	Allows uniform stack height (3) 6.0	No radiative or conductive barrier (3) 4.5	Built and tested on A. F. and L. S. S. S. A. (2) 2.2	24.5	1
BACKSIDE TRANSVERSE	Nominal width impact, weight increase over edge mounted (2) 4.4	Same as above (3) 4.5	Single function, easy access (3) 5.1	Uniform stack height - sophisticated termination (2) 4.0	Some view factor effects (2) 3.0	Mod. of the above sim. to Skylab structure (1) 1.1	22.1	2
PRIMARY SUBSTRATE	Possibility of dual function weight savings (2) 4.4	Dual function so separate disassembly steps required (2) 3.0	Access dependent on placement, tied to entire array (2) 3.4	Non uniform stack height, bad pre-loading (1) 2.0	Diff. backside thermal barrier (1) 1.5	No dem, testing or flight experience --	14.3	5
PANTOGRAPH	Additional mandatory width (1) 2.2	Same as edge mounted and backside transverse (3) 4.5	Interfaces to mech. function (2) 3.4	Must perform mech function with low section members (1) 2.0	No barrier (3) 4.5	No dem., testing or flight experience --	16.6	4
SEGMENTED PRINTED CIRCUIT	Additional mandatory width (1) 2.2	Must disassemble several bridge wire sets to remove module (1) 1.5	Feasible for segment replacement (3) 5.1	Uniform stack height (3) 6.0	No barrier (3) 4.5	Under development and test for CTS (2) 2.2	21.5	3

\*Points out of 10

○ Point Value of Concept for Specific Function

□ Weighted Product of \* and ○

Figure 2-30 Power Feeder Harness Concept Tradeoffs

Minimal Thermal Effects - For a most uniform temperature profile across the face of the solar array there should be uniformity in the cross section of the array with the reverse side array material held to a minimum, and with minimum protuberances which will affect view factor for thermal radiative rejection. If a harness is uniformly adhered to the back some of the radiative losses can be compensated by conduction and re-radiation. However if delamination should occur, heat transfer is locally dramatically reduced.

Prior Use - Prior use is a factor for consideration of a concept, largely due to the "off the shelf hardware", "cost effectiveness", "flight qualified" leverage such status implies. However this evaluation criteria was assigned the lowest point value because little use data exists and it is of insufficient quantity to have statistical validity.

As a result of the tradeoffs performed the Edge Mounted Power Feeder Concept is the baseline selection and the Backside Transverse Concept is the backup.

2.4.2.2.3 Harness Sizing Calculations. Using the electrical conductivity value for aluminum and conservative conductor spacing and insulation density factors, calculations were performed to assess what the general weight allocation for the power feeder harness should be. It was determined, as shown in the analysis contained in Appendix A, that for one array wing the weight budget should be 2.75 Kg for a 200 volt system when maintaining a voltage drop not in excess of 5.75 volts at 1 au. The minimum weight of a harness for a 100 volt system occurs with the same voltage drop, 5.75 volts, and is 5.50 Kg for one wing at 1 au. The harness design data is shown in Table 2-5.

#### 2.4.2.3 Solar Array Performance

It is assumed that angle of incidence effects on reflectivity of the solar spectrum are such that by maintaining constant temperature of the solar cells by tilting provides constant illumination energy to the solar cell. Fresnel's formulas, Ref. 10, indicate that the reflectivity of the solar cell covers for longer wavelengths will increase at a slightly higher rate than for shorter wavelengths as the array is tilted.

TABLE 2-5  
FCC HARNESS DESIGN

$$\frac{L}{A}_{\text{opt}} = 21.174 \times 10^6$$

One of two edge harnesses/wing,  
conductor thickness = 0.0762 mm (0.003 in)

Panel No.	Length Ft.	Conductor Width 2 ea. req'd.	Cable No.	Panel No.	Length Ft.	Conductor Width 2 ea. req'd.	Cable No.
41	108	6.22 mm (8.245 in)	1	9	28.0	1.61 mm(0.0635 in)	6
40	105.5	6.08 mm (0.239 in)	1	8	25.5	1.47 mm (0.0578 in)	6
39	103.0	5.93 mm (0.234 in)	1	7	23.0	1.33 mm (0.0522 in)	6
38	100.5	5.79 mm (0.228 in)	1	6 } 5 } 4 } 3 } 2 } 1 }	15.5	5.35 mm (0.211 in)*	6
37	98.0	5.65 mm (0.222 in)	1&2				
36	95.5	5.50 mm (0.217 in)	2				
35	93.0	5.36 mm (0.211 in)	2				
34	90.5	5.21 mm (0.205 in)	2				
33	88.0	5.07 mm (0.200 in)	2	Instrumentation			
32	85.5	4.93 mm (0.194 in)	3	54	1.33 mm (0.0522 in)	7	
31	83.0	4.78 mm (0.188 in)	3				
30	80.5	4.64 mm (0.183 in)	3				
29	78.0	4.49 mm (0.177 in)	3				
28	75.5	4.35 mm (0.171 in)	3				
27	73.0	4.21 mm (0.166 in)	3				
26	70.5	4.06 mm (0.160 in)	4				
25	68.0	3.91 mm (0.154 in)	4				
24	65.5	3.77 mm (0.149 in)	4				
23	63.0	3.63 mm (0.143 in)	4				
22	60.5	3.49 mm (0.137 in)	4				
21	58.0	3.34 mm (0.132 in)	4				
20	55.5	3.20 mm (0.126 in)	5				
19	53.0	3.05 mm (0.120 in)	5				
18	50.5	2.91 mm (0.115 in)	5				
17	48.0	2.77 mm (0.109 in)	5				
16	45.5	2.62 mm (0.103 in)	5				
15	43.0	2.48 mm (0.0975 in)	5				
14	40.5	2.33 mm (0.0919 in)	5				
13	38.0	2.19 mm (0.0862 in)	5				
12	35.5	2.05 mm (0.0805 in)	6				
11	33.0	1.90 mm (0.0749 in)	6				
10	30.5	1.76 mm (0.0692 in)	6				

\*Paralleled panels to maintain minimum conductor width of 0.050 in.

Angle of Incidence (Deg)	Wavelength (microns)	n	Reflectivity (no AR coating)	Increase from 0 to 65 Deg
0	0.4	1.470	0.0362	3.18 times
65	0.4	1.470	0.1151	
0	0.8	1.4525	0.0340	3.29 times
65	0.8	1.4525	0.1118	

At constant temperature this effect should shift the relative energy peak of the spectrum incident on the cell toward the blue and decrease the relative amount of long wave energy incident on the cell. These two effects while maintaining constant temperature tend to be offsetting as far as cell power is concerned. Test data on the SEPS cell will be required to accurately define the array performance.

The predicted  $P/P_o$  for the SEPS solar cells vs au is shown in Figure 2-30a. The array operating temperature vs au is based on calculations performed under this study. The  $P/P_o$  data vs illumination intensity and cell operating temperature is based on 2 ohm-cm cell data presented in Ref. 3. The curve does not include degradation effects. The maximum power point,  $P/P_o = 1.41$  occurs at  $r = 0.65$  au, cell temperature =  $136^{\circ}\text{C}$ . Maximum array energy is obtained if tilting starts at this  $P/P_o$  value and  $r = 0.65$  au to hold cell temperature at  $136^{\circ}\text{C}$ . A tilt of 75 degrees occurs at about 0.31 au. At this point, tilting is stopped and temperature is allowed to increase to  $150^{\circ}\text{C}$  as  $r$  decreases to 0.3 au and  $P/P_o$  decreases from 1.41 to 1.32. At 0.3 au, 73 degrees tilt and  $160^{\circ}\text{C}$  cell temperature,  $P/P_o$  is equal to 1.17.

Table 2-6 summarizes the predicted array performance over the design solar distance range. The E. O. L. values assume a 16 percent solar array base power degradation. The array harness design is optimized for weight at 1 au. The harness average temperature is assumed to be  $20^{\circ}\text{C}$  cooler than the solar cells since it is behind the solar array blanket for the most part. A thermal analysis should be performed on the harness to evaluate the effect of sun impinging on the edge of one harness at high array tilt angles and the effect of increased harness currents going toward the sun.



TABLE 2-6  
SEPS SOLAR ARRAY PERFORMANCE

Sun Distance AU	Harness Power Loss - B.O.L. (Percent of Cell Power)	E.O.L. Module* Voltage at Base	P/P <sub>o</sub> Cells		P/P <sub>o</sub> Array Base	
			B.O.L.	E.O.L.	B.O.L.	E.O.L.
0.3	25 percent	50 V	1.32	1.11	1.10	0.92
0.31 to 0.65	15 percent	63 V	1.41	1.18	1.32	1.11
1.0	4.0 percent	122.2V	1.0	0.84	1.0	0.84
2.0	0.38 percent	189.2	0.35	0.29	0.364	0.306
6.0	0.03 percent	252V	0.08	.067	0.0405	0.034

P<sub>o</sub>Base = 25 KW

P<sub>o</sub>Cells = 27.17 KW

\*Two modules are in series in vehicle when module voltage is less than 200V, four modules are in series when module voltage is less than 100V.

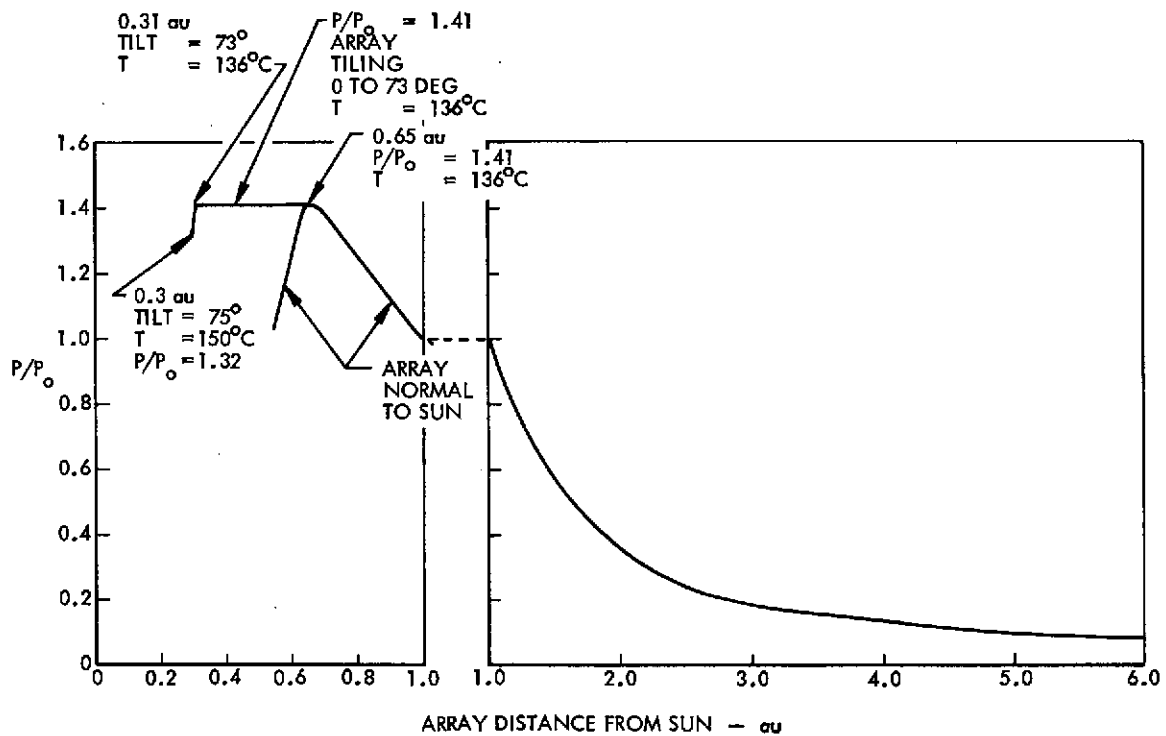


Figure 2-30a Array P/P<sub>o</sub> Vs Distance From Sun - No Degradation

## 2.5 DESIGN SUPPORT STUDIES

This section presents the results of dynamics, thermodynamics, space radiation and structural design studies.

### 2.5.1 Dynamic Analysis

The dynamic characteristics of the SEPS flat-fold solar array were studied. During the study, finite element models were constructed to accurately represent the array and to evaluate its characteristics. The results indicate some verification of previous analytical treatments and disclose some facets of the array dynamics which can be helpful in optimization of the structure during later phases of the program. In particular, a combination of pretensioning and boom stiffness was determined which maintains a specified minimum first mode frequency of 0.04 Hz while minimizing the required boom stiffness.

The models that were developed incorporated preloaded elements and in-plane and out-of-plane partitioning, to allow the most accurate definition of the array properties. Models were developed using SOLAR\*DYN, a specially written preprocessing computer program for solar array dynamic analysis and were analyzed using ASTRO, a general finite element routine which has the capability for inputting preloaded elements, specifically, the preloaded beam and membrane plate elements presented by Reference . Details of the development of the SEPS solar array baseline model with SOLAR\*DYN are presented, and representative dynamic characteristics of the array are discussed. Results agree qualitatively with those presented in Reference 8.

#### 2.5.1.1 Study Approach

The SEPS/Solar Array is a 32.0m x 4.1m flat-fold array. The array with the extension device has approximately 154 Kg of extensible weight. The blanket of the array is subjected to a dual-level tensioning system to provide control of the

frequency response of the system with partial and full extension. The base (inboard edge) of the array is pretensioned to a level  $T(1)$  at full extension through the use of a negator system. The tension value of the system is maintained at this level over dimension variations due to system temperature changes and also during spacecraft maneuvers. An outboard section of the array is maintained at a slightly higher preload,  $T = T(1) + T(2)$ , through the use of negator loaded wires attached to the intermediate tension bar between the two sections. The array has a single extension mast which is precompressed in reaction to the blanket pretension. The general arrangement of the array is shown in Figure 2-31.

In the model developed, a 4 x 6 mesh of preloaded membrane plates is used to represent the blanket for out-of-plane freedoms, with a set of preloaded light beams (wires) for characterization of the in-plane blanket motion. The boom is represented by a nine-element precompressed beam. In addition, tension wires and cross beams are included to model the corresponding sections of the actual array. The model general arrangement is shown in Figure 2-32. Here, the wire (in-plane) elements are shown separately since they form a separate partition in the model. This partitioning permits characterization of different allowable freedoms for the same node points in different partitions, thus allowing the in-plane and out-of-plane models to be combined in one problem solution.

Previous studies (Reference 8) have shown that a relationship exists for the blanket/boom arrangement of the SEPS array wherein there is some minimum value of boom stiffness ( $EI$ ) which, when combined with the proper blanket tension, produces a specified frequency of the array system. For this study, it was desirable to demonstrate that this relationship did exist, and to evaluate the correspondence of the relationship produced analytically with that determined numerically here. For this reason, a parametric study was performed to evaluate the frequency response of the system vs boom stiffness and pretensioning of the blanket.

#### 2.5.1.2 Finite Element Models

The finite element models used in this study were developed with program SOLAR\*DYN. This program generates data for an ASTRO model of the array, given a set of general geometry and blanket properties input by the user. The model is generated in three

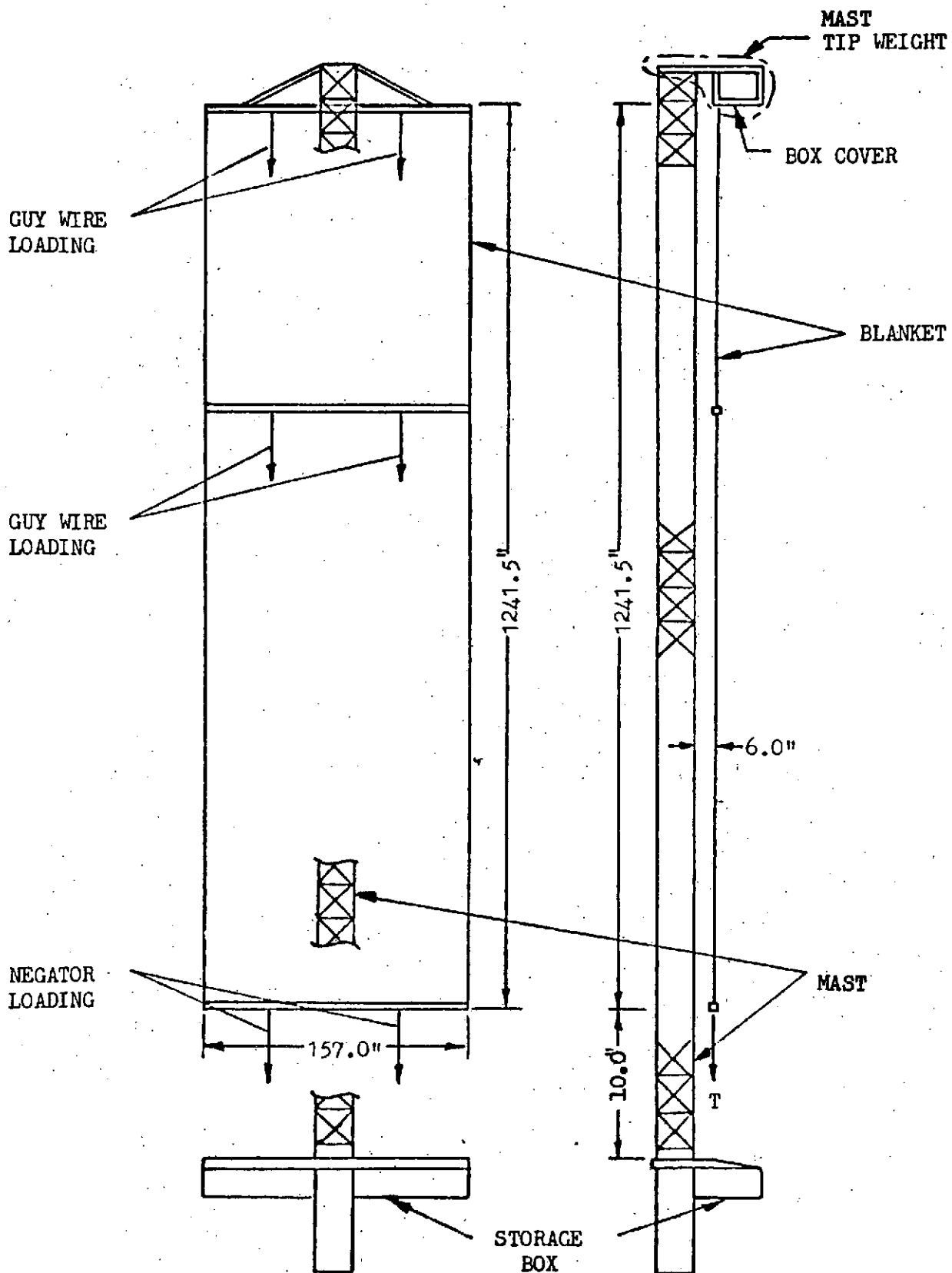


Figure 2-31 SEPS Solar Array Configuration

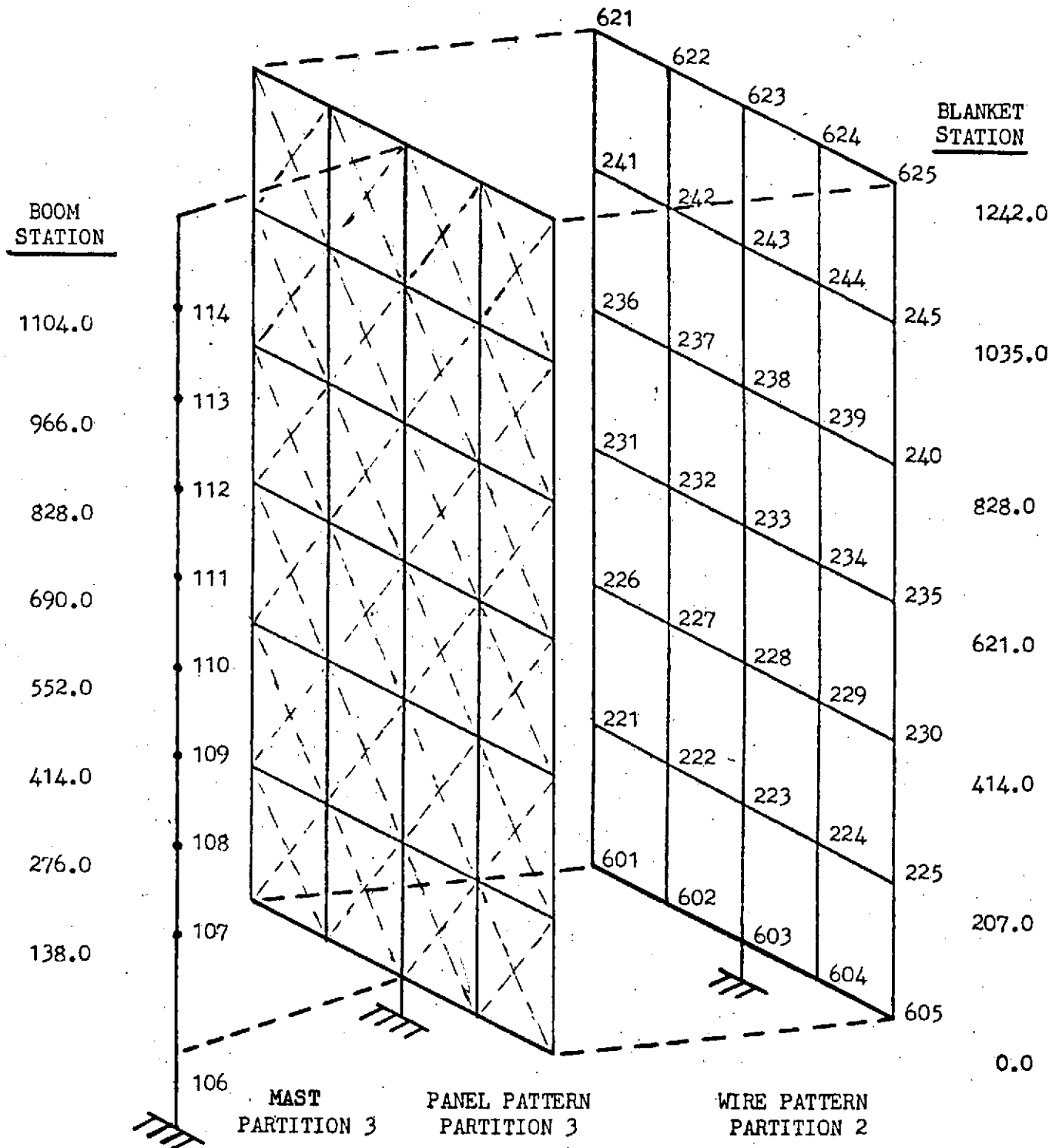


Figure 2-32 Array Finite Element Model

partitions, an out-of-plane partition 3, an in-plane partition 2, and a merge and solution partition 1. This format follows the general format for analysis of a partitioned problem using ASTRO (Ref. 9). The in-plane and out-of-plane characteristics are assumed to be uncoupled in this model. Partition 3 includes elements modeling the boom, solar array panels, cross beams and tension wires. Because of the nature of the quadrilateral element used to model the blanket in this partition, only out-of-plane stiffnesses, those due to the pretensioning of the panel, are generated. In-plane freedoms are allowed, but no contributions to in-plane stiffnesses are generated. However, all contributions to blanket mass, both in-plane and out-of-plane, are generated in this partition. This allows identical mass characteristics for in- and out-of-plane freedoms to be used. The precompressed beam elements used to model the boom are also generated in this partition. Both in-plane and out-of-plane masses and stiffnesses for the boom are generated.

Partition 2 includes a set of wires (slender beam elements), preloaded in the length of the array, which outline the blanket panels of partition 3. The pretension generates stiffness for the in-plane motion of the array. Wires in the width of the array are sized to maintain the wire pattern and to eliminate individual string modes.

Partition 1 merges the mass and stiffness matrices generated by partitions 2 and 3 and initiates the eigensolution calculations for the frequencies and modes of the array.

#### 2.5.1.2 Parametric Study Particulars

The basic premise of the parameter study indicated that, for a given base model of the array, a variation of boom stiffness and blanket pretension could indicate the minimum boom stiffness for a given frequency requirement. Analytically, for a given frequency, the relationship between stiffness and pretension can be determined by varying the pretension and calculating the required stiffness. This was the method of Reference 8. Numerically, however, both stiffness and pretension must be varied over the ranges of interest, with the frequency as the output. The relationship for  $EI$  vs  $T$  for a given frequency is then determined by interpolation of the data which results. This is the method employed.

Stiffnesses were varied over the range 4.29 to 8.53 KN/m<sup>2</sup> (15.0 to 30.0 x 10<sup>6</sup> lb-in<sup>2</sup>), and pretensions T (l) ranged from 35.6 to 88.9 N (8.0 to 20.0 pounds) total.

To describe the baseline array, the following parameters were defined:

SAL	=	Solar Array Length	=	1242.0 in.
SAW	=	Solar Array Width	=	157.0 in.
BMOFF	=	Boom Offset From Blanket	=	6.0 in.
DTR	=	Dual Tension Length Ratio, (Inboard/Total)	=	0.500
BDI	=	Inboard Blanket Density	=	0.200 lb/ft <sup>2</sup>
BDO	=	Outboard Blanket Density	=	0.200 lb/ft <sup>2</sup>
ESTWT	=	Blanket Weight	=	274.80 lb
EPWT	=	End Panel Weight	=	23.58 lb
GWTNS	=	Guide Wire Tension (2 at 1.0 lb)	=	2.00 lb

Interrelated parameters that were varied for data points are:

BMSTF	=	Boom Stiffness (EI)	-	lb-in <sup>2</sup>
TORSTF	=	Boom Torsion Stiffness(GJ)	-	lb-in <sup>2</sup>
BTNSI	=	Inboard Blanket Tension	-	lb.
BTNSO	=	Outboard Blanket Tension	-	lb.

A total of nine stiffness-pretension combinations were analyzed for the base configuration, with pertinent results tabulated in Table 2-7.

### Study Results

Modes and frequencies have been calculated for each of the configurations in the parametric study, up to the third boom-blanket bending mode. A representative ordering and description of the modes is given in Table 2-8. Collective data for the out-of-plane primary bending mode, taken from Table I, was used to construct the plot presented in Figure 2-33. Interpolation of the frequency values shown for each pair of parameters (T(l), EI) produce the curve shown. The result compares qualitatively with the results of Reference 8 wherein a minimum value of boom stiffness can be found which produces the desired array frequency response for the proper

TABLE 2-7  
DYNAMICS STUDY RESULTS

Baseline Model Results

Model Name	EI (lb-in <sup>2</sup> )	T(1) (lb)	Modal Frequencies Z - Bending - X Torsion		
NEWDATA2	25. x 10 <sup>6</sup>	8.0	.0410	.0440	.0477
NEWDATA5	25. x 10 <sup>6</sup>	11.0	.0433	.0467	.0543
NEWDATA7	25. x 10 <sup>6</sup>	14.0	.0448	.0481	.0600
NEWDATA8	20. x 10 <sup>6</sup>	8.0	.0386	.0423	.0475
NEWDATA10	20. x 10 <sup>6</sup>	11.0	.0403	.0443	.0540
NEWDATA11	20. x 10 <sup>6</sup>	14.0	.0412	.0450	.0596
NEWDATA9	30. x 10 <sup>6</sup>	8.	.0427	.0452	.0478
NEWDATA12	30. x 10 <sup>6</sup>	11.0	.0456	.0485	.0545
NEWDATA14	15. x 10 <sup>6</sup>	14.0	.0366	.0407	.0590
NEWDATA15	15. x 10 <sup>6</sup>	17.0	.03678	.0399	.0638
NEWDATA16	15. x 10 <sup>6</sup>	20.0	.03675	.0385	.0681

Baseline Model with DTR = .167

NEWDATA1	25. x 10 <sup>6</sup>	8.0	.0411	.0444	***
NEWDATA4	25. x 10 <sup>6</sup>	11.0	.0425	.0454	.0529

Baseline Model with DTR = .833

NEWDATA3	25. x 10 <sup>6</sup>	8.0	.0411	.0444	***
NEWDATA6	25. x 10 <sup>6</sup>	11.0	.0433	.0477	.0557



TABLE 2-8  
SOLAR ARRAY MODES

Model Name: NEWDATA15

Mode No.	Frequency	Generalized Mass	Characteristics	Max @ Node No.
1	.03678	.4425	1st Z Boom-Blanket Bending	625
2	.03987	.4746	1st X Boom-Blanket Bending	625
3	.0638	.1473	1st Blanket Torsion	231
4	.0765	.2365	Z Blanket (W)	225
5	.0809	.2366	Z Blanket (W)	240
6	.0873	.1366	Z Blanket (N)	221
7	.0923	.1417	Z Blanket (N)	241
8	.0965	.3802	2nd Z Boom-Blanket Bending	226
9	.0985	.3988	2nd X Boom-Blanket Bending	228
10	.1080	.1178	Z Blanket (S)	228
11	.1142	.1185	Z Blanket (V)	238
12	.1232	.2145	2nd Blanket Torsion	245
13	.1518	.4098	3rd Z Boom-Blanket Bending	225
14	.1570	.4156	3rd X Boom-Blanket Bending	238

( ) - Indicates blanket deformed mode shape

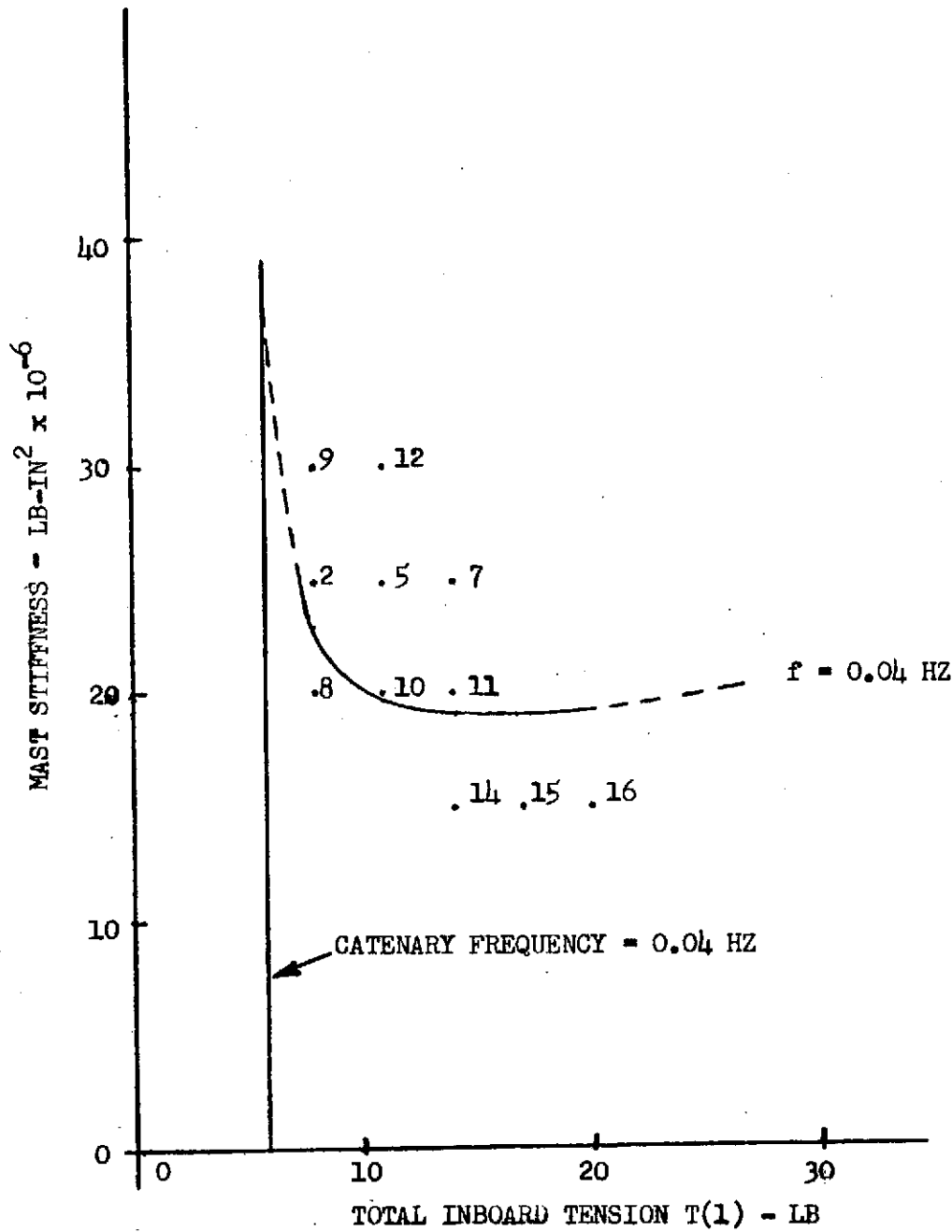


Figure 2-33 First Mode Frequency Variation

blanket preload. The preload-stiffness values for the minimum stiffness point here are:

$$\begin{aligned} T(2) &= 8.9 \text{ N (2 lb.)} \\ T(1) &= 75.6 \text{ N (17 lb.)} \\ EI &= 55.2 \text{ KN/m}^2 (19.3 \times 10^6 \text{ lb-in}^2) \end{aligned}$$

The preload required for a blanket catenary mode at .04 Hz is determined by:

$$f = \frac{0.5}{L} \sqrt{\frac{T}{\sigma}} \text{ Hz}$$

where

$$\begin{aligned} L &= \text{Length of the array blanket} \\ \sigma &= \text{Blanket mass per unit area} \\ T &= \text{Tension per unit width} \end{aligned}$$

The total base preload for the SEPS for this mode is:

$$P = T \cdot W = 5.8 \text{ lb.}$$

This is the preload required to give a blanket catenary frequency of .04 Hz for an infinitely stiff boom ( $EI = \infty$ ).

### 2.5.1.3 Tensioning and Mast Stiffness Requirements

The application of tension to the intermediate array position for partial retraction operation allows the reduction of the bottom tension applied to blanket, while still providing control of the mast plus blanket natural out-of-plane vibration frequency. As the mast is retracted from full extension to partial extension, the outboard portion of the array remains tensioned by the amount  $T_2$  as shown in Figure 2-34. The study is evaluating the variation of the partial retraction fraction,  $L_1/(L_1+L_2)$ , on tensioning requirements and the possible use of a dual density blanket. In the dual density design, the outboard section of the array wing is exposed to the total space radiation environment and has an appropriate cell/cell cover thickness. The inner section is retracted during most of the solar proton flare event durations and may have a thinner cell/cover design. Average array power is conserved and the total blanket weight meets the BOL specific power requirements.

Tension in the blanket can be zero for frequency control if the mast stiffness is

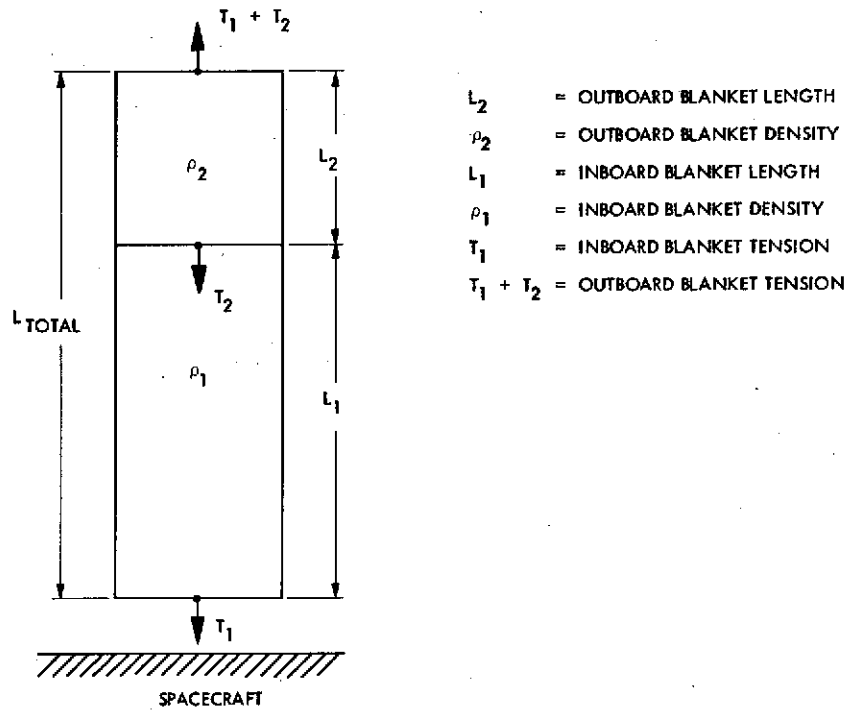


Figure 2-34 Array Blanket/Tension System Model

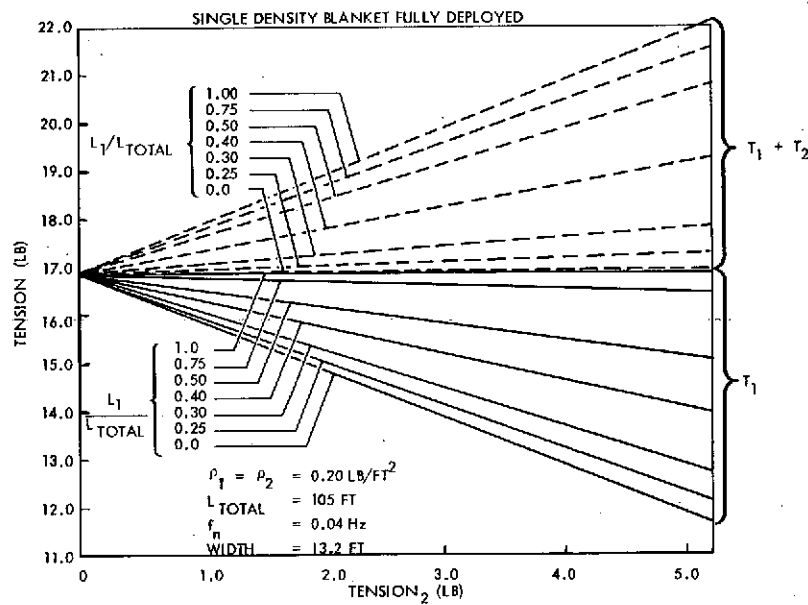


Figure 2-35 Tension for Minimum Mast EI

infinite. As the tension is increased, the mast stiffness required for a given system vibration frequency reduces to a minimum. If the tension is increased further, the required mast stiffness also increases. Figure 2-35 shows the tension required in the lower section of a single density array blanket as a function of partial retraction fraction and tension in the outer blanket section. The total blanket tension applied to the mast,  $T_1 + T_2$ , is also shown. The same data for a dual density blanket is shown in Figure 2-36. Extension mast stiffness requirements for a dual density blanket vs partial retraction fraction are shown in Figure 2-37.

Recommended further studies are:

1. Perform a more detailed parametric analysis to determine the array characteristics for other variables.
2. Analyze the non-linear features of the array and the characteristics under specific loading conditions.

#### 2.5.2 Thermodynamics Analysis

This section briefly describes the THERM model of the SEPS solar array developed for this study. Two areas unique to this model are described in greater detail. One is the effective conduction resistance,  $R_c$ , between the solar cell mode and the average base temperature node that is estimated for this model. The second is the development of the analytical method to predict solar cell performance as a function of solar incidence angle that is used in the study.

The THERM temperature predictions are presented. Steady-state solutions of solar array temperatures are presented as a function of distance from the sun and solar incidence angle. A transient failure mode temperature solution was also made for sun to the solar array backside at 0.3 au.

Each solar array wing is 4.06m wide and about 32.0m long fully extended. It uses a coilable, continuous longeron, fiberglass mast. An articulated stainless steel mast for extension, retraction and support of the array is an alternate design. The forty-one flexible and folding panels of each solar array will be covered with 2 cm x 4 cm solar cells welded to the 1 mil thick copper foil conduction traces sandwiched between two overlays of 0.5 mil Kapton plus 0.5 mil adhesive of the flexible substrate base.

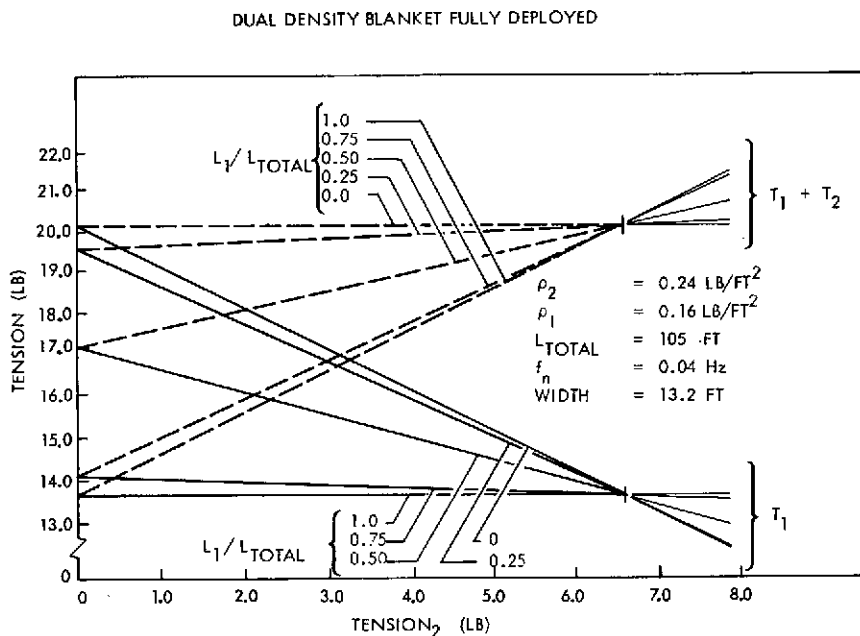


Figure 2- 36 Tension for Minimum Mast EI, Dual Blanket Density

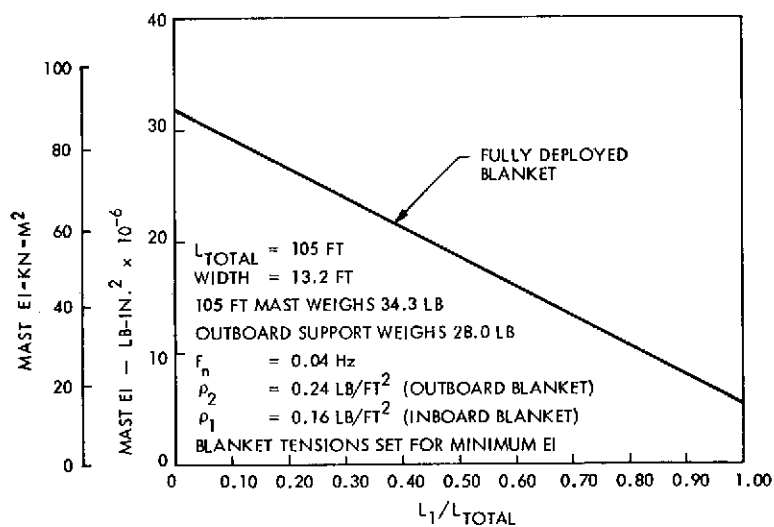


Figure 2- 37 Extension Mast Stiffness Requirements

The copper foil conduction traces will occupy 25% of the base substrate area, in a pattern which allows series-parallel connection of the solar cells. The configuration concept of an elemental area of the solar array panel is shown in Figures 2-38 and 2-39.

#### 2.5.2.1 Description of Model

For this study of the expected solar array temperatures, a simple THERM model of the solar array panel was constructed. A one foot long section of the 157 in. wide solar array panel was chosen from the center of the solar array. Only direct solar incidence and radiation to deep space was considered in the inter-planetary model, no radiation from the SEPS spacecraft or planetary earthshine and albedo was included.

This section of the solar array was divided into two modes, one which represents the temperature of the solar cells on the front of the array, and one which represents the average of base substrate temperature at the back of the array. These two modes are connected by conduction and radiation resistors. The infrared and solar radiation in the spaces between the solar cells, as seen in Figure 2-39 was also considered, and solar transmittance was included through the 10.49% of the base substrate area at the bottom of the cell spacings. Both infrared and solar values of absorptance, reflectance, and transmittance were estimated for the base substrate thickness of Figure 2-38, for both the base substrate alone and for the base substrate against the solar cell backs. Radiation and thermal properties of the substrate base and solar cells were obtained from Refs. (10) and (11) and are shown in Table 2-9.

Elements of the mast longerons and battens were located 6 inches behind the center of the back of the solar array section. Mast elements of stainless steel and of fiberglass were included in the model, and coupled by both infrared and solar radiation to the back of the substrate base through appropriate view factors. A complete thermal model of the triangular masts was not attempted, and the mast elements were not connected by conduction resistors since the objective was to obtain an initial estimate of mast temperatures behind the array for the two potential mast material considered.

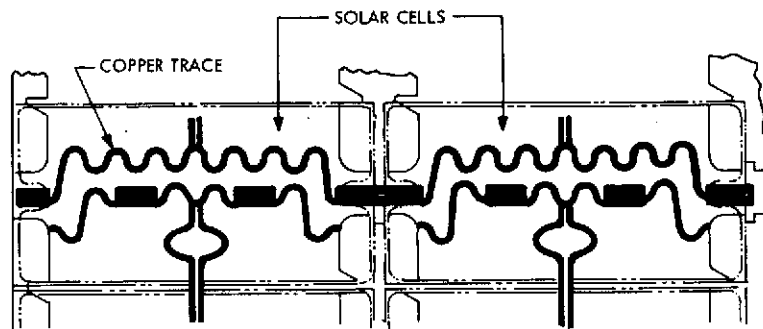


Figure 2-38 Substrate Copper Trace Pattern

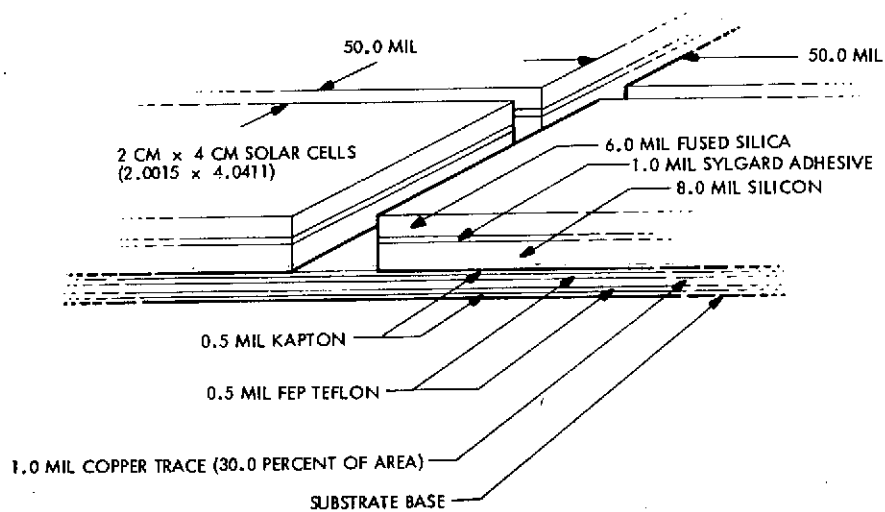


Figure 2-39 Array Panel Detail



TABLE 2-9  
SURFACE RADIATION PROPERTIES USED IN THERM MODEL OF THE SEPS  
SOLAR ARRAY

Node No.	Surface Description	Solar Absorptance, $\alpha$	Infrared Emittance, $\epsilon$
1	Solar Cell, front surface	0.77	0.81
1	Solar Cell, back surface	0.16	0.07
2	Substrate Base, 30% Cu trace (backed by Solar Cells)	0.33	0.87
2	Substrate Base, 30% Cu trace (not backed by Solar Cells)	0.20	0.87
3, 4	310 Stainless Steel Mast (commercial grade, as received)	0.50	0.30
5, 6	Epoxy-bound Fiberglass Mast (non-colored fiberglass)	0.70	0.85

The major simplification involved in constructing this THERM model was to treat the substrate base as being at one average temperature. Actually, the substrate base with 25% copper trace will have temperature gradients in the small area beneath a single solar cell, because of the high conductivity of the copper and the low conductivity of the Kapton plus adhesive between the copper traces. The substrate base area was treated as one node at an average temperature, and an effective conduction resistance  $R_c$  between the solar cell node and the substrate base node was defined based upon the results of Ref. (11). That report analyzed the Space Station flexible solar array in earth orbit. Steady state temperatures of the 25 nodes of the substrate base below a solar cell are given in that model for the sub-solar point (hot case) of the orbit and for the opposite orbital point in the earth's shadow (cold case). These temperatures were then area averaged, to obtain an average base temperature for the two cases reported.

An energy balance was then performed on the total base substrate area, using the average base substrate temperature computed above, to determine an effective conduction resistor  $R_c$  between the base and solar cells. These energy balances, which included radiation heat transfer between the substrate base and solar cell backs, resulted in the selection of an effective conduction resistance between the base and solar cells of  $R_c = 0.32 \text{ hr-ft}^2\text{-}^\circ\text{R/Btu}$  for the present study.

The second area of concern in the development of this model was to accurately predict the solar cells reflectance and absorptance of solar energy as a function of solar incidence angle  $\theta$ . The incidence angle  $\theta$  as used here is defined in the optical sense, being the angle between the solar vector and the normal to the solar cell surface. From Fresnel's formulas of Ref. (12), it is possible to define the surface reflectance  $\rho(\theta)$  as a function of incidence angle  $\theta$  for a glass surface on a transparent cover plate, but without anti-reflective (AR) coatings.

Since the fused silica cover plate has an index of refraction,  $n = 1.46$ , then the normal reflectance for this surface without an AR coating would have the value  $\rho(\theta) = 0.035$ . From Fresnel's relation for  $\rho(\theta)$ , the surface reflectance would be as shown by the dashed curve in Figure 2-40 where the reflectance approaches unity as  $\theta$  approaches 90 degrees.

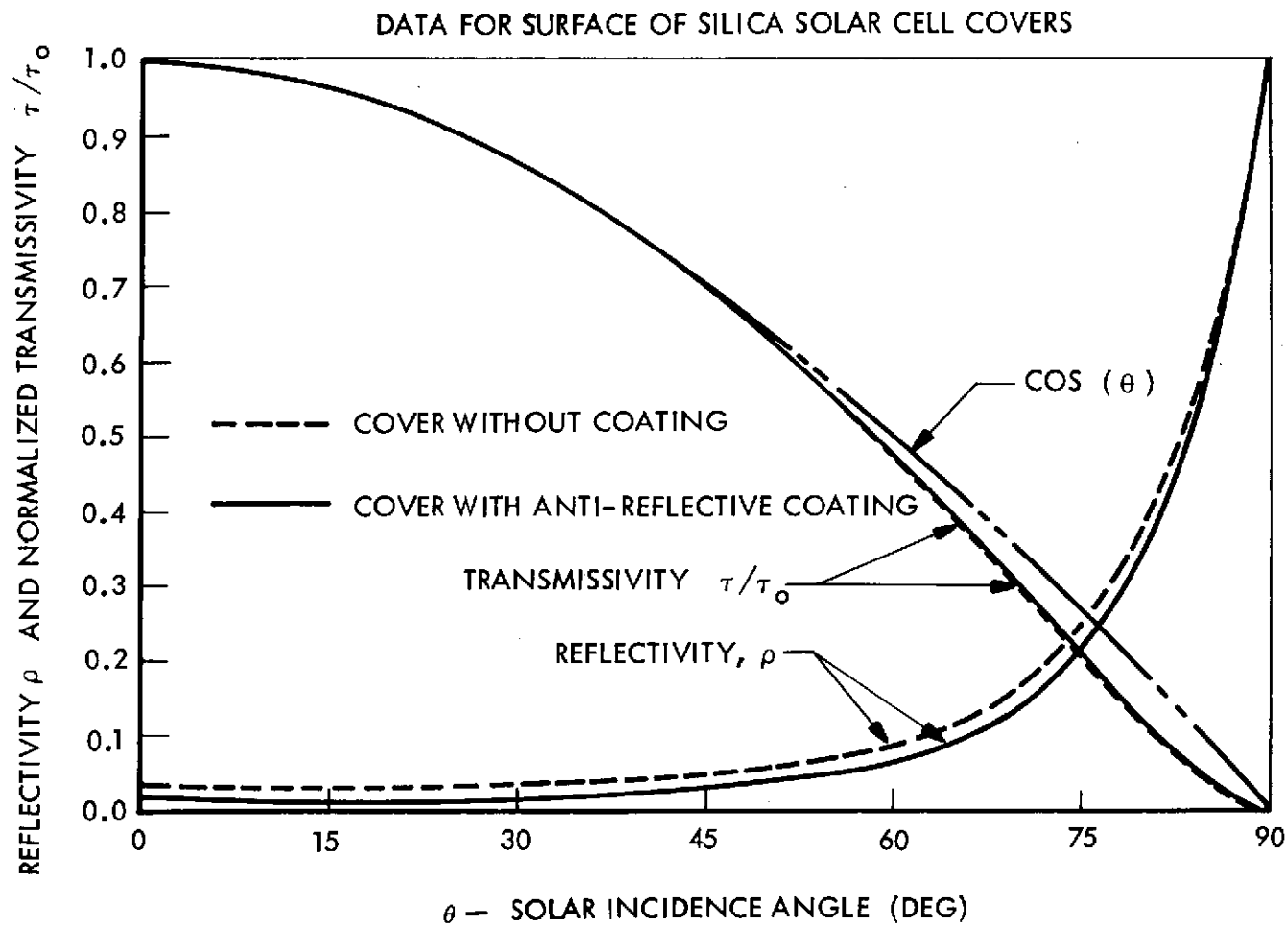


Figure 2-40 Reflectivity and Transmissivity vs Solar Incidence Angle

The actual fused silica cover surface of the solar cells is treated with an AR coating, so that the normal surface reflectance has the value  $\rho(\theta) = 0.020$ . In this case, Fresnel's formula should not apply, but it can be used to make an effective estimate of the surface reflectance  $\rho(\theta)$  with an AR coating. This relationship is shown as the solid reflectance curve in Figure 2-40, for the actual normal surface reflectance of  $\rho(\theta) = 0.020$ . The normalized transmitted solar energy is also shown in Figure 2-40 for both the untreated and anti-reflective coated surface. It is noted that for high angles of incidence the normalized transmissivity curve is much lower than the  $\cos \theta$  curve, and only a small fraction of the incident energy is transmitted through the surface.

Ref. 13 shows the importance of the normalized transmissivity curve in solar cell electrical power generation. In that study, solar cells similar to those used in this study were exposed to solar incident energy at various angles of incidence.

Figures 5, 6 and 7 of Ref. 13 show that the normalized electrical power generation of the solar cells falls on top of the normalized solar transmissivity curve, and hence the electric power generation is directly proportional to the solar energy transmitted into the cell. This fact that electric power generation is proportional to solar transmitted energy at any angle of incidence supports the earlier assumption that the solar absorptance and internal reflectance in the solar cell are effectively independent of the incidence angle. A solar cell efficiency of 10 percent is used for the analysis.

#### 2.5.2.2 Temperature Results

Figure 2-41 shows the solar cell and average base substrate temperature as a function of au distance from the sun for normal illumination of the solar cells. This curve of solar cell temperature for normal solar incidence shows that in order not to exceed solar cell temperatures in the range  $120^{\circ}\text{C}$  to  $150^{\circ}\text{C}$  the angle of incidence of the solar array will have to be increased for  $r^*$  values less than about 0.64 au.

Figure 2-42 shows solar cell temperature,  $T_c$ , as a function of distance from the sun and solar incidence angle. This data was run using a normal solar cell absorptance value of  $\alpha = 0.77$  and a normal surface reflectance of  $\rho(\theta) = 0.02$  for the AR coated fused silica cover.

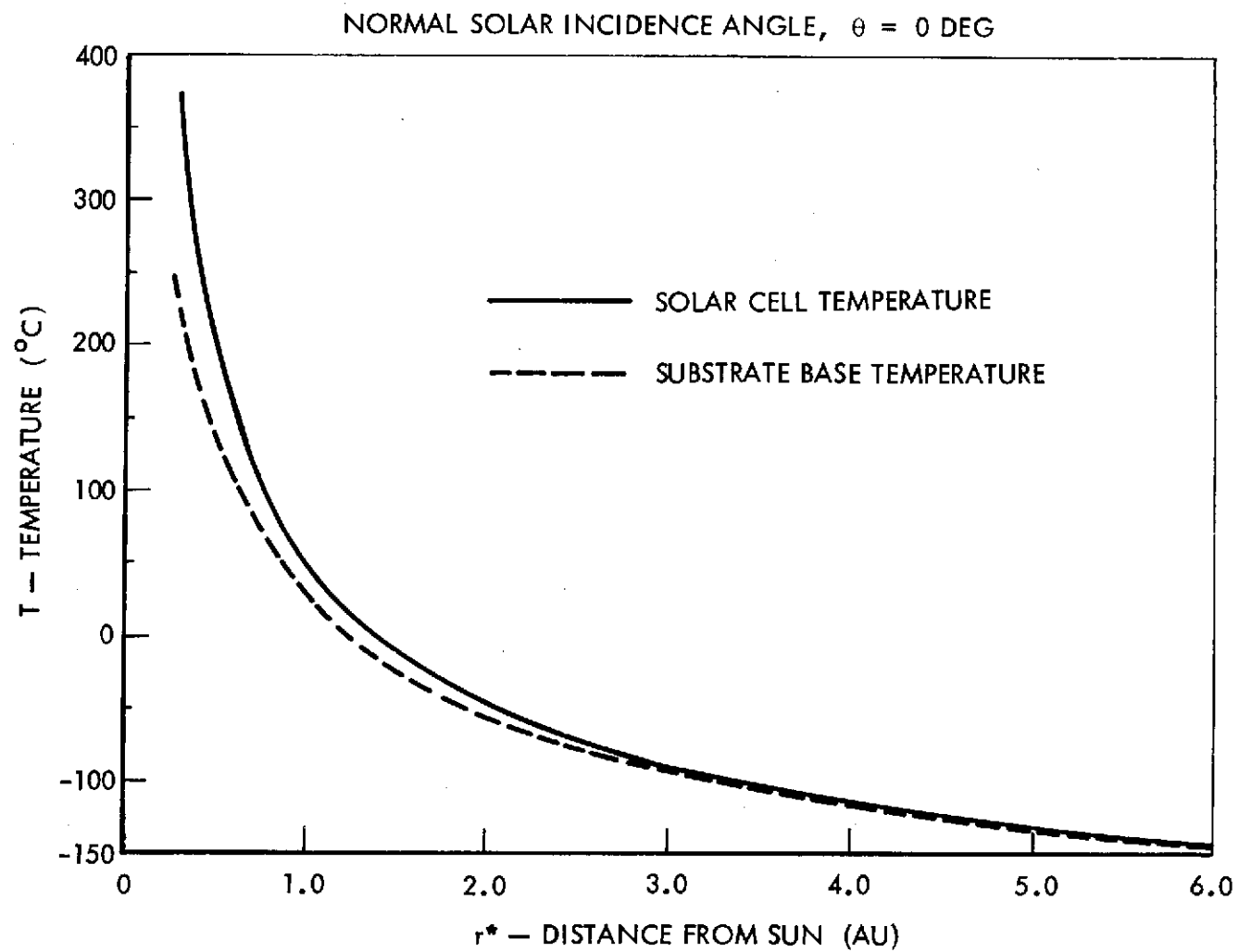


Figure 2-41 Solar Cell and Substrate Base Temperature vs Sun Distance

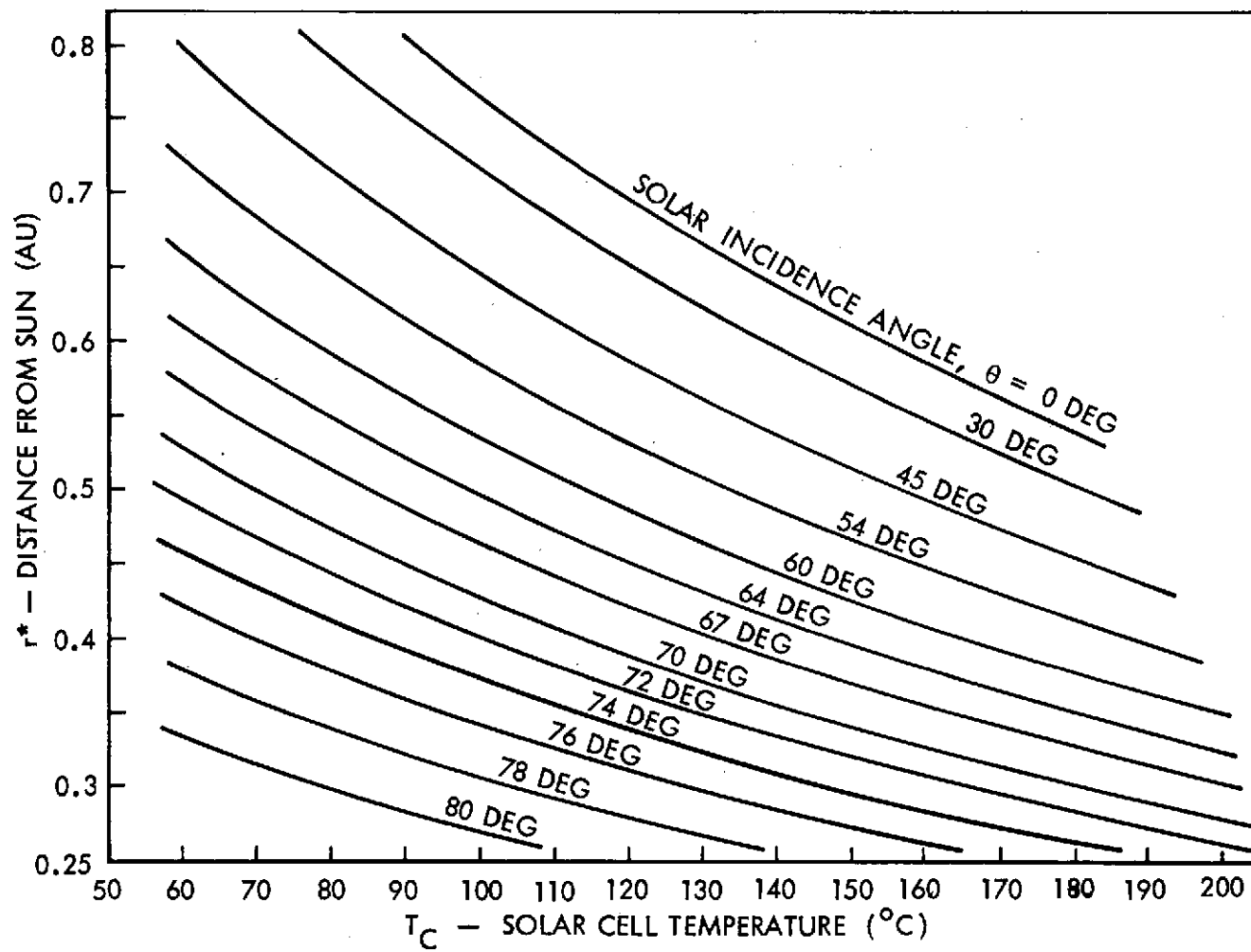


Figure 2-42 Solar Cell Temperature vs Heliocentric Distance and Array Tilt

Figure 2-43 is a graph of solar cell to substrate backside temperature difference  $\Delta T$  as a function of au distance from the sun.

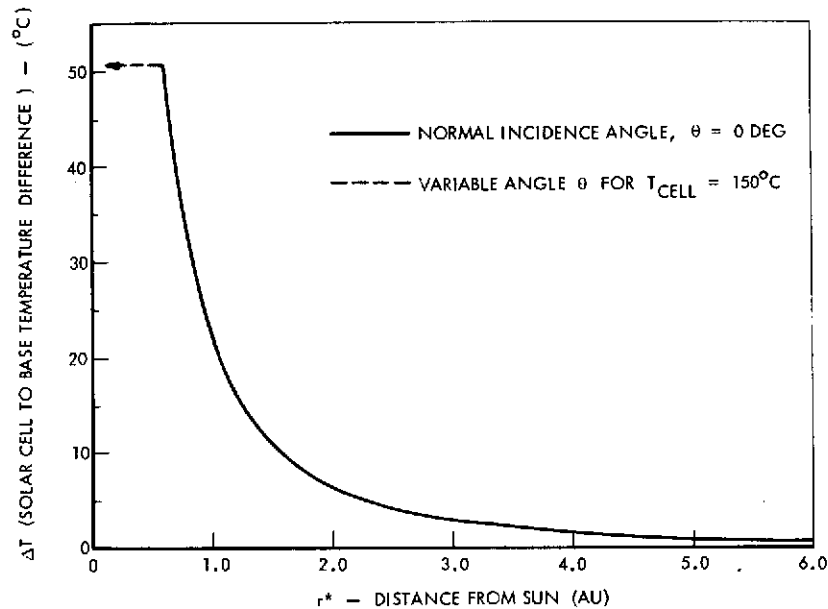


Figure 2-43 Array Front-to-Back Temperature Difference

The solar absorptance and infrared emittance of the mast elements are listed below, and are based upon commercially available epoxy bound S-type fiberglass and 310 stainless steel, without any special surface finish or surface coatings.

Epoxy Bound S Type Fiberglass

$$\alpha = 0.70$$

un-colored

$$\epsilon = 0.85$$

310 Stainless Steel

$$\alpha = 0.50$$

$$\epsilon = 0.30$$

A transient failure mode study of array and mast temperatures was performed at 0.3 au, with normal sun instantaneously applied to the backside of the array.

Figure 2-44 shows the transient response of all the node temperatures. A solar reflectance value of  $\rho_s = 0.55$  was used for the backside of the base substrate, based upon experimentally measured values supplied by Ref. (8). If the SEPS were to lose attitude control and turn its backside to the sun at 0.3 au, the base substrate warms so quickly that there would probably not be time to take corrective action on the attitude control system to keep from overheating the substrate base.

### 2.5.3 Solar Cell Radiation Analysis

An initial selection of solar cell parameters to meet the power requirements for the deployed array for the five year SEPS mission at one au (but external to the geomagnetosphere) has been performed based on the (large event) solar flare proton model environment provided by NASA Huntsville. In addition, the effect of the proposed retraction system in reducing the power requirements by shielding the retracted array during solar flare proton events has also been assessed based on the same solar flare proton model. These analyses have been performed using the BUFES computer program which evaluates the equivalent normally incident 1 MeV electron fluence ( $\Phi_{eq}$ ), evaluated at the sensitive cell volume, that gives the same change in the desired solar cell characteristic as does the specified (isotropically) incident solar flare proton spectrum on the actual solar cell. Before giving the results of applying this program in the indicated fashion, a brief description of the procedures followed in using the program follows.

#### 2.5.3.1 Prediction of Solar Array Degradation

The method used to predict the degradation of the output the solar cells is based on the base layer diffusion length of the solar cell material. This correlation exists for electrons or protons if they have energy above a certain minimum required to produce lattice displacements in the base layer of the solar cell that lead to increased minority carrier recombination and a reduction in collection efficiency for the cell. The 1 MeV electron equivalent terminology is based then on laboratory measurements of the lattice displacement effects produced by protons, electrons and other particles as a



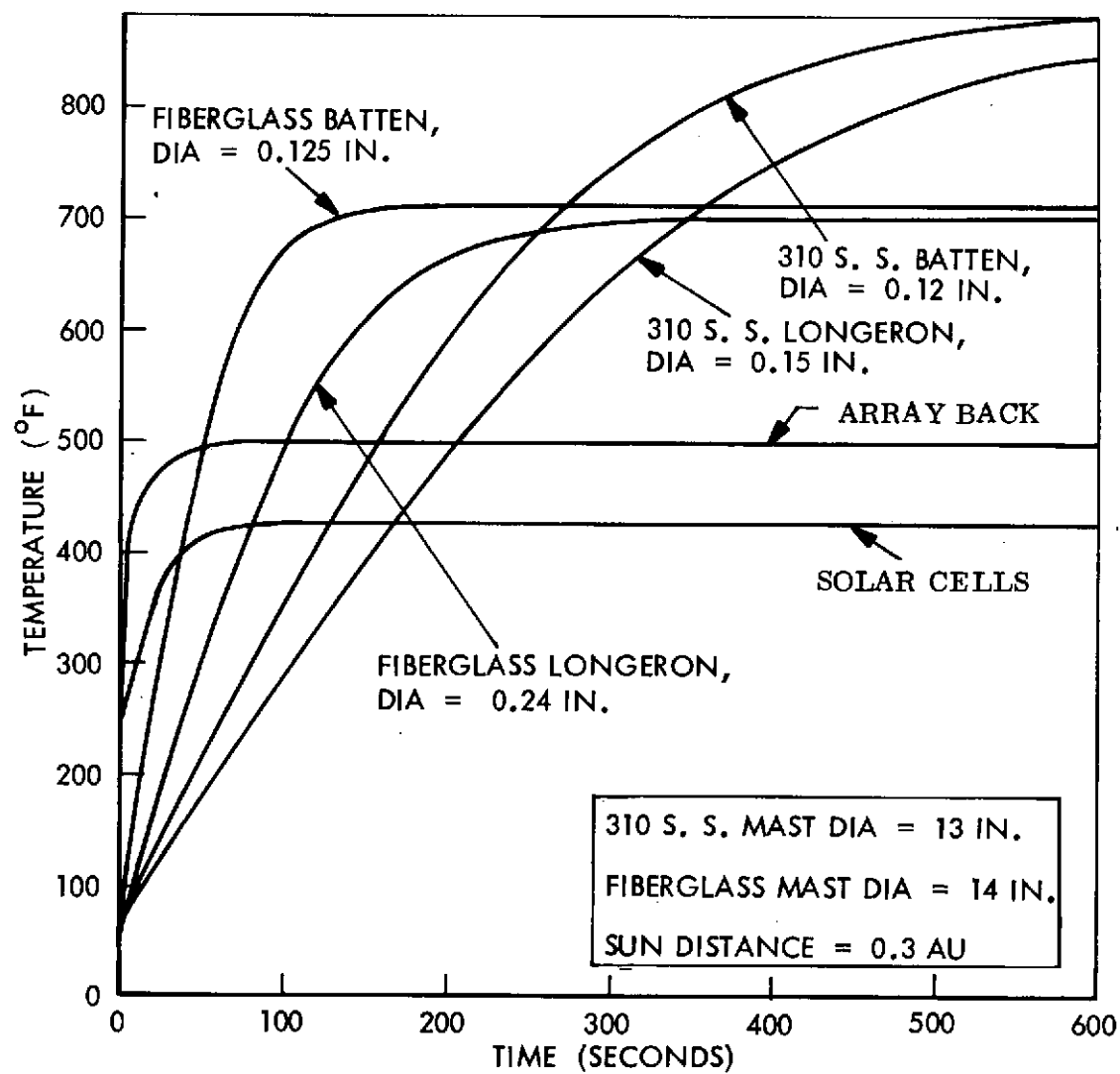


Figure 2-44 Transient Temperature Response of Mast Elements

function of particle energy and solar cell material parameters. As a result of these measurements the changes derived were of the form  $\Delta\left(\frac{1}{L^2}\right) = K(E) \phi$  where  $\phi$  is

the particle fluence and  $E$  is energy and  $K(E)$  the proton or electron damage coefficient that depends on energy and on the bulk material parameters. It has been observed that contributions from different particles and with different energies based on the 1 MeV electron equivalent doses are simply additive. Using measured values to determine  $K(E)$  for electrons and protons, the equivalent 1 MeV electron equivalent doses are simply additive. Using measured values to determine  $K(E)$  for electrons and protons, the equivalent 1 MeV electron fluence can be defined as

$$\phi_{eq} = \frac{\int K_e(E) \phi_e(E) dE}{K_e(l)} + \frac{\int K_p(E) \phi_p(E) dE}{K_e(l)} \quad (1)$$

where  $\phi_e(E)$  is the fluence per energy interval for electrons and correspondingly by  $\phi_p$  for protons.

To apply this technique to solar cell geometries requires the evaluation of the particle energy spectrum that penetrates to the p-n junction region of the solar cell for an isotropic incident spectrum on the cover slide and for an incident spectrum on the backside of the panels. Computer programs that have been developed to evaluate both the ionizing dose and the equivalent 1 MeV electron fluence for the both normal incidence and isotropic incidence of general electron and proton energy spectra, have been specialized to the case of one dimensional slab shields with infinite cell backside shielding. For this particular case the results of a number of such evaluations for a range of fused silica cover slide thicknesses has led to the use of an alternate form of the original equation; i.e.,

$$\phi_{eq}(t) = \int_0^\infty dE_o K_R(E_o, t) \phi(E_o)$$

Where  $\phi(E_o)$  is now the incident particle spectrum and the altered damage coefficient,  $K_R$ , depends on both the incident energy and the fused silica shield thickness,  $t$ . For protons and electrons, analytical fits of the energy dependence of  $K_R$  on  $E_o$  for a series of selected shield thicknesses allows this evaluation to be done easily. A single computer program has been written to evaluate  $\phi_{eq}$  for tabular inputs of the incident proton and electron environments.

One of the fundamental limitations is related to the tacit assumption that each particle reaching junction region will uniformly damage the effective collection volume. Due to the finite range and high damage effectiveness of low energy protons this condition will not be valid for shield thicknesses less than 6 mils of fused silica for generally observed trapped proton and solar flare proton environments. Evaluations for 3 and 4 mils should be considered as upper limits.

Finally, in order to apply this procedure to the evaluation of the contribution from the backside of the panel, it is only necessary to evaluate the shielding characteristics of the cell, adhesive, panel components and any additional shielding present in the form of an equivalent fused silica coverslide thickness; and then to add the  $\phi_{eq}$  for this thickness to that evaluated for incidence from the other side to obtain the total  $\phi_{eq}$  for the panel.

This shielding equivalence procedure has been based on comparison of the total stopping power,  $\epsilon(E)$  for each material layer as a function of particle energy, with that for fused silica and on the determination of the best choice for a single multiplicative factor to use as the equivalent thickness of silica ( $\text{gm/cm}^2$ ). Since most of the materials encountered are either aluminum, silica, silicon; or contain silica compounds this procedure is justified.

#### 2.5.3.2 Solar Array Degradation for the Deployed Panels

This panel construction uses a flexible Kapton, FEP Teflon laminant that is bonded to a 1 mil copper interconnect structure that may cover about 30% of backside of each cell. The equivalent fused silica thickness of the flexible laminant is about 1.6 mils while that of the copper interconnect plus the laminant is 6 mils. The average  $\phi_{eq}$  for laminant only and laminant plus interconnect portions has been evaluated using the computer program. The resulting total  $\phi_{eq}$  for the 20% interconnect area coverage case has been evaluated for 6, 8, and 12 mil cell thicknesses and 3, 6, 8, and 12 mil cover slide thicknesses and is given in Table 2-10 for one and seven solar flare events. Also given in this table are the estimated final fractional maximum power for the seven flare case for both two and ten ohm-cm N/P cells.

TABLE 2-10  
SEPS EQUIVALENT 1 MeV ELECTRON FLUENCE

Fused Silica Cover Slide Thickness (mils)	Cell Thickness (mils)	Total $\phi^1$ Equiv. -one flare	Total $\phi$ Equiv. -7 flares	P/Po 2-ohm cm -7 flares	P/Po 10-ohm cm -7 flares
3	6	1.62 (14)	1.134 (15)	0.765	.822
	8	1.51 (14)	1.057 (15)	0.728	.775
	12	1.42 (14)	9.94 (14)	0.696	.723
6	6	1.27 (14)	8.89 (14)	0.777	0.842
	8	1.18 (14)	8.26 (14)	0.745	0.791
	12	1.00 (14)	7.00 (14)	0.707	0.742
8	6	1.17 (14)	8.19 (14)	0.785	0.849
	8	1.10 (14)	7.70 (14)	0.753	0.798
	12	1.00 (14)	7.00 (14)	0.722	0.747
12	6	1.06 (14)	7.42 (14)	0.795	0.858
	8	9.62 (13)	6.73 (14)	0.763	0.809
	12	8.62 (13)	6.03 (14)	0.734	0.758

<sup>1</sup>Flexible Substrate is 1 mil Kapton + 1 mil FEP Teflon + 20% area 1 mil copper

### 2.5.3.3 Effects of Retraction of Cell Degradation

The concept of retraction to reduce the radiation degradation over the mission life is most significant for the missions discussed here in which there is 1) absence of any significant contribution to  $\phi_{eq}$  from a "background" radiation environment (such as due to the trapped radiation belts) either before or after mission initiation and 2) all of the mission  $\phi_{eq}$  is due to a "small" number of discrete solar flare proton events so that the number of times the array must be retracted is reasonable.

For the proposed retraction system, in which only a fraction (70%) of the total number of folded panels are fully retracted,  $\phi_{eq}$  has been evaluated as a function of location in the retracted panel stack assuming the depth of the stack is much less than the minimum lateral dimension and all the folded fully retracted panels are in a planar array. The analysis was done for the prescribed incident solar flare proton model environment and repeated for several combinations of cover slide and solar cell thicknesses with the results given in Table 2- 11. The upper and lower side equivalent 1 MeV electron fluences cited refer to the upward and downward (with respect to the containment box) facing half of each folded pair.

Figure 2-45 shows the power degradation of the array due to space radiation vs the fraction of the array that is partially deployed during flares at 1 au for 5 years. The allowed power degradation from 25 KW to 21 KW is 16 percent. Six percent is allocated to thermal control degradation, cell cover transmission degradation and cell inter-connect failures. The remaining 10 percent is allocated to radiation degradation. The analysis indicates that retraction to 30 percent or less partially extended is required to meet the above 10 percent limit with the design cell and cover thickness single density blanket. The performance of dual density blanket designs with the same blanket total weight are shown in Figure 2-35. While a dual density design may be found that performs better than the single density blanket, the 70 percent retraction requirement is not expected to be significantly changed with the present design, degradation requirements, and the flare model and probability model used. The probability of more than a given number of solar flares being experienced at a point on a circle around the sun in 5 years is shown in Table 2- 12.

Additional analysis for specific SEPS missions and radiation degradation testing of the SEPS solar cell will be required in the future.

TABLE 2-11

## PARTIALLY STORED SEPS EQUIVALENT 1 MeV ELECTRON FLUENCE

LAYER NO. (1)	UPPER SIDE EQUIV. 1 MeV FLUENCE, e/cm <sup>2</sup>			LOWER SIDE EQUIV. 1 MeV FLUENCE			AVERAGE EQUIV. 1 MeV FLUENCE - 1 FLARE		
	CELL/COVER COMBINATION - MILS								
	12/6	8/6	8/4	12/6	8/6	8/4	12/6	8/6	8/4
1	7.1(13)	7.2(13)	9.0(13)	2.3(13)	2.8(13)	4.2(13)	4.7(13)	5.0(13)	6.6(13)
4	1.8(13)	2.1(13)	3.1(13)	1.2(13)	1.5(13)	1.7(13)	1.5(13)	1.8(13)	2.4(13)
10	0.63(13)	0.75(13)	0.87(13)	0.55(13)	0.65(13)	0.77(13)	0.59(13)	0.70(13)	0.82(13)
20	0.35(13)	0.43(13)	0.49(13)	0.34(13)	0.41(13)	0.51(13)	0.34(13)	0.42(13)	0.50(13)
40	0.27(13)	0.34(13)	0.38(13)	0.28(13)	0.35(13)	0.39(13)	0.28(13)	0.35(13)	0.39(13)
60	0.50(13)	0.60(13)	0.67(13)	0.56(13)	0.67(13)	0.74(13)	0.53(13)	0.64(13)	0.71(13)
68	1.5(13)	1.6(13)	1.7(13)	2.4(13)	2.4(13)	2.5(13)	2.0(13)	2.0(13)	2.1(13)

(1) 34 panels of 41 total panel are in box (68 layers of 82 layers)

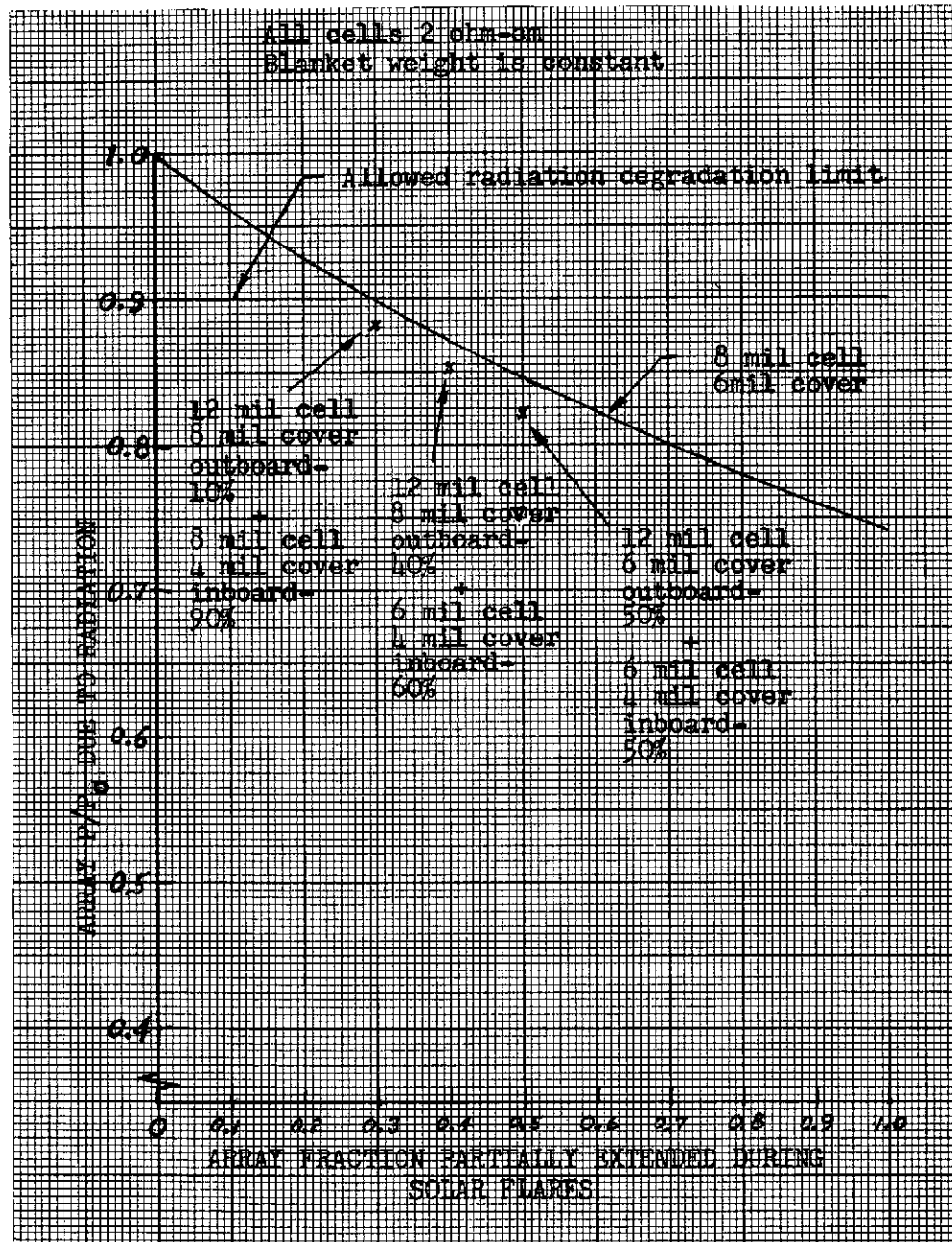


Figure 2-45 SEPS Solar Array Degradation

TABLE 2-12  
PROBABILITY OF SOLAR FLARE EVENTS

Number of Events, N	Probability of Exactly N Events, P	Probability of More Than N Events
0	0.0743	0.9257
1	0.193	0.7327
2	0.251	0.4817
3	0.218	0.2637
4	0.141	0.1227
5	0.0736	0.0491
6	0.319	0.0172
7	0.0118	0.0054
8	0.00385	0.0015
9	0.00111	0.00044
10	0.000289	0.00015
11	0.0000683	0

$$P = e^{-\lambda t} (\lambda t)^N / N!$$

$$\lambda = 0.01 \text{ events/week}$$

$$t = 5 \text{ years} = 260 \text{ weeks}$$



#### 2.5.4 Structures Analysis

The SEPS solar array is required to be capable of various lengths of extension. It is also required to re-stow itself so the array can be returned by the Space Shuttle for the refurbishing. The stress analysis effort was directed, for the most part, to determining the analysis method best suited for the array loading conditions.

##### 2.5.4.1 Solar Array Pretension

The analysis method was taken from Reference 14, "Elastic Foundation" by M. Hetenyi, 1946. The method will allow selection of a buffer panel that will have a spring rate different from 32 m long substrate and provide a nearly uniform load into the substrate. This will provide minimum shear wrinkles in the array. A computer program was written to allow various combinations of array and buffer sheet to be included to find the best design. Future effort is required to determine the actual properties of the substrate and the buffer to give satisfactory results. The analysis was used to produce a series of computer plots that indicate the amount of variation in distribution of load into the substrate panels depending on their physical properties.

The model used is shown in Figure 2-46. An example of the results is shown in Figure 2-47. The ideal design would result in uniform deflection of the first hinge across the array width. Further analysis is also required to optimize the buffer design which could include the use of an appropriate hole pattern in the buffer elastic material.

##### 2.5.4.2 Array Extension Mast

###### 2.5.4.2.1 Mast Sizing

###### Mast Stiffness Requirement

The required mast plus canister bending stiffness is  $19 \times 10^6$  lb-in.<sup>2</sup>. Flexibility at the mast-canister interface exists because of the eccentric manner in which the boom rollers bear on the nut, which causes local bending of the longerons. The bending stiffness of that interface is given by:

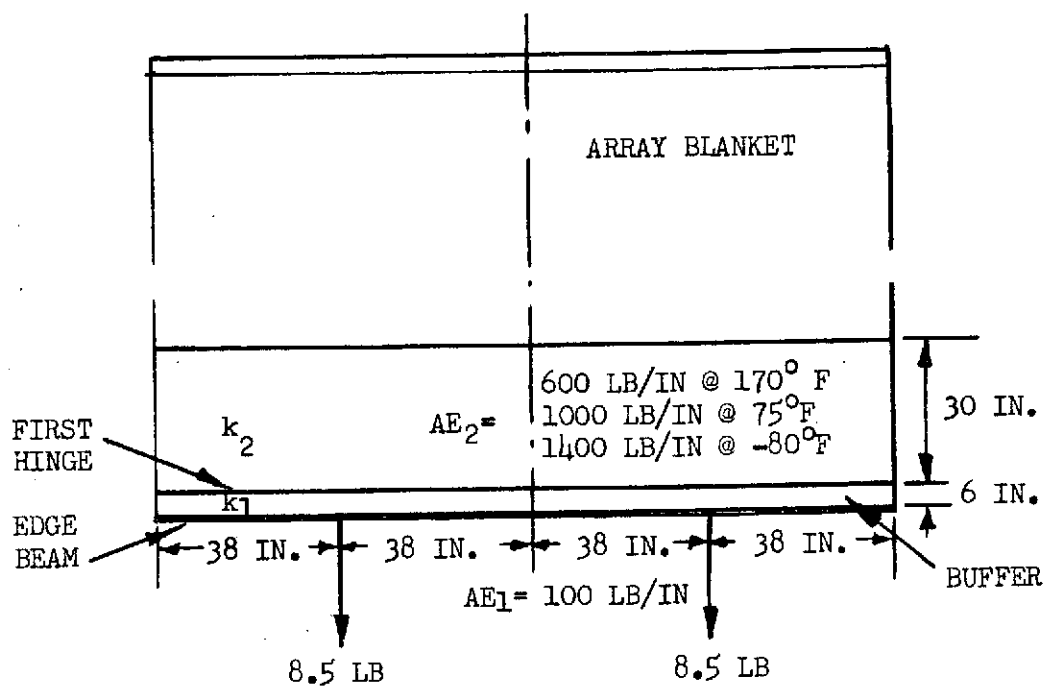


Figure 2-46 Inboard Tension Distribution Model

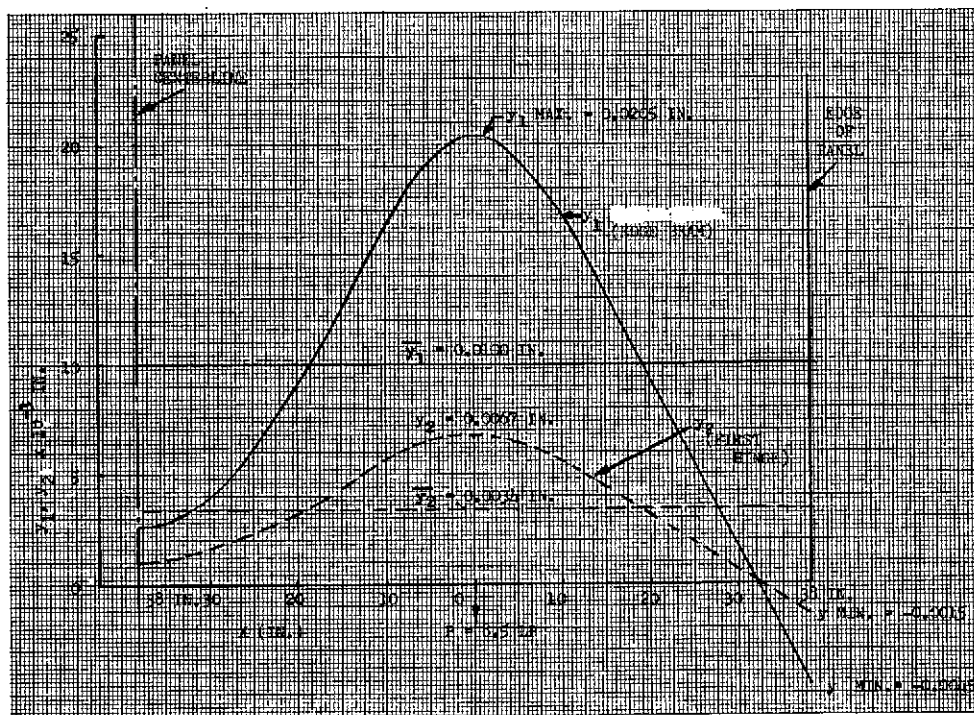


Figure 2-47 Deflection of Edge Beam and First Hinge

$$K = M/\theta$$

where  $K$  = stiffness

$M$  = bending moment applied to the boom (in.-lb)

$\theta$  = the result rotation or slope of the boom (radians)

From a detailed analysis of the eccentric support of the longerons,  $K$  is formulated as:

$$K = 4.5 R^2 \frac{EI_\ell}{\ell^2}$$

where  $R$  = boom radius

$EI_\ell$  = longeron bending stiffness

$e$  = eccentric distance at which longeron loads are reacted

$\ell$  = bay length

The function of the mast, even though it is flexibly supported, is to provide a certain vibration frequency when it supports a concentrated mass at its free end. Assuming that the boom is relatively weightless, the increased bending stiffness of the boom necessary to provide the same vibration frequency is:

$$EI \text{ (mast + canister)} = EI_{\text{required}}/1+(S/K)$$

where  $S = (1/2)(\pi/2)^4 EI_{\text{required}}/L$

and  $L$  = boom length

Since longeron bending stiffness and overall boom bending stiffness are related, one can derive:

$$S/K = 37.9 R/L$$

The value of  $EI_{\text{required}}$  was calculated to be:  $23.1 \times 10^6 \text{ lb-in}^2$

More refined analyses will be required if the cited assumptions are too inaccurate.

Boom Sizing

Bending stiffness of an Astromast with coilable longerons (of square cross sections) is calculated by the equation:

$$EI_{\text{required}} = 6ER^4 \epsilon^2$$

where

E = Young's modulus (psi)

R = boom radius (in.)

and

$\epsilon$  = working strain given by  $\epsilon = S/D$

where S is the longeron thickness

and D is the boom diameter

The safe value of the working strain used here is  $\epsilon = 0.0135$ .

The above equation can therefore be solved (using  $E = 7.5 \times 10^6$  psi)

for R giving:

$$R = 7.29 \text{ in.}$$

Longeron Sizing

The cross-sectional dimension of a square longeron is:

$$S = D\epsilon$$

Therefore,

$$S = 0.197 \text{ in.}$$

Diagonal and Batten Sizing

Diagonal and batten properties as given in the summary of design data, Table 2-2, are derived empirically.

Boom Bending Strength

For bending that equally compresses two of the longerons, the ultimate bending strength M of the boom is calculated by:

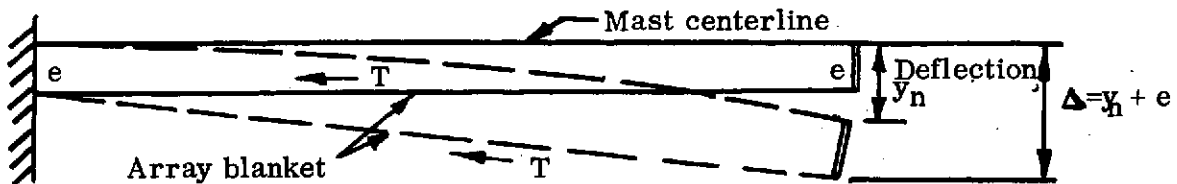
$$M = 32E \epsilon^4 R^3$$

Using the previously cited values of  $\epsilon$  and R,

$$M = 3100 \text{ in.-lb}$$

## 2.5.4.2.2 Mast Loads and Deflections

The array blanket is tensioned to a nominal value of 17 lbs at the base plus 2 lbs intermediate tension. This total tension plus 2 lbs of guide wire tension provides a load of 21 lbs on the mast tip in space. The resulting deflections are shown below:



$$y_n = \frac{Ml^2}{2EI}$$

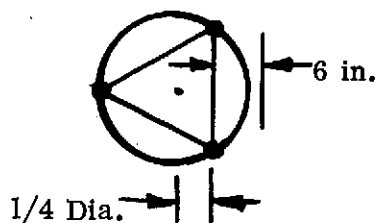
$$l = 105 \text{ ft.}$$

$$EI = 23.1 \text{ lb-in}^2$$

$$T = 17 + 2 + 2 = 21 \text{ lbs. (T max. allowed = 173 lbs.)}$$

$$M = Te$$

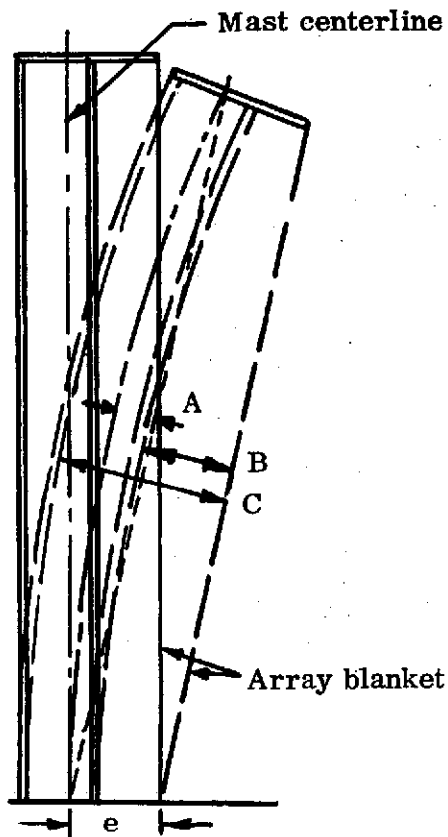
$$y = 6.96 \text{ in.}$$



$$\text{Mast dia.} = 14.6 \text{ in.}$$

$$e = 1/4 \text{ dia.} + 6 \text{ in.} = 9.65 \text{ in.}$$

$$\Delta = 6.96 \text{ in.} + e = 16.6 \text{ in.}$$



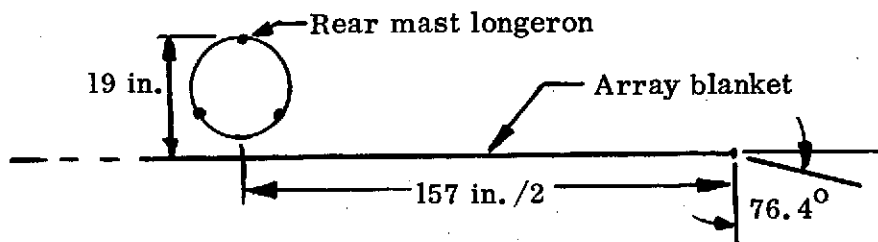
Assume circular curvature of final mast shape:

A = centerline deflection = 2 in.

B = blanket/front longeron separation = 8 in.

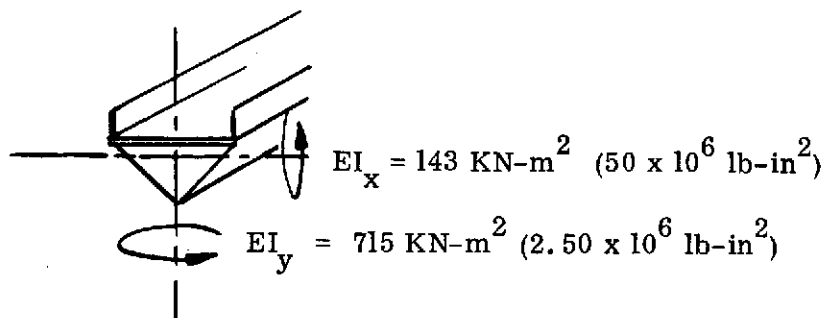
C = blanket/rear longeron separation = 19 in.

The amount of array tilt that may occur before the sun strikes the rear longeron is 76.4 degrees:



#### 2.5.4.3 Containment Box Bending Stiffness

The bending stiffness of the array containment box is based on the triangular beam composed of two 0.020 in. magnesium panels and the 1/2 in. honeycomb panel box bottom.



## 2.6 STATE OF THE ART ASSESSMENT

As an aid to design evaluation, state of the art assessments were conducted on selected SEPS array components and processes during the first phase of the program. The photovoltaic and associated technologies are undergoing continuous changes and refinements, therefore in accordance with the program plan, to implement design and analysis functions on as current a technology base as possible, the state of the art assessment task was completed and the summary reports are incorporated herein. Each component is treated as a separate entity with cited references incorporated within the sections. The sections are as follows:

- 2.6.1 Cell Cover
- 2.6.2 Solar Cells
- 2.6.3 Solar Cell Interconnect
- 2.6.4 Cell Joining Techniques
- 2.6.5 Solar Array Flexible Substrate
- 2.6.6 Module Joints
- 2.6.7 Array Electrical Harness
- 2.6.8 Composite Material for Containment Box Structure
- 2.6.9 Extension and Retraction Mast
- 2.6.10 Extension Mast Motors
- 2.6.11 Lubricants

Table 2-4 summarizes the criteria used for categorizing the state-of-the-art.



TABLE 2-13  
CRITERIA FOR STATE OF THE ART ASSESSMENT

STATE OF THE ART STATUS				
CATEGORY	I-SUFFICIENT	II-INSUFFICIENT, DEVEL. PROGRESS WILL ACHIEVE READINESS	III-INSUFFICIENT, ALTERNATE FEASIBLE	IV-INSUFFICIENT, NO ALTERNATES, NO DEVICE POTENTIAL
Determin- ation Criteria	<ul style="list-style-type: none"> <li>. Successfully used for similar missions.</li> <li>. Not in use but substantiated by test and analysis.</li> <li>. Qualified by similarity &amp; material compatibility.</li> <li>. Substantiation achievable within span &amp; scope of this technology program.</li> </ul>	<ul style="list-style-type: none"> <li>. Insufficiency due to lack of analytical or test data &amp; not due to known functional or physical limitation.</li> <li>. Insufficiency because of material or component specified for environment &amp; duration marginal without modification, but develop. program may verify capability of material or component.</li> </ul>	<ul style="list-style-type: none"> <li>. Basic material, component or concept limitation but feasible options available.</li> <li>. Known life or environment insufficiency but direct substitutions feasible.</li> </ul>	<ul style="list-style-type: none"> <li>. Does not satisfy any of the preceding category determination criteria.</li> </ul>
Action Required	<ul style="list-style-type: none"> <li>. Submit necessary data to MSFC to justify capability.</li> </ul>	<ul style="list-style-type: none"> <li>. Submit assessment report to MSFC with details of program required to achieve state-of-the-art readiness, with emphasis on program cost plus cost, weight, etc. advantages if qualified.</li> </ul>	<ul style="list-style-type: none"> <li>. Submit assessment report to MSFC specifying feasible alternates &amp; their time-cost factors for implementation.</li> </ul>	<ul style="list-style-type: none"> <li>. Submit assessment report to MSFC identifying design elements or areas not achievable for the intended application.</li> </ul>

## STATE OF THE ART ASSESSMENT

## 2.6.1 Cell Cover

Several terms have been used synonymously with "cell cover" such as, cover filter, cover glass, coverslip, filter, cover. Cell covers were incorporated initially to enhance the surface thermal optical properties of a solar array and to act as a shield against micrometeoroid erosion. Their initial use was prior to a knowledge of the Van Allen belt. The selection of the cell cover parameter of thickness is now associated with the projected radiation environment and the role of micrometeoroid protection has diminished because initial projections were grossly overrated and definitive micrometeoroid environments and degradation factors have never been specified. For many years the cell cover options were confined primarily to microsheet glass and fused silica. Some use occurred with sapphire, however, it did not exhibit significant advantages and its cost was prohibitive. In recent years three new cover systems have been under development. These are integral covers, ceria doped glass and FEP. Three other systems were briefly investigated but are not under active consideration at this time. EOS proposed the use of PVF, Polyvinylidene fluoride, in a NASA Technical Brief. Marks of LMSC developed an organometallic coating in 1964 which could be sprayed on cells, however, due to thermal coefficient mismatch problems it was not developed further. Investigations were also made at Heliotek and Ryan under JPL sponsorship on the use of ribbon glass as cell covers. (Section 4.1.3.4 of the NAS9-11039 First Topical Report, LMSC-A981486, and the Topical Report Update, LMSC-D159124, provide detailed summary discussions of solar cell covers).

At this time eight different solar cell cover systems are in use, under development, or have some utilization potential. Three of the systems are variations of FEP. The eight systems are listed below.

1. Fused Silica
2. Cerium Stabilized Glass
3. Microsheet
4. FEP - Tape
5.       - Heat laminated
6.       - Spray on
7. Integral Covers
8. ES Bonded 707

These cover systems were subjected to a State of the Art review for the SEPS program with results which are summarized as follows.

#### Fused Silica

Corning 7940 fused silica has been used extensively for cell covers on most Air Force satellites and on many NASA and communication satellite programs. It is favored for its environmental stability. Its state of the art status is Category I because of demonstrated successful use in mission applications which are similar to those projected for SEPS.

The drawbacks associated with use of fused silica are cost and fragility. Projected costs for 6 mil fused silica are the same as or higher than for 12 mil because of the process and handling breakage that occurs in the thinner configuration.

#### Cerium Stabilized Glass

Of the cover options other than fused silica, more recent effort has been expended on the development and evaluation of cerium stabilized microsheet including flight experiments. This type of cover has been subjected to component type approval tests in accordance with RAE specifications (Ref. 1), has been subjected to extensive comparative tests with fused silica and microsheet (Ref. 2) and has demonstrated favorable characteristics on flight experiments (Ref. 3). Ceria glass covers will be used on the CTS, Canadian Technology Satellite, and the Esso OTS, Orbital Test Satellite. Fabrication of covers as thin as 4 mils has been demonstrated. Recently many European space programs have switched to the use of the cerium stabilized covers. The lower cost, higher strength and thinner options associated with microsheet can be taken advantage of with incorporation of the ceria dopant which counters color center darkening.

Cerium Stabilized Microsheet is a Category I option with substantiation achievable within the span of this program. Because of different measured thermal optical properties an array with ceria covers is analytically projected to run 1° to 2° C hotter than with fused silica. However, on the flight experiment previously cited, Ref. 3, the ceria glass covered cells ran slightly lower in temperature than the fused silica covered specimen.

#### Microsheet

Microsheet is feasible for short term use where particulate radiation levels are low, however, it is not feasible for the SEPS application. It therefore is a Category III component, the ceria doped version previously discussed being an available feasible option.

#### FEP

As previously reported in Ref. 4, FEP is under evaluation as a cell cover. TRW under contract to NASA Lewis is evaluating heat-pressure applied FEP. It was initially investigated by LMSC and NASA Lewis. The general impetus for the use of FEP is its low cost, flexibility and potential adaptability to large areas in one application process. The three different types of FEP cover candidates are discussed as follows.

Tape - Preliminary temp cycle evaluation of FEP tape has been encouraging. A system that uses a silicone adhesive has successfully withstood 50 cycles from -150°C to +160°C and 232 cycles from -65°C to 100°C. The cycle time peak to peak is 10 minutes with 5 minute dwell at upper and lower temp regions. UV and temp cycle tests are continuing with a modified adhesive for the tape which is UV stable.

Heat Laminated - The application of sheets of FEP film to cells and modules is still under active investigation at LeRC, TRW and LMSC using heat-pressure lamination methods. Indications are that systems which apply FEP to both sides of the modules (encapsulated) have better survivability than those with application to the cell topside only. The former method provides a more symmetrical cross section for stress alleviation, however, the extra layer introduces a weight penalty.

Sprayed On FEP - The LMSC R&D Labs have developed solvents for FEP and methods of spraying, brushing or dipping the component to be coated. The initial limitation of this method was that coatings of more than 1 mil were difficult to obtain. With more recent formulations, coatings from 1 to 10 mils have been obtained. The LMSC Spralyn coating has demonstrated very good UV stability. The current status of this coating is reported in Ref. 5.

The major limitation associated with the FEP cover concepts is the inherent high thermal coefficient of the material which introduces high shear stresses to the cell. For mission applications that experience deep cold cycles approaching the  $-180^{\circ}\text{C}$  range, high contraction stresses occur in the film. The tape system appears most promising for deep cycle applications because the adhesive acts as a stress relief plane. From the standpoint of preliminary comparative tests for temp cycle survivability the FEP systems would be ranked as follows:

- 1st FEP Tape
- 2nd Spraylon
- 3rd Encapsulated Laminated
- 4th Single Surface Laminated

The State of the Art Categories for the FEP systems are as follows.

FEP Tape	Category II
Spraylon	Category II
Heat Laminated	Category III

### Integral Covers

The primary limitations associated with integral covers are process rate, cost and induced stresses (potato chip effect). Advances have been made in application methods and composition that result in lower stresses. However, for the array sizes being considered production rates are too low without making high facility capital expenditures. The Integral Cover is a Category III component.

Electrostatic Bonding for Application of 7070 Boro Silicate Glass Integral Covers

Ref. 6

Simulation Physics started a program 15 January 1974 sponsored by WP-AFAPL to investigate the bonding of glass covers directly to solar cells using an electrostatic bonding process patented by P. R. Mallory Company. This process has been licensed to Simulation Physics (1-5% royalty). The technique is to elevate the cell and glass to a temperature of  $350^{\circ}\text{C}$  ( $680^{\circ}\text{F}$ ), apply an electric field of approximately 1000 volts and 0.5 ma for 30 seconds. The glass is adhered to the cell via an ion transfer mechanism. In specimens examined the devices appeared to be homogenous with no visible transitional plane between the cell and cover. Simulation Physics indicates that there are no discernable assembly losses using this method of cover application.

The 7070 glass has been selected because it has the closest thermal coefficient match to silicon, much closer than fused silica and because under particulate radiation,  $5 \times 10^{15}$  equivalent 1 MeV electrons, it exhibited, next to fused silica, the best radiation stability.

The AFAPL funded work is focused toward radiation hardened concepts. Seven hundred (700)  $2 \times 2$  cm 7070 covers are being obtained from OCLI and Centralab is building the solar cells for the test modules to be fabricated by Simulation Physics.

Cost projections are quite low compared to conventional covers. Using a Corning quote of \$50,000 for one ton of 7070 glass, Simulation Physics projects that they could cover  $5 \times 10^6$   $2 \times 2$  cm cells with 10 mil covers for .01¢ ea. material cost.

The preliminary evaluations indicate that the process can accommodate a wide range of cover thicknesses--specimens 10 mil and 1/4 mil thick were displayed. It is planned to evaluate several methods of heating the cell and cover including infrared, induction, microwave and hot plate. It is only necessary to apply heat until just before the plastic flow stage is achieved. An electrical field is then applied. The materials become ionically conductive and "wetting" (bonding) occurs in 2-3 seconds. The temperature and field are held for 27 more seconds to assure fusion occurs.

Samples have been made with the cell grids formed on the underside of the cell cover glass prior to ES bonding. Simulation Physics suggested the possibility of designs where sub-modules could be fabricated with the interconnect design and cell grids formed on the glass. This may be practical with rigid substrate arrays.

The Simulation Physics investigations on ES bonded 7070 will be monitored and a State-of-the-Art Assessment will be conducted on this system for incorporation in the present program final report. The wraparound electrode cells are chem etched with some pillowing (contouring) around the cell edges. It would be valuable to submit 2 x 4 cm wraparound cells similar to the SEPS baseline to determine if proper full face adhesion occurs. ES bonded 7070 would be considered at this time a category III cover option, however, this status may change after some development history has accrued on the system.

Cover Status Summary

Table 1 lists the state of the art status for the cell cover candidates. The recent and continuing development of Ceria Glass makes it a viable alternate to Fused Silica for the SEPS application. The status of the FEP systems will be monitored periodically to determine compatibility with the SEPS requirements.

TABLE 1  
STATE OF THE ART STATUS  
SOLAR CELL COVERS

CANDIDATE	CATEGORY
FUSED SILICA	I
CERIUM STABILIZED GLASS	I
MICROSHEET	III
FEP - TAPE	II
- HEAT LAMINATED	III
- SPRAY ON	III
INTEGRAL COVERS	III
ELECTROSTATIC BONDED 7070	III



# REFERENCES

- Ref. 1 "Type Approval Tests on PPE Ceria Stabilized Solar Cell Coverslips",  
A. A. Dollery, R.A.E., Tech. Memo Space 172
  
- Ref. 2 "Evaluation of Cerium Stabilized Microsheet Coverslips for Higher Solar  
Cell Outputs", R. L. Crabb, p 185, Ninth Photovoltaic Specialists Conference
  
- Ref. 3 Letter, Perkin-Elmer, F. H. Marchionna to G. F. Turner, 8/22/72, 120  
Day Flt. Test Data, Ceria Glass vs Fused Silica
  
- Ref. 4 "Investigation of FEP Teflon as a Cover for Silicon Solar Cells", Greenberg  
et al, Final Report NAS3-14398, NASA CR-72970
  
- Ref. 5 "A Highly Stable Clear Fluorocarbon Coating for Thermal Control and Solar  
Cell Applications", Haslim, Greenberg et al, LMSC, A.I.A.A. 12th  
Aerospace Sciences Mtg., January 1974
  
- Ref. 6 Private Conference, Alan Kirkpatrick, Simulation Physics, Burlington, Mass.,  
3/19/1974

## STATE OF THE ART ASSESSMENT

## 2.6.2 Solar Cells

The current state-of-the-art flight proven solar cells have been used with much success on satellites which require solar arrays as a source for electrical power. With the development of and the need for more sophisticated satellites, it is becoming more and more apparent that higher efficiency solar cells are required to prevent the solar array size and weight from becoming a major limiting design constraint in the design of future satellites.

Both solar cell vendors (Heliotek and Centralab) and Comsat Corp. have developed solar cells which have a conversion efficiency in the 12.4 to 13.5 percent range. The current production state-of-the-art solar cells have a conversion efficiency in the 10 to 11 percent range. See Table I for comparison of the different types of solar cells. It should be pointed out the 13.4 and 13.5 percent conversion efficiency solar cells were lab developed solar cells and the solar cell vendors at this time estimate the typical production type solar cells will have a conversion efficiency in the 12.4 to 12.8 percent range. Table 1 summarizes the solar cell technology status.

Listed below are the basic design changes that have been made to increase the efficiency of solar cells.

A. Diffusion (P/N Junction Depth)

Historically the trend in solar cell diffusion has been toward lower temperatures and shorter schedules in order to gain improved output. The improvements observed are in two regions of the cell's response, the short wavelength (blue) because the junction depth is reduced, and the long wavelength (red) because degradation of minority carrier lifetime is reduced. The two major reasons for lifetime degradation are fast diffusing impurities such as copper and iron and the thermal shock that silicon receives in cooling from the diffusion temperature, lower temperature and shorter times both act to moderate these effects. From the standpoint of the panel maker it is the short wavelength improvement that is important since this response is relatively insensitive to particulate radiation effects.

TABLE I  
SOLAR CELL TECHNOLOGY STATUS

	TYPICAL IMSC PRODUCTION CELLS						
	2x4 Conventional 2 $\Omega$ cm, Centralab Coverglassed	2x4 Conventional 10 $\Omega$ Heliotek or Centralab Coverglassed	Heliotek K6-B Cover- glassed	COMSAT Violet	Centralab Violet Pro- duction Quantities	Heliotek High Efficiency Production Quantities	2x4 cm End Tab Wrap Around (Development Quantities)
Efficiency (Based on Total Area and 140 MW/cm <sup>2</sup> illumination	10%	10.3%	13.4%	13.5%	12.4%	12.8%	11.0%
Efficiency (after irradiation)	7.6% <sup>(1)</sup> (1x10 <sup>15</sup> , 1 MeV e/cm <sup>2</sup> )	7.7% <sup>(2)</sup> (1x10 <sup>15</sup> , 1 MeV e/cm <sup>2</sup> )	10.1% (1x10 <sup>15</sup> MeV e/cm <sup>2</sup> )	10.4 (1x10 <sup>15</sup> MeV e/cm <sup>2</sup> )	Test will be con- ducted	>10% (1x10 <sup>15</sup> , 1 MeV e/cm <sup>2</sup> )	Not tested
Diffusion Depth	3500A	3500A	1500- 2000A	1000- 1500A	1000- 1500A	1200- 2000A	3500A
Base Resistivity	2 $\Omega$ cm	10 $\Omega$ cm	20 $\Omega$ cm	2 $\Omega$ cm	2 $\Omega$ cm	20 $\Omega$ cm	2 $\Omega$ cm
Solar Cell AR Coating	Si O <sub>x</sub>	Si O <sub>x</sub>	Ta <sub>2</sub> O <sub>5</sub>	Ta <sub>2</sub> O <sub>5</sub>	Ta <sub>2</sub> O <sub>5</sub>	Ta <sub>2</sub> O <sub>5</sub>	Si O <sub>x</sub>
Back Surface Field	No	No	P +	P+	P+	P+	No
Contact Grids & Number Material	8/2 cm	8/2 cm	>12/2 cm Ag-Ti-Pi	60/2 cm (N/Avail.)	60/2 cm (N/Avail.)	12/2 cm Ag-Ti-Pd	Centralab=8/2 cm Heliotek: 12/4 cm
Coverslide Cuton (nm)	410	410	350	350	350	350	410
Coverslide Adhesive	XR6-3409	XR6-7489	DC 93-500	XR6-3489	XR6-3489	DC 93-500	XR6-3489
Sizes	2x4 cm nom	2x4 cm nom	2x2, 2x6 nom	2x2	2x2	2x2 nom	2x4 nom
Cell Thickness (mils)	12	12	9-12	10	10	9-12	12
Coverslide Material	Fused silica	Fused silica	Fused silica	Ce Doped Micro- sheet	Ce Doped Micro- sheet (5%)	Fused silica	Fused silica
Coverslide Thickness (mils)	12	12	12	6	6	12	12
STATE-OF-THE-ART CATEGORY	I	I	II	II	II	II	II

**B. Contact Configuration**

The configuration of the contact (including grids) have been optimized by increasing the number of grids to reduce the sheet resistance, but is limited by number and size (width) so as not to significantly reduce the active area of the cell.

**C. Antireflective Coating**

The antireflective coating has been changed from silicon monoxide (SiO) to tantalum pentoxide ( $\text{Ta}_2\text{O}_5$ ) since it has the best transmission in the shorter wavelength range.

**SUMMARY**

At this time the state of the art status for the higher efficiency solar cell is listed as Category II because of: (1) Lack of/or unavailability of radiation test data from the cell vendors and (2) unavailability of cells for in-house evaluation of solar array manufacturing and test.

However, it should be noted that the first spaceborne test of higher-efficiency "Violet solar cells" developed by Comsat Laboratories, is currently underway on the Explorer 50 interplanetary monitoring platform (Imp-S), launched Oct 25, 1973. Additional tests planned on board the NASA Sphinx spacecraft were aborted by launch vehicle failure. A third test of the solar cells will be on board the ATS-F spacecraft.

## STATE OF THE ART ASSESSMENT (CONT.)

## 2.6.3 Solar Cell Interconnect

A fairly large variety of metals, alloys and plated metals have been used for solar cell interconnects. The primary function of an interconnect in a solar array is to provide an electrical conductor to a) interconnect the solar cells in series to provide selected levels of voltage, and b) to interconnect the solar cells in parallel to provide selected current levels. It is therefore necessary that interconnect terminations can be made at both the negative (N) and positive (P) contacts on the solar cell.

Interconnect Design Categories

Interconnect design falls into two main categories as associated with solar arrays; Independent - that is where the interconnect is separately fabricated and assembled to the solar cells as a piece part or subassembly, and Integral - where the interconnect is printed-etched and laminated as part of a larger entity such as a submodule, module or entire array panel. The typical assembly procedure with "independent" interconnects is to take the interconnected cell subassembly and glue it to the rigid or lightweight flexible substrate, whereas with the "integral" printed circuit concept supplementary laydown adhesives are eliminated and the electrical joint is also the mechanical joint that provides structural attachment for the cell to the solar array. Because of major weight and cost advantages the integral printed circuit interconnect concept has been chosen for SEPS.

Candidate Interconnect Metals

Many different metals and combinations thereof have been used for solar cell interconnects. The majority of solar arrays that have been orbited have used silver (usually in the expanded metal mesh form), Kovar, copper or Molybdenum. The Kovar and Molybdenum are silver plated for this application.

Recently work has been conducted to determine by research or test the important physical properties of candidate interconnect metals over the broad temperature range from  $-200^{\circ}\text{C}$  to  $+200^{\circ}\text{C}$ . The properties of copper, silver, aluminum, Kovar and Molybdenum were investigated under Contract NAS8-28432 by LMSC and the data obtained is presented in Reference 1. JPL under contract NAS7-100 has developed properties data on Kovar, molybdenum, palladium, silver, aluminum and lead-tin solder alloys. The JPL work was done in conjunction with stress analysis of selected rigid substrate array designs using soldering as the interconnection technique. (Ref. 2). Summary Table 1 is from Ref. 3.

In addition to the general physical and mechanical properties associated with the interconnect metals, an important factor associated with ductility is crystallographic space lattice characteristic of the metal. The face-centered cubic metals copper and aluminum maintain ductility substantially unimpaired at very low temperatures down to  $-240^{\circ}\text{C}$ . All metals and alloys that have a face-centered cubic lattice appear to maintain ductility substantially unimpaired at very low temperatures. Body-centered cubic metals and alloys generally suffer a marked decrease in ductility and impact strength at even moderately low temperatures (Ref. 4). Space lattice grouping of some metals is as follows:

Face-Centered Cubics

Aluminum  
Copper  
Gold  
Lead  
Nickel  
Platinum  
Silver

Body-Centered Cubics

Chromium  
Iron (e.g. Kovar, Invar)  
Molybdenum  
Tungsten

It should be noted that the primary flexure inducing mechanism in orbit, other than minor substrate deformation during array deployment or retraction, is thermal expansion and contraction. Moly, Kovar and Invar are in the low expansion category so their body-centered cubic deficiencies would be somewhat ameliorated.

TABLE 1  
PHYSICAL AND MECHANICAL PROPERTIES OF METALS USED IN INTERCONNECTS

PROPERTY	METAL											
	Al	Ti	Ni	Cu	Mo	Pb	Ag	Sn	Au	Kovar <sup>a</sup>	Si	Sn 62 Solder
Density (lb/in <sup>3</sup> )	0.098	0.163	0.322	0.324	0.369	0.41	0.379	0.208	0.698	0.302	0.084	0.303
Coef. thermal expansion (μ-in/in°C)	23.0	4.67	13.3	16.5	4.90	29.0	17.0	23.0	14.2	5.0	3.0	24.0
Thermal conductivity (cal/sq cm/cm°C/sec)	0.57	.04	0.22	0.941	0.34	0.083	1.0	0.15	0.71	0.40	0.20	.12
Electrical conductivity (% IACS) <sup>b</sup>	64.9	3.1	25	103	34	8.3	106	15.6	73.4	3.5		11.9
Electrical resistivity (μ-ohm-cm)	2.65	42	6.84	1.73	5.2	20.6	1.59	11.5	2.19	49	10x10 <sup>6</sup>	14.5
Magnetic susceptibility (10 <sup>-6</sup> cgs)	0.6	1.25		-0.08	0.04	-0.1	-0.2	0.03	-0.15		-0.13	
Modulus of elasticity (10 <sup>6</sup> psi)	10	16.8	30	16	47	2.6	11	6	12	19	10	6
Specific stiffness (E/ρ x 10 <sup>6</sup> in.)	92.0	103	93	49.4	127	4.9	29	28.9	15.8	99.3	119.0	.20
Tensile strength (10 <sup>3</sup> psi)	6.8	34	46	37	115	1.9	18.2	2.2	19	77.5	30	10
Yield strength (10 <sup>3</sup> psi)	1.7	20	8.5	6.5	100	0.8	7.9	1.3	40	59.5	24	7.5
Elongation (%)	60	54	30	40	4	30	50	40	45	16.8		32
Solderability*	2	3	1	1	2	1	1	1	1	2	3	--
Melting Temperatures (°F)	1220.4	3300	2651	1981.4	4760	621.3	1760.9	449.4	1945.4	2642	2605	364

<sup>a</sup>Kovar is not a pure metal, but rather an alloy of the following composition: 29 Ni, 17 Co, 53 Fe

<sup>b</sup>International Annealed Copper Standards

\* 1. Solders under normal conditions, 2. Solders under special conditions, 3. Not normally soldered

ALUMINUM - There are significant weight advantages associated with aluminum, it has electrical conductivity characteristics that place it third next to copper and silver and it is easy to fabricate and etch into interconnects. However, vast quantities of electricity are used in its manufacture and prices of aluminum are increasing dramatically which will also affect availability. It can be joined to Al and Ag-Ti contacted solar cells using ultrasonic bonding, however, joint survivability under temp cycling is poor with Al contacted cells and not greatly improved with Ag-Ti contacted cells (Ref. 1, pg 3-44). Therefore, for the SEPS application as a printed circuit interconnect material, aluminum has a Category III status because there are feasible alternates available and it would not be schedule or cost effective to develop the required improvements in ultrasonic bonding and cell Al contact adhesion at this time.

KOVAR & INVAR - Both Kovar and Invar are highly ferrous alloys, are therefore magnetic materials and they are at the lowest end of the candidate interconnect material scale on electrical conductivity. This has a formidable impact on required cross sectional area, which is further compounded because of the resulting weight increase. An interest exists in these metals, especially Invar, because of its favorable low coefficient of thermal expansion.

For the SEPS application Kovar and Invar have a Category III state of the art status because copper is a feasible alternate. The basic limitations on Kovar and Invar are low electrical conductivity combined with high relative weight and producibility limitations.

SILVER - Silver has excellent electrical conductivity and has a demonstrated good flight history--primarily in the expanded metal mesh category. However, it is the heaviest of the candidate metals (density  $10.6 \text{ g/cm}^3$ ) and it would be very costly for a solar array the size of SEPS. It therefore has a Category III status.

MOLYBDENUM - Of the low expansion candidates (which incidentally also all require plating) Moly, Invar and Kovar, Moly is favored because it is non magnetic, unlike Kovar and Invar; it is more than 10X better as an electrical conductor in the unplated form than Kovar and Invar; and it has a lower coefficient of expansion than Kovar.



It does require unique facilities and procedures to be properly plated in the SEPS module size so there are producibility constraints plus on a side by side comparison with Copper Moly is the heaviest system. Its current state of the art status is II.

COPPER - For tradeoffs and State of the Art Status based entirely on the physical properties of the metals Mo would be a first selection and copper a second selection as is indicated in Table 2 reproduced from Reference 1. However, the specific utilization factors of producibility and SEPS weight restraints dictate the use of copper as the baseline interconnect metal. Its excellent low temperature ductility, good producibility, availability in a variety of foil gauges and generally good test results result in it being categorized as State of the Art Status I.

#### INTERCONNECT STATUS SUMMARY

Table 3 lists the status for the candidate interconnect metals. The status of Molybdenum may be upgraded in the future if reduction in cell thickness can occur without compromising power thereby gaining a better weight allocation for the array circuitry, and if more amenable large moly circuit fabrication procedures are developed.

TABLE 2A  
PHYSICAL PROPERTIES COMPARISONS

Property	Preferred Range	Rank	Weighting* Factor	Comments
- Thermal Expansion Coefficient	Low	1st	2.4	- The closer to silicon coefficient the lower the temperature induced stresses
- Ductility	High	2nd	2.2	- Important in lower fatigue and higher metal cycle life
- Electrical Conductivity	High	3rd	1.7	- Primary factor for proper electrical function. Also important in making weld bond
- Ultimate Shear Strength	High	4th	1.5	- Factor in ability to resist loading
- Density	Low	5th	1.2	- Important, as arrays become larger, for weight reduction
- Thermal Conductivity	High	6th	1.0	- Conducts heat away from solar cells

\*Point value out of 10 total.

TABLE 2B  
GENERAL INTERCONNECT METAL TRADEOFFS-  
ALL CANDIDATE METALS

WEIGHTING FACTOR	1.0	1.2	1.7	1.5	2.2	2.4		
METAL	THERMAL COND	DENSITY (G/CM <sup>3</sup> )	CONDUCTIVITY (REQUIRED CROSS SECTION FOR CONSTANT VOLTAGE DROP)	ULTIMATE SHEAR STRENGTH	DUCTILITY	COEFFICIENT OF EXPANSION (IN./IN.-°C)	TOTALS	RANKING
Cu	<u>2</u> (2)	<u>8.9</u> (3) <u>10.7</u>	<u>1.7</u> (2) 1.0	<u>3.0</u> (2)	<u>2.2</u> (1)	<u>16.5</u> (3) <u>39.6</u>	59.2	2
Ag	<u>1</u> (1)	<u>10.6</u> (5) <u>12.7</u>	<u>1.7</u> (1) 0.97	<u>4.5</u> (3)	<u>4.4</u> (2)	<u>17.0</u> (4) <u>40.8</u>	65.1	3
Al	<u>3</u> (3)	<u>2.7</u> (1) <u>3.2</u>	<u>2.7</u> (3) 1.59	<u>6.0</u> (4)	<u>6.6</u> (3)	<u>23.0</u> (5) <u>55.2</u>	76.7	4
Mo	<u>4</u> (4)	<u>9.01</u> (4) <u>10.8</u>	<u>4.9</u> (4) 2.85	<u>1.5</u> (1)	<u>11.0</u> (5)	<u>4.9</u> (1) <u>11.8</u>	40.4	1
Ko	<u>5</u> (5)	<u>8.36</u> (2) <u>10.0</u>	<u>50.0</u> (5) 29.43	<u>7.5</u> (5)	<u>8.8</u> (4)	<u>5.0</u> (2) <u>12.0</u>	93.3	5

( ) DENOTES RANK FIRST, SECOND, ETC.  
\* EQUATED TO COPPER AS 1  
— WEIGHTED PRODUCT

TABLE 3  
STATE OF THE ART STATUS  
SOLAR CELL INTERCONNECT

CANDIDATE	STATUS
COPPER	I
MOLYBDENUM	II
ALUMINUM	III
SILVER	III
KOVAR	III
INVAR	III

## REFERENCES

Reference 1 - Phase III Progress Report, LMSC-D338388, Nov 1973, "Solar Array Flexible Substrate Design Optimization, Fabrication, Delivery & Test Evaluation Program", Appendix B - Material Properties

Reference 2 - TM 33-626, "Thermoelastic Analysis of Solar Cell Arrays and Their Material Properties", JPL, Sept 1973

Reference 3 - MSC-07161/LMSC-D159618, Design Data Handbook for Flexible Solar Array Systems, NAS9-11039, March 1973

Reference 4 - LMSC-A995719, Second Topical Report, Design and Analysis, Space Station Solar Array Technology Program, NAS9-11039, Nov 1971

## STATE OF THE ART ASSESSMENT (CONT.)

## 2.6.4 CELL JOINING TECHNIQUES

Solar cells are connected electrically with a metallic connector network. The cells are fabricated with a metallization contact layer (positive and negative) and joints are made between the interconnect metal and the cell contact. The joining technique may be solder or solderless. The solderless techniques include ultrasonic bonding, parallel gap electric resistance welding, thermocompression bonding and laser welding. The selection of various techniques is dependent on the metals being joined, the speed and the degree of automation that the technique may afford, the array lifetime, the thermal cycling temperature range and number of cycles, and the state of development of the bonding technique.

Soldered Joining

Solder joining is the most common joining technique used to date. Its major disadvantage is that under deep thermal cycling or high number of thermal cycles, 500 to 1,000, it often causes silicon divots and solder cracks. This is a result of high stresses in a relatively large solder joint and the mismatch in coefficient of thermal expansion between solder and silicon. The flight systems that have used solder successfully have controlled the amount of solder used, the thickness and configuration of the interconnect material. In addition the combined mission lifetime and thermal environment have not exceeded the soldered system capability. The soldered joints are easily made, inspected and repaired. In the SEPS application the weight of solder is a penalty over non-soldered systems, the solder would be the weakest link in non-nominal temperature spikes, and the five year geosynchronous mission thermal cycling environment for a lightweight array makes solder a doubtful technique. Solder is classed as a Category III item which could be used with an anticipated reduction in mission lifetime. Alternate techniques are available.

### Ultrasonic Bonding

In ultrasonic bonding, the two materials to be joined (the interconnect metal and the contact of the solar cell) are securely held between a supporting platform and a bonding tip by means of a static clamping force. A transducer-coupling-tip system converts high-frequency electrical power from a suitable source into mechanical vibrations and transmits this vibratory energy through the bonding tip into the material area to be joined. The ultrasonic vibration causes local heating and cold flow of the interconnect in the immediate interface region, and a bond between the interconnect and the solar cell contact is obtained.

The use of ultrasonic bonding techniques for interconnecting solar cells is reported in Ref. 1 (Appendix C) and Ref. 2. Bonding parameters have been developed and good contact pull strengths are achieved with aluminum interconnects on Al and on Ag-Ti contacted solar cells where cell contact thickness is at least 5 microns. An advantage of ultrasonic bonding is that the heating effects are limited in depth in the solar cell and the potential for cell junction damage is small. In a printed circuit array, some problem has been noted when the encapsulating substrate holds the interconnect material too stiffly near the bond area. The work by Hughes on the Air Force Hardened Solar Power System (HASPS) has also furthered the development of aluminum interconnect/aluminum contact ultrasonic bonding. Bonders with sufficient reach for solar panel work are available. From a weight standpoint, the use of an aluminum system in SEPS would provide a significant weight reduction. However, as noted in the state of the art assessment for interconnect metals, aluminum interconnect joints are not performing well under thermal cycling. The ultrasonic bonding technique by itself making mechanical joints is classed as Category I but as part of a system utilizing aluminum interconnects and surviving thermal cycling it is classed as Category III with feasible alternates available.

### Parallel Gap Electric Resistance Welding

Resistance welding of solar cell interconnects is the non-soldered joining technique that has seen the most development activity. Two closely spaced electrodes are used to press the interconnect material against the cell contact. An electric current is then passed between the electrodes. Since the contact resistance between the interconnect

and the cell contact is high, the temperature rise causes the two materials to weld. The electrodes are of high temperature material. They are also heated and produce some heat input to the joining process. Ref. 1 reports the results of a study to determine the requirements for cell surface finish, cell metallization thickness, weld voltage, weld pressure and pulse duration that produce a strong bond without damage to the cell. This latter consideration is due to the relatively large amount of energy that is introduced into the cell during the joining process. A current Air Force satellite program at LMSC is developing a rigid solar panel that uses parallel-gap welding between silver plated 1 mil molybdenum and Ag-Ti contacted cells. The cell junction is of conventional depth. A printed circuit copper interconnect, parallel gap welded to Ag-Ti contacted cells, has also been used to fabricate small test modules at LMSC. These have been thermal cycled between  $+60^{\circ}$  and  $-180^{\circ}\text{C}$  for over 700 cycles successfully. The use of parallel gap welding for the SEPS array on conventional solar cells is classed as Category I. The shallow junction of high efficiency cells is a potential problem area for parallel gap welding. There is limited data in this area because the cells are new and welding evaluations are incomplete. COMSAT Laboratories has reported their cell, before being licensed to Centralab, could not be safely resistance welded. Centralab says that it can be. Hughes has reported successful parallel gap welding of the Heliotek high efficiency cell. For the high efficiency cell, parallel gap welding is classed as Category II with the weld schedules to be developed with no, or acceptable, degradation in cell power.

The array fabrication process using parallel gap welding is presently limited in printed circuit flexible panel technology as far as automated place and weld systems are concerned. This technology does not limit the fabrication of SEPS panels but does have a cost impact on large area array fabrication. The adhesive used in the substrate lamination, if it flows with heat as does FEP Teflon, has an effect on the contamination of the electrodes. The electrode cleaning and replacement cycles also have an impact on the cost of array fabrication. This latter effect is of more concern than automation and the substrate design/electrode design for array fabrication using parallel gap welding is classed as Category II.

## Thermal Compression Bonding

Most methods of welding rely on achieving a bond by developing sufficient heat to cause some degree of melting of the two parts to be joined. Parallel gap resistance welding is an example of this type of welding (electron beam, laser, gas, etc. are others). Thermocompression bonding on the other hand does not depend on bringing the parts to their melting point but on the microscopic diffusion of each material into the other (or one into the other). The classical diffusion equations relating time, temperature, and diffusion coefficient for the materials can be used to describe the theoretical process. Thus a microscopic thermal diffusion bond which develops sufficient mechanical as well as electrical characteristics can be achieved for a variety of semiconductor material and fabrication methods. The basic process is accomplished by providing intimate contact (pressure) between the mating surface and using temperature and time to control the diffusion process. Thus a detail time vs temperature schedule must be developed to control the bonding process. However, the temperature and time profile is highly dependent on the degree of intimate contact (cleanliness, smoothness, oxides, etc.) and as such requires sufficient control of the mating part 1) mechanical properties, 2) topography of the surface, 3) presence of inorganic or organic films, 4) and the actual bonding device design as well as the compliant tool/fixture. Pressure is used to maximize the actual contact area thus overcoming some surface irregularities. This has also resulted in soft material providing high quality bonds as opposed to very hard materials which would on a microscopic basis provide insufficient area contact. For these reasons the following materials have been used very extensively by the semiconductor industry for thermocompression bonding.

- 1) Aluminum to Aluminum
- 2) Gold to Gold
- 3) Aluminum to Gold

Since Silver is not generally used in the semiconductor industry less is known about its overall bondability. However, it can be said that it is an acceptable material for thermal compression bonding. Gold is the primary material in the semiconductor device fabrication due to the ease of attaching devices through forming a gold-silicon eutectic. The devices are then interconnected in the artwork or by thermocompression wire bonding (1-2 mil diameter wires). The semiconductor industry has extensive knowledge of this process for integrated circuits to microcircuits and over 10 companies manufacture specially designed thermocompression bonding machines for automated and production line systems. These processes include "ball" bonding of gold to gold or aluminum and wedge or stitch bonding of aluminum to aluminum.



Based on the general capabilities of thermocompression bonding LMSC has investigated its applicability to the bonding of solar cells. The most promising method of bonding large area thick lead interconnects to solar cells was determined to be the wedge type bond over the available ball or stitch type bonders. This was mainly a function of material considerations and mechanical strength requirements. For example, at present the most desirable materials for solar cell bonding are silver plated Kovar or moly using a silver plated/ contacted solar cell with silver thicknesses on the cell and interconnect material of from  $3-7\mu$ . The wedge type bonders used for lead frames was the most apparent choice to investigate for solar cell application. As such several solar cell samples and interconnects were sent to Jade Corporation (a designer of special wedge type bonders) for tests. The cells were 4 cm x 2 cm cells with approximately  $4\mu$  of Ag. Jade was able to bond a flight type Ag plated Molybdenum interconnect to both the "N" contact and "P" using several weld schedule (pressure and time) on a standard bonder. The process was deemed to be an acceptable method of bonding solar cells together. Therefore an inquiry as to tooling cost and equipment costs were made. Based on these discussions it was decided to delay any further studies on the thermocompression bonding since a tailor made machine to weld solar cell modules would be required costing close to \$50K. This was beyond the study at that time and LMSC decided to base welding of silver plated solar cells to silver plated Moly interconnects on parallel gap welding techniques.

Some concern has been expressed over the acceptability of parallel gap welding versus thermal compression for the newer shallow diffused junction solar cells ( $.5\mu$  versus  $.3\mu$  junctions). However, with the available data it was concluded that parallel gap welding would be acceptable for the slightly shallower junctions since the heated zone can be controlled to the silver layer with a reasonable time and voltage weld setting.

Thermocompression bonding has very major disadvantages as compared to parallel gap 1) high pressures over a larger working area, and 2) much longer time durations required per bond. In addition, the tool and wedge design requires specific pressure control (compliance) and would require fairly complex fixtures to account for solar cell tolerances.

Thermocompression bonding could relatively easily be adapted to bonding of solar cells to solar cells if sufficient expenditures for equipment and process development were expended. It is questionable at this time whether there is any major advantage or disadvantage for this bonding technique. However a great deal more available equipment in the parallel gap field is available for adaption and as such has received considerable more attention.

For SEPS, thermocompression bonding is classed as a Category III item with feasible alternates available. If high efficiency cells are selected for SEPS, the Category changes to II, but development for SEPS should await the determination that parallel gap welding will not be satisfactory. It is noted that no additional effort has been expended by either Hughes or Boeing on thermocompression bonding for solar cells since the work reported in Refs. 2 and 3.

#### Laser Welding

The development of a laser welding technique is reported by Hughes in Ref. 2. While adequate welding of silver plated molybdenum on Ag-Ti contact cells was attained, voids were often observed in microsections. The state-of-the-art in this area is rudimentary and it is classed as Category III.

TABLE 1  
STATE OF THE ART STATUS  
CELL JOINING TECHNIQUES

<u>CANDIDATE</u>	<u>STATUS</u>
Parallel Gap Electric	
Resistance Welding	
a. Conventional Solar Cells	I
b. Shallow Junction Cells	II
c. Electrode Cleaning and Replacement	II
Soldered Joining	III
Ultrasonic Bonding	III
Thermocompression Bonding	III
Laser Welding	III

## REFERENCES

1. "Solar Array Flexible Substrate Design Optimization, Fabrication, Delivery and Test Evaluation Program", Phase III Progress Report, LMSC-D338388, November 1973, Contract NAS8-28432
2. Eakins, T. C., "Results of Solar Cell Welded Interconnection Development", Paper No. 729101, 7th I. E. C. E. C., September 1972
3. Clarke, D. R., "High-Temperature Annealable Solar Array", Paper, 7th Photovoltaic Specialists Conference, November 1968

## STATE OF THE ART ASSESSMENT (CONT.)

## 2.6.5 Solar Array Flexible Substrate

Flexible substrate design activities have been underway since 1964 by both U. S. and foreign agencies. The term, lightweight flexible substrate, refers to the fact that flexible substrates designs using high-strength thin film plastic materials produce array panels lighter than those using rigid substrates such as magnesium castings or aluminum honeycomb core panels with facesheets of various materials. Several prototype flexible arrays have been built and tested (Ref. 1-6) and one has been flight tested (Ref. 7). The SEPS specific power requirement, however, emphasizes the need for a flexible substrate that is lighter in weight than most of the flexible systems developed to date. The candidate substrates (excluding the metallic electrical interconnect system) vary in design from single plastic films to laminated sandwiches of 4 layers of materials. The choice of the substrate design is tied to considerations of how the solar cells are mounted mechanically to the substrate, how the interconnect system is integrated with the substrate, the substrate manufacturing process and the cell joining technique. Additional consideration is required for electrical insulation, array thermal operation, interaction of substrate thermal cycling stresses with cell joints, mechanical environments, outgassing requirements and the mission space environment effects. The availability of substrate materials in thicknesses less than 1 mil and in sufficient widths to allow efficient array fabrication is of considerable importance to SEPS weight requirements.

The mechanical mounting of solar cells on flexible substrates is accomplished by either an adhesive or adhesiveless system. The adhesive system treats the flexible substrate as similar to a rigid panel with an insulated surface. Solar cells are joined to form modules using separate interconnect piece parts. Adhesive is then applied either to the back of the solar cell modules or to the flexible substrates and the solar cells are then pressed to the substrate to complete the mechanical mounting. The adhesiveless system employs a metallic cell interconnect system that is mechanically integrated with substrates. The solar cells are then joined to the interconnect system to provide

both an electrical joint and a mechanical joining of the solar cell to the flexible substrate. The printed circuit is an example of a cell interconnect system that is integral with the substrate. The etched printed circuit is considered the best approach to the SEPS design because it represents a low cost method of producing a large quantity of thin solar cell interconnecting networks, eliminates the physical handling of the many pieceparts associated with separate interconnect systems and can be used in an adhesiveless solar cell mounting system. Similarly, the flexible substrate technology desired is one useable with printed circuit technology.

The flexible printed circuit is built by 1) adhering a metal foil to a plastic substrate on underlay, 2) photo-etching the desired circuit configuration, and 3) adhering a plastic coverlay over the circuit to provide an encapsulated and, therefore, an insulated circuit.

The thin film substrate material requirements for either a single film or a laminate of several films are:

- o Be stable in the space environment (hard vacuum, radiation and temperature extremes) with minimum outgassing
- o Be highly flexible and capable of repeated bending to the smallest design radius over the operating temperature range
- o Have high tensile strength with minimum creep over lifetime, operating temperature and tension loads
- o Be an electrical insulator and have low moisture absorption
- o Be highly transmissive to infrared wavelengths to transfer heat directly from the cell back surface to space or be compatible with thermal control coatings
- o Conduct heat well
- o Have good tear strength
- o Be useable with printed circuit technology and resistant to damage from soldering and other manufacturing operations such as welding of solar cells to the interconnect system
- o Be a minimal contributor to welding electrode contamination

(THIS PAGE LEFT BLANK)

Based upon these requirements, the candidate materials that have been evaluated include Kapton, Aclar, Nomex, Mylar, FEP Teflon, and Teflon impregnated fiberglass (FEP and TFE 50-50% by weight). The FEP Teflon and the Aclar are candidate adhesive systems for the printed circuit encapsulation or lamination. (Section 4.1.3.1 of the NAS9-11039 First Topical Report, LMSC-A981486, provides a summary of the physical, thermal, electrical and chemical properties of the candidate materials noted above. Table 1 summarizes significant characteristics of the films. Additional candidate adhesives for printed circuit encapsulation or lamination are TME 300 (modified epoxy), Pyrolux (acrylic adhesive) and Tefzel (ETFE fluoropolymer film). Table 2 summarizes the significant characteristics of the adhesive systems.

Based on the experience of both foreign and domestic flexible substrate developers, the use of Kapton as the main structural material in the printed circuit substrate is highly favored. The required SEPS laminated substrate structure, however, is composed of thinner forms of both Kapton, laminating adhesive and printed circuit metal than has been heretofore fabricated and tested.

The candidate substrate laminations are

1. 0.5 mil Kapton/0.5 mil FEP Teflon/1.0 mil copper/0.5 mil FEP Teflon/  
0.5 mil Kapton
2. 0.5 mil Kapton/0.5 mil Tefzel/1.0 mil copper/0.5 mil Tefzel/0.5 mil Kapton
3. 0.5 mil Kapton/0.5 mil TME 300/1.0 mil copper/0.5 mil TME 300/0.5 mil  
Kapton
4. 0.5 mil Kapton/0.5 mil Pyralux/1.0 mil copper/0.5 mil Pyralux/0.5 mil  
Kapton

#### Kapton (0.5 mil)/FEP Teflon (0.5 mil)

The use of these materials in printed circuits and flexible cables is well established for a Kapton thickness of 1 mil. In several LN<sub>2</sub> convection chamber tests at LMSC the combination has been cycled between +60°C and -180°C for up to 1000 cycles without apparent degradation in mechanical or electrical properties. Tensile, tear, and creep tests are reported in Ref. 8 (Section 1.2) and Ref. 9 for a substrate system using 2 mils of Kapton, temperatures to 77°C (171°F) and loading up to 4 lbs per inch.



**TABLE 1**  
**PROPERTIES OF FLEXIBLE SUBSTRATE MATERIALS**

PARAMETER	MATERIAL			
	KAPTON H-FILM (POLYIMIDE) (1 MIL)	TEFLON FEP (FLUOROPLASTIC) (1 MIL)	MYLAR (TYPE T) (POLYESTER) (1 MIL)	FEP IMPREGNATED FIBERGLASS (DODGE 368-5) (5 MIL)
RELATIVE COST	1.0	0.62	0.08	6.0
PROPERTY TEMPERATURE UNLESS OTHERWISE NOTED	25°C	25°C	25°C	25°C
ULTIMATE TENSILE STRENGTH (PSI)	25,000	3,000	45,000	125 LB./IN. WIDTH
YIELD POINT AT 3% (PSI)	10,000	1,700	NOT REPORTED	-
STRESS TO PRODUCE 5% ELONGATION (PSI)	13,000	1,800	23,000	-
ULTIMATE ELONGATION (%)	70	300	40	5%
TENSILE MODULUS (PSI)	430,000	70,000	800,000	-
FOLDING ENDURANCE (CYCLES)	10,000	4,000	100,000	-
INITIAL TEAR STRENGTH (GRAVES) (GM/MIL)	510	270	450	10,000
PROPAGATING TEAR STRENGTH (EMELDORF) (GM/MIL)	8	125	20	-
SPECIFIC GRAVITY	1.42	2.15	1.377	2.20
CREEP RESISTANCE	GOOD	POOR	GOOD	EXCELLENT
MELTING POINT (°C)	NONE	260-280	250	260-280 (FEP MELT)
ZERO STRENGTH TEMPERATURE (°C)	815	255	248	-
COEFFICIENT OF THERMAL EXPANSION (IN./IN./°C)	$2.0 \times 10^{-5}$ (14° TO 38°C)	$2.55 \times 10^{-5}$ AT -77°C $5.0 \times 10^{-5}$ AT 100°C	$1.7 \times 10^{-5}$ (30° TO 50°C)	-
COEFFICIENT OF THERMAL CONDUCTIVITY (CAL) (CM) (CM <sup>2</sup> ) (SEC) (°C)	$3.72 \times 10^{-4}$	$4.65 \times 10^{-4}$	$3.7 \times 10^{-4}$ (25° TO 75°C)	-
SPECIFIC HEAT (CAL/GM/°C)	0.261 AT 40°C	0.28	0.28	-
HEAT SEALABLE	NO	YES (280° TO 370°C)	NO (UNLESS COATED OR TREATED)	YES (SAME AS FEP-TEFLON)
SHRINKAGE	0.3% AT 250°C, 0.5% AT 300°C, 3% AT 400°C (FOR 30 MIN)	0.7% STRETCH (IN M.D.), 2.2% SHRINK (IN T.D.), 150°C, 30 MIN		
USABLE TEMPERATURE LIMITS (°C)	-269 TO 400	-240 TO +200	-70 TO 150	-
EMISSIVITY	.80	.85	NOT REPORTED	-
ABSORPTIVITY	NOT REPORTED	3% FROM 0.5 TO 3.8 μM	NOT REPORTED	-
TRANSMISSIVITY	0.66	96% FROM 0.5 TO 3.8 μM	.86 AT 0.8 μM	-
REFLECTIVITY	~0.13	1%	NOT REPORTED	-
DIELECTRIC STRENGTH (1 MIL, 60 CYCLES (VOLTS)	7,000	6,500	7,500	-
MOISTURE ABSORPTANCE	2.9% IN H <sub>2</sub> O FOR 24 HR AT 23.5°C	<0.01% IN H <sub>2</sub> O FOR 24 HR AT 23.5°C	<0.8% IN H <sub>2</sub> O FOR 24 HR AT 23.5°C	<0.01 IN H <sub>2</sub> O FOR 24 HR
OUTGASSING WEIGHT LOSS	0.25% IN HELIUM FOR 2 HR AT 400°C	-	NOT REPORTED	-
RADIATION RESISTANCE	NO LOSS IN TRANSMISSION AFTER 10 <sup>14</sup> , 800 KEV PROTONS/CM <sup>2</sup> , 2.6 X 10 <sup>17</sup> , 1 MEV ELECTRONS/CM <sup>2</sup> OR UV UP TO 9600 ESH	NO LOSS IN TRANSMISSION AFTER 10 <sup>14</sup> , 800 KEV PROTONS/CM <sup>2</sup> OR 2.6 X 10 <sup>17</sup> , 1 MEV ELECTRONS/CM <sup>2</sup> , 4.5% LOSS IN TRANSMISSION AFTER 2 EQUIVALENT SOLAR YEARS OF UV.	NO LOSS IN TRANSMISSION AFTER 10 <sup>14</sup> , 800 KEV PROTONS/CM <sup>2</sup> , 5% LOSS AFTER 2.6 X 10 <sup>17</sup> , 1 MEV ELECTRONS, 20% LOSS AFTER 3510 ESH	EXCELLENT
AVAILABILITY	0.25 TO 5 MILS, 60 IN. MAX. WIDTH	0.5 TO 20 MILS, 48 IN. MAX. WIDTH	0.5 TO 1.5 MILS	39 IN. MAX. WIDTH

TABLE 1 (Cont.)  
TEFZEL ETFE FLUOROPOLYMER

## Relative Cost to Kapton H Film

Ultimate Tensile Strength (psi)	11,000	-70°C	
	7,500	23°C	
	1,200	155°C	
Ultimate Elongation (%)	300	23°C	
Tensile Modulus (psi)	230,000	-70°C	
	125,000	23°C	
	7,000	155°C	
Folding Endurance	30,000 Flexes	9 Mil	180° MIT
Initial Tear Strength (Graves) (gm/mil)	Not reported		
Propagating Tear Strength (Emeldorf) (gm/mil)	650/950 MD/TD		
Specific Gravity	1.7		
Creep Resistance	Not reported		
Melting Point, °C/°F	270/520		
Zero Strength Temperature (°C)	Not reported		
Coefficient of Thermal Expansion (in/in°C)	6.7 x 10 <sup>-5</sup>	32-86°F	
	4.7 x 10 <sup>-5</sup>	284-302°F	
Coefficient of Thermal Conductivity (Cal)(Cm)(Cm <sup>2</sup> )(Sec)(°C)	Not reported		
Specific Heat	Not reported		
Heat Sealable	Yes	270°C	
Shrinkage (230°C, 6 & 48 hrs, 36" sample)	0 in		
Useable Temperature Limits	to +180°C		
Emissivity	Not reported		
Absorptivity	Not reported		
Transmissivity	Not reported		

Reflectivity	Not reported
Dielectric Strength (v/mil)	3500
Moisture Absorption, %	< 0.02      ASTM D-570
Outgassing Weight Loss	Not reported
Radiation Resistance	>50% elongation at 10 <sup>8</sup> rad exposure
Availability	0.5 mils to 10 mils
Low Temperature Embrittlement	-150°F      D746

TABLE 2  
 PROPERTIES OF LAMINATING ADHESIVES

	DuPont Pyrallux	TME-300	Rexham MKC 12069
Adhesive Type	Acrylic	Modified Epoxy	Phenolic Butyral
Available Kapton Thickness	1 Mil	0.5 Mil	1 Mil
Shrinkage in Laminate (in/in)*			
Longitudinal	.001	.001	0
Transverse	.001	.002	0
Solder-Dip-Temperature Shock, Humidity/ Temperature and Peel Strength Tests per LAC 3238*	Passed	Passed	Passed
Peel Strength on Copper Foil (lbs/linear inch) RT	10-14	8	5.4

\*Tests on 2 mil Kapton substrate, 2 mil Kapton coverlay

The maximum loading in the SEPS array is 0.15 lbs/in, so that creep at temperatures below 77°C for a 1 mil Kapton system will not be excessive. The creep rate at 250°F for this candidate system is required for SEPS and will be determined in this program.

The tensile strength data for 1 mil Kapton at 200°C (392°F) indicates a yield point (at 3%) of 6,000 psi. The maximum design static SEPS stress is 145 psi in the total substrate. With a tensile modulus of 260,000 psi at 200°C, the strain in the 115 ft array substrate is 0.8 in.

The tested initial tear strength of the basic substrate (2 layers, each 1 mil Kapton/0.5 mil FEP) is 390 gm/mil or 780 gms total in the SEPS substrate at 75°F. This value will be determined in this program.

The folding endurance of the substrate system at the low temperatures associated with 6 a.u. partial retraction and redeployment will be determined in this program.

The effect of UV radiation on mechanical and electrical properties will also be determined during this program.

The 0.5 mil Kapton/0.5 mil FEP layer (two layers per substrate) is classed as a Category I item due to ground testing in the following areas:

- o Thermal cycling material stability in a synchronous equatorial mission
- o Creep strength stability in missions with blanket temperatures below 77°C
- o Tensile strength capability up to 200°C

It is considered a Category I item to be substantiated in this program in the areas of:

- o Substrate initial tear strength at room temperature and at 250°F
- o Low temperature retraction and redeployment capability
- o Effect of UV radiation on mechanical and electrical performance
- o Creep strength of substrate at 250°F
- o Addition of thin scrim material in substrate laminate as backup to possible tear strength limitations
- o Compatibility with manufacturing of the laminate and the techniques used to join the solar cells to the printed circuit.

This substrate is classed as a Category II item in the areas of:

- o Radiation damage effects on mechanical and electrical properties
- o Thermal cycling testing of substrate with interconnect, solar cells, and cell joining technique to determine effect of substrate stresses on system
- o Creep testing of the total panel makeup with substrate, hinges, hinge reinforcement, and edge reinforcement. Test at maximum load and temperature expected.

Kapton (0.5 mil)/Tefzel (0.5 mil)

Tefzel is apparently a tougher material than FEP and is considered an alternate to FEP. It is not presently available in the Kapton laminated form desired but separate 0.5 mil films of Kapton and Tefzel are available and will be laminated in this program to evaluate its potential application to the SEPS program. It is classed as a Category I item to be substantiated in this program in the areas of:

- o Creep strength at 77°C and at 121°C
- o Tensile strength at 77°C and at 121°C
- o Substrate initial tear strength at 77°C and at 121°C
- o Low temperature retraction and redeployment capability
- o Effect of UV radiation on mechanical and electrical performance
- o Compatibility with manufacturing of the laminate and solar cell welding operations

This substrate is classed as a Category II item in the areas of:

- o Large volume laminating in the required thickness and width
- o Radiation damage effects
- o Thermal cycle testing
- o Creep testing of the total panel makeup

Kapton (0.5 mil)/TME 300 (0.5 mil)

The high specific gravity of both FEP and Tefzel is a drawback to the lightweight substrate design desired. The flowing of both materials during laminations of prepunched Kapton sheets and the floating of circuits in the heated laminate adversely affect dimensional control and the cleanliness of exposed printed circuit areas.

TME 300 (modified epoxy) is available applied to Kapton in the desired thicknesses. This substrate will be evaluated with the Tefzel design in the areas noted for Tefzel but it is classed as a Category II item since 1) it has no known sufficiency for the SEPS design and 2) a significant weight savings over the FEP design will result if it can be applied. The preliminary tests in this program will determine if further development is recommended.

#### Kapton (0.5 mil)/Pyralux (0.5 mil)

Pyralux is an acrylic adhesive that is made and applied to Kapton film by DuPont. It is not presently available on Kapton thinner than 1 mil. It also has potential for solving FEP problems in fabrication and reducing substrate weight. It is classed as Category II requiring a development of the thinner design by DuPont and development testing of the substrate.

Table 3 summarizes the substrate area density of current designs and proposed concepts.

#### Flexible Substrate Status Summary

Table 4 lists the state-of-the-art status for flexible printed circuit substrate candidates for the SEPS application. The lowest category of various substrate performance requirements is noted.

TABLE 3  
SUBSTRATE DESIGNS

DESIGN	AREA DENSITY (Kg/m <sup>2</sup> )	COMPONENT	REF
Hughes FRUSA	0.0360	1 mil Kapton	7
	0.0175	1 mil Fiberglass cloth	
	0.0298	Adhesive	
	<u>0.0833</u>		
LMSC Space Station	0.0720	2 mil Kapton (total)	5
	0.0546	1 mil FEP (total)	
	<u>0.1266</u>		
LMSC SEPS Baseline (Proposed)	0.0360	1 mil Kapton (total)	--
	0.0546	1 mil FEP (total)	
	<u>0.0906</u>		
GE 110W/Kg (Proposed)	0.0384	2 mil Kapton ( 50% holes)	10
	0.0333	Proton protection adhesive	
	<u>0.0617</u>		
RAE	0.0370	2 mil Kapton (50% holes)	6-1
	0.0220	Proton protection adhesive	
	<u>0.0590</u>		
LMSC SEPS Design - FEP Replaced	0.0360	1 mil Kapton (total)	--
	0.0360	1 mil Adhesive (total)	
	<u>0.0720</u>		
LMSC SEPS - TEFZEL (Concept)	0.0360	1 mil Kapton (total)	--
	0.0431	1 mil TEFZEL (total)	
	<u>0.0791</u>		

TABLE 4  
STATE OF THE ART STATUS  
FLEXIBLE SUBSTRATES

CANDIDATE (ONE SIDE OF LAMINATE)	CATEGORY
0.5 mil Kapton/0.5 mil FEP	II
0.5 mil Kapton/0.5 mil TEFZEL	II
0.5 mil Kapton/0.5 mil TME 300	II
0.5 mil Kapton/0.5 mil PYRALUX	II



## REFERENCES

- Ref. 1-1 "Feasibility Study of 30 Watts per Pound Rollup Solar Array", Final Report, June 1968, General Electric, JPL Contract 951970.
- Ref. 1-2 "Rollup Sub-solar Array", Final Report, October 1970, General Electric, JPL Contract 952314.
- Ref. 2-1 "Fabrication Feasibility Study of A 30 Watt Per Pound Rollup Solar Array", Final Report, August 1968, Fairchild-Hiller, JPL Contract 951969.
- Ref. 2-2 "Positive Deployment Solar Array Development Program" Phase I, II & III Reports, June 1966 through July 1968, Fairchild-Hiller, Contract NAS5-9648.
- Ref. 3 "Feasibility Study 30 Watts Per Pound Rollup Solar Array", Final Report, June 1968, Ryan Aeronautical, Contract JPL 951107.
- Ref. 4 IECEC Paper 699094, "40 Watts/Pound Spacecraft Solar Array", September 1969, Thomson-Ramo-Wooldrige Sys., Inc.
- Ref. 5-1 IECEC Paper, "Flat-Pack Flexible Solar Cell Array", August 1968, LMSC.
- Ref. 5-2 Space Station Solar Array Program, Third Topical Report, "Design Support, Major Hardware, and System Level Testing", September 1972, LMSC, Contract NAS9-11039.
- Ref. 6-1 "A Study of Advanced Solar Array Designs", 1st, 2nd, and 3rd Quarterlies, through November 1969, British Aircraft Corporation, Contract ESRO No. 623/68.
- Ref. 6-2 8th Photovoltaic Specialist Conf. "Progress in Advanced Solar Array Development", August 1970, Royal Aircraft Establishment (RAE).
- Ref. 6-3 7th Photovoltaic Specialist Conf., "Large Solar Array Development in U.K.", November 1968, Royal Aircraft Establishment (RAE).
- Ref. 6-4 "Development of a Deployable & Self Rigidizing Solar Cell Array in the Multi-Kilowatt Range", August 1970, Messerschmitt-Bolkow-Blohm Space Div.
- Ref. 7 "Flexible Rolled Up-Solar Array" (FRUSA) Final Technical Report, 1 July 1968 through 31 May 1972, Hughes Aircraft Company, AFAPL-TR-72-61, Contract AF33(615)-68-C-1676.

## ASSESSMENT OF STATE OF THE ART (CONT.)

## 2.6.6 Module Joints







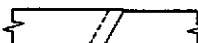
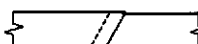
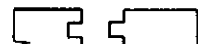

To minimize the cost impact resulting from damage to a part of the solar array blanket and to provide a unit of the blanket assembly which can be easily illuminated for manufacturing tests, the array blanket is manufactured in mechanically separate modules which are joined to form the total blanket. The desired module joint characteristics are:

1. Joints easily assembled and disassembled
2. Module interchange is readily allowed by joint techniques
3. The planar space occupied by the joint is a minimum resulting in higher packing factors
4. Joints easily manufactured
5. The joint design is compatible with low tear propagation materials


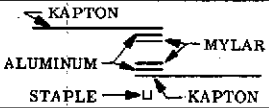

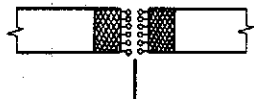



An additional requirement in a flat fold array for SEPS under the present technology evaluation is that the intermediate tensioning distribution bar is easily integrated with the module joint over the 25 to 75 percent blanket partial retraction range.

Table 1 from Ref. 1 presents substrate joining techniques which have been developed for various flexible array designs. Table 2, also from Ref. 1., summarizes the module joining techniques evaluated for the Large Space Station Solar Array Program. The methods used generally fall into the three categories of adhesive, tape, or mechanical. Mechanical methods such as the use of lacing, velcro, or pin splicing (piano hinging) require more labor and tooling than the other categories; however, they appear best for removal and disassembly. The early joint investigations in the Lockheed Independent Development programs favored the use of Fluoroplastics Adhesive 80. Later work pointed up advantages of Kapton-silicone adhesive tape.

**TABLE 1**  
**FLEXIBLE SUBSTRATE JOINING TECHNIQUES**

NO.	APPLICATIONS	METHOD	DESCRIPTION	TEST	EASE OF REMOVAL
1	LMSC 50 FT <sup>2</sup> ID FLAT PACK	 LAP BOND	ADHESIVE 80 FLUORO PLASTICS, INC. PHILADELPHIA, PA.	LAP SHEAR TESTS	FAIR
2	LMSC 80 FT <sup>2</sup> ID ARRAY	 SHEAR BOND (DOUBLE SIDED TAPE)  LAP BOND (TAPED)	KAPTON TAPE PERMACEL EE-6761	LAP SHEAR TESTS	FAIR
3	LMSC ID MODULE JOINING EVALUATION 1968	SEE FOLLOWING CHART	SEE FOLLOWING CHART	PRODUCIBILITY EVALUATION	
4	GENERAL ELECTRIC 30 W/LB ROLLUP SOLAR ARRAY	 LAP BOND	KAPTON-TO-KAPTON WITH G.E. SMRD 745 COMPOUND	LAP SHEAR TEST KAPTON TO GOLD PLATED COPPER ~>98 LB/IN	FAIR
5	HUGHES FLEXIBLE ROLLUP SOLAR ARRAY	 LAP BOND	0.25 IN. LAP BOND KAPTON TO KAPTON (0.003) BONDED WITH HUGHES FORMULATED ADHESIVE	SOLAR PANEL (CELLS BONDED TO FIBER- GLASS SUBSTRATE) WAS TEMP. CYCLED +80 TO -300°F SUCCESSFULLY. TENSILE LAP SHEAR ~73 LB/IN.	FAIR
6	FAIRCHILD-HILLER 30 W/LB ROLLUP SOLAR ARRAY	 LAPPED AND LACED  LAP BOND	0.002 KAPTON WITH HOLE PATTERN ALONG EDGE OF 2 x 3 FT. SUBSTRATE SECTIONS. TWO SUCH SECTIONS ARE LACED TOGETHER BY LAPPING THE HOLES. FIX WAS TO BOND END OF LACE WITH ADHESIVE.  H-FILM TO HFO FILM THERMAL SET; DOW A-1000 SILICONE ADHESIVE; AND PERMACEL 18	LAP SHEAR TEST ~9 LB/IN. FAILED BY UNLACING. ADEQUATE SINCE DESIGN LOAD EXPECTED WAS 0.1 LB/IN	GOOD  FAIR
7	RYAN 30 W/LB ROLLUP SOLAR ARRAY	 LAP BOND	KAPTON-TO-KAPTON WITH FM 1044R ADHESIVE	PEEL STRENGTH ~2.3 PSI; SHEAR STRENGTH >109 PSI	FAIR
8	TACONIC PLASTICS, INC. TFE GLASS CATALOG	 PIN SLICE  SEWN SEAM	ALLIGATOR LACING THROUGH WHICH A PIN IS PLACED TO COMPLETE THE SPLICE.  SUBSTRATE IS OVERLAPPED AND SEWN (MORE APPLICABLE TO IMPREGNATED FIBERGLASS CLOTH)		GOOD  POOR

**TABLE 2**  
**LOCKHEED KAPTON JOINING TECHNIQUES INVESTIGATION**

NO.	DESCRIPTION	METHOD	BOND PEEL STRENGTH LB/IN	EASE OF APPLICATION	ROOM TEMP CURE	NUMBER OF OPERATIONS	METHOD OF APPLICATION	CATALYST	EASE OF REMOVAL	REPAIR- ABILITY
1	ADHESIVE 80, FLUOROPLASTICS, INC.	 LAP JOINT	4+	GOOD	YES	2	BRUSH OR SPRAY	NOT REQUIRED	FAIR	GOOD
2	DUPONT ADHESIVE 46970		3	GOOD	NO	3	BRUSH OR SPRAY	RC-805	FAIR	GOOD
3	DUPONT ADHESIVE 46960		3	GOOD	NO	3	BRUSH OR SPRAY	RC-805	FAIR	GOOD
4	DUPONT ADHESIVE 46950		3	GOOD	NO	3	BRUSH OR SPRAY	RC-805	FAIR	GOOD
5	ALUMINUM REINFORCED - 5 MIL AL. BONDED WITH ADHESIVE 80 TO MYLAR. LAP BONDED AND STAPLED	 KAPTON ALUMINUM MYLAR STAPLE	4	GOOD	-	4	BRUSH OR SPRAY AND STAPLER	N/A	GOOD	GOOD
6	VELCRO PAD BONDED TO KAPTON WITH ADHESIVE 80	 VELCRO KAPTON	4	FAIR	-	3	PRESSURE	N/A	GOOD	GOOD
7	20 MESH AL. SCREEN SANDWICHED BETWEEN 2 LAYERS OF 6 MIL. MYLAR, BONDED TO KAPTON WITH ADHESIVE 80, WIRE THRU HOOKS		4	FAIR	-	4	-	N/A	GOOD	GOOD
8	20 MESH AL. SCREEN SANDWICHED AND BONDED BETWEEN AL. FOIL AND KAPTON WIRE THRU HOOKS	SIMILAR TO ABOVE	4	FAIR	-	4	-	N/A	GOOD	FAIR
9	DOUBLE BACK TAPE, 1-IN. WIDE MYSTIC TAPE, BORDEN CHEMICAL CO.	 LAP JOINT	1	GOOD	-	2	PRESSURE	N/A	GOOD	GOOD
10	LOOPED MYLAR BONDED TO KAPTON AND FORMED INTO "PIANO HINGE"	 MYLAR WIRE KAPTON	4	FAIR	-	4	LACE	N/A	GOOD	POOR
11	KAPTON IS LAPPED, HOLE PUNCHED, AND LACED WITH KAPTON STRIP		-	POOR	-	3	LACE	N/A	GOOD	POOR

One of the longest term evaluations of adhesive for Kapton joining (breakstrength and creep tests) has been conducted at NASA-Goddard. The testing was initiated to determine if Kapton substrates could be feasibly joined by adhesives for solar array applications. Break strength testing was performed on a Hunter Spring (Division of Amtek) tester. The samples are 2-1/16 in. wide, 7-9/16 in. long, and 2 mils thick and all bonded with approximately 5 mil thick adhesive with a 1/2-in. overlap except for some unbonded Kapton controls. On the tester, the distance between sample clamps was 5-9/16 in. The tester separates the clamps at a constant rate regardless of tension and indicates the breakpoint force and the accumulated separation movement at the breakpoint. The tests were performed at room temperature. All the Kapton material breaks occur in the total tension force range of 80 to 100 lb, and variation is ascribed to variations in the sample parameters such as in thickness and in local defects. The bonding is preceded by a chemical etch or abrasion with No. 40 emory paper of the surfaces to be bonded. Prior to break testing, the samples were cycled 25 times in liquid nitrogen and boiling water. With the exception of Sylgard 182, all bonded joints with the adhesives used held to the point at which the Kapton broke, in an area other than at the joint. The adhesives used were Sylgard 182 and Sylgard 186, RTV 41 and RTV 8243.

The objective of the NASA-Goddard tests, namely the demonstration of the feasibility of bonding Kapton to Kapton, has been accomplished. Etching or mechanically preparing the surfaces to be bonded prior to bonding appeared to be required.

#### Mechanical Joint

The joining technique developed for the Space Station is shown in Figure 1. It is stronger than is required for SEPS and is also considered too heavy. These aluminum bars on SEPS would weigh 17.7 kg per wing. A lighter weight joint, similar to No. 10, Table 2, is the mechanical joint candidate design for SEPS. Heat sealed loops of Dodge Industries FEP impregnated fiberglass cloth are a prime candidate for lamination in the substrate sandwich during substrate fabrication. A candidate piano hinge design is 0.8 mm diameter aluminum which would weigh 0.226 kg per wing.

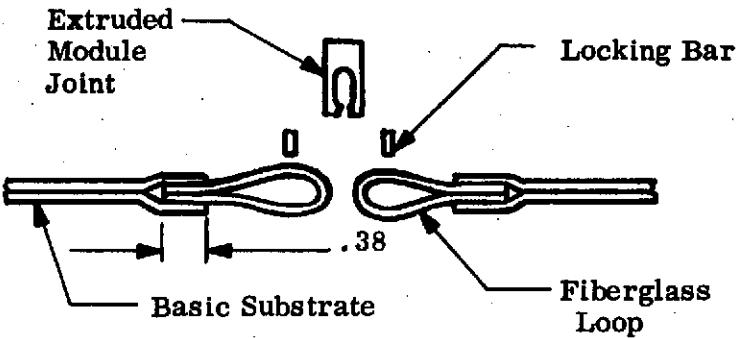
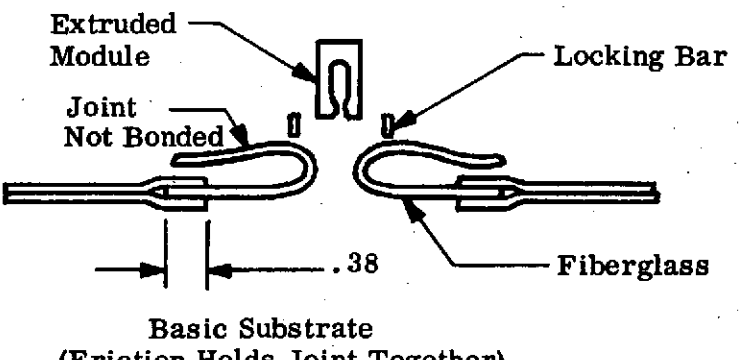
Config. No.	Joint	Tensile Strength (Lb/In)		
		-80°F	70°F	170°F
1		44.7	36.7	33.3
2		42.7	33.0	29.7

Figure 1 Space Station Module Joint Design

### Adhesive Joint

The use of 1) a soluble adhesive or 2) a heat sealable thermoplastic such as FEP Teflon or TEFZEL either alone, on a Kapton backing or impregnated in a fiberglass cloth are alternate module joint techniques. The incorporation in the joint of a loop that is formed on the rear of the blanket will be required in the flat fold array to allow the attachment of the tension distribution bar for partial retraction.

The module hinge joint is classed as Category II. The current program will fabricate a mechanical and a heat sealable joint design and evaluate strength, fabricability, integration with the tension distribution bar and with the thin substrate design. An enlarged design and evaluation test program for various configurations, materials and environments to determine creep at elevated temperatures, tooling requirements and a quick attach and release system is recommended.

### REFERENCE

1. First Topical Report "Evaluation of Space Station Solar Array Technology and Recommended Advanced Development Programs", LMSC-A981486, December 1970, Contract NAS9-11039

## STATE OF THE ART ASSESSMENT (CONT.)

## 2.6.7 Array Electrical Harness

Two basic functions are served by solar array electrical harnesses. The primary function is to provide a conduction path to route power inboard from the array solar cell modules and panels. These harnesses are categorized as Power Feeder Harnesses (PFH). The secondary function is for instrumentation and control purposes such as temperature transducers, accelerometers, strain gauges and in some instances for sun sensors and other control inputs and outputs. The secondary harnesses are termed Instrumentation and Control Harnesses (ICH).

Two general types of cables exist as options for harnesses, those containing flat (rectangular) conductors and those containing round conductors in either solid or multistrand configuration. A flat cable with flat conductors is called FCC and a cable in flat form having round conductors is called a ribbon cable. Another term, round-wire cable RWC is used denoting a bundle, harness or cable using round conductors. The RWC term could refer to a round tied bundle typical of harnesses generally used or of the flexible type. Therefore when the latter is referred to it will be defined as a RWC ribbon cable. There is no multistrand version of FCC, it is a solid conductor.

FLAT CONDUCTOR CABLE

There is universal agreement that flat conductor cabling should be considered for large deployable arrays. Compared to round conductors, the flat conductor is easier to package, is more flexible and is lighter in weight. The weight advantage comes from the fact that there is less insulation required, the insulation material used is of lighter weight, and a higher current density can be used because of the higher surface area (heat radiating area) in relation to cross-section area. Some favor the use of aluminum conductors and some favor copper; however, for larger arrays such as the SEPS solar array the use of aluminum conductors can result in significant weight savings.



Preliminary investigations indicate that the majority of FCC fabricators do not have off the shelf aluminum FCC, nor have they had past production of significant quantities even though the weight advantages have been recognized since the inception of FCC work. Quoting from reference 1:

The sealed construction of FCC makes the use of aluminum conductors feasible. Aluminum has a lower weight-per conductivity ratio, is more economical, and is not affected by shortages or procurement priorities as copper often is.

The economy and availability factors associated with aluminum have changed since 1968 when the work cited above was conducted.

Due to the current energy situation, concern has been expressed on the cost and production of aluminum due to its process dependency on large quantities of electrical energy. The shortages have been associated primarily with aluminum for structural applications where large quantities are needed in the aerospace and construction industries. Even with a solar array as large as SEPS, the quantity of conductor metal required for harness is minute compared to general non electrical uses. Therefore cost of aluminum for FCC could increase dramatically and still be insignificant compared to solar cell cost. Aside from these recently changed factors on cost and availability, consideration of the two properties of density and resistivity for aluminum and copper indicate dominant weight advantages for aluminum. From reference 2 the following comparison is made.

	<u>EC ALUMINUM</u>	<u>ETP COPPER</u>
Density	2.70 grams/cm <sup>3</sup>	8.89 grams/cm <sup>2</sup>
Resistivity	2.688 microhm-cm	1.724 microhm-cm

for equal resistance

$$\text{Aluminum weight} \frac{2.688}{1.724} \times 2.70 = 4.12 \text{ grams/cm}^3$$

$$\text{which is a weight savings of } \frac{8.89 - 4.12}{8.89} \times 100 = 53.8\% \text{ over copper}$$

STATE OF THE ART STATUS

RWC tied bundles (generally circular in cross section) are not a candidate for consideration because of severe weight and poor flexibility disadvantages. RWC-ribbon cable with stranded conductors exclusively has some termination advantages and possible flexibility advantages, however, there are viable alternates. FCC has many advantages, especially those associated with weight, flexibility and low profile (minimum thickness). The latter is of prime importance in integrating either for PFH or ICH applications on a lightweight flexible substrate solar array. FCC has two potential conductor options--aluminum and copper. There are two areas where action is required associated with aluminum FCC, confirmation of a manufacturing source and development of acceptable joining methods between aluminum and copper. This is being accomplished under the current NAS8-30315 contract, therefore, aluminum conductor FCC is therefore categorized as State of the Art Status I. With the demonstrated use of copper FCC in many array and general applications and with the potential that downstream weight advantages may be realized via higher efficiency cells and or mast, structure, substrate weight improvements copper conductor FCC is also categorized as status I. Several sources are available for FCC-copper and development of engineering, fabrication, test and use has progressed to the point where a definitive specification is available on FCC-copper with the preferred polyimide insulation. Ref. 3.

The state of the art status for the candidates for the SEPS array electrical harness-PFH and ICH application are listed below.

STATE OF THE ART STATUS  
ARRAY ELECTRICAL HARNESS

CANDIDATE	CATEGORY
FCC-Aluminum	I
FCC-Copper	I
RWC-Ribbon Cable (stranded only)	III
RWC-Round Bundle	IV

ARRAY ELECTRICAL HARNESS

- Ref. 1      Handbook for Flat Conductor Cable System Design and Manufacturing,  
McDonnell Douglas, July 1968, p 2-7
- Ref. 2      "Aircraft Flat Conductor Cable Power Feeders", J. P. Morris,  
Boeing, IPC Meeting 9/29/69
- Ref. 3      40M38295, Cable, Electrical, Flat Conductor, Polyimide/FEP  
Insulated-Specification for, MSFC, 1/15/74

## ASSESSMENT OF STATE OF THE ART (CONT.)

## 2.6.8 Composite Material For Containment Box Structure

Advanced composite materials can be utilized in fabrication of the solar array ascent container box and the container cover as well as the tension distribution bars. Both the box base and cover can be of aluminum honeycomb core and graphite/Kevlar 49/epoxy face sheet sandwich construction similar to lightweight sandwich panel construction produced and tested under LMSC development studies. Hybrid panels approximately 48 square feet in area have been built utilizing three ply hybrid face sheets of very high modulus graphite and Kevlar 49 woven fabric. This type construction is current state-of-the-art.

The tension bars are similar to plates, strip and tube of various configurations fabricated previously at LMSC. The fibers and resin system can be the same as those used on the lightweight panels. Design and fabrication are current state-of-the-art, Category I. Verification of environmental behavior in the specific environment of temperature extremes in vacuum coupled with space radiation must be extended to the five year life time requirements. This testing should be accomplished during the development program.

This material and construction, therefore, is placed in Category II for state-of-the-art assessment. The action required is to develop a test plan for exposure and test of representative specimens to the necessary environments and then to perform the simulated space exposure, tests and evaluation.

Generally, space composite laminates are fabricated using 350°F curing systems suitable for continuous usage at 350°F, so no problems are anticipated.

Bonding of face sheets to honeycomb core may be accomplished by cocuring without use of supplemental adhesive. This procedure would employ the prepreg epoxy matrix as the bonding agent. Cocuring may also be employed using supplemental adhesive.

If a two stage cure is required, an adhesive will be selected to meet the performance requirements of the assembly. Performance should be verified by mechanical testing and simulated environmental exposure followed by test. If thermal control coatings are required, adhesion, peel and thermal-optical stability of the assembly will be evaluated.

## STATE OF THE ART ASSESSMENT (CONT.)

## 2.6.9 Extension and Retractions Mast

The flexible solar array is extended and tensioned to provide the required array planar surface and the required vibration frequency control. The array extension mast for SEPS must support a tip load created by the array tensioning system and provide sufficient bending stiffness and torsional stiffness to control array dynamics. Automatic extension, retraction and partial retraction of the mast is required. The mast assembly must be of low weight in both the mast element and its storage and drive components. The mast storage volume for integration of the mast in the SEPS vehicle should be minimal. The thermal deflection of the mast when heated by thermal radiation coming from one side in space should also be minimal. Ref. 1 contains an extensive review of deployment devices for space application with the source of these devices noted. The review covers:

- o Beam Basic Cross-Section Forms
- o Beam and Beam Member Cross Section Variations
- o Truss Configuration Variations
- o Basic Stowage Methods and Variations
- o Extension/Retraction Methods
- o Deployable Structures Survey (existing designs and development status)

Ref. 2 contains an update of the existing designs and development status. Several different mast designs that have application to the 80 to 115 ft long SEPS mast requirement have been developed and have demonstrated low weight, high efficiency structures. Steel, aluminum and fiberglass have been used in their construction. These mast designs, in their largest sizes, are listed in Table 1. The weight and performance of the various mast designs can be determined semi-empirically. The minimum weight mast element design is a function of material and the actual bending stiffness and column load requirement. The minimum combined weight of mast element and storage system will add the mast length and the storage container material as a parameters. In SEPS, the weight of the extended mast element contributes to the mast

TABLE 1  
LARGE FABRICATED DEPLOYABLE MASTS

Application	Antenna Support for Use on Lunar Surface (Eng. Model)	Support for Space Station Solar Cell Array (Eng. Model)	Antenna Support Jeep Mounted (Prototype)
Mast Type	Coilable Continuous Longeron, Motor Driven	Articulated Longeron	Articulated Longeron
Mast Material	S-Fiberglass	Steel	Steel
Storage Container Material	Aluminum	Aluminum	Aluminum
Mast Diameter (in)	10	20	13.4
Mast length (ft)	100	84	40

bending stiffness requirement for array system dynamics control. The temperature range of mast operation affects the strength of the mast and the clearances between parts that move with respect to each other. The candidate extension mast types for SEPS that are of low storage volume and high stiffness per unit weight are:

- A. Cylindrical Section
  - 1. STEM
  - 2. Bi STEM
  - 3. Bi Sinusoid or Quasi-Biconvex
- B. Lattice Structure
  - 1. Coilable Lattice (Lanyard Deployed and Motor Deployed)
  - 2. Articulated Lattice

### STEM Mast

The STEM (Storable Tubular Extendible Member) mast element is a pre-formed spring tape that are flattened and rolled up on a reel for storage. The reel is rotated by an electric motor and gear train. Retraction is accomplished by reversing the motor. The Bi-STEM is formed by nesting two overlapping STEM elements that are typically stored on two separate reels. The STEM and Bi STEM boom schematics are shown in Figure 1.

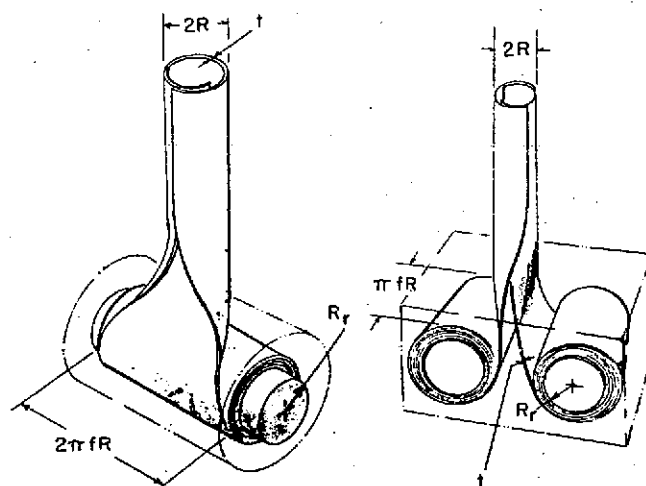


Figure 1 Schematic  
of Stem Boom

Schematic of  
Bi-Stem Boom



The STEM and Bi-STEM booms are manufactured by SPAR Aerospace Products, Ltd. The deployed configurations are relatively stress free except for the interference pressure between overlapping surfaces which creates frictional resistance to shearing and torsion loads. A modification to the overlapping configuration of the Bi-STEM incorporates interlocking element edges (Trade Name: Interlocked Bi STEM). The torsional stiffness of this configuration approaches that of a seamless tube. Fairchild Hiller has developed a similar design (Trade Name: Edgelock and Hingelock Tubular Extendible Element (TEE)). Six Interlocked Bi-STEMs under 2 inches in diameter and 60 to 120 feet in length were flown on NRL gravity gradient experiment satellites. Four 750 foot Edgelock TEEs have also been flown.

#### Bi Sinusoid or Quasi-Biconvex

The quasi-biconvex boom is a form of lenticular welded beam. Two pieces of spring tape are preformed to approximately a hat section or a sine wave configuration. The two tapes are welded together at the flanges. For stowage, the section is flattened and rolled up on a reel. A motor driven reel provides extension and retraction capability. A schematic of this mast from Ref 1 is shown in Figure 2.

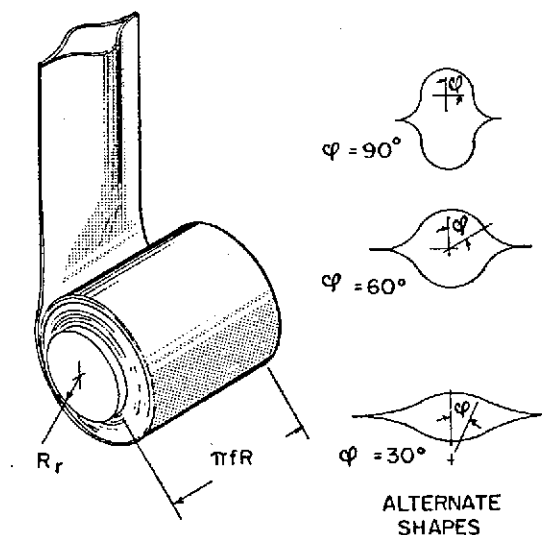


Figure 2 Schematic of Quasi-Biconvex Boom

The alternate shapes in Figure 2 allow variation of the mast stiffness across the flanges and perpendicular to the flanges. Masts of this type have been developed by Boeing Co., Astro Research Corp., and Celesco Industries. The Celesco design is the most developed as a 3 in. diameter mast is being qualified as the Sampler Boom for the Viking Program. The closed section of this mast provides good torsional strength.

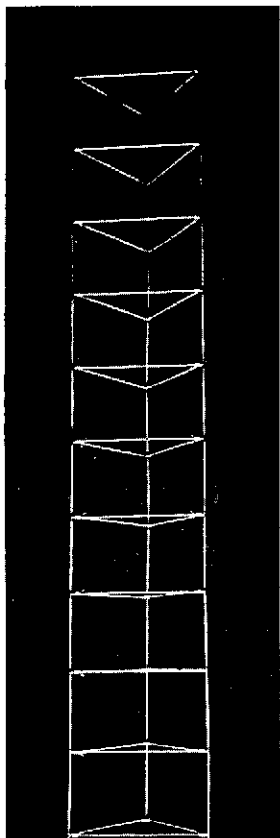
All the cylindrical booms above require control of element thickness to element radius, element thickness to storage drum radius, and deformation during flattening for storage. Material selections and fabrication processes have been developed to provide the required control.

#### Coilable Lattice Mast

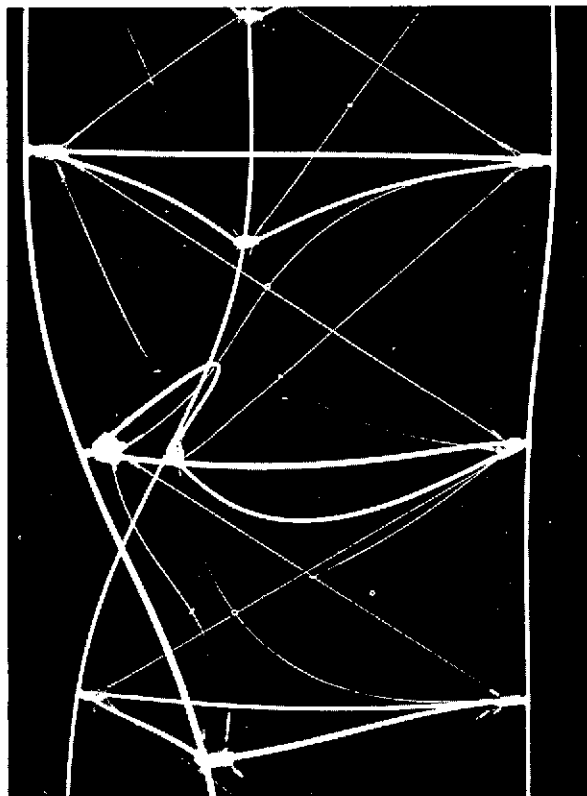
Astro Research Corp. has developed two lattice structure mast types which can be automatically deployed from and retracted into compact stowage volumes. One of these is the coilable continuous longeron mast which can be elastically coiled into a cylindrical storage canister. This type of mast is shown in Figure 3. The lattice structure of fiberglass rods shear-stiffened by diagonal cables, is retracted by forcibly twisting it about its axis. This twisting causes the horizontal "batten" members to buckle. The joint design attaching the battens to the longerons allows the mast to be retracted into a compact stored configuration. The maximum thickness allowable for the longerons is related to the radius of the mast and the elastic strain limit of the longeron material. Epoxy impregnated S-type fiberglass is an ideal material for coiling at minimum mast radius. Other materials, such as metals, can be coiled but these usually require a larger radius, a larger stowage volume and a larger heavier stowage canister.

When structural performance is not required of the mast unless it is fully deployed, an axial lanyard can be payed out to control deployment rate. The lanyard can be reeled in to retract the mast if desired. The SEPS application requires intermediate retraction position strength capability and a motor driven nut at the top of the canister would be required. This nut controls the extension and retraction of lugs protruding from the horizontal frames of the mast. A full section of the mast is always deployed and contained in the canister as the mast is deployed.

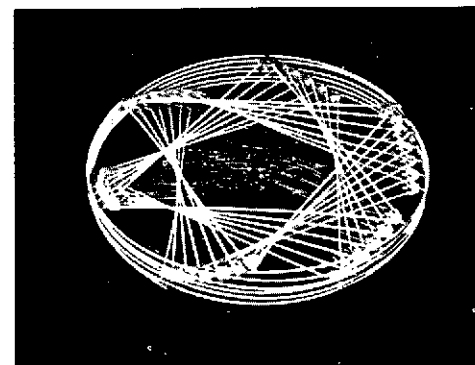
2-186



Segment of Flexible  
ASTROMAST Column



Buckled Battens of Column



Packaged Configuration

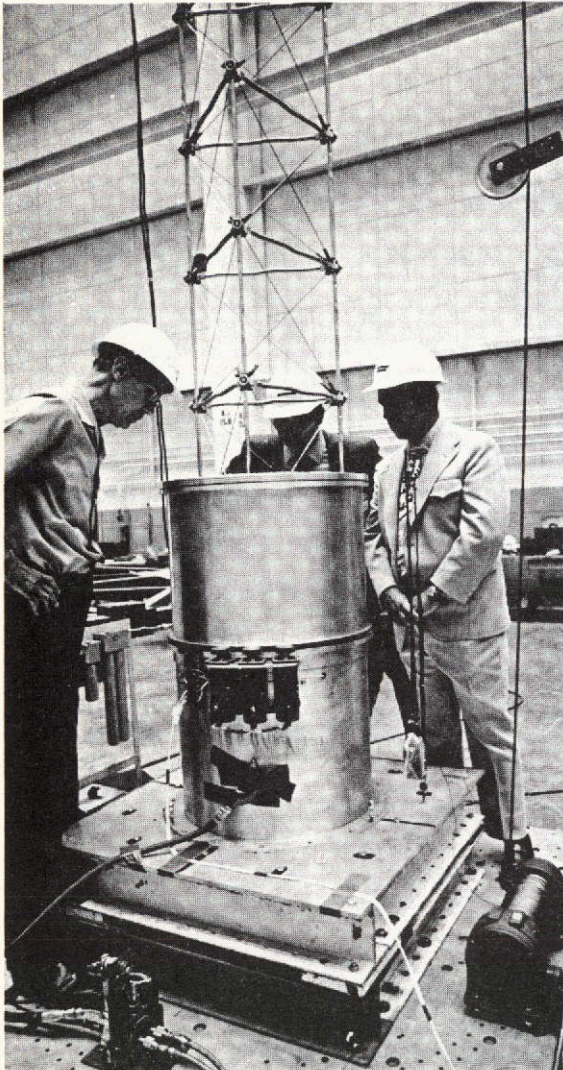
Figure 3 Continuous Longeron ASTROMAST Concept

LMSC-D384250

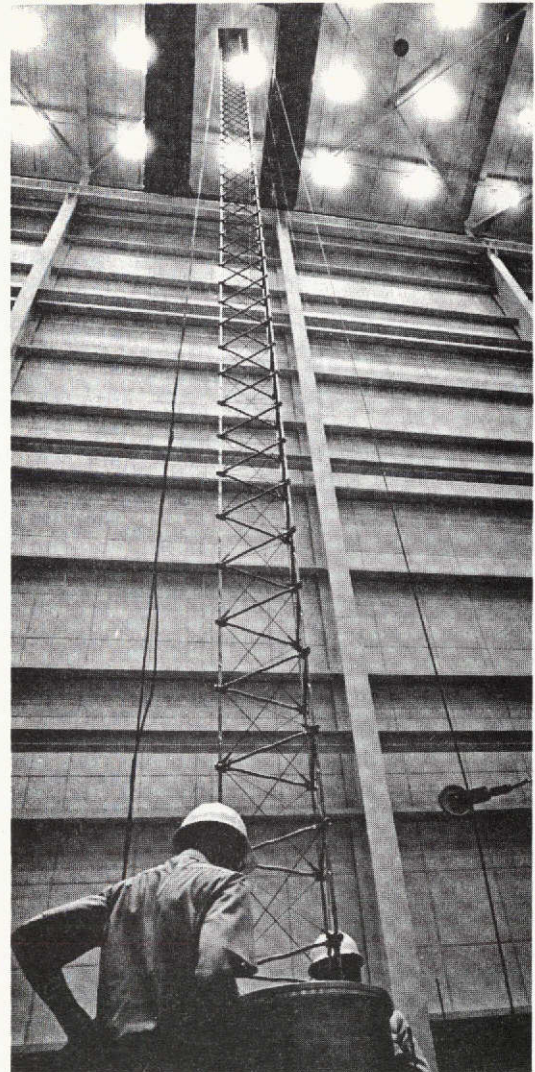
### Articulated Longerons Mast

The articulated longeron Astromast (Astromast Research Corp.) is shown in Figure 4. In this concept, the longerons are in segments and connected by hinge joints to the batten frames. The assembly is shear-and torsion-stiffened by diagonal cables extending across each rectangular face in the lattice structure. Three of the six diagonal cables contain linkages which are actuated by the deployer to "set up" the section during extension or unlatched to allow the mast to retract into a folded configuration. The members of the articulated mast may be as large in cross section as the application dictates. A limitation of the articulated mast is that the completed longeron of many pieces cannot be made without a significant accumulation of play. The resulting dead band of little or no resistance to deflection can be a problem in dynamic control of the deployed solar array.

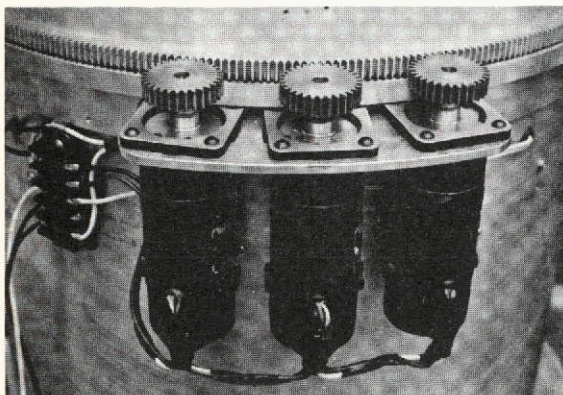




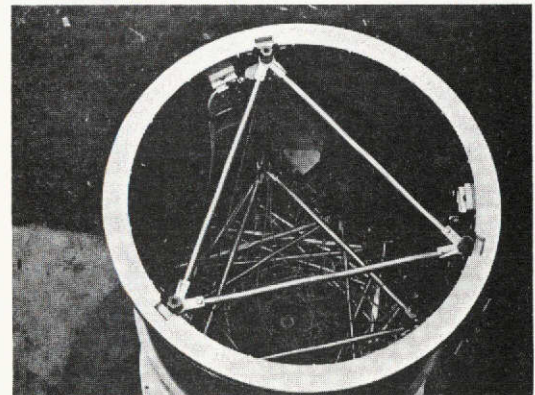
Astromast Deploying  
Automatically



Fully Extended Mast  
(84 ft long, 20 in. diam., 214 lb)



Deployment Motors



Retracted Configuration  
400 lb Mast plus Canister

Figure 4 Articulated Astromast

### Mast Performance

The SEPS mast for the flatfold array will have a maximum length requirement of 115 ft. The bending stiffness requirement for dynamics control is in the range of  $3 \text{ to } 6 \times 10^4 \text{ N-m}^2$  ( $15 \text{ to } 30 \times 10^6 \text{ lb-in}^2$ ). The weights vs bending stiffness of the masts plus their storage elements are shown in Figures 5 and 6 for conventional materials. Those data were generated using the equations and data contained in Refs. 3, 4 and 5. The major limitations in the calculated data are:

1. Bi-STEM Deployer weights are extrapolated from data in a range of mast diameters from 3/8" to 2".
2. All Astromast canister weights are extrapolated from a 10 inch diameter mast design for the fiberglass continuous longeron lunar antenna mast.
3. The stiffness of masts is best obtained from tests of actual designs.
4. The ratio of Astromast element weights to the weight of one longeron (F) is based on a few samples of both mast types that have been built.

The weight of the Bi-STEM mast is greater than that of the Bi-Convex and Astromasts in this application and is not considered a viable candidate.

The coilable fiberglass longeron Astromast is the most attractive design from a simplicity and weight standpoint. It has been fabricated at long length. It has application over a wide range of SEPS missions but suffers from over temperature strength loss if exposed to the sun in near sun missions. At  $93^\circ\text{C}$  ( $200^\circ\text{F}$ ) the material has lost 10 percent of its room temperature capability. The possible substitution of graphite epoxy composite for the fiberglass is a possible approach to raising the mast temperature capability to  $149^\circ\text{C}$  ( $300^\circ\text{F}$ ) without increasing storage canister diameter and weight.

The articulated longeron Astromast can be made with a large number of metals and element sizes. High temperature capability is not a problem in near sun missions and it has been built in a long length configuration. The deflection force dead band mentioned earlier for this mast is a potential problem. The complexity of the hinges

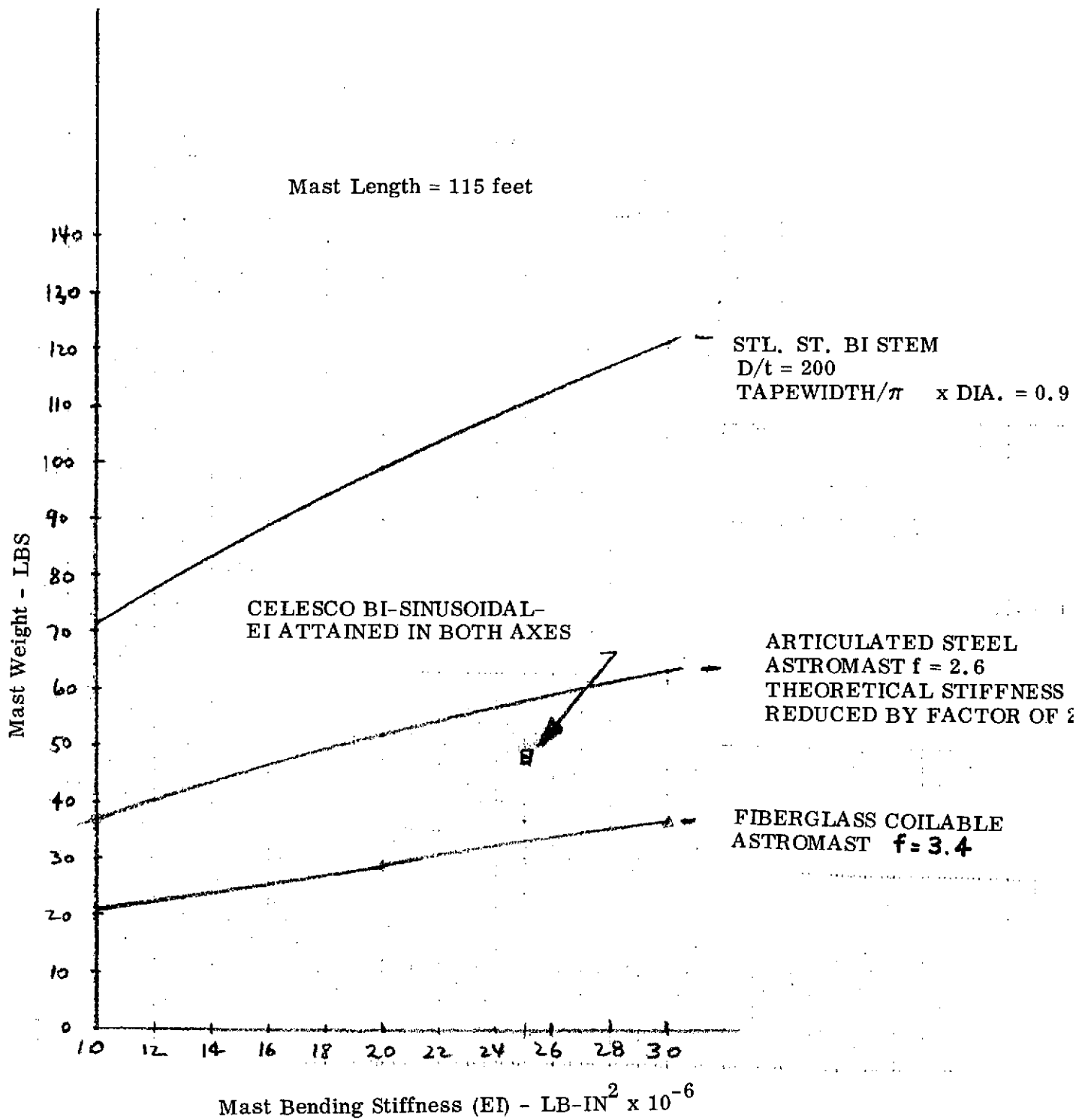


Figure 5 Deployable Mast Element Weight Vs Bending Stiffness



Mast Length = 115 feet

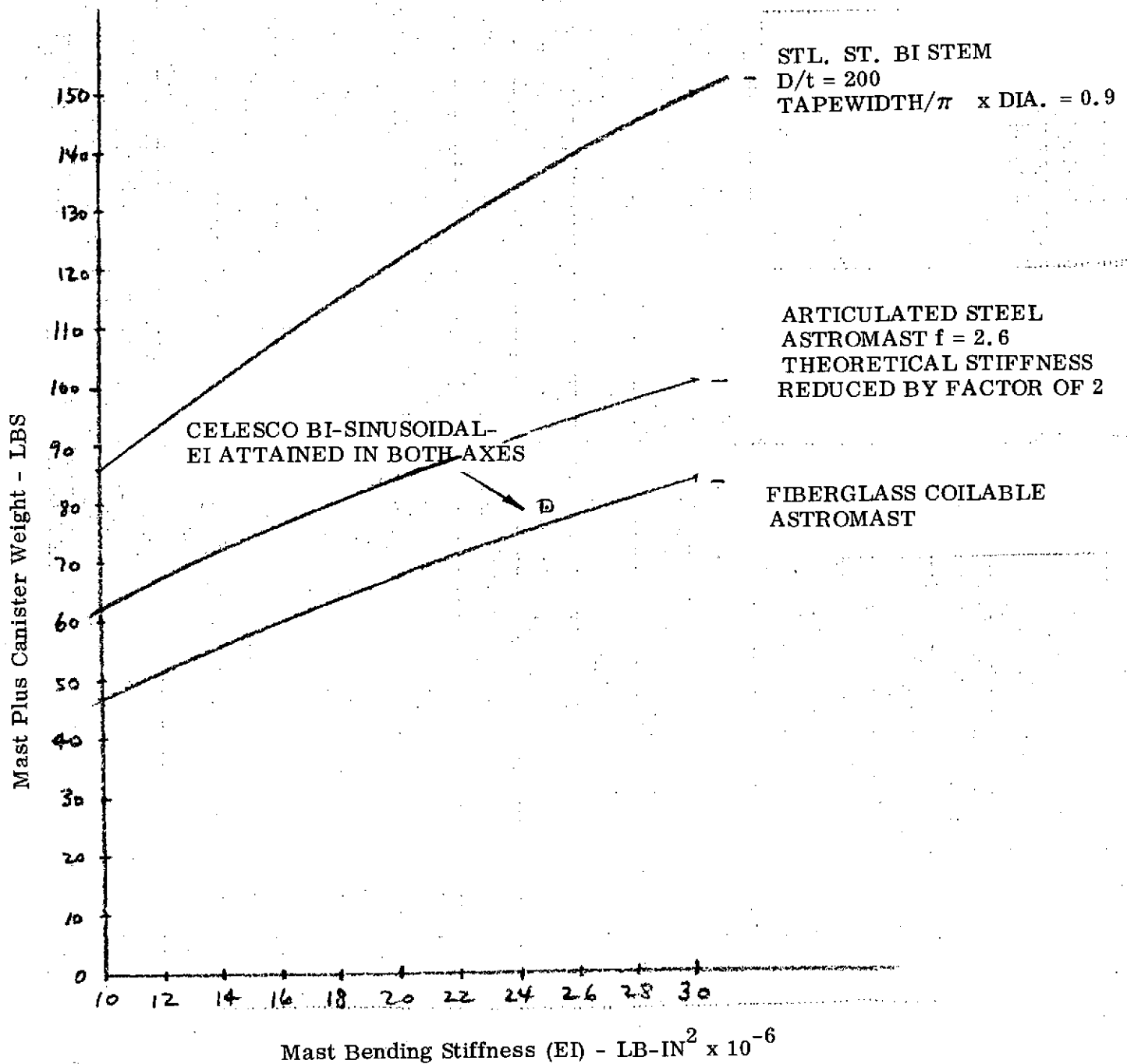


Figure 6 Total Mast Plus Canister Weight Vs Bending Stiffness



and latches required for articulation increases the cost of this mast in steel about 20 percent over the continuous longeron fiberglass mast.

The Celesco Bi-Sinusoid appears to be viable candidate for the SEPS mast. It has high temperature capability and does not have a deflection dead band problem. Being a closed configuration, it does have a greater thermal deflection than does the lattice structure boom. It has not been built in a large diameter in a long length and therefore lacks fabrication experience.

The extension mast technology is classed as Category II. This is primarily because of 1) the wide SEPS operating temperature range requirements from 0.3 au to 6 au, 2) the need to investigate the cost and fabrication aspects of material substitutions to reduce mast and storage container weights and 3) the fabrication of a test section of the mast design in the SEPS size is required to assure that the full scale design strength and stiffness can be obtained.

## STATE OF THE ART ASSESSMENT (CONT.)

## 2.6.10 Extension Mast Motors

The primary requirement for the extension mast motors is reliable intermittent operation for 5 years in the space environment. A large variety of motors have been flown in space. These include:

## Brushless

DC Stepper

DC Torquer

AC Servo

## Brush Type

DC Torque

Table 1 contains a summary of motor characteristics. Table 2 lists typical motors that have flight experience.

The motor used successfully in flight on the SPAR 2.0 in diameter Bi-STEM is a dc brush type, AiResearch 36790-2-1. The motor selected for the CTS solar array deployment mast is a Kearfott dc brush type which runs at 3350 RPM and is geared down to 33.5 RPM shaft output. The stall torque is 5.64 N-m and the motor weighs 0.341 kg (0.75 lb). The use of brush type motors for deployment booms to date has been justified in part by the short term lifetime requirement. Quite often only one deployment operation is required shortly after attaining orbit. The Celestec Sampler Boom for Viking will use three Singer-Kearfott brush type dc torque motors which are magnetically coupled to gearing through a hermetic seal. The motor torque is limited by the magnetic coupling torque which then allows the motor to break away and run at no load speed. The largest motor has a torque capability of 6.77 N-m (960 oz-in.). While brush type motors have flown successfully, the use of brushless motors is usually favored from a reliability and EMI control standpoint. The magnetic control requirements for SEPS will also be a factor in the selection of a permanent magnet motor over a wound field motor. While the latter draws more power, there is no magnetic field when it is off.

Two dc stepper motor types that have application are the 1) permanent magnetic and 2) variable reluctance (no permanent magnet). The control electronics for intermittent operation of the mast can be turned off. The efficiency of both motors is relatively high when they are run at high stepping rates.

The dc torque motor is essentially a servo actuator that can be directly attached to the load it drives. In general, it is designed for high torque, low-speed operation, for speed control systems or optimum torque at high speeds for positioning, rate, or tensioning systems.

An ac servomotor is basically a two-phase reversible induction motor which has been modified for servo operation. To achieve the rapid and accurate response characteristics, they have small diameter high resistance motors. The small diameter results in low inertia for fast starts, stops, and reversals, while the high resistance provides for a nearly linear speed-torque curve for accurate control.

The temperature limits for motor operation are usually in the range of  $-34^{\circ}$  to  $74^{\circ}\text{C}$  ( $-30^{\circ}\text{F}$  to  $+165^{\circ}\text{F}$ ). The Bi-STEM Airesearch motor was qualified for  $-54$  to  $121^{\circ}\text{C}$  ( $-65^{\circ}$  to  $+250^{\circ}\text{F}$ ). The temperature limits are based on lubrication capabilities and insulation high temperature limits.

The technology status for SEPS mast motors is classed as Category I. The development approach is to survey existing motor designs against mast drive and mission requirements with a view toward limiting new motor development. SEPS thermal control design is required to maintain the motor within its allowable temperature limits.

TABLE 1  
MOTOR TRADE OFF TABLE

Motor Type	Torque Efficiency Lb-Ft/Watt	Control System Compatibility	Remarks
DC Brush Type Torque	0.027	Excellent	Can handle large inertia loads. Impressive history of successful space applications
DC Brushless Type Torque	0.022	Electronic Complexity Otherwise Excellent	Can handle large inertia loads. Very complex electronics.
Servo Motor	0.00025 at motor	More complex electronics to control AC	Poor torque per watt ratio. Inverter losses must be charged against drive.
DC Stepper	0.022	Complicated electronics	High surge currents, does not drive inertia loads well. Detent torque could be useful.
AC Stepper	0.00002	Complicated electronics	Poor torque efficiency, high surge currents does not drive inertia loads well.
Induction	0.0007	More complex Electronics to control AC	Low starting torque, high starting surge current. Inverter inefficiency must be charged to drive.
AC Synchronous	Poor - depends on starting method	More complex electronics to control AC	Poor starting torque without aux. means. Inverter losses must be charged to drive
AC Torque	0.002	More complex electronics to control AC	Poor torque per watt ratio. Poor torque per pound ratio. Inverter losses charged to drive.

TABLE 2  
SPACEFLIGHT MOTORS

Program	Motor Type & Manufacturer	Application		Torque N-m	RPM	Remarks
OSO I-IV	DC Torque, Brush, Inland Motor T-4006 & T-2907-B	Solar Array tracking drive		2.43	312	Performance satisfactory for all launches. OSO III operated over 42 months
Nimbus I-III	AC Servo, Brushless			2.12 (-3)	800	Motor bearings failed on Nimbus I at 3 months. Nimbus II, III, and IV no failures after 36 months
OLSCA	DC Torque, Brushless Aeroflex 47-3P			3.66	250	Performance satisfactory
OLSCA	Inland T-51134D, Brush, Inland T-5134D			3.66	22	Performance excellent
Type I, II	DC Stepper, Brushless, Superior Electric SS-150-1014			2.12 (max)	--	Array deployment failures experienced--not motor failures
Type III	AC Induction, Brushless			5.64	6000	9 flights, 30 days to 12 months
OGO	AC Servo, Brushless, Kearfott Size 11			4.23 (-3)		12 units flown, no failures

# REFERENCES

1. "Evaluation of Space Station Solar Array Technology and Recommended Advanced Development Programs", First Topical Report, December 1970, LMSC-A981486, Contract NAS9-11039.
2. "Evaluation of Space Station Solar Array Technology", First Topical Report Update, July 1972, LMSC-D159124, Contract NAS9-11039.
3. Crawford, R. F., "Strength and Efficiency of Deployable Booms for Space Applications", AIAA Paper No. 71-396.
4. "STEM Design and Performance", published by SPAR Aerospace Products, Ltd., Toronto, Canada
5. "Astromasts for Space Applications", published by Astro Research Corp., Santa Barbara, California

## STATE OF THE ART ASSESSMENT (CONT.)

## 2.6.11 Lubricants

The long life space environment requirement for the SEPS solar array and outgassing constraints will require special attention to lubricant system selection in gears and bearings. There is a preference for solid lubricants over oils and greases wherever applicable. Similarly a system utilizing replenishment of lost lubricant will have to be sized for the mission environment and lifetime.

Solid Lubricant

Solid lubricants are used in space primarily in two ways for gears: either as a thin film of lubricant applied to the surface of gear, or as a continually replenished film transferred, to the gear from an idler gear that is made of lubricant and that is in mesh with the train.

Solid-lubricant films that are bonded or burnished to the surface of the gear may be satisfactory for a fixed amount of sliding action between gear teeth. When the film is worn through, its lubricating capability is ended. One of the advantages of the idler gear technique is that the film is continually replenished, resulting in long life. The idler can be a Mo S<sub>2</sub> loaded polyimide composite such as Duroid 5813 or Fluralon.

Another way gears can be lubricated in space is by hard-surface coatings that provide wear resistance and prevent cold welding of unlubricated surfaces. These inert surface coatings are either anodized aluminum or oxidized, nitrided or carborized steel gears. The use of solid lubricant on hard cased gears would be a plus.

The use of solid lubricants on bearings is most effective at high loads and slow speeds. They are applied to surfaces by the following techniques.

- 1) Burnishing of parts in pigment powders
- 2) Dispersion of pigment in greases or liquids
- 3) Precoating of parts with resin-, metal salt-, or ceramic-bonded films containing pigments

4) Incorporation of pigment in a solid metal or plastic bearing material.

The most frequently used solid lubricants are graphite, Mo S<sub>2</sub> and PTFE. Mo S<sub>2</sub> is used in space for its stability at temperature extremes, -200°C to 1000°C, and in radiation and vacuum environments.

For motor bearings, the use of oil impregnated phenolic ball bearing spacers provides replenishment of lubrication. DuPont Krytox 143 fluorinated oil is a low volatility, high radiation resistance material that may be used for this application. Krytox 240-AC is a highly inert fluorinated grease that may be used in a sealed unit. Krytox may also set in bushings.

The lubricants required for SEPS are classed as Category I. The vendors of motors and actuating mechanisms have a variety of materials and systems to select from in order to tie in the best lubrication system for the particular application and mechanical rating.



## 2.7 COMPONENT DESIGN, FABRICATION AND TEST

### 2.7.1 On Array Padding

A series of tests were performed to determine the relative performance capabilities of the various on-array padding concepts and to provide a guide for further design efforts. The capability parameters being investigated are cell power degradation (over cell concepts), slip resistance, preload, vibration and extension/retraction.

#### 2.7.1.1 Test Specimens

The test specimens for each padding concept are shown in Figure 2-48. The "no pad" specimen is shown to the left. It consists of four panels with 20 each 2x4 cm x 12 mils thick glass slides in a 4x5 cell pattern. The slides are taped to a 2 mil Kapton substrate with 0.25 inch wide pressure sensitive adhesive transfer tape. This slide attachment method allows for intermittent specimen repair if required. The four panels are taped together with FEP/Silicone tape to fold into the flatfold stowed position.

Two "over-cells" specimens are shown in the second row from the left in Figure 2-43. The top specimen is a "button" concept. The substrate glass slides, and attachment methods are the same as the no pad specimen. Sylgard 182 was cast into a sheet 0.020 in. thick with a 1 mil FEP mold release agent. The FEP produced a clear transparent pad rather than being cloudy which occurred with other mold release agents (note: the buttons were capped for the photo to make them visible). In addition, it serves as a means to prevent adhesion between the pad and the mating cell. The "buttons" were applied to the slides on every other panel with more Sylgard 182. To supplement the data for this concept with power degradation data, a wrap-around 2x4 cm cell was modified by applying a button to its center. The button material was varied from a completely opaque to the Sylgard combination used on the panel specimens. The lower "over cells" concept consisted of a 2x5 pattern of 2x4 cm cells soldered to a typical LMSC flexible substrate. Two of these assemblies were mounted to a locking bar as shown in Figure 2-9. The padding material was an embossed FEP 2 mils thick attached at the locking bars only



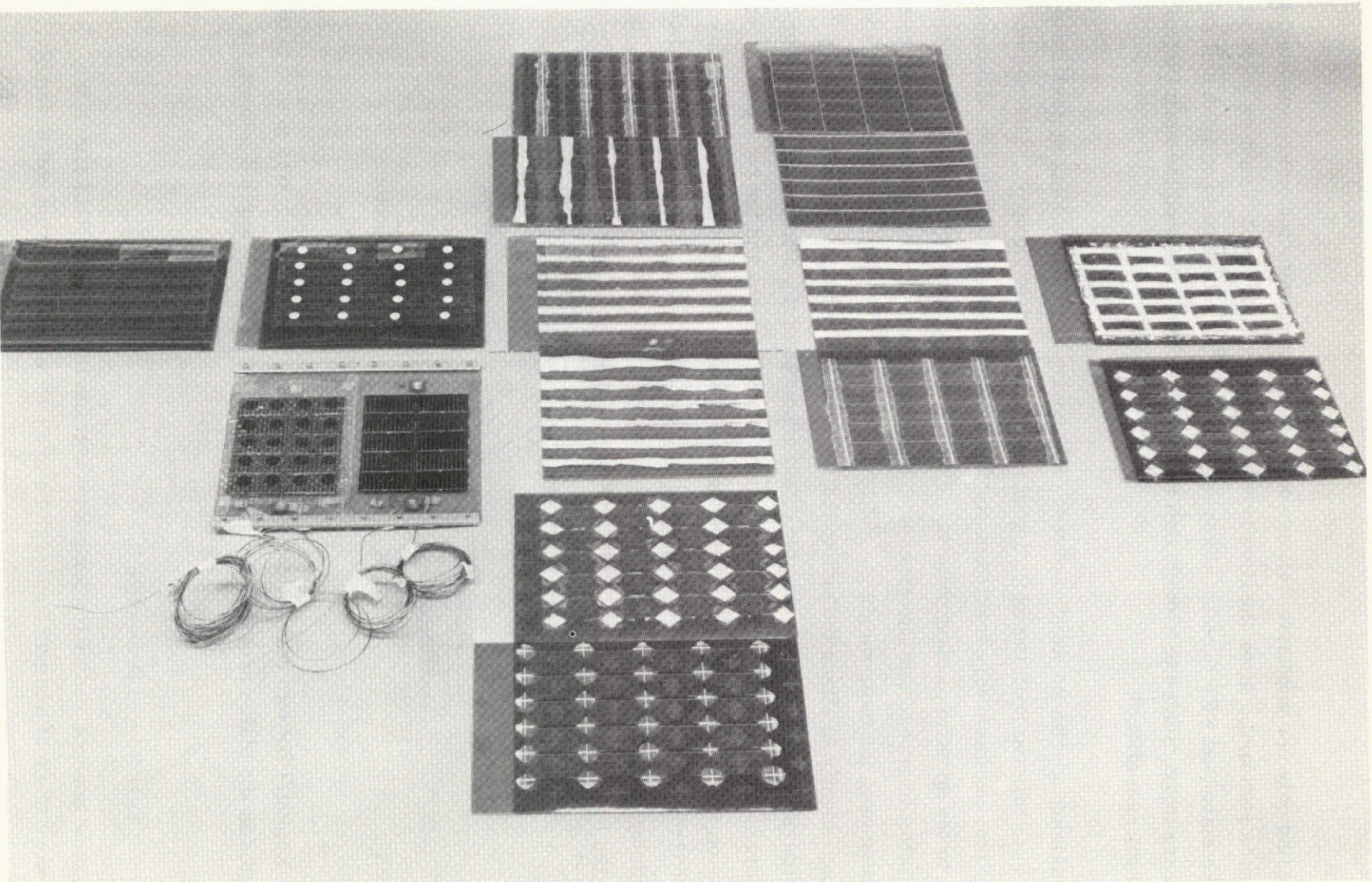


Figure 2- 48 On-Array Padding Test Specimen

REPRODUCIBILITY OF THE  
ORIGINAL PAGE IS POOR

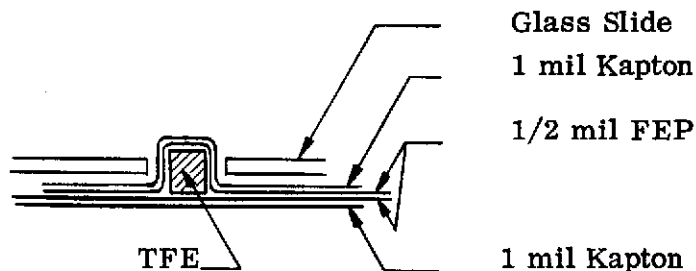
2-201

LOCKHEED MISSILES & SPACE COMPANY



and covering only one substrate/cell assembly. The remaining assembly was used as a reference standard. After the first series of testing 2-1/2 inch diameter holes were cut in the embossed FEP directly above each cell. Two solder pads on each cell substrate were instrumented to provide cell temperature and to record the magnitude of the "greenhouse effect".

The remaining specimens were "between cell" concepts. The padding material used was RTV-41 silicone with the exception of one "criss-cross" concept. The silicone pads for the specimen were formed on the 2 mil Kapton substrate using an aluminum tool cut to the specific padding pattern. The tool was sprayed with a separating agent and the silicone spread into the grooves. The Kapton was locally abraided and primed, then placed over the tool, weighted, and left to cure. After curing, the flash was removed sufficiently to attach the cell to the Kapton. Referring to Figure 2-43, the above process was used to develop the offset concepts in the center row, the lower "criss-cross" specimen in the column second from the right and the two "perimeter" concepts on the right. The upper "criss-cross" pad specimen (second from right) used 0.032x0.032 in. TFE ribs integrated into the substrate. The lay up shown below was made by covering an aluminum tool with a layer of 1.5 mil Kapton/FEP and inserting the 0.032 in. x 0.032 in. TFE strips into the tool grooves. Another layer of



1.5 mil Kapton/FEP was added along with armalon. The assembly was placed between caul plates in the platen press and sufficient heat and pressure applied to form the substrate.

#### 2.7.1.2 Test Up and Procedure

The "button" concept was tested for power degradation with an OCLI simulator. I-V curves were made at ambient temperature prior to and after button pad assembly.

The embossed Kapton and reference standard specimens were tested side by side in a thermal vacuum chamber with an  $\text{LN}_2$  cold wall and illuminated with an X-25 solar simulator (1 au) in situ. It was suspended from the upper locking bar and a 1 lb. weight hung from the lower locking bar. The specimen was subjected to 1 cycle between  $+94^\circ\text{C}$  and  $-80^\circ\text{C}$ .

The test fixture for slip resistance (acceleration) and vibration tests was designed to apply 0.5, 1, 2, 3, and 4  $\text{lbs/in}^2$  preloads to the padding specimens. The fixture shown in Figure 2-49 consists of two  $3/8$  in thick honeycomb plates (aluminum skins-fiberglass core). Two 0.5 in. square beams are bonded to the upper plate while the lower plate is bonded to a base made from 0.25 inch thick aluminum. The inner surfaces of the upper and lower plates are covered with a  $1/8$  inch thick polyurethane foam to distribute the loads in any discontinuity areas. Four pins are press fit into the base and they pass through clearance holes in the upper plate beams. Compression springs 91  $\text{lbs/in}$ . are used to provide the specimen preload levels. Spacers with a  $\pm 0.0005$  inch length tolerance are used to control the preload to required levels and when properly adjusted limit the vibration amplitude between upper and lower plates to a negligible level. With a specimen in the fixture and the fixture assembled, the preload is adjusted by screwing the jamb nuts down to the spacers until the spacer will still rotate when a light torque is applied, and yet exhibit a negligible end play.

For the slip resistance tests, the tab on the central panel in the folded specimen was clamped as shown in Figure 2-50. Weights were added to a hook at the end of the cable until panel movement was observed. The movement of these weights and specimen was controlled by a hand operated lift. The lift was slowly lowered until the weights were free. If no slippage occurred, the lift was raised, more weights were added and the procedure repeated until slippage was apparent.

Vibration tests were performed with the padding test specimens mounted in the test fixture and preloaded to a value related to its slip resistance (higher slip resistance - lower preload). This assembly was mounted to the shaker. A three axis accelerometer was mounted to the base plate to monitor the input levels. The specimen in its fixture was subjected to a  $1/2$  g (O-peak) sinusoidal resonance sweep from 10 to 250 Hz to ensure



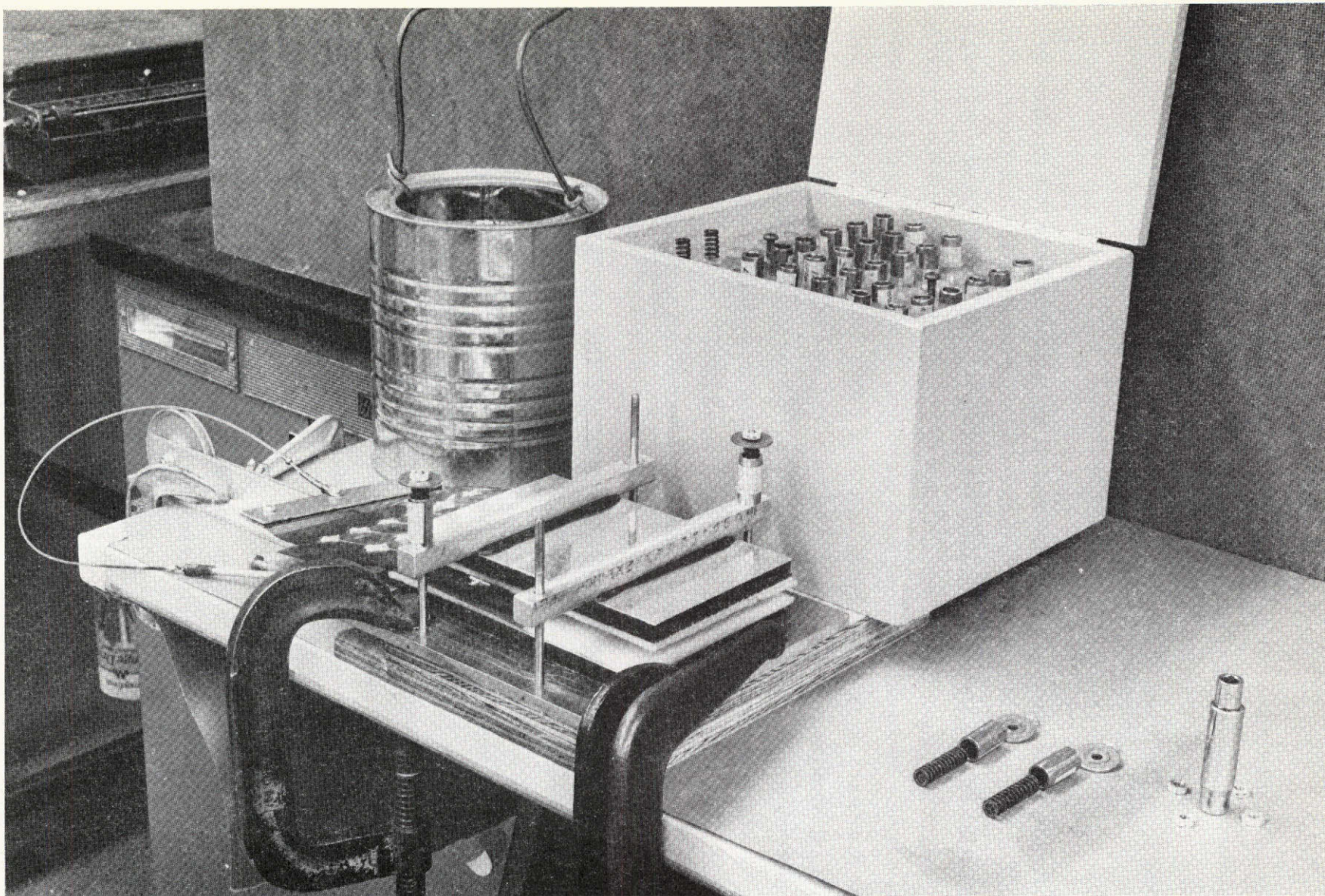


Figure 2-- 49 Slip Resistance Test Fixture



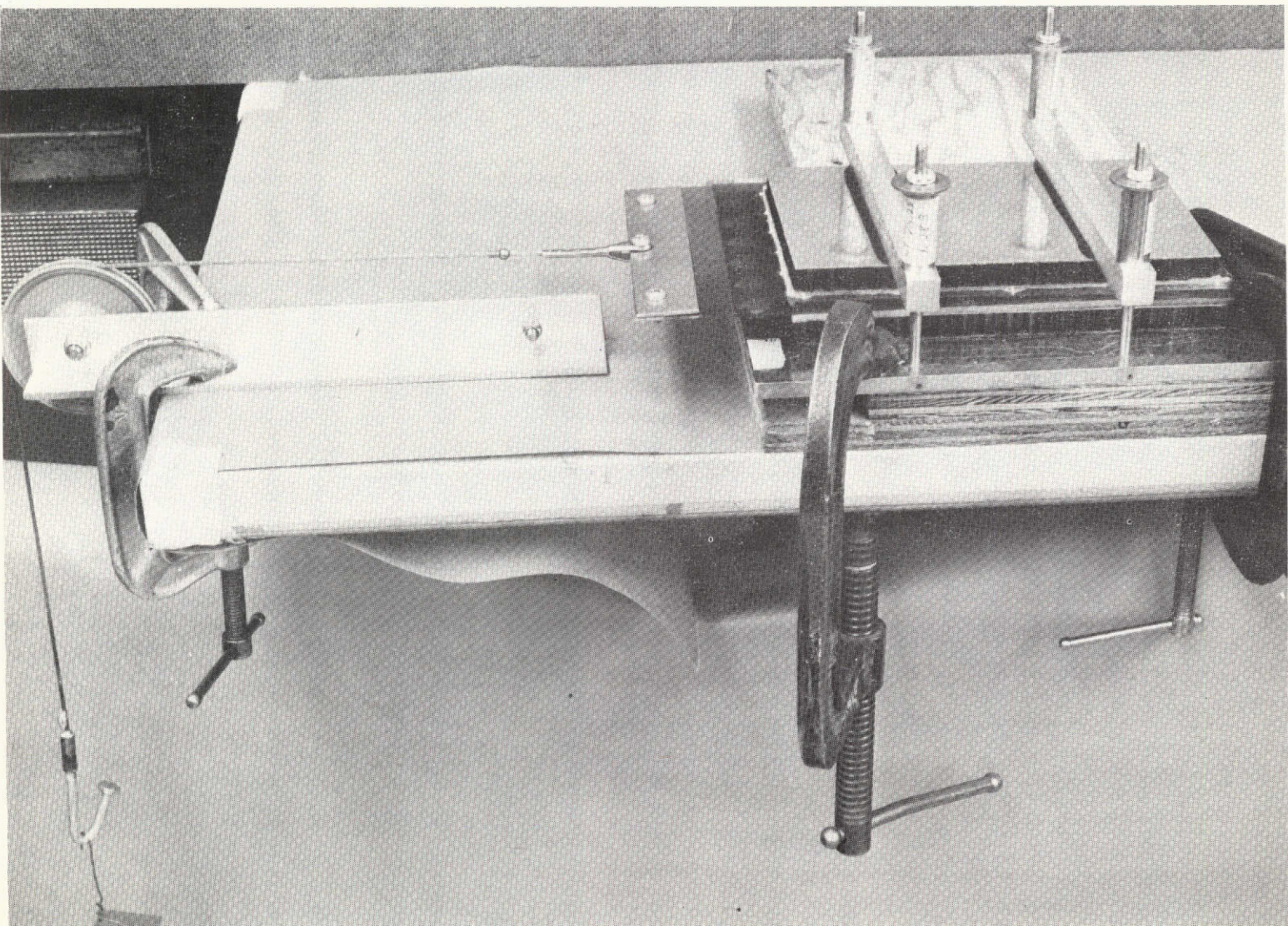


Figure 2-50 Padding Slip Resistance Test Setup

that no major fixture or other resonances were experienced.

The specimens were subjected to sinusoidal vibration mutually perpendicular axes to levels comparable to Shuttle/Titan III ranges (do directly simulate final flight conditions which are dependent on several other factors).

Frequency Range	Amplitude or Acceleration G's (0-Peak)
5-10	0.25 in DA
10-50	2.5
50-200	2.0

After experiencing the above levels the specimen was visually inspected and any damage was noted.

Each padding specimen was subjected to Shuttle launch random vibration levels along 3 mutually perpendicular axes. This level is significantly higher than the Titan III ascent or Shuttle re-entry levels shown in Figure 2-51 and higher than normal for a module the size of the SEPS solar array. The specimens were visually inspected after each axis of vibration and any damage was noted.

#### 2.7.1.3 Results

The transmission losses associated with the cast Sylgard/FEP circular "button" or "annulus" were less than 1% and with an opaque button 4.2%.

The losses given below with the 2 mil embossed padding overlay showed significant improvements in power with the addition of holes, but still results in a serious penalty in area, cells and weight as shown in Figure 2-8.

	Greenhouse Loss	Transmission Loss	Total
Non Perforated	10%	6%	16%
Perforated	5.5%	4.4%	9.9%

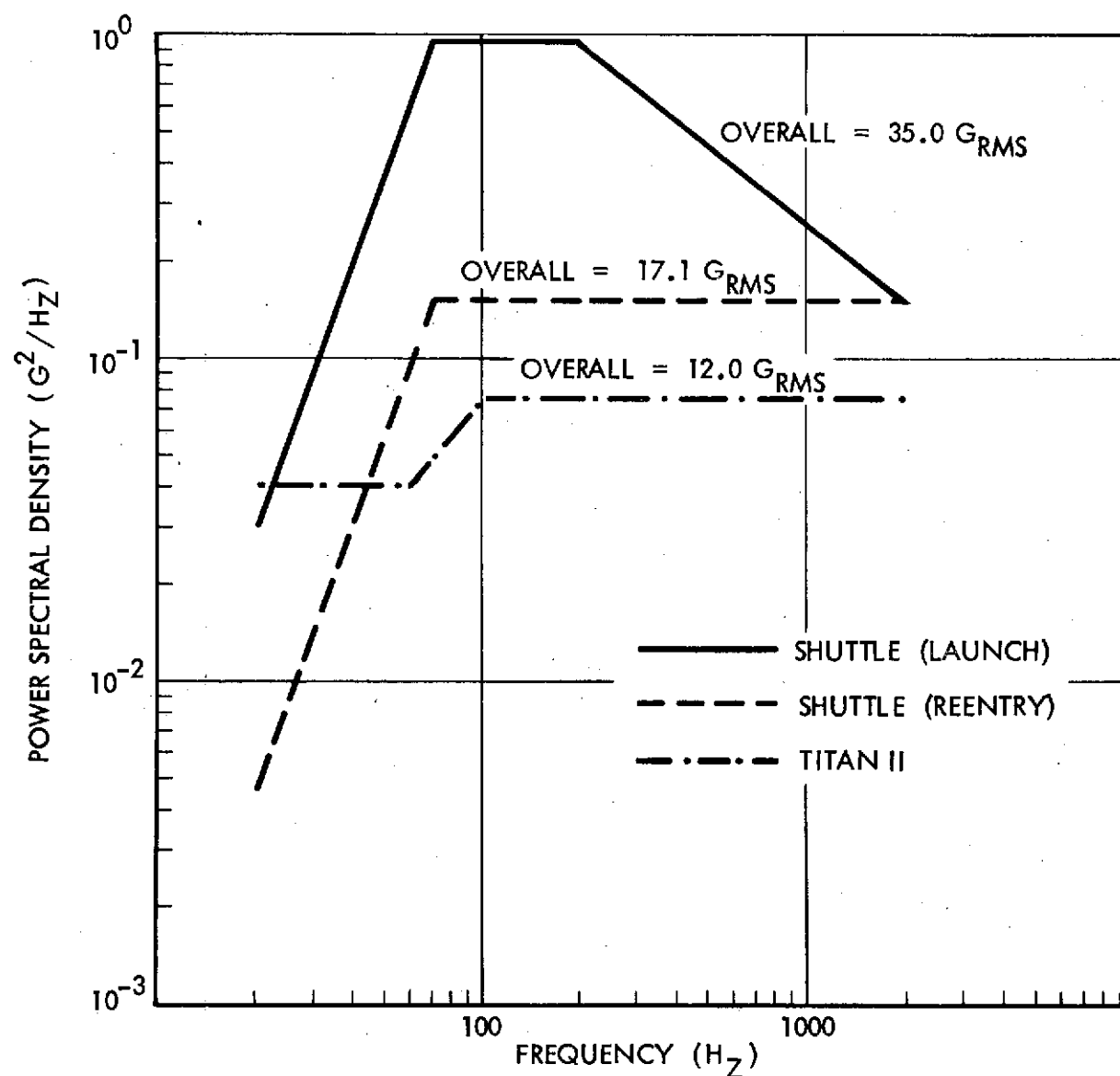


Figure 2-51 Qualification Test Levels - Random Vibration



The slip resistance test results are shown in Figures 2-52 and 2-53. The criss-cross concept performed best. The results of the vibration tests are shown in Table 2-14.

### 2.7.2 Harness Joining Techniques

The design harness conductor material is aluminum in a flat conductor cable (FCC) configuration. This design provides a significant weight savings over the alternate material copper. The printed circuit substrate solar cell interconnect material is copper. Silver plated molybdenum is a preferred interconnect material from a thermal cycling survivability standpoint. It is too dense for the lightweight SEPS array and copper is the next best selection. Copper is lighter and less expensive than silver which would otherwise be a leading candidate material.

The aluminum harness must be reliably connected to the copper interconnect system. An evaluation of joining techniques was performed. The candidates are:

- o Solder using special fluxes and solders - planar joint configuration.
  - Alcoa X69 Flux/X807 Solder
  - Epatam 673 Flux/SN63 Solder (QQ-S571d)
  - Alu-sol Aluminum Solder
- o Electroless nickel plate aluminum interconnect areas. Conventional solder. High or low temperature.
- o Electroless nickel plate aluminum and/or copper interconnect areas. Weld.
- o Electroless nickel plate on aluminum followed by silver plate. Weld.
- o Solder plate copper. Resistance solder to aluminum using special flux.
- o Pin and washer mechanical concept. Special flux for bond to alum.

Each of the candidate techniques has been used to make sample joints in order to evaluate 1) the feasibility of the technique, and 2) the ease of joint fabrication. The pin and washer concept utilizes several small parts. While a strong joint is produced, it has been discarded because other techniques will work and the fabrication of this joint is time consuming. The soldering techniques using a caustic flux on the aluminum, which is carefully cleared away before remelting, produced strong bonds. Pull

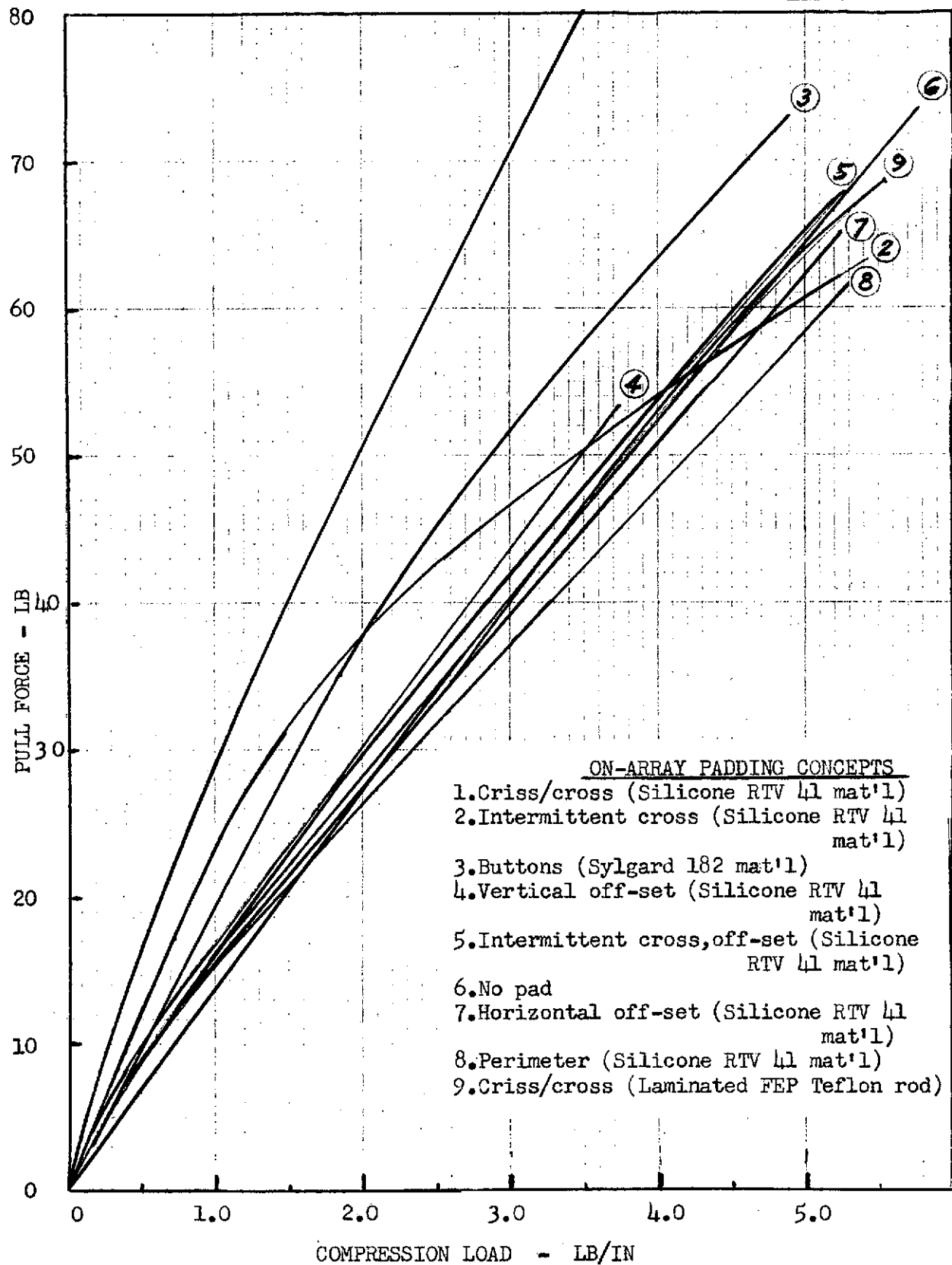


Figure 2-52 Padding Concept Slip Resistance

(SR • F/N) F = PULL FORCE (LB)  
N = PRELOAD (LB/IN<sup>2</sup>) X AREA (26 IN<sup>2</sup>)

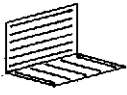
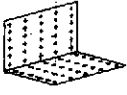
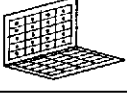
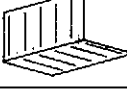

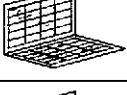



SPECIMEN	CONFIGURATION	PAD MATERIAL	1.00 LB/IN <sup>2</sup>			2.00 LB/IN <sup>2</sup>			3.00 LB/IN <sup>2</sup>			4.00 LB/IN <sup>2</sup>			COMMENTS
			F	N	SR	F	N	SR	F	N	SR	F	N	SR	
CRISS/CROSS		SILICONE RTV 41	29.0	26.0	1.115	50.5	52.0	.973	70.5	78.0	.904	-	104	-	AT 3.00 LB/IN <sup>2</sup> TOP FOLD ADHERED TO CUSHION ON THE COVER. RELEASED PRIOR TO COVER CLEARING HOLD DOWN STUDS.
INTERMITTENT CROSS		SILICONE RTV 41	23.5		.904	37.8		.727	46.6		.597	54.1		.520	
BUTTOUS		SYLGARD 182	19.2		.783	37.6		.723	51.5		.660	59.7		.574	AT 3.00 LB/IN <sup>2</sup> DAMAGED GLASS ON FOLD NO. 1 & 2. REPAIRED SPECIMEN AND CHANGED TO HARDER CUSHION MATERIAL. AT 4.00 LB/IN <sup>2</sup> DAMAGED ON FOLD 2 & 4.
VERTICAL OFF-SET		SILICONE RTV 41	18.0		.692	30.3		.582	43.5		.558	-		-	AT 3.00 LB/IN <sup>2</sup> DAMAGED GLASS ON FOLD NO. 1 AT APPLICATION OF PRE-LOAD. PERFORMED STORAGE TEST OVER A 68 HR PERIOD AT 3.00 LB/IN <sup>2</sup> PRE-LOAD. NO APPRECIABLE ADHESION BETWEEN PADS AND GLASS.
INTERMITTENT CROSS (OFF-SET)		SILICONE RTV 41	17.3		.665	29.7		.571	42.0		.538	65.0		.625	
NO PAD		-	17.3		.665	27.4		.527	40.4		.518	64.0		.615	
HORIZONTAL OFF-SET		SILICONE RTV 41	15.5		.596	27.3		.525	39.0		.500	62.3		.599	AT 3.00 LB/IN <sup>2</sup> FOLD NO. 1 ADHERED TO CUSHION ON COVER. RELEASED PRIOR TO COVER CLEARING HOLD DOWN STUDS.
PERIMETER		SILICONE RTV 41	15.2		.584	26.0		.500	37.0		.474	58.5		.563	PERFORMED STORAGE TEST OVER 68 HR AT 3.00 LB/IN <sup>2</sup> PRE-LOAD. NO APPRECIABLE ADHESION BETWEEN PADS AND GLASS.
CRISS/CROSS		LAMINATED TEFLON ROD	13.6	26.0	.523	27.2	52.0	.523	40.4	78.0	.518	63.6	104	.611	AT 1.00 LB/IN <sup>2</sup> TO 4.00 LB/IN <sup>2</sup> VERTICAL PAD CAUGHT BETWEEN GLASS OF MATING FOLD. DAMAGED GLASS ON FOLD NO. 1 & 4. REPAIRED SPECIMEN AND CHANGED TO HARDER CUSHION MATERIAL. AT 2.00 LB/IN <sup>2</sup> 3.00 LB/IN <sup>2</sup> & 4.00 LB/IN <sup>2</sup> VERTICAL PAD CAUGHT BETWEEN GLASS OF MATING FOLD.

Figure 2-53 Summary of Slip Resistance Tests

TABLE 2-14 SUMMARY OF VIBRATION TEST

## AXES IDENTIFICATION

1. THRUST: PARALLEL TO CENTERLINE OF HINGE/FOLD LINE
2. LATERAL: NORMAL TO FOLDED SPECIMEN

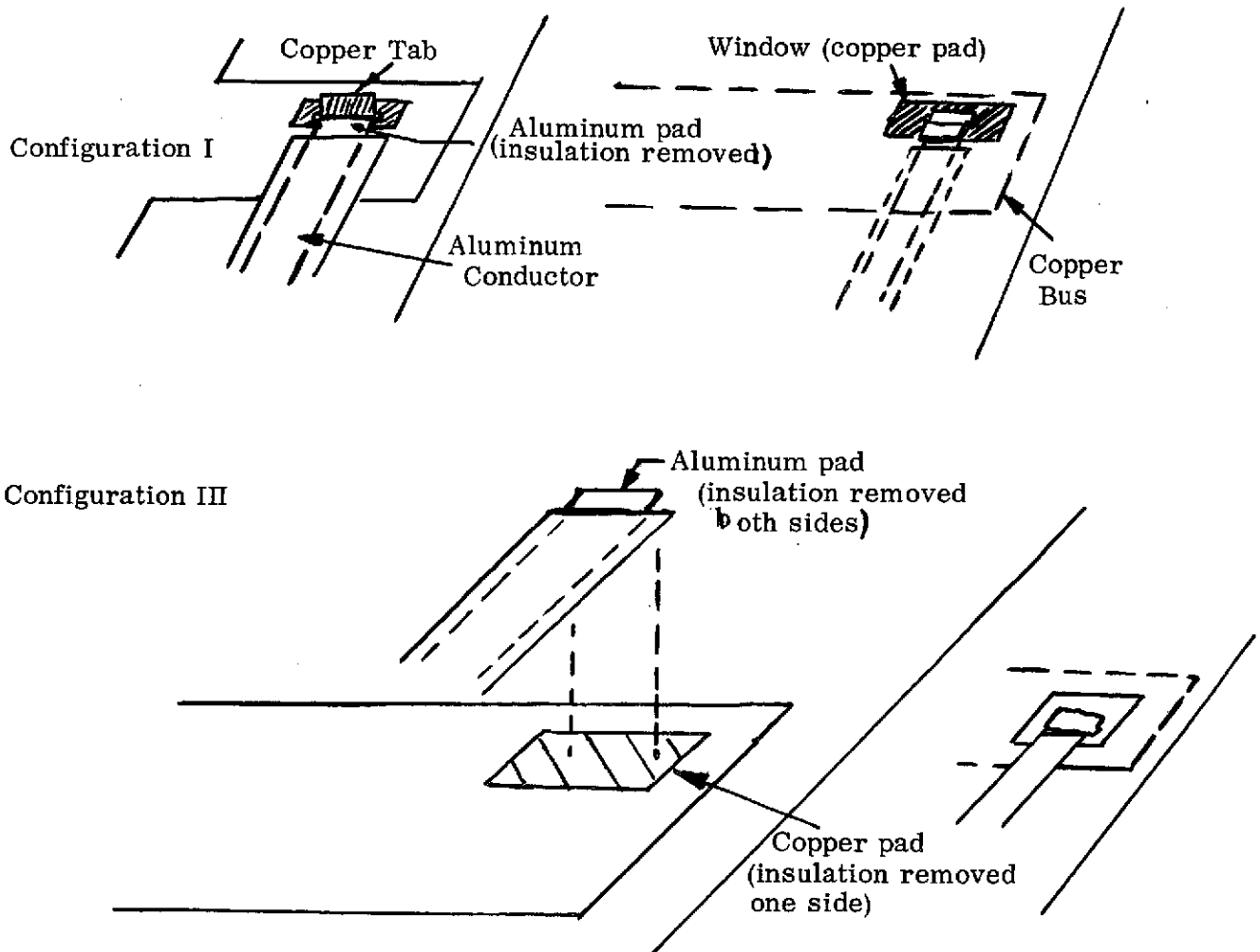
## LEGEND:

1. OK - NO APPARENT DAMAGE

SPECIMEN	MATERIAL	SINUSOIDAL LEVEL		RANDOM LEVEL THRUST & LATERAL AXIS
		THRUST AXIS	LATERAL AXIS	
		5-10 cps, 0.25 DA 10-50 " , 2.5 g's 50-200 " , 2.0 g's	5-8 cps, 0.25 DA 8-21 " , 1.6 g's 21-200" , 1.25 g's	+8 db g <sup>2</sup> /cps, 20-70 cps, - g RMS .95 " , 70-200 " , 26 " -2.5 db " , 200-2000 cps, - "
Criss/Cross	Silicone RTV 41	OK	OK	OK
Intermittent Cross	Silicone RTV 41	OK	OK	OK
Buttons	Sylgard 182	OK	OK	OK
Vertical Off-Set	Silicone RTV 41	Broken Glass on Fold No. 1	--	--
Intermittent Cross (Off-Set)	Silicone RTV 41	OK	OK	OK
No Pad	--	OK	OK	OK
Horizontal Off-Set	Silicone RTV 41	OK	OK	OK
Perimeter	Silicone RTV 41	OK	OK	OK
Criss/Cross	Laminated Teflon Rod	Vertical Pads Caught Between Glass	Vertical Pads Caught Between Glass	Vertical Pads Caught Between Glass

strength testing, high humidity testing and UV exposure testing was performed.

The pull test results for the two promising joint configurations (I and III) were 2 to 7 lbs (90° peel) on 0.040 aluminum conductor widths.



Two samples each of the two joints were exposed to 95% (min) relative humidity for 14 days at 70°F and one sample each of the two designs were exposed to UV (5 suns, 3210 E. S. H.) with no significant degradation in pull strength observed.

Based on the findings, the recommended termination techniques for the SEPS array are as follows:

1. Solder interface configuration joint.
2. Copper pad of "outrigger" exposed one side only.
3. Copper pad solder tinned (may be "hydrosqueezed" for uniform thin coating).
4. Aluminum conductor pad exposed both sides.  
NOTE: A means of stripping insulation without damage to aluminum conductor will have to be established. Chemical stripping of Kapton is possible.
5. Aluminum conductor pad (interface side) tinned with aluminum solder/#673 flux. Cleaned thoroughly for removal of flux residues.
6. Termination made by positioning aluminum conductor on copper pad and reflow solder with conventional solder iron. Resin flux could be used for better heat conductivity.
7. Solvent clean joint and surrounding area.
8. Reinforce joint with suitable compound.

### 2.7.3 Thin Array Substrate Fabrication and Test

The SEPS array baseline substrate is thinner than previously built printed circuit designs. The laminate employs 0.5 mil Kapton/0.5 mil adhesive film. A printed circuit is encapsulated between two sheets of this film when they are heat laminated together in a platen press. Depending on press size and electrical module size, a step laminating process may be used to make a large panel if the "adhesive" is thermoplastic in nature. FEP exhibits this characteristic but is also denser than desired for a lightweight substrate. Other adhesive materials were evaluated for this application. The other candidate systems are:

- o 0.5 mil Kapton/0.5 mil TME 300 (high temperature polyester)
- o 0.5 mil Kapton/0.5 mil Pyralux (acrylic adhesive)
- o 0.5 mil Kapton/0.5 mil TEFZEL (ETFE Fluoropolymer)
- o 0.5 mil Kapton/0.5 mil high temperature adhesive (CMC-122)

Pyralux on 0.5 mil Kapton is presently been made by DuPont but not yet in the desired width (15 to 18 in.). The adhesion of TEFZEL to Kapton is reported as a problem by DuPont and the combined system film is also not available in the desired width.

Three thin printed circuit substrate designs were tested for:

- 1) Exposure to 150<sup>0</sup>C for 96 hours
- 2) Temperature/humidity exposure followed by dielectric strength measurements

- 3) Dielectric strength measurements
- 4) Peel strength tests: a) coverlay to underlay bond and b) coverlay to copper foil bond

The substrate designs were:

- 1) 0.5 mil Kapton/0.5 mil FEP Teflon (1 oz Cu)
- 2) 0.5 mil Kapton/0.5 mil TME 300 (1 oz Cu)
- 3) 0.5 mil Kapton/0.5 mil high temperature polyester adhesive (CMC-122) (1 oz Cu)

The test results are summarized in Table 2-15

In fabricating test segments, the CMC-122 -1/2 -1/2 has demonstrated that it is handled and laminated with the best control after the Pyralux. The FEP Teflon and TME 300 adhesives were very difficult to handle in the thin designs. Since the Pyralux system is not available in the desired width, the CMC-122 is the preliminary design selection.

#### 2.7.4 UV Testing

In addition to the two sample aluminum to copper Alusol solder joints, mentioned previously, several candidate materials coupons were exposed to 3210 E. S. H. at 5 suns. One of these was a cross pattern of RTV-41 on-array padding molded on a 1 in. square sheet of 2 mil Kapton. A force vs. deflection determination was made before and after testing. The padding cross section was 0.020 in x 0.032 in. A 1.25 in. flat round mandrel was pressed against the face of the sheet and padding. The before and after measurements were:

<u>Deflection (in.)</u>	<u>Load (lbs)</u>	
	<u>Before</u>	<u>After</u>
0.005	0.30	0.40
0.010	2.93	2.40
0.015	8.35	7.00
0.020	18.60	17.80

TABLE 2-15

## THIN FLEXIBLE PRINTED CIRCUIT SUBSTRATE TESTS

TESTS	REQUIREMENTS	RESULTS		
		TME	CME	DUPONT
Elevated Temperature	No Separation, Charring, Discoloration	None	None	None
Humidity/Temperature	No Delamination, VOIDS, Swelling $72.4 \times 10^{11}$ Ohms/ $\square$ @ 500 VDC	Pass $5.7 \times 10^{14}$	Pass $2.9 \times 10^{10}$	Pass $7.4 \times 10^{13}$ Ohms/ $\square$
Dielectric withstand	No. Flashover, Breakdown @ 1 KVAC hms	Pass	Pass	Pass
Peel Strength	Coverlay-Conductor 3#/in. (Min.)	Covering broke @ 8.5#	Covering broke @ 12#	Covering broke @ 1.4#
	Coverlay-base dielectric 3#/in. (Min.)	Covering broke @ 6.6# & 9.7#	Covering broke @ 9# & 11#	Covering broke @ 1.6#



The RTV-41 white color, its adhesion to the Kapton and the padding capabilities were not significantly changed by this exposure. The temperature of the specimen, which is held near a water cooled block (corners clamped), was under 100°C.

The following items, 1 inch square, were similarly exposed with, no observed change in physical properties:

- a. 1 mil Kapton/0.5 mil Pyralux adhesive (two sheets laminated together)
- b. 0.5 mil Kapton/0.5 mil high temperature Polyester adhesive (CMC-122)
- c. 1 mil Kapton/0.5 mil Pyralux (two sheets laminated over 0.040 in wide aluminum conductors, 3 mils thick, 9 conductors.
- d. 1 mil Kapton/0.5 mil Pyralux part way laminated over a 5 mil thick Teflon impregnated fiberglass cloth.

#### 2.7.5 Effect of On-Array Padding Shadows

If the array is tilted 75 degrees to the sun and the 0.032 in high between cell padding is right next to the cell edge (worst case) a portion of the solar cell will be shaded, 0.06 in. of the 1.591 in. long cell (3.8%) shading occurs on 1/2 the array since the on-array padding runs in a direction on the other half of the panel that does not result in a shadow. A 10 cell module of 12 mil wraparound 2x4 in. solar cells was taped to provide a 0.1 in. mask on every cell. The module was illuminated before and after taping. The resulting power loss was proportional to the active area loss and therefore the same assumption can be made for the SEPS solar array. The nominal or average spacing of cells and padding causes a 3 percent shadow on one-half the panel or 1.5 percent on the whole array at 75 degrees tilt.

## 2.8 Root Section Model

The root section model is a modification to the flight design which uses existing components, such as the Astromast "Moonbeam" and where there are significant costs or availability impacts.

The model design includes 4 each hinge to hinge panels comprising an area of 4.0 m X 3.05 m (13.1 ft. X 10 ft.). A 0.25 m (10 in.) diameter coilable fiberglass longeron Astromast with a 3.66 m (12 ft.) extension length and its canister are used for extension/retraction/blanket preload operations. Aluminum FCC harnessing is used to represent the first 3.05 m of the wing harness (inboard end). The containment box uses honeycomb panels for the box bottom and top. The model contains the blanket tensioning and guide wire systems. Two live electrical modules composed of 765 2x4 cm wraparound contact, 200 micron (8 mil) cells with 150 micron (6 mil) fused silica covers are located in the model blanket. The selected criss-cross on-array padding design is used on one-half of the panels. The electrical modules are of welded assembly design. The remainder of the model blanket employs glass chip solar cell mass simulators.

The completion of the model fabrication has been delayed due to delays in the delivery of the solar cells and covers. The results of planned model functional testing will be reported in an addendum to this final report when the tests scheduled for October 1974, are completed.

SECTION 3.0  
SEPS SOLAR ARRAY TECHNOLOGY DEVELOPMENT  
WORK PLAN

### 3.1 Introduction

The purpose of this plan is to describe a cost effective approach to demonstrate technology readiness for the SEPS solar array. As a result of the technology evaluation program, several areas requiring technology development have been defined and these are included in this plan. The major effort in the demonstration of technology readiness involves the design, fabrication, and test of a full scale array wing with less than a full compliment of live solar cells. To accomplish this, a review of SEPS solar array design requirements, and of the state-of-the-art of applicable technology is required. A significant cost savings in the technology demonstration program can be achieved if a design, meeting the SEPS requirements, for the flight array wing is arrived at as soon as possible. Design optimization is not required. It is required that the design adequately display the array components and their functions to insure that any of the new technology that is required will be identified and covered in the technology demonstration program. A second cost savings should be achieved by performing component tests in the configurations that they have in the array design, and assuring that testing is performed specifically for the SEPS environments that are reasonable expected to affect the performance of the components. Similarly technology development should be emphasized rather than design developments where there is confidence that the design is sufficiently developed to identify all necessary technology. To save costs, where technology readiness risk is low, components shall be incorporated and tested in the full scale array tests.

### 3.2 Component Evaluation and Technology Development

#### 3.2.1 Technology Status

Each component in the array design should be reviewed to determine level of technology

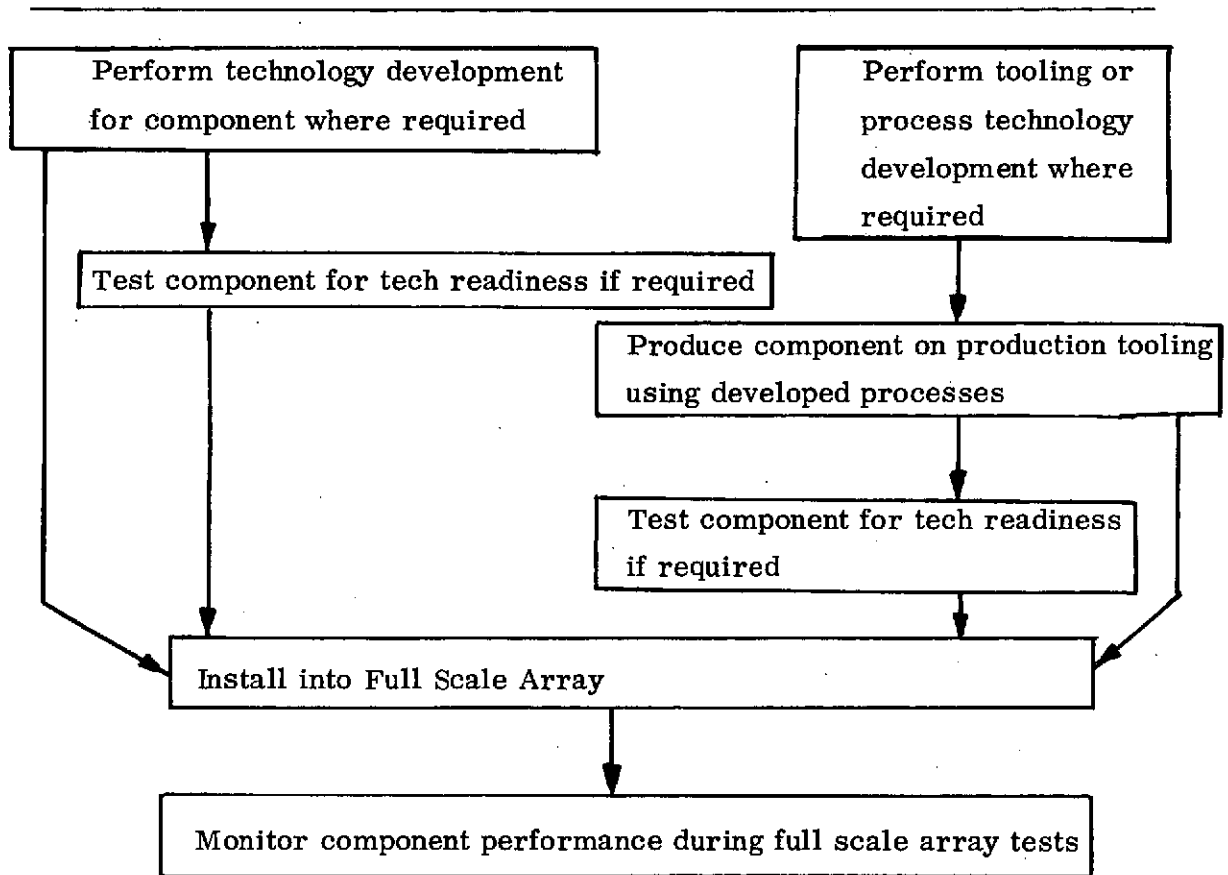
readiness as it relates to SEPS requirements.

- o Is component flight design weight predicted with confidence and safe margin?
- o Has component been proven in similar application?
- o Has full scale hardware been produced? (If full scale hardware production has a technology question).
- o Have production tooling and process techniques technology been developed fully for SEPS application?
- o Can ready date be established now with high confidence?
- o What developments in hardware design are necessary for readiness (i. e., full scale test)?
- o What developments in production tooling process technology are necessary before full scale SEPS production?

Technology readiness was assessed under this study with components technology classified as: I-Sufficient, II-Insufficient but development progress will achieve readiness, III Insufficient but an alternate is feasible, and IV, Insufficient with no alternatives and no device potential. For those components required for SEPS which are less than sufficiently developed for technology readiness (Category II, III or IV), programs should be instituted for developing technology in time for the SEPS Solar Array Technology readiness date.

Determine technology status for fabricating each component into assemblies and subsystems. Where fabrication technology is lacking, institute programs (with alternatives) for developing fabrication techniques in time for SEPS technology readiness. This effort should parallel development of component technology where applicable. All articles used for these tests shall be manufactured with fabrication tooling and processes which are either actually for production of SEPS or are directly similar in operating technique, panel capacity, controls, etc. Where deviations are necessary, the capability of the process or equipment must be determined to be non-critical to the performance of the item produced. In addition, availability of actual equipment for SEPS production must be highly probable. Adherence to this restriction will ensure that performance of components produced and tested during this program can be related directly to SEPS mission requirements.

COMPONENT TECHNOLOGY DEVELOPMENT  
AND VERIFICATION OF TECHNOLOGY READINESS



The technology state-of-the art status reviewed in section 2.6 is summarized below:

<u>Solar Cell Covers</u>	<u>Cat.</u>
Fused Silica	I
Cerium Stabilized Glass	I
Micro Sheet	III
FEP-Tape	II
-Heat Laminated	III
-Sprayon	III
Integral Covers	III
Electrostatic Bond 7070	III

<u>Solar Cells</u>	<u>Cat. II</u>
--------------------	----------------

Preliminary design requires development of 11.4% efficiency 8 mil end-tab wrap-around 2 x 4 cm cells. LMSC has received samples of such cells which were produced under laboratory conditions. A plan for implementing a pilot production and test program is required. It is expected that refinement of full-scale production methods will be successful.

<u>Solar Cell Interconnect</u>	<u>Cat.</u>
Cu	I
Mo	II
Al	III
Ag	III
Kovar	III
Invar	III

<u>Cell Joining Technique</u>	<u>Cat.</u>
Parallel Gap	I, II
Solder	III
Ultrasonic	III
TC Bonding	II
Laser	III

<u>Substrate</u>	<u>Cat.</u>
0.5 mil Kapton/0.5 mil FEP Teflon	II
0.5 mil Kapton/0.5 mil Tefzel	II
0.5 mil Kapton/0.5 mil TME 300	II
0.5 mil Kapton/0.5 mil Pyralux	II
0.5 mil Kapton/0.5 mil Polyester adhesive (CMC-122)	II

<u>Module Hinge Joint</u>	<u>Cat.</u>
Electrical Harness	II
FCC Al	I
FCC Cu	I
RWC Ribbon	III
RWC Round Bundle	IV

<u>Containment Box Structure</u>	<u>Cat.</u>
	II

<u>Extension and Retraction Mast</u>	<u>Cat.</u>
	II

<u>Mast Motors</u>	<u>Cat.</u>
	I

<u>Lubricants</u>	<u>Cat.</u>
	I

### 3.2.2 Recommended Technology Development Projects

#### A. Temperature Cycling Program, Category II

Background: The SEPS Solar Array must survive over 440 temperature cycles in geosynchronous orbit over the 5 year design life plus additional cycles in a spiralling out mode. The low mass of the SEPS array results in on-orbit rates of temperature which are 3-4 times greater than for conventional rigid panel designs. The high altitudes and low mass also result in very low temperatures in the shade periods. The effect of this thermal environment on the SEPS array padding, interconnect material, substrate tension, cell joining design, and material thickness and

geometries should be defined by test.

Desired Output: This program should provide (1) a temperature cycling facility capable of "in-situ" output measurement and of cycling samples to  $-196$  to  $-200^{\circ}\text{C}$ , (2) Validation of accelerated and low cost testing methods such as convective cycling, (3) Comparative low temperature cycle data on candidate flexible solar array assemblies for up to 1000 cycles, (4) An understanding of basic failure mechanisms, and, ultimately the ability to analytically model and predict failure modes. Results from these tests can be factored in the SEPS array panel design during the development phase.

Recommended Program Elements: The program should include as key elements (1) A preliminary or parallel analytical effort to predict performance of the test designs and to evaluate convective vs radiative testing effects. (2) A parallel radiative and convective test program to attempt to validate (or invalidate) the less expensive convective techniques, (3) Fabrication of test facility with capability for "in situ" electrical output measurement and  $-196$  to  $-200^{\circ}\text{C}$  testing, (4) Early initiation of flexible assembly testing to temperatures and rates as determined by SEPS solar array thermal analysis, (5) Continued addition of candidate assemblies as they become available such as thermal compression bonding modules, (6) Detailed failure analysis of samples, (7) Continuous analytical support for data analysis and failure mode refinement.

The testing should allow the addition of test samples to the program on a near continuous basis so that companies and centers that care to submit samples can do so.

#### B. UV and Irradiation Tests of Flexible Substrates, Category II

Background: The SEPS Solar Array must survive up to 5 equivalent sun years of UV on missions to 0.3 au and 5 years of space radiation and vacuum. Of major concern is the long term effect of these environments on the structural and thermal properties of the tensioned polymeric substrate materials since the array substrate is a major structural element of the array system. Creep, tear and tensile data and UV effects on these properties must be evaluated to insure technology readiness. An abundance



of radiation effects studies have been performed on polymeric materials to determine insulation property degradation. The present application requires strength and thermal-optical properties characterization as a function of environmental stress. For example the relationship between creep and combined environmental effects is not known. Data on particle and high level UV irradiated material is needed before technology readiness can be demonstrated for the selected substrate material.

Desired Output: Data on the combined effects of UV, penetrating radiation and vacuum on structural, thermal-optical and electrical properties of the candidate substrate materials.

Recommended Program Elements:

This program should include several thin candidate substrate materials such as 1/2 mil Kapton with candidate adhesives. The following tasks should be included:

- (1) Prediction of degradation in properties based on available data
- (2) Creep and tensile testing in the  $-196^{\circ}\text{C}$  to  $+150^{\circ}\text{C}$  range
- (3) Particle radiation and UV exposure to 5 equivalent sun years
- (4) Post radiation testing of
  - a. Thermal-optical properties
  - b. Tensile and creep strength
  - c. Electrical insulation

C. NDT Inspection - Acceptance Techniques, Category II

BACKGROUND: The visual appearance of soldered joints (filleting, geometric symmetry, etc.) have been used as criteria of acceptance for interconnect to cell joints. Parallel gap welding creates a joint nugget non discernable visually and slightly larger in diameter than the weld tips. There is a need for NDT inspection of non-soldered cell assembly joints. Efforts have concentrated on In Process and Post Bond evaluation methods. Some success has occurred with the In Process category using resistive measurement techniques and under NAS8-28432 Acoustic Emission methods have given favorable results. Post Bond evaluation has been a more difficult problem with many systems evaluated and only one, Infrared Videography, showing any possibilities.

The advent of large arrays with high cell quantities incorporating multiple joints per cell creates a dominant requirement for a reliable generally rapid rate of assessing joint integrity both in fabrication and as a pre-flight checkout.

Following completion of NAS8-28432 in November 1974, the best approaches and the general requirements for the evaluation hardware will be defined. The program can proceed from that point.

DESIRED OUTPUT: Definition of on-line procedures and equipment to perform the NDT Inspection/Acceptance functions for welded solar array modules.

RECOMMENDED PROGRAM ELEMENTS:

- 1) Write specification for selected system
- 2) Procure and set-up the testing system
- 3) Develop processes and procedures for system application
- 4) Fabricate module using NDT inspection/acceptance system
- 5) Generate handbook describing acceptable on-line procedures for NDT inspection/acceptance for solar array module fabrication

D. Improved Solar Cell for SEPS, Category II

BACKGROUND: The SEPS array preliminary design requires an 8 mil silicon solar cell with 11.4 percent efficiency where the conventional solar cell in production is in the range of 10 to 11 percent efficient. A low cost SEPS solar array depends on achieving an improved production cell that has a minimum cost. Thus, the lowest cost "high efficiency" cell techniques and the minimum number of these techniques should be identified to arrive at the desired cell performance.

In arriving at the applicable SEPS cell improvement techniques and to predict array performance the performance of the SEPS solar cell design as a function of the following conditions should be determined;

- a. Particle radiation and UV exposure
- b. Effect of variation of illumination intensity, of temperature and

of angle of incidence.

- c. Thermal cycling
- d. Compatibility of cell design for higher efficiency with cell joining techniques.

DESIRED OUTPUT: Data on the effects of particle radiation, both front and back exposure, on cell  $I_{sc}$ ,  $I_{mp}$ ,  $V_{mp}$  and  $V_{oc}$  as a function of 1 MeV fluence (electrons) is desired. The cell performance under the temperature and illumination values that the cells will see will improve array performance predictions. Demonstration of cell joining techniques that 1) have minimum effect on cell performance, 2) provide good thermal cycling performance and 3) are of low cost in application to array fabrication. Candidate cell joining techniques can be used on the cells when they are available and these cells can be included in the "Temperature Cycling Program".

#### Recommended Program Elements

The program should include effort by solar cell vendors to develop a low cost "intermediate" efficiency 8 mil solar cell where single or combined "high efficiency" techniques are investigated. These techniques include  $P^+$  backside treatment, new grid designs,  $Ta_2O_5$  AR coatings, and shallow junctions. The best cell candidate should then be characterized by electron irradiation testing, UV testing, and temperature, illumination, intensity and illumination angle testing. Compatibility of the cell design with parallel gap electric resistance welding and other joining techniques should be evaluated.

#### E. Array Blanket Module Mechanical Joint Technology, Category II

BACKGROUND: The SEPS Solar Array will be made up of physical modules which are economically handled, illumination tested and can be mechanically joined in the array or removed for replacement of damaged modules. Candidate joints require evaluation for strength, fabricability, integration with the tension distribution bar and with the thin substrate design. Design and evaluation for various joint configurations, materials and environments is required to determine creep at elevated temperatures, tooling requirements and a quick attach and release system.

DESIRED OUTPUT: Data on several module joint designs that integrate well with the thin substrates, retract well during full and partial retraction, allow easy joining and separating of modules, allow easy integration of the blanket tension system and withstand the SEPS environments.

RECOMMENDED PROGRAM ELEMENTS: This program should include several candidate hinge designs and materials. The following tasks should be included.

- (1) Evaluate fabrication techniques and tooling requirements
- (2) Evaluate ease of joint assembly and separation, and integration with tension distribution bar
- (3) Particle radiation and UV exposure of joints to SEPS levels
- (4) Post-radiation tensile and creep testing
- (5) Evaluate geosynchronous environmental effects on disassembly operations

F. Parallel Gap Electric Resistance Welding, Category II

BACKGROUND: The electric resistance welding of solar cell interconnects is the non-soldered joining technique that has seen the most development. This development has been in both weld schedules and weldable solar cell design. The use of this joining technique in SEPS on a hybrid or high efficiency cell is classed as Category II. The successful parallel gap welding of the hybrid cell is not well established and some concern exists as to the  $P^+$  surface treatment on the P contact area.

The adhesive used in the substrate lamination, if it flows with heat, as does FEP Teflon, has an effect on the contamination of the electrodes. The electrode cleaning and replacement cycles also have an impact on the cost of array fabrication. Thus, the substrate design/electrode design for parallel gap welding is in need of technology advancement.

DESIRED OUTPUT: The program should provide 1) Definition of the acceptability of parallel gap welding for the SEPS cell, the weld schedule and the cell design requirements, 2) Improved substrate/electrode designs providing more welds between electrode cleaning and replacement operations.

RECOMMENDED PROGRAM ELEMENTS: The program should include as key elements (1) Procurement of SEPS design cells, (2) Pre-weld and post-weld cell output determinations as a function of weld schedules, (3) Evaluate electrode contamination as a function of substrate lamination materials, (4) Vary electrode design and materials to improve electrode life.

G. Composite Material for Containment Box Structure, Hinge Pin Tension Distribution Bar, Category II

BACKGROUND: The use of an aluminum honeycomb core with a graphite/Kevlar 49/epoxy face sheet construction is a current state-of-the-art light weight panel design. Verification of environmental behavior in the SEPS temperature ranges, in vacuum coupled with space radiation must be extended to the five year lifetime requirement.

DESIRED OUTPUT: Data on mechanical performance of sandwich structure following simulated environmental exposure.

RECOMMENDED PROGRAM ELEMENTS: The program should include:

- 1) Fabrication of candidate single stage and two stage cure systems with prepreg epoxy and with supplemental adhesive
- 2) Perform pre-environmental exposure tests
  - a) Flat-wise tensile
  - b) Sandwich flexure
  - c) Drum peel
- 3) Expose test specimens to temperature/vacuum environments of SEPS
- 4) Repeat mechanical tests at SEPS operating temperatures
- 5) If thermal control coatings are required, adhesion, peel, and thermal-optical stability of the control assembly will be tested following UV, particle radiation, temperature, vacuum environmental exposure

H. Extension Mast Technology Program, Category II

BACKGROUND: The SEPS Extension Mast operating temperature range requirements from 0.3 au to 6 au require the evaluation of materials and weights of various candidate mast designs to provide technology readiness. The mast stowage volume must be compact and the bending stiffness requirements must be met at all operating temperatures. The exposure of the mast to the sun at 0.3 au is a non-nominal condition that can strongly impact the selection of mast materials for the close sun mission. The cost and fabrication aspects of material substitutions to reduce mast and storage container weights should be evaluated to identify the best design approaches.

DESIRED OUTPUT: Data on:

- (1) Other coilable, high temperature mast materials for continuous longeron design of the Astromast type.
- (2) Design modifications to articulated metal masts of the Astromast type that eliminate or reduce "deadband" in mast deflection
- (3) Mast and canister weight reductions with the substitution of materials, and cost impact of these changes
- (4) Designs that are capable of operation over the SEPS mast temperature range

RECOMMENDED PROGRAM ELEMENTS: The program should include the following tasks.

- (1) Develop a preliminary design of an Extension Mast meeting the design performance requirements.
- (2) Assess the state-of-the-art for all elements within the design. In areas where the state-of-the-art is judged inadequate to support the development and fabrication of an extension mast meeting the design requirements, identify and define the research program necessary to the adequate advancement of the state-of-the-art

- (3) Evaluate the cost and fabrication aspects of substituting materials to provide a low weight design
- (4) Fabricate and test such extension mast components that are required to adequately validate the mast design concept proposed by the contractor
- (5) Fabricate and test a section of the full scale extension mast design
- (6) Fabricate and test the full scale extension mast design

### 3.2.3 Component Tests

#### 3.2.3.1 General

1. Materials and small component testing to the SEPS environment are required to verify Category I status.
2. The testing will proceed from component tests to full scale assembly tests.
3. Functional tests can be performed at the component level and at the full scale assembly level.
4. Environmental testing will tend to be limited to components and to limited configurations of the full scale wing due to cost of large volume or tall environmental chambers.
5. The fabrication of the full scale array wing components shall demonstrate and verify technology readiness of fabrication methods and production tooling.

#### 3.2.3.2 Component Functional Tests - Ambient Environment

- a. Extension/Retraction Mast Assembly
  - 1) Electrical continuity and insulation resistance
  - 2) Motor operation and mast movement direction
  - 3) Water table mast extension for testing in two axes
    - Deadband
    - Bending stiffness test
    - Torsional stiffness test
    - Operation with offset tip loads

- 4) Vertical extension tests prior to assembly with stowage container
  - Check 1 "g" counterbalance system
  - Extension/retraction rates
- 5) Flight weight design verification
  
- b. Electrical Modules
  - 1) Dielectric performance at operating voltage
  - 2) Illumination testing
  - 3) Weld schedule verification
  
- c. Array Stowage Container, Preload, and Testioning System
  - 1) Tensioning system and guide wire system
    - tension vs extsion (two directions)
  - 2) Blanket preload system (without mast)
    - build up compression load to design value
  - 3) Blanket extension/retraction verification in simulated zero g environment such as underwater testing.
  - 4) Flight weight verification
  
- d. Array Blanket
  - 1) Alignment of panels into strip checked as blanket is assembled
  - 2) Panel replacement
  - 3) Flight weight verification

### 3.2.3.3 Component Environmental Tests

- a. Extension/Retraction Mast Assembly
  - Thermal bending
  - Temperature Extremes Operation - Design and test for short term operation at ambient pressures at highest and lowest mission temperature
  
- b. Electrical Modules
  - Thermal/vacuum/ascent pressure profile with post environment illumination



- c. Array Stowage Container, Preload, and Tensioning System
  - Vibration testing with blanket and padding installed
  - Temperature/vacuum/ascent pressure profile
  - Tension system operation at temperature extremes
- d. Array Blanket  
(Vibration testing with storage container, c.)

The test model fabrication will follow procedures which will represent SEPS production.

Design and fabrication of the test fixtures will be approached similarly.

### 3.3 Full Scale Array Design, Fabrication and Testing

#### 3.3.1 Design and Fabrication

This technology development effort will be culminated in the design, fabrication and test of a full scale array model which will show that technology status is sufficient to permit SEPS Solar Array flight design development. A detailed design of the full scale array test model will be performed. Differences from the preliminary flight unit design will be identified and justified. Whenever possible, however, full scale, flight-like components which are produced on production type tooling will be used in the full scale test model. The array wing blanket shall contain approximately 10 percent live electrical modules, 25 percent cell mass simulators on design substrates and the remainder plastic film.

#### 3.3.2 Full Scale Wing Tests

##### 3.3.2.1 Functional Tests - Ambient Environment

- a. Check counterbalance system for 1 "g" extension testing
- b. Mast integration with preload system and testing up to design preload
- c. Blanket release, extension, tensioning at partial extension

- d. Buildup mast extension/retraction rates
- e. Vary sequence of array position changes
- f. Vary partial extension

3.3.2.2 Environmental Testing

- Acoustic Test - Perform at ambient conditions in stowed configuration

(Vibration, Acceleration & Shock, and Combined temperature/vacuum testing are recommended for performance during a flight design development program.)

SECTION 4  
REFERENCES

1. Optimized Silicon Solar Cells for Space Exploration Power Systems - Final Report. Nov. 30, 1971, P.A. Isles, CENTRALAB, JPL Contract 952865
2. Electrical Characteristics of Silicon Solar Cells As A Function of All Temperature and Solar Intensity, J. D. Sandstrom, IECEC, 1968 p 138
3. Parametric Performance Characteristics and Treatment of Temperature Coefficients of Silicon Cells for Space Application, R. E. Patterson, R. K. Yasui, JPL, TR 32-1582, May 1973
4. Second Topical Report, Design and Analyses, Space Station Solar Array Technology Evaluation Program, LMSC-A995719, Nov. 71
5. Final Report - Feasibility Study of A 110 Watt per Kilogram Lightweight Solar Array System, G. E. 73SD4256, May 1973, JPL Contract 953387 pg 3-28
6. Layout and Technology of the CTS Solar Array Blanket, R. Bohs, AEG-Telefunken, 1973 Photovoltaics Specialists Conference, p 296
7. "Parametric Study of the Performance Characteristics and Weight Variations of Large Area Roll-Up Solar Arrays," JPL TR 32-1502, J. V. Coyner, Jr. and R. G. Ross, Jr.
8. Space Station Solar Array Technology Evaluation Program, NAS9-11039, LMSC A995719, Nov. 1971.
9. Program Manual for ASTRO, Version C, 22 May 1973.
10. G. D. Rhoads, LMSC, Personal communication.
11. M. A. Saunders, S. C. Downing, and T. Meuldyk, "Steady-State and Transient Thermal Analysis of Space Station Solar Array, " TXA 2512, LMSC, Sept. 16, 1971. (Published in Reference 4)
12. F. W. Sears, Optics, Addison-Wesley Publishing Co., Reading, Mass., 1949, page 174
13. B. E. Anspaugh, Solar Cell Performance as a Function of Temperature and Illumination Angle of Incidence, Jet Propulsion Laboratory, CIT-JPL- TM-33-495, Sept. 15, 1971
14. "Beams on a Elastic Foundation", M. Hetenyi, University of Michigan Press. 1946
15. MIL-HDBK-5B.

# APPENDIX A HARNESS CALCULATIONS

## A.1 Derivation of conductor length/conductor area for maximum array watts/lb.

$$X = \frac{\text{WATTS DELIVERED}}{\text{LBS OF BLANKET} + \text{HARNESS}}$$

$$X = \frac{\frac{P_{\text{DELIVERED}}}{P_{\text{DEL}} + \text{ONE CONDUCTOR LOSS} \cdot (n)}}{\frac{\text{WATTS/LB OF ARRAY BLANKET}}{+ \text{HARNESS WEIGHT}}}$$

where  $n$  = number of conductors

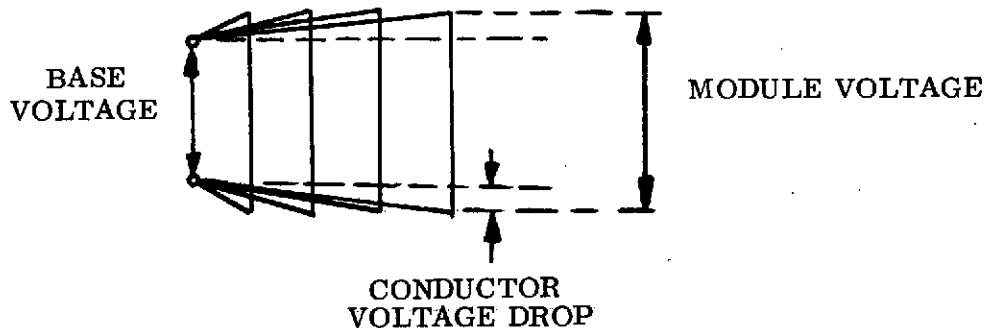
$$\text{one conductor loss} = I_M \Delta V = I_M (I_M R_{\text{COND}})$$

$$\text{one conductor loss} = I_M^2 \rho \frac{L}{A}$$

$I_M$  for each module is the same

$\Delta V$  for each conductor is held the same

$\therefore R$  and thus  $\frac{L}{A}$  is the same for each conductor



$$\begin{aligned} \text{HARNESS WT} &= \text{DENSITY} \times \sum L \cdot A \text{ (all conductors)} \\ &= \text{DENSITY} \times \left[ L_1 A_1 + L_2 A_2 + \dots + L_n A_n \right] \\ &= \text{DENSITY} \times \left[ \frac{L_1 A_1}{L_1/A_1} \times \frac{L_1}{A_1} + \dots \right] = \text{DENSITY} \times \left[ \frac{L_1^2}{A_1} + \frac{L_2^2}{A_2} + \dots \right] \\ &= \text{DENSITY} \times \left( \sum L^2 \right) / \frac{L}{A} \text{ (all conductors)} \end{aligned}$$

$$X = \frac{P_{DEL}}{P_{DEL} + n I_M^2 \rho \frac{L}{A}} + \frac{DENSITY \cdot \Sigma L^2}{\frac{L}{A}}$$

$$d \frac{u}{v} = \frac{v du - u dv}{v^2} = 0 \text{ at maximum } \frac{u}{v}$$

$$X = \frac{P_D \cdot \frac{L}{A} \cdot \frac{W}{LB}}{P_D \frac{L}{A} + n I_M^2 \rho \left( \frac{L}{A} \right)^2 + \frac{W}{LB} \cdot DENSITY \Sigma L^2}$$

$$\frac{L}{A} = \sqrt{\frac{\frac{W}{LB} \cdot DENSITY \Sigma L^2}{n I_M^2 \rho}} \quad \text{for maximum X, watts delivered/lb.}$$

where

$\frac{W}{LB}$  = watts/lb of array blanket

Density = lbs of FCC/cuft of conductor

$\Sigma L^2$  = sum of the lengths of all conductors squared

n = total number of conductors

$I_M$  = module current, each module has two conductors

$\rho$  = resistivity of conductor

### A.2 $\Sigma L^2$ FOR 41 PANELS

PANEL WIDTH = 2.5 ft.

5 ft ADDED TO REACH CENTER OF BASE

PANEL NO.	L	$L^2$
1	8.0	64.0
2	10.5	110.25
3	13.0	169.0
⋮	⋮	⋮
39	103.0	10,609.0
40	105.5	11,130.25
41	108.0	11,664.0

$$\Sigma L^2 = 173,799 \quad \text{for one conductor per panel position}$$

$$(\Sigma L^2 \text{ for 4 conductors at each L value} = 4 \times 173,799)$$

### A.3 Conductor Resistivity

	$\rho \sim \text{Ohms (Cirmil-Ft)}$				Sp. Gr.
	20°C	55°C	150°C	-145°C	
Cu	10.371	11.796	15.667	3.65	8.99
Al	17.01	19.41	25.927	5.69	2.71

$$\frac{\frac{\pi d^2}{4}}{d^2} = \frac{\pi}{4}, \quad 1 \text{ CM} = 0.7854 \text{ square mil}$$

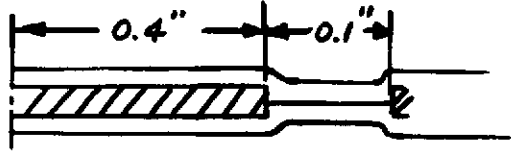
$$1 \text{ ohm (CM-Ft)} = 0.7854 \text{ ohm (sq mil-ft)} = 0.7854 \text{ ohm } (1 \times 10^{-6} \text{ in}^2 - \text{ft})$$

$$= 0.7854 \times \frac{1 \times 10^{-6}}{144} \text{ ohm (sq ft-ft)}$$

$$\text{ohm (sq. ft-ft)} = \text{ohm (CM-Ft)} \times 5.454 \times 10^{-9}$$

$$\rho_{\text{Al}} (55^\circ \text{C}) = 19.41 \times 5.454 \times 10^{-9} = 1.059 \times 10^{-7} \text{ ohm (sq. ft-ft)}$$

#### A.4 EFFECTIVE DENSITY OF FCC (in terms of Al Conductor Area)



1 mil Kapton + 1 mil High temperature polyester adhesive

$$2 \text{ mils Kapton, } A = 0.002 \times 0.5 = 0.0010 \text{ in}^2, \text{ sp. gr.} = 1.42$$

$$2 \text{ mil adhesive, } A = 0.002 \times 0.5 = 0.001 \text{ in}^2, \text{ sp. gr.} = 1.40$$

$$3 \text{ mil Al, } A = 0.003 \times 0.4 = 0.0012 \text{ in}^2, \text{ sp. gr.} = 2.71$$

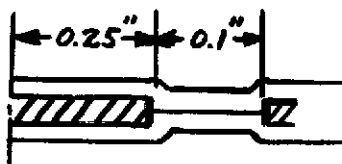
$$1 \text{ cu ft of Al conductor takes } L \text{ of } \frac{1728 \text{ in}^3}{0.0012 \text{ in}^2} = 1,440,000 \text{ in} \\ = 120,000 \text{ ft}$$

$$\text{Wt of } 1 \text{ ft}^3 \text{ of Al} = 2.71 \times 62.4 \text{ lbs/ft}^3 = \underline{169.104 \text{ lbs}}$$

$$\text{Wt of Kapton} = 1.42 \times 62.4 \times \frac{0.0010 \text{ in}^2}{144} \times 120,000 \text{ ft} = \underline{73.84 \text{ lbs}}$$

$$\text{Wt of adhesive} = 1.40 \times 62.4 \times \frac{0.0010}{144} \times 120,000 = \underline{72.80 \text{ lbs.}}$$

$$\text{Effective density of FCC} = \frac{299.9 \text{ lbs.}}{1 \text{ cu ft of Al}} = \boxed{315.74 \text{ lbs/ft}^3 \text{ Al}}$$



$$\text{Area Kapton} = 0.002 \times .35 = 0.0007 \text{ in}^2$$

$$\text{Area adhesive} = 0.001 \times .35 = 0.0007 \text{ in}^2$$

$$\text{Area Al} = 0.003 \times .25 = 0.00075 \text{ in}^2$$

$$1 \text{ cu ft of Al takes } L \text{ of } \frac{1728 \text{ in}^3}{0.00075} = 2,304,000 \text{ in} = 192,000 \text{ ft}$$

$$\text{Wt of Al} = 2.71 \times 62.4 = \underline{169.104 \text{ lbs}}$$

$$\text{Wt of Kapton} = 1.42 \times 62.4 \times \frac{.0007}{144} \times 192,000 = \underline{82.70 \text{ lbs}}$$

$$\text{Wt of adhesive} = 1.40 \times 62.4 \times \frac{0.0007}{144} \times 192,000 = \underline{81.54 \text{ lbs}}$$

$$\text{Effective density of FCC} = \boxed{\frac{333.34 \text{ lbs}}{\text{ft}^3 \text{ of Al}}}$$

A.5 Harness WeightsOne Wing, 100 volt modules to base4 conductors to each panel  
or L value

$$T = 55^{\circ}\text{C}$$

$$\frac{L}{A}_{\text{opt}} = \sqrt{\frac{50 \text{ W/Lb} \times 350 \text{ lbs/ft}^3 \times 4 \times 173,799 \text{ ft}^2}{4 \times 41 \times (1.25)^2 (1.059 \times 10^{-7})}}$$

$$\frac{L}{A} = 21.174 \times 10^6$$

$$\text{At 108ft, } A = \frac{108}{21.174 \times 10^6} = 5.101 \times 10^{-6} \text{ ft}^2 = 0.000734 \text{ in}^2$$

(.003" x .245")

$$\text{At 8 ft, } A = \frac{8}{21.174 \times 10^6} = 0.000734 \times \frac{8}{108} = 0.0000544 \text{ in}^2$$

(.003" x 0.0181")

$\text{Wt. of Harness} = \frac{350 \times 173,799 \times 4}{21.174 \times 10^6} = 11.49 \text{ lbs} = 5.22 \text{ Kg}$
--

$$\Delta V_{\text{Module}} = 2 \cdot I \cdot R = 2 \cdot (1.25) \times (1.059 \times 10^{-7}) \times (21.174 \times 10^6) = 5.61$$

One Wing, 200 volt modules to base2 conductors to each panel  
or L value

$$T = 55^{\circ}\text{C}$$

$$\frac{L}{A} = \sqrt{\frac{50 \text{ W/Lb} \times 350 \times 2 \times 173,799 \text{ ft}^2}{2 \times 41 \times (1.25)^2 (1.059 \times 10^{-7})}}$$

$$\frac{L}{A} = 21.174 \times 10^6$$

$$\text{At 108ft, } A = \frac{108}{21.174 \times 10^6} = 0.000734 \text{ in}^2$$

(.003 x .245")

$$\text{At ft, } A = (.003") \times (.0133")$$

$\text{Wt of Harness} = \frac{11.49 \text{ lbs}}{2} = 5.75 \text{ lbs} = 2.61 \text{ Kg}$
---

$$\Delta V_{\text{Module}} = 2 \cdot I \cdot R = 2 \cdot (1.25) \times (1.059 \times 10^{-7}) \times (21.174 \times 10^6) = 5.61 \text{ V}$$